Vol. 63 May, 1959 No. 5

THE JOURNAL OF PHYSICAL CHEMISTRY

(Registered in U. S. Patent Office)

CONTENTS

NOTES

COMMUNICATION TO THE EDITOR

THE JOURNAL OF PHYSICAL CHEMISTRY

(Registered in U. S. Patent Office)

Published monthly by the American Chemical Society at 20th and Northampton Sts., Easton, Pa.

Second-class mail privileges authorized at Easton, Pa. This publication is authorized to be mailed at the special rates of postage prescribed by Section 132.122.

The *Journal of Physical Chemistry* is devoted to the publication of selected symposia in the broad field of physical chemistry and to other contributed papers.

Manuscripts originating in the British Isles, Europe and Africa should be sent to F. C. Tompkins, The Faraday Society, 6 Gray's Inn Square, London W. C. 1, England.

Manuscripts originating elsewhere should be sent to W. Albert Noyes, Jr., Department of Chemistry, University of Rochester, Rochester 20, N. Y.

Correspondence regarding accepted copy, proofs and reprints should be directed to Assistant Editor, Allen D. Bliss, Department of Chemistry, Simmons College, 300 The Fenway, Boston 15, Mass.

Business Office: Alden H. Emery, Executive Secretary, American Chemical Society, 1155 Sixteenth St., N. W., Washington 6, D. C.

Advertising Office: Reinhold Publishing Corporation, 430 Park Avenue, New York 22, N. Y.

Articles must be submitted in duplicate, typed and double spaced. They should have at the beginning a brief Abstract, in no case exceeding 300 words. Original drawings should accompany the manuscript. Lettering at the sides of graphs (black on white or blue) may be pencilled in and will be typeset. Figures and tables should be held to a minimum consistent with adequate presentation of information. Photographs will not be printed on glossy paper except by special arrangement. All footnotes and references to the literature should be numbered consecutively and placed in the manuscript at the proper places. Initials of authors referred to in citations should be given. Nomenclature should conform to that used in *Chemical Abstracts*, mathematical characters marked for italic, Greek letters carefully made or annotated, and subscripts and superscripts clearly shown. Articles should be written as briefly as possible consistent with clarity and should avoid historical background unnecessary for specialists.

Notes describe fragmentary or incomplete studies but do not otherwise differ fundamentally from articles and are subjected to the same editorial appraisal as are articles. In their preparation particular attention should be paid to brevity and conciseness. Material included in Notes must be definitive and may not be republished subsequently.

Communications to the Editor are designed to afford prompt preliminary publication of observations or discoveries whose value to science is so great that immediate publication is imperative. The appearance of related work from other laboratories is in itself not considered sufficient justification for the publication of a Communication, which must in addition meet special requirements of timeliness and significance. Their total length may in no case exceed 500 words or their equivalent. They differ from Articles and Notes in that their subject matter may be republished.

Symposium papers should be sent in all cases to Secretaries of Divisions sponsoring the symposium, who will be responsible for their transmittal to the Editor. The Secretary of the Division by agreement with the Editor will specify a time after which symposium papers cannot be accepted. The Editor reserves the right to refuse to publish symposium articles, for valid scientific reasons. Each symposium paper may not exceed four printed pages (about sixteen double spaced typewritten pages) in length except by prior arrangement with the Editor.

Remittances and orders for subscriptions and for single copies, notices of changes of address and new professional connections, and claims for missing numbers should be sent to the American Chemical Society, 1155 Sixteenth St., N. W., Washington 6, D. C. Changes of address for the *Journal of Physical Chemistry* must be received on or before the 30th of the preceding month.

Claims for missing numbers will not be allowed (1) if received more than sixty days from date of issue (because of delivery hazards, no claims can be honored from subscribers in Central Europe, Asia, or Pacific Islands other than Hawaii), (2) if loss was due to failure of notice of change of address to be received before the date specified in the preceding paragraph, or (3) if the reason for the claim is "missing from files."

Subscription Rates (1959): members of American Chemical Society, $8.00 for 1 year; to non-members, $16.00 for 1 year. Postage free to countries in the Pan American Union; Canada, $0.40; all other countries, $1.20. Single copies, current volume, $1.35; foreign postage, $0.15; Canadian postage $0.05. Back volumes (Vol. 56–59) $15.00 per volume; (starting with Vol. 60) $18.00 per volume; foreign postage, per volume $1.20, Canadian, $0.15; Pan-American Union, $0.25. Single copies: back issues, $1.75; for current year, $1.35; postage, single copies: foreign, $0.15; Canadian, $0.05; Pan-American Union, $0.05.

THE JOURNAL OF
PHYSICAL CHEMISTRY

(Registered in U. S. Patent Office)

VOLUME 63 MAY 20, 1959 NUMBER 5

RADIATION-INDUCED EXCHANGE OF HYDROGEN CHLORIDE-Cl^{36} AND PROPYL CHLORIDES[1]

BY ROWLAND E. JOHNSON[2] AND CHARLES E. MILLER, JR.[3]

Contribution from the Department of Chemistry, Florida State University, Tallchassee, Fla.

Received March 7, 1958

The γ-irradiation of the two propyl chlorides has been studied, both alone and admixed with hydrogen chloride-Cl^{36}. The principal radiolysis product is hydrogen chloride; G_{HCl} values are 3.38 for *n*-PrCl and 3.82 for *i*-PrCl. The isotopic exchange reaction is zero order in hydrogen chloride; G_{exchg} values are 3.32 for *n*-PrCl and 1.27 for *i*-PrCl. A mechanism is suggested for the exchange.

Introduction

The identification of products from the γ-irradiation of materials has been hampered both by the small yields available and by the transient nature of many of the species produced. Special techniques such as gas chromatography and mass spectroscopy have been used to overcome these difficulties. Another possible technique is the incorporation of a small amount of a radioactive tracer in the system during irradiation; the tracer is available to react with transient species as they are produced and the label can be used to follow small amounts of material. Other workers have used this approach; a recent paper by Schulte[4] gives an application in the CCl_4–Cl_2 system.

In our work, we were interested in testing the method to compare the reactions of two similar materials. We chose for irradiation one of the simplest systems available, the two propyl chlorides. We expect in such small organic halides that the major interaction of radiation will be with the halide atom.[5] We find that there is negligible thermal exchange of the organic halide with other halogen atoms present in compounds in the system.[6] Chlorine has a radioactive isotope of convenient energy, half-life and accessibility. Finally, we might hope to correlate any difference in reaction rates with the structural difference between the molecules.

Our experimental procedure consisted of the γ-irradiation of propyl chloride alone and admixed with hydrogen chloride-Cl^{36}. The hydrogen chloride is quite soluble in propyl chloride. The relatively high ratio of propyl chloride to hydrogen chloride ensures that the main portion of the radiolysis occurs in the propyl chloride; we assume that the hydrogen chloride is not affected by the γ-radiation. Loss of activity from the hydrogen chloride-Cl^{36} is assumed to indicate the production of some intermediate species leading to isotopic exchange between propyl chloride and hydrogen chloride.

Experimental

Materials.—Hydrogen chloride, Matheson, 99+%, was bubbled through an aqueous solution of hydrogen chloride-Cl^{36} (received on allocation from the Atomic Energy Commission). The gas then was passed through a trap at −78° and a phosphorus pentoxide tube. It was stored in a stainless steel tank until used.

Isopropyl chloride (*i*-PrCl), Matheson, Coleman and Bell, was used without further purification. A gas chromatogram showed no (<0.1%) impurities.

Normal propyl chloride (*n*-PrCl), Matheson, Coleman and Bell, was used without further purification. A gas chromatogram showed the presence of negligible amounts (<0.5% total) of *i*-PrCl, *n*-propyl alcohol and a third component.

Pyridine, J. T. Baker, purified grade, was distilled and stored over potassium hydroxide.

Radiation Source.—All irradiations were carried out in the Florida State University cobalt-60 facility. During our irradiations, the activity was approximately 388 curies. In the work position, approximately 1.64×10^{19} e.v. ml.$^{-1}$ hr.$^{-1}$ were available as measured by an 0.8 *N* H_2SO_4 ferrous

(1) Supported in part by the Research Corporation. Presented at the American Chemical Society Meeting, San Francisco, April, 1958.

(2) Texas Instruments, 6000 Lemmon Avenue, Dallas, Texas.

(3) Work performed in partial fulfillment of the requirements for Master of Science degree.

(4) J. Schulte, *J. Am. Chem. Soc.*, **79**, 1643 (1957).

(5) B. M. Tolbert and R. M. Lemmon, *Rad. Res.*, **3**, 52 (1955).

(6) P. B. D. de La Mare, *J. Chem. Soc.*, 3169 (1955).

sulfate dosimeter using $G(Fe^{++} \rightarrow Fe^{+++})$ to be 15.5.[7] (By comparison, the radiation from the tracer was at least a factor of 10^8 less.) Rough calculations indicated that the mass absorption coefficients of the dosimeter solution and the propyl chlorides were very similar; we assumed the coefficients to be identical. Corrections for decay of the cobalt-60 were made as necessary. All irradiations were carried out at ambient temperatures, 25 ± 1°.

Experimental Procedures.—The procedures used for both propyl chlorides were identical. Samples for irradiation were pipetted into thin-wall Pyrex bulbs. A bulb was attached to a vacuum system and degassed by the standard procedure of cycles of freezing, pumping and melting. After a final freezing, the bulb was sealed off if it were to be used for the irradiation of pure propyl chloride. If the run were to measure isotopic exchange, labeled hydrogen chloride was introduced from an auxiliary dosing system before the bulbs were sealed off. The gaseous volumes of the sealed bulbs were kept as small and reproducible as possible. The bulbs were placed in the cobalt-60 source to be removed at preselected times.

After irradiation, isotopic exchange mixtures were separated with pyridine. The bulb was opened in an evacuated container having a side arm containing excess pyridine. The reaction mixture was distilled into the pyridine, then all volatile components distilled away from the pyridinium hydrochloride. The latter was hydrolyzed, the chloride converted to silver chloride by standard methods, and counted as suggested by Kahn.[8] No attempt was made to analyze the extremely low activity of the propyl chloride.

In a series of runs on irradiation of propyl chloride alone, the amount of hydrogen chloride produced during irradiation was measured by direct titration. The bulb was opened in an evacuated container containing a few ml. of water and a drop of phenolphthalein solution. The container was vigorously agitated, opened, and the solution titrated with 0.1 *N* sodium hydroxide.

In another series of runs on irradiation of propyl chloride alone, the bulb (after irradiation) was opened in an evacuated container having a side arm containing excess pyridine to which a measured dose of labeled hydrogen chloride had been added. The propyl chloride mixture was distilled into the pyridine mixture and out again as described above. Care was taken to ensure complete mixing of the labeled and unlabeled pyridinium hydrochlorides. Chloride activity was determined as above.

Preliminary investigations showed that there was negligible thermal exchange between propyl chloride and hydrogen chloride-Cl^{36} at room temperature. We find half-times of exchange at 50° of >82 days for *i*-PrCl and >107 days for *n*-PrCl. (The difference may not be significant.) Attempts to find some exchange reaction occurring after irradiation proved fruitless. Samples separated immediately (~20 minutes) after irradiation showed the same fraction of isotopic exchange as those separated 150 hours after irradiation, other conditions being equal.

Analysis of species produced as a result of the irradiation was attempted using a Model 154B Perkin–Elmer gas chromatograph. Pure chloride was irradiated and a portion of the sample evaporated. The peaks of this aliquot were identified by comparison runs with known compounds.

Results

Formation of Hydrogen Chloride by Radiolysis.—All runs in which the isotopic exchange rate is to be determined must be corrected for the hydrogen chloride produced by radiolysis of the propyl chloride. The rate of production of hydrogen chloride could be measured by titrating as described above; the experimental values were (9.24 ± 0.19) × 10^{-4} mmole ml.$^{-1}$ hr.$^{-1}$ for *n*-PrCl and (10.44 ± 0.62) × 10^{-4} mmole ml.$^{-1}$ hr.$^{-1}$ for *i*-PrCl. The rates were constant over the period of our runs. These results correspond to G_{HCl} values (molecules yield per 100 e.v.) of 3.38 and 3.82, respectively.

To define further the experimental conditions, we examine the runs in which we diluted the hydrogen chloride produced during the irradiation with labeled hydrogen chloride introduced during the separation procedure. From the decrease in specific activity of the chloride we can calculate the amount of chloride species produced during irradiation which are permanent and are capable of exchanging. The results agree with the values for the production of hydrogen chloride given above.

Calculation of Fraction of Isotopic Exchange.—Since we have a non-equilibrium system, the usual isotopic exchange expressions[9] do not apply to the present case. The specific activity of the hydrogen chloride (had no dilution occurred) S at any time t depends upon the original specific activity and the amount of exchange. S may be calculated from S_{exp}, the experimentally determined specific activity, by

$$S = S_{exp}(A + k't)/(A) \qquad (1)$$

where A is hydrogen chloride originally present, k' is the rate of production of hydrogen chloride, and parentheses indicate concentrations.

The rate of exchange, R, then is given by the expression

$$R = -\frac{(A + k't)(B)\,\mathrm{d}\ln(1 - F)}{(A + k't + B)\,\mathrm{d}t} \qquad (2)$$

where B is propyl chloride and F is the fraction exchange calculated by the usual methods using the values of S calculated from eq. 1. We neglected the small change in concentration of propyl chloride during a run. In our experiments, the concentration of propyl chloride was much greater than the amount of hydrogen chloride (including that produced during the irradiation), $(B) >> (A + k't)$. Then

$$R = -\frac{(A + k't)\,\mathrm{d}\ln(1 - F)}{\mathrm{d}t} \qquad (3)$$

and

$$R = k''(A + k't)^n(B)^m(I)^p \qquad (4)$$

where k'' is the specific rate constant of the exchange reaction, I is the radiation density, and n, m and p are constants describing the kinetic order of each of the reactants. Since B is the solvent whose concentration remains essentially constant during the runs and since the radiation density remained constant during the runs, the last two terms remain constant and may be incorporated in k'' to give k.

Equating eq. 3 and 4 then gives

$$\mathrm{d}\ln(1 - F) = -k(A + k't)^{n-1}\,\mathrm{d}t \qquad (5)$$

and

$$\ln(1 - F) = -\frac{k}{nk'}[(A + k't)^n - (A)^n] \quad (n \neq 0) \qquad (6a)$$

$$\ln(1 - F) = -\frac{k}{k'}\ln\frac{(A + k't)}{(A)} \quad (n = 0) \qquad (6b)$$

Table I gives the experimental data of the runs made with labeled hydrogen chloride added. The data of each run were applied to eq. 6a and 6b trying various values of n in the former case. Only

(7) R. M. Lazo, H. A. Dewhurst and M. Burton, *J. Chem. Phys.*, **22**, 1370 (1954).

(8) M. Kahn, *et al.*, *Nucleonics*, **13**, #5, 58 (1955).

(9) A. C. Wahl and N. A. Bonner, Editors, "Radioactivity Applied to Chemistry," John Wiley and Sons, Inc., New York, N. Y., 1951, Chp. 1.

eq. 6b gave consistently constant values of k and this equation is used to calculate the values of k in Table I. Table II shows the data for a typical run. Calculations show the G_{exchg} values (molecules exchanged per 100 e.v.) to be 3.32 for n-PrCl and 1.27 for i-PrCl.

TABLE I

PROPYL CHLORIDE–HYDROGEN CHLORIDE-Cl^{36} RUNS

Run	Initial HCl, mmoles ml.$^{-1}$	t_{max} [c] hr.	$k \times 10^4$,[d] mmoles hr.$^{-1}$ ml.$^{-1}$
	Normal propyl chloride[a]		
1	0.085	84.25	9.18
2	.170	66.5	9.16
3	.170	97.5	8.74
4	.170	63.5	9.15
5	.350	96.0	9.24
6	.350	88.5	8.64
7	.350	92.0	9.16
		Av.	9.04 ± 0.25
	Isopropyl chloride[b]		
8	0.085	120 0	4.57
9	.170	96 0	3.65
10	.170	74 0	3.98
11	.350	140 5	2.66
12	.350	56.0	2.46
		Av.	3.46 ± 0.72

[a] n-PrCl concentration, 12.30 mmoles ml.$^{-1}$. [b] i-PrCl concentration, 11.88 mmoles ml.$^{-1}$. [c] Time at which last point in run was removed from irradiator. [d] For a radiation density of 1.64×10^{19} e.v. ml.$^{-1}$ hr.$^{-1}$.

TABLE II

DATA OF A TYPICAL RUN[a]

Sample	HCl at time t, mmoles ml.$^{-1}$	$\frac{(HCl + k't)}{(HCl)}$	$1 - F$	t, hr.
1	0.170	1.00	1.00	0.0
2	.184	1.08	.90	16.0
3	.196	1.15	.90	28.5
4	.213	1.25	.85	47.5
5	.235	1.38	.71	71.8
6	.257	1.51	.68	97.5

[a] Initial concentration of hydrogen chloride was 0.170 mmole ml.$^{-1}$, n-PrCl was 12.30 mmoles ml.$^{-1}$.

The gas chromatography data showed the formation of very small amounts of hydrogen, methane and hexane during radiolysis of the pure chlorides. In addition, a very small amount of ethane was produced from n-PrCl during radiolysis but not from i-PrCl. Propane and hydrogen chloride were the only species found in larger amounts.

Discussion

From the results, we see that hydrogen chloride and propane are the major products of the γ-irradiation of propyl chloride. In addition, exchange occurs between propyl chloride and hydrogen chloride *via* some transient species produced during irradiation. The reaction is zero order in hydrogen chloride and pseudo-zero order in propyl chloride. However, we assume that the reaction is actually first order or higher with respect to propyl chloride and that the first reaction is the rupture of the C–Cl bond, neglecting the small amount of reaction to produce other species.

The rates of hydrogen chloride production are very similar for the two chlorides. The exchange rate for the n-PrCl is about the same as the rate of production of hydrogen chloride and is almost three times as fast as the exchange rate of the i-PrCl. From these data we might imagine that the reactions to produce hydrogen chloride are very similar for the two chlorides and that the exchange reactions depend more upon the structures of the two molecules. We suggest a series of equations to explain the main reactions

$$RCl \xrightarrow{\sim} R\cdot + Cl\cdot \quad (7a)$$

$$Cl\cdot + RCl \longrightarrow HCl + \cdot R'Cl \text{ (production of HCl)} \quad (7b)$$

$$R\cdot + HCl \longrightarrow RH + Cl\cdot \text{ (loss of HCl)} \quad (7c)$$

$$Cl\cdot^* + RCl \longrightarrow Cl\cdot + RCl^* \text{ (exchange reaction)} \quad (7d)$$

$$Cl\cdot^* + RCl \longrightarrow HCl + \cdot R'Cl^* \text{ (exchange reaction)} \quad (7e)$$

In addition, propane may be produced by

$$R\cdot + RCl \longrightarrow RH + \cdot R'Cl \quad (8)$$

We also expect the exchange of radioactivity to be very rapid between chlorine atoms and hydrogen chloride molecules.

The production of hydrogen chloride would depend upon the reactions of eq. 7a, 7b and 7c though the latter will be relatively unimportant because of the low concentration of hydrogen chloride. The rates for the two chlorides would be quite similar since neither eq. 7a nor eq. 7b differentiates greatly between the normal or iso form with the latter being only slightly favored in each case. If the primary process involves instead the rupture of a C–C bond, we expect methane or ethane (plus other fragments) from the n-PrCl and methane from the i-PrCl. The very small amounts of these species found confirm that this type of reaction is negligible in our system. Of course, hexane would be expected from recombination of propyl radicals. Propane will be produced by the reactions of eq. 7c and 8.

The exchange reaction would occur *via* eq. 7d and 7e. In our proposed mechanism, none of the other reactions given above would lead to exchange. We assume also that reactions of an organic radical to extract a chlorine atom from labeled hydrogen chloride or the recombination reaction of a propyl radical and a labeled chlorine atom, eq. 9a and 9b, are negligible.

$$R\cdot + HCl^* \longrightarrow RCl^* + H\cdot \quad (9a)$$

$$R\cdot + Cl\cdot^* \longrightarrow RCl^* \quad (9b)$$

In either case, 7d or 7e, we expect a difference in rate depending on whether RCl is n-PrCl or i-PrCl. Bimolecular substitution reactions are known involving radicals[10]; in a bimolecular substitution reaction, n-PrCl would be expected to react faster than i-PrCl. The relative importance of the two exchange reactions is unknown but we believe that 7d is the more important. Our conclusion, then is that the exchange reaction and hydrogen chloride production are essentially separate reactions and that there is a fortuitous agreement of the two rates in the case of n-PrCl.

We are grateful to Drs. Ernest Grunwald and Russell H. Johnsen for helpful discussions and the latter for help with the irradiations.

(10) R. A. Herrman and R. M. Noyes, *J. Am. Chem. Soc.*, **78**, 5761 (1956).

MASS SPECTROMETRIC STUDY OF THE SUBLIMATION OF LITHIUM OXIDE[1]

BY JOSEPH BERKOWITZ, WILLIAM A. CHUPKA AND GARY D. BLUE AND JOHN L. MARGRAVE

Argonne National Laboratory, Lemont, Illinois
Department of Chemistry, University of Wisconsin, Madison, Wisconsin

Received June 19, 1958

Lithium oxide sublimes mainly by decomposition to the elements at 1400°K., but an appreciable partial pressure of $Li_2O(g)$ in equilibrium with the solid is indicated by mass spectrometric studies of Li_2O sublimation from a platinum Knudsen cell. From absolute pressures and estimated thermodynamic functions, the following heats were obtained: $Li_2O(s) = Li_2O(g)$, $\Delta H_0^0 = 104 \pm 5$ kcal./mole; $LiO(g) = Li(g) + O(g)$, $D_0^0 \leq 83$ kcal./mole (3.6 e.v.). LiO(g) is of very minor importance as a vapor species, but LiONa(g), formed when Na is present as an impurity, appears to have considerable stability.

Introduction

The nature of the gaseous species subliming from solid alkali metal oxides has been the subject of considerable speculation and experimentation. Brewer,[2] from a consideration of the data available in 1951, decided that there was no evidence for the existence of important alkali metal oxide gaseous molecules except possibly Li_2O and LiO. Theoretical calculations by Brewer and Mastick[3] treating the M_2O molecule as a linear assemblage of three ions, suggest the Cs_2O, Rb_2O, K_2O and Na_2O should vaporize by decomposition to the elements with no appreciable contribution due to M_2O gaseous molecules. These calculations do indicate the possible importance of Li_2O, but the uncertainty is large. Experimental determinations of the vapor pressures of Li_2O and Na_2O have been made by Brewer and Margrave[4] using the Knudsen effusion technique. The observed pressures of both substances agreed within experimental error with the pressures expected for simple decomposition to the metal gases and O_2. However, when the same investigators measured the volatility of Li_2O in streams of argon and oxygen, no decrease in volatility upon changing from argon to oxygen at one atmosphere was observed, thus demonstrating that the partial pressure of Li_2O gaseous molecules must be comparable to that of the elements in the saturated vapor of Li_2O.

In this work on lithium oxide, a mass spectrometer has been used to investigate the vapor in thermodynamic equilibrium with solid Li_2O inside a Knudsen cell. Observation of ion masses and measurement of ion currents then provide a means of identifying the species in the vapor and obtaining thermodynamic data for the gaseous equilibria inside the Knudsen cell. With this experimental arrangement it is possible to obtain more unambiguous information than that which may be obtained from either Knudsen weight loss or flow type experiments.

Experimental

The mass spectrometer and associated Knudsen cell assembly have been described in detail earlier by Chupka and Inghram,[5] and Porter, Schissel and Inghram.[6] In this experiment, the Knudsen cell was made of platinum and was contained within an Inconel oven. It was necessary to contain the sample completely in platinum since the Inconel acts as a reducing agent as was evidenced in the earliest runs without a platinum lid where the vapors were in contact with the Inconel cover.

The temperature of the cell was measured with a calibrated optical pyrometer, which was sighted through a Pyrex window and a slot in the radiation shields onto a black-body hole in the cell. A correction was made for the transmission of the window.

The vapor effusing from the Knudsen cell entered directly into the ionization chamber of the mass spectrometer where the neutral atoms and molecules were bombarded with electrons of controlled energy and thus ionized. An electron multiplier was used for ion detection. The output of this multiplier was measured by a vibrating reed electrometer and recorded by a strip chart recording potentiometer. This provided ready measurement of ion currents as low as 10^{-19} amp.

The lithium oxide was prepared by heating lithium carbonate to about 1000° for 1.5 to 2 hours and pumping off the CO_2. Brewer and Margrave[4] discuss the chemical and physical properties of the product obtained in this manner. A small amount of sodium impurity (about 0.3%) threatened to thwart efforts to determine the existence of a gaseous LiO molecule since $^{23}Na^+$ and $^7Li^{16}O^+$ both occur at mass 23. To overcome this difficulty, some lithium oxide used in one run was prepared from ^6Li metal as

$$2^6Li + 2H_2O = 2^6LiOH + H_2$$
$$(NH_4)_2CO_3 + 2^6LiOH = {}^6Li_2CO_3 + 2NH_3 + 2H_2O$$
$${}^6Li_2CO_3 = {}^6Li_2O + CO_2$$

The $^6Li^{16}O^+$ ion has mass 22, a relatively "clean" position compared to mass 23 with its continuously varying amount of $^{23}Na^+$ due to depletion of the sodium impurity with time.

Experimental Results

A. Identification of the Gaseous Species.—When the decomposition reaction of the lithium carbonate apparently was complete and the pressure due to the evolved CO_2 gas was reduced, a mass scan was made and the species produced by electron bombardment of the effusing vapor were identified. Peaks at masses 7, 30 and 32 were shown to be $^7Li^+$, $^7Li_2{}^{16}O^+$ and $^{16}O_2{}^+$, respectively. A subsequent investigation of the isotopic structure of the peaks due to the two lithium isotopes provided a positive check on the identity of the lithium-containing species. Using normal lithium oxide, a peak at mass 23 was found to be due to Na^+, as mentioned before. However, when one run was made with a sample of lithium oxide en-

(1) Work performed under the auspices of the U. S. Atomic Energy Commission.

(2) L. Brewer, *Chem. Revs.*, **52**, 1 (1953).

(3) L. Brewer and D. F. Mastick, *J. Am. Chem. Soc.*, **73**, 2045 (1951).

(4) L. Brewer and J. Margrave, *J. Chem. Phys.*, **59**, 421 (1955).

(5) W. A. Chupka and M. G. Inghram, THIS JOURNAL, **59**, 100 (1955).

(6) Porter, Schissel and M. G. Inghram, *J. Chem. Phys.*, **23**, 339 (1955).

riched with the ^6Li isotope, a peak at mass 22, attributable to $^6Li^{16}O^+$ was observed. Appearance potential curves for Li^+, LiO^+ and Li_2O^+ are shown in Fig. 1. With the known ionization potential (5.36 e.v.) of gaseous lithium atoms as a standard, it was determined that A.P. (LiO^+) = 9.0 ± 0.2 e.v. and A.P. (Li_2O^+) = 6.8 ± 0.2 e.v.

A peak observed at mass 46 was at first attributed to $Li_2O_2^+$, but later identified as $LiONa^+$ produced by ionization of LiONa which was formed by the reaction of the Na with the Li_2O. Evidence for the identity of the species observed at mass 46 was the fact that the intensity at mass 46 followed the decline in intensity of the sodium impurity as the activity of the latter diminished. In addition, the mass 46 peak was much more intense during the initial runs under reducing conditions which is contrary to the effect one would expect for an Li_2O_2 species.

B. The Equilibrium: $Li_2O(s) = 2Li(g) + {}^1/_2O_2(g)$.—It was possible to calculate the equilibrium constant for the decomposition reaction and hence the equilibrium partial pressures of gaseous lithium and oxygen over the temperature range investigated by making use of thermodynamic data which were available in the literature. For such calculations, the heat of formation and entropy for formation of solid Li_2O at 298°K. have been given by Johnston and Bauer.[7] The relative enthalpy, $H_T^0 - H_{298}^0$ and the relative entropy, $S_T^0 - S_{298}^0$, of the solid were evaluated by extrapolating the equations of Shomate and Cohen[8] from 1045°K., the highest temperature at which their data were obtained, to 1600°K. All the necessary functions for lithium and oxygen were obtained from the tabulation of thermodynamic properties of the elements by Stull and Sinke.[9] The results of these calculations are presented in Table I.

The partial pressure of a particular species is related to the observed ion intensity by the equation $P = kI^+T$ where P = vapor pressure, k = proportionality constant, I^+ = positive ion current, and T = absolute temperature.[10] It is possible to evaluate the proportionality constant in the ion current–pressure equation (and therefore the absolute partial pressure of a gaseous species inside the Knudsen cell) from a sensitivity calibration with a substance of known pressure and an estimate of the relative ionization cross sections.[5,11]

In this experiment it was assumed that the effusing vapor had the composition of the solid. The relative ionization cross sections σ then were evaluated for Li and O_2 by comparing the observed ion intensities of these species on the detector and using the factor $m_1/m_2^{1/2}$ as a correction for speed of transit across the ion chamber. The observed ion intensity of Li_2O^+ was converted to pressure of Li_2O by assuming that $\sigma(Li_2O) = 2\sigma(Li) + {}^1/_2\sigma(O_2)$ and

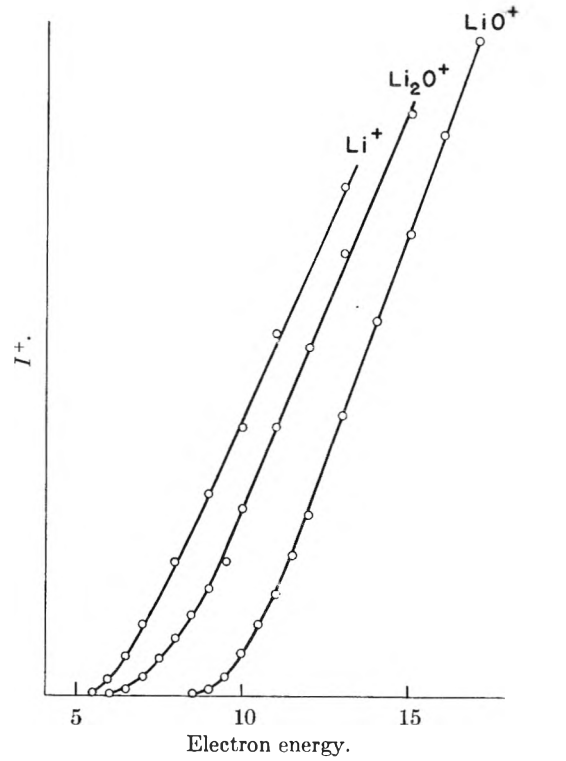

Fig. 1.—Ionization efficiency curves for lithium oxide vapor species.

comparing to $I_{O_2^+}$ and the previously calculated pressure of O_2. In a like manner the pressure of LiO was obtained from the ion intensity of LiO^+ by assuming that $\sigma(LiO) = \sigma(Li) + {}^1/_2\sigma(O_2)$. Taking $\sigma(O_2) = 1$, it was found that $\sigma(Li) = 1.1$, $\sigma(Li_2O) = 2.7$, and $\sigma(LiO) = 1.6$. The calculated cross sections of Otvos and Stevenson[12] show that $\sigma(Li)/\sigma(O_2) = 1.26$. Insofar as these calculations may be assumed to approximate the true cross sections, experimental evidence is thus obtained for the absence of reduction and for the validity of the above assumption that the vapor and solid have very nearly the same composition.

C. The Equilibrium: $Li_2O(s) = Li_2O(g)$.—Two independent methods were employed to extract the heat of sublimation of the Li_2O from the experimentally observed ion currents of Li_2O^+. By making use of the ion current–pressure relationship, $P = kI^+T$, and the Clausius–Clapeyron equation

$$\frac{d \ln P}{d(1/T)} = -\frac{\Delta H^0_{sub}}{R}$$

a value of ΔH^0_{sub} which is independent of the proportionality constant, k, may be found from the slope of the curve obtained when plotting ln (I^+T) *vs.* $1/T$. A Clausius–Clapeyron plot for the sublimation of Li_2O is shown in Fig. 2. The slope of this plot yielded a heat of sublimation of 108.3 kcal./mole^{-1} over the temperature range 1248–1534°K., and a heat of sublimation of 115.9 kcal./mole^{-1} at absolute zero.

The alternative procedure was to use k, the calibration constant evaluated as previously discussed, to determine the absolute pressure of Li_2O. The

(7) H. L. Johnston and T. W. Bauer, *J. Am. Chem. Soc.*, **73**, 1119 (1951).

(8) C. H. Shomate and A. J. Cohen, *ibid.*, **77**, 285 (1955).

(9) D. R. Stull and G. C. Sinke, "Thermodynamic Properties of the Elements," Advances in Chemistry Series No. 18 (American Chemical Society, 1956).

(10) W. A. Chupka and M. G. Inghram, *J. Chem. Phys.*, **21**, 371 (1953).

(11) M. G. Inghram, W. A. Chupka and Porter, *ibid.*, **23**, 2161 (1955).

(12) J. W. Otvos and D. P. Stevenson, *J. Am. Chem. Soc.*, **78**, 546 (1956).

TABLE I

$Li_2O(s) = 2Li(g) + {}^1/_2O_2(g)$

T (°K.)	$1/T \times 10^4$	log K_{eq}	log P_{O_2}	$P_{O_2(atm)}$	$P_{Li(atm)}$
1000	10.000	−30.32	−12.61	2.46×10^{-13}	9.84×10^{-13}
1050	9.524	−28.07	−11.71	1.95×10^{-12}	7.80×10^{-12}
1100	9.091	−26.02	−10.89	1.29×10^{-11}	5.16×10^{-11}
1200	8.333	−22.45	− 9.46	3.47×10^{-10}	1.39×10^{-9}
1300	7.692	−19.44	− 8.26	5.50×10^{-9}	2.20×10^{-8}
1400	7.143	−16.88	− 7.23	5.89×10^{-8}	2.36×10^{-7}
1500	6.667	−14.67	− 6.35	4.47×10^{-7}	1.79×10^{-6}
1600	6.250	−12.74	− 5.58	2.63×10^{-6}	1.05×10^{-5}

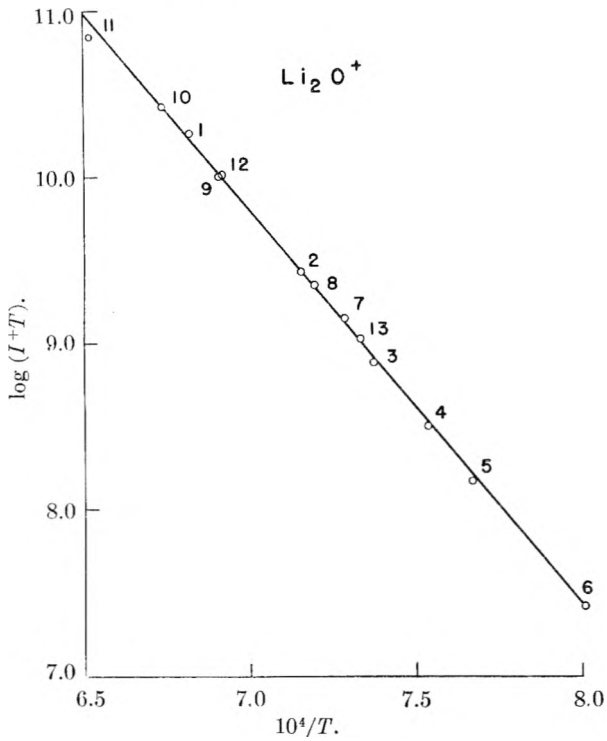

Fig. 2.—Clausius–Clapeyron plot for $Li_2O(g)$ above $Li_2O(s)$.

heat of sublimation then was obtained from an estimate of ΔS^0_{sub} and the relationships

$$\Delta F^0 = -RT \ln P$$
$$\Delta F^0 = \Delta H^0 - T\Delta S^0$$

In a like manner, the heat at absolute zero was then obtained from an estimate of $\Delta[(F^0 - H_0^0)/T]_{sub}$ and the relationship

$$\frac{\Delta H^0}{T} = \frac{\Delta F^0}{T} - \Delta\left(\frac{F^0 - H_0^0}{T}\right)$$

The ion currents of Li_2O^+ and the partial pressures of Li_2O gas are listed in Table II at various temperatures.

The entropy and free energy function of solid Li_2O were derived from the previously mentioned sources of data. However, an estimation of the entropy and free energy function of the gas necessitated the formulation of a molecular model and an estimation of vibrational frequencies. The internuclear distance and stretching bond constant were chosen by comparison of LiO to the iso-electronic molecule BeF which is included in the compilation of molecular data by Herzberg.[13] An estimated stretching bond constant of 6×10^5 dynes cm.$^{-1}$ yielded a ground-state vibration frequency of 1450 cm.$^{-1}$. The Li_2O molecule was assumed to be bent with an Li–O–Li bond angle of 105° and a bending force constant of 0.65×10^5 dynes cm.$^{-1}$, obtained by comparison to similar molecules such as D_2O. The valence-bond approximation[14] was used to determine the three frequencies of vibration. The frequencies 1270, 740 and 1650 cm.$^{-1}$ were used in the computations. Table III presents the computed thermodynamic functions for the LiO and Li_2O gaseous molecules which were used in the absolute pressure treatment of the mass spectrometric data.

TABLE II

$Li_2O(s) = Li_2O(g)$

T (°K.)	$1/T \times 10^4$	$I^+_{Li_2O}$	log P_{Li_2O}	P_{Li_2O} (atm.)
1248	8.013	2.123×10^4	−9.530	2.95×10^{-10}
1304	7.669	1.144×10^5	−8.780	1.66×10^{-9}
1327	7.536	2.453×10^5	−8.451	3.54×10^{-9}
1356	7.375	5.720×10^5	−8.064	8.63×10^{-9}
1364	7.331	7.920×10^5	−7.920	1.20×10^{-8}
1372	7.289	1.042×10^6	−7.798	1.59×10^{-8}
1390	7.194	1.617×10^6	−7.602	2.50×10^{-8}
1398	7.153	1.980×10^6	−7.521	3.01×10^{-8}
1447	6.911	7.810×10^6	−6.900	1.26×10^{-7}
1448	6.906	7.590×10^6	−6.912	1.22×10^{-7}
1467	6.817	1.238×10^7	−6.694	2.02×10^{-7}
1485	6.734	1.771×10^7	−6.533	2.93×10^{-7}
1534	6.519	4.545×10^7	−6.110	7.76×10^{-7}

These values for the entropy and free energy function of the gaseous Li_2O, together with the observed absolute pressure, yielded the values of ΔH_T^0 and ΔH_0^0 which are presented in Table IV. The average values are $\Delta H_T^0 = 96.1$ kcal. mole^{-1} and $\Delta H_0^0 = 103.7$ kcal. mole^{-1}. The difference between the slope and third law values of ΔH_0^0 is thus about 10.5%. Its most likely cause is temperature inhomogeneity within the Knudsen cell.

TABLE III

STATISTICAL ENTROPIES AND FREE ENERGY FUNCTIONS

T (°K.)	LiO Gas S^0	LiO Gas $\frac{-F^0 - H_0^0}{T}$	Li_2O Gas S^0	Li_2O Gas $\frac{-F^0 - H_0^0}{T}$
1300	58.126	50.301	70.384	59.551
1400	58.761	50.947	71.351	60.358
1500	59.356	51.488	72.263	61.123

D. The Equilibrium: $LiO(g) = Li(g) + {}^1/_2O_2(g)$.—In the run with the isotopically enriched sample, the isotope ratio was $^6Li/^7Li = 0.825$.

(13) G. Herzberg, "Molecular Spectra and Molecular Structure. I. Spectra of Diatomic Molecules," D. Van Nostrand Co., Inc., New York, N. Y., 1950.

(14) G. Herzberg, "Infra-Red and Raman Spectra," D. Van Nostrand Co., Inc., New York, N. Y., 1945, pp. 172, 180.

TABLE IV

STATISTICAL HEATS OF REACTION FOR $Li_2O(s) = Li_2O(g)$

T (°K.)	ΔS_T^0	$\frac{\Delta H_T^0}{T}$	ΔH_T^0	$-\Delta\left(\frac{F^0 - H_0^0}{T}\right)$	$\frac{\Delta H_0^0}{T}$	ΔH_0^0 (kcal.)
1248	35.420	79.030	98.6	40.294	83.904	104.7
1304	35.034	75.209	98.1	40.106	80.281	104.7
1327	34.865	73.536	97.6	40.023	78.694	104.4
1356	34.651	71.551	97.0	39.918	76.818	104.2
1364	34.592	70.834	96.6	39.889	76.131	103.8
1372	34.533	70.217	96.3	39.860	75.544	103.6
1390	34.400	69.185	96.2	39.794	74.579	103.7
1398	34.341	68.758	96.1	39.765	74.182	103.7
1447	33.991	65.567	94.9	39.573	71.149	103.0
1448	33.984	65.615	95.0	39.569	71.200	103.1
1467	33.848	64.481	94.6	39.494	70.127	102.9
1485	33.720	63.617	94.5	39.423	69.320	102.9
1534	33.379	61.338	94.1	39.220	67.179	103.1

This was verified by monitoring the ^6Li and ^7Li peaks as well as the $^7Li_2{}^{16}O$ and $^7Li^6Li^{16}O$ peaks. The mass 28 peak could not be used due to the high background of carbon monoxide.

Absolute pressures of LiO were then determined from the observed ion currents of $^6Li^{16}O^+$ and combined with the free energy functions to yield the values of ΔH_0^0 in Table V. The average value, $\Delta H_0^0 = 24.1$ kcal. mole^{-1}, combined with the dissociation energy of oxygen, $\Delta H_0^0 = 118.0$ kcal. mole^{-1}, yielded the value $D_0^0(LiO) = 3.6$ e.v. for the dissociation energy of the LiO gaseous molecule. This is in qualitative agreement with the slope value $D_0^0(Li_2O) = 7.0$ e.v. or the 3rd law value $D_0^0(Li_2O) = 6.5$ e.v. since it is to be expected that the addition of one lithium atom to oxygen will release slightly more energy than the addition of a second lithium atom. The $D_0^0(LiO)$ obtained must be considered only an upper limit, since the LiO^+ was all assumed to be produced by simple ionization of the LiO molecule. The appearance potential of LiO (9.0 e.v.) is considerably higher than that of Li_2O^+ (6.8 e.v.). If the observed LiO^+ were produced by fragmentation of the Li_2O molecule, this value would indicate that the ionization potential of the LiO molecule is about 5.5–6.0 e.v. (assuming that ΔE for the reaction $Li_2O \rightarrow LiO + Li$ is about 3–3.5 e.v., *i.e.*, slightly less than one-half the atomization energy of Li_2O).

TABLE V

STATISTICAL HEAT OF REACTION FOR $LiO(g) = Li(g) + \frac{1}{2}O_2(g)$

T (°K.)	$-R \ln K_{eq}$	$-\Delta\left(\frac{F^0 - H_0^0}{T}\right)$	$\frac{\Delta H_0^0}{T}$	ΔH_0^0 (kcal.)
1346	7.00	11.54	18.54	24.9
1351	5.81	11.54	17.35	23.4
1390	5.54	11.55	17.09	23.8
1400	5.58	11.55	17.13	24.0
1444	5.22	11.58	16.80	24.3
1470	4.76	11.60	16.36	24.1

If the LiO^+ were produced by fragmentation of Li_2O, the absence of an ion intensity of LiO^+ below 9.0 e.v. enables one to estimate the maximum partial pressure of LiO that would evade detection. This partial pressure, about one-thirtieth of that shown in Table VI, would imply that $D_0(LiO)$ is less than 3.2 e.v. Since the atomization energy of Li_2O is about 7.0 e.v., this implies that the addition of a second Li atom releases more energy than the first, which is unlikely. For the above reasons it appears quite probable that the observed LiO^+ ion is a parent ion and that the value obtained for the dissociation energy of LiO is correct.

TABLE VI

COMPOSITION OF THE VAPOR AT 1400°K.

Species	P (atm.)	Mole % of vapor
Li	2.36×10^{-7}	72.2
O_2	5.89×10^{-8}	18.0
Li_2O	3.10×10^{-8}	9.5
LiO	9.5×10^{-10}	0.3

TABLE VII

HEATS OF VARIOUS REACTIONS IN THE Li–O SYSTEM*

Reaction	ΔH_T^0 (kcal.)	Method
$Li_2O(s) = Li_2O(g)$	$\Delta H_{1400}^0 = +108.3$	Exptl. slope
	$\Delta H_0^0 = +115.9$	Exptl. slope
	$\Delta H_{1400}^0 = +96.1$	Exptl. 3rd law
	$\Delta H_0^0 = +103.7$	Exptl. 3rd law
$Li_2O(s) = 2Li(g) + \frac{1}{2}O_2(g)$	$\Delta H_{298}^0 = +219.3$	Available thermodynamic data
	$\Delta H_{1400}^0 = +214.6$	Available thermodynamic data
$Li_2O(g) = 2Li(g) + O(g)$	$\Delta H_0^0 = +161.7$	Available data and slope ΔH_{sub}^0
	$\Delta H_0^0 = +173.9$	Available data and 3rd law ΔH_{sub}^0
$LiO(g) = Li(g) + \frac{1}{2}O_2(g)$	$\Delta H_0^0 = +24.1$	Experimental 3rd law
$LiO(g) = Li(g) + O(g)$	$\Delta H_0^0 = +83.1$	Available data and 3rd law ΔH

* NOTE ADDED IN PROOF.—Since this paper was submitted for publication, some experimental data on the structure of the Li_2O molecule have become available. Electron diffraction studies by P. A. Akishin and N. G. Rambidi (*Doklady Akad. Nauk S. S. S. R.*, **118**, 973 (1958)) yield the value r(Li–O) = 1.82 Å. and angle 110° for Li–O–Li. The use of these values in the calculation of thermodynamic functions results in an increase of S by 1.156 e.u. for LiO(g) and by 1.701 e.u. for $Li_2O(g)$. The correct thermodynamic functions, together with the absolute pressure data, give these corrected results:

$Li_2O(s) = Li_2O(g)$	$\Delta H^0{}_{1400} = +98.5$ kcal.
	$\Delta H_0^0 = +106.1$ kcal.
$Li_2O(g) = 2Li(g) + O(g)$	$\Delta H_0^0 = +171.5$ kcal.
$LiO(g) = Li(g) + 1/2O_2(g)$	$\Delta H_0^0 = +22.5$ kcal.
$LiO(g) = Li(g) + O(g)$	$\Delta H_0^0 = +81.5$ kcal.

Discussion

The saturated vapor in equilibrium with solid Li_2O contains gaseous Li, O_2 and Li_2O in comparable amounts with LiO as a minor constituent. The composition of the vapor at 1400°K. is shown in Table IV. In addition to the previous results, calculations using the limited data available for the LiONa (mass 46) peak show that $\Delta F_{1400}^0 = -5.2$ kcal./mole^{-1} for the reaction Na(g) + Li_2O(g) = LiONa(g) + Li(g). The existence of detectable amounts of gaseous Na_2O molecules over solid sodium oxide is thus suggested.

The heats of various reactions are given in Table VII. In order to see what effect the shape of the molecule has on the third law heats of reaction involving this molecule, a recalculation of the entropy at 1400°K. was made assuming a linear model, but with the same bond constants. The resulting third law entropy for the linear model was 66.82 e.u., compared with 71.35 e.u. for the bent model. At 1400°K., the difference in ΔH would be $T\Delta S$ or 6.34 kcal. mole^{-1}. Closer agreement between the slope and third law values of the heats is obtained using thermodynamic quantities calculated for a bent model. This is to be expected since both covalent and ionic[15] models predict a bent form for the Li_2O molecule. In the case of the ionic model this bent form is a result of the large polarizability of the oxygen ion and the high polarizing power of the lithium ion. The large amount of polarization in this molecule can also be considered as a large covalent contribution to the bond.

The third law heats are considered more reliable since the slope of the log P *vs.* $1/T$ curve could easily be too high if temperature gradients exist in the Knudsen cell.

(15) F. Hund, *Z. Physik*, **32**, 1 (1925).

SURFACE CHEMICAL PROPERTIES IN AQUEOUS SOLUTIONS OF NON-IONIC SURFACTANTS: OCTYL GLYCOL ETHER, α-OCTYL GLYCERYL ETHER AND OCTYL GLUCOSIDE

BY KŌZŌ SHINODA, TERUKO YAMANAKA AND KYOJI KINOSHITA

Department of Chemistry, Faculty of Engineering, Yokohama National University, Minamiku, Yokohama, Japan

Received June 30, 1958

The surface tension, critical micelle concentration (c.m.c.), surface excess, foaminess and foam stability of aqueous solutions of octanol, octyl glycol ether, octyl glyceryl ether and octyl glucoside have been determined. The surface activity and/or c.m.c. values of non-ionic surfactants, containing the octyl group as the hydrocarbon chain, are similar to those of ionic surfactants containing the undecyl or dodecyl group as the hydrocarbon chain. As the foaminess and foam stability of the compounds in the series improved markedly with the increase in the size of the hydrophilic moiety, these properties are probably dependent upon the hydrophilic–lyophilic balance of the molecule.

Introduction

In spite of the industrial importance of non-ionic surface active agents, few reports[1-3] concerning the surface chemical properties of the pure materials have been published, probably because the pure compounds are difficult to obtain; both the synthesis of pure polyoxyethylene alkyl ethers and the purification of commercial non-ionic surfactants are troublesome.

We have investigated the surface chemical properties of a series of octyl polyol ethers to determine the effect of differences in the hydrophilic group. The relatively short hydrocarbon chain, C_8, was chosen as the hydrophobic group because (1) the c.m.c. values of these non-ionic surfactants are close to those of ionic surfactants containing the dodecyl group; (2) with C_8 as the hydrocarbon chain, the hydrophilic–lyophilic balance changes considerably with an increase in the number of oxygen atoms from 1 to 6; and (3) the synthesis, purification and measurements of longer chain compounds are more difficult.

(1) C. R. Bury and J. Browning, *Trans. Faraday Soc.*, **49**, 209 (1953).

(2) T. Nakagawa, *et al.*, *J. Chem. Soc. Japan*, **77**, 1563 (1956); **79**, 345, 348 (1958)(in Japanese).

(3) L. M. Kushner, W. D. Hubbard and A. S. Doan, THIS JOURNAL, **61**, 371 (1957).

Experimental

Materials.—Octanol obtained from the Kaō Soap Co. Ltd. was purified by fractional distillation through a 100 cm. column to give a product boiling at 96° (16 mm.).

Octyl glycol ether, synthesized[4] from octyl bromide (b.p. 94–95° at 20 mm.), and ethylene glycol (b.p. 116° at 40 mm.), was purified by fractional distillation through a 60 cm. column, b.p. 132° (21 mm.); $n^{20}D$ 1.4355, $n^{30}D$ 1.4357.[4] α-Octyl glyceryl ether prepared[5] from glycerol α-monochlorohydrin (b.p. 125–130° at 21 mm.) and sodium octylate, was purified by distillation, b.p. 132–133° (0.5 mm.); d^{20} 0.9614; $n^{20}D$ 1.4517.

β-D-Octyl Glucoside.—Glucose was acetylated to give β-pentaacetyl glucose (m.p. 127.5–128.5°) which upon bromination yielded acetobromoglucose, m.p. 87–88°. This bromo compound reacted with octanol in the presence of silver oxide to give β-tetraacetyl octyl glucoside[6,7] (m.p. 61.5–62.5°), which was deacetylated in sodium methylate solution in 24 hours at 10–20° to yield β-octyl glucoside; m.p. 63.8–65° (62–65°,[7] 65–99°[6]); $[\alpha]^{20}D$ −33.8° in 4% aqueous solution ($[\alpha]^{20}D$ −34°).[7] Careful purification, drying and crystallization were indispensable in the synthesis of this compound.

Procedures.—Surface tension was measured by the drop weight method, with a tip 0.249 cm. in diameter, in an air thermostat at 25 ± 0.2°. There was no appreciable change of surface tension with time within two minutes after the

(4) F. C. Cooper and M. W. Partridge, *J. Chem. Soc.*, 459 (1950).

(5) G. G. Davies and W. M. Owens, *ibid.*, **132**, 2542 (1930).

(6) C. R. Noller and W. C. Rockwell, *J. Am. Chem. Soc.*, **60**, 2076 (1938).

(7) W. W. Pigman and N. K. Richtmyer, *ibid.*, **64**, 369 (1942).

TABLE I

Surfactant	C.m.c., mole/l.	Solubility (mole/l.)	Surface excess (mole × 10^{-10})	Area per molecule (Å.²)
R_8OH	...	0.0038	5.6	30
$R_8OCH_2CH_2OH$	0.0049	.0075	5.2	32
$R_8OCH_2CHOHCH_2OH$	.0058	.012	5.2	32
R_8OCH–$(CHOH)_5$	.025	.1+	4.0	41
$R_8NC_5H_5Cl$	.23[a]	...	4.9[a]	34[a]
$R_{12}OSO_3Na$	.0081[b]	...	4.0[c]	33,[b] 40[c]
$R_{12}O(CH_2CH_2O)_{5.8}H$	.00025[d]	.0013+	4.9[d]	34[d]

[a] Ref. 1. [b] Ref. 11. [c] Ref. 12. [d] Ref. 2.

formation of droplets. The correction of Harkins and Brown[8] was applied.

The foaming properties of a given surfactant are characterized by at least two parameters; one is the foaminess and the other the foam stability.[9] The foaminess was measured by the procedure described previously.[10] The foam stability was expressed as the time required for the foam height to decrease to one-half of the initial height in a closed test-tube.

Results

The surface tension–log concentration curves are shown in Fig. 1. For the sake of comparison, the data for polyoxyethylene dodecyl ether[2] and sodium dodecyl sulfate[11] were included. The value of octyl glucoside obtained by Bury and Browning[1] is in excellent agreement with our value. The inflections in the curves correspond to the c.m.c. values (or the maximum concentration of molecular dispersion) of non-ionic surfactants. Because the activity of solute is constant over the flat portion of the surface tension–concentration curve for a two component system, the concentration of molecularly dispersed solute stays approximately constant over the flat portion, provided the solution is dilute. The c.m.c. values thus obtained from Fig. 1 are given in Table I. The flat portions of the surface tension–log concentration curves increased remarkably with the size of the hydrophilic group, *i.e.*, the larger the hydrophilic group, the larger the ratio of solubility to c.m.c. This flat portion (micellar region) is very significant, since surfactants, which do not show this phenomenon, possess little solubilizing power, detergent action, etc. Table I gives the c.m.c., surface excess and residual area per molecule estimated from the data in Fig. 1 under the assumption that $\partial \ln a/\partial \ln c = 1$. The values for octylpyridinium chloride[1] were included for comparison. The solubility was obtained from the turbidity change. The surface tension measurements were extended to the emulsified solution in some cases in order to obtain a clearer flat portion.

Foaminess and foam stability are plotted as functions of the concentration in Fig. 2. The foaminess of octanol (30 seconds after shaking) was zero over the concentration range examined. The arrows indicate the c.m.c. values. It is evident that there is a close relation among foaminess, foam stability, c.m.c. and hydrophilic–lyophilic balance.

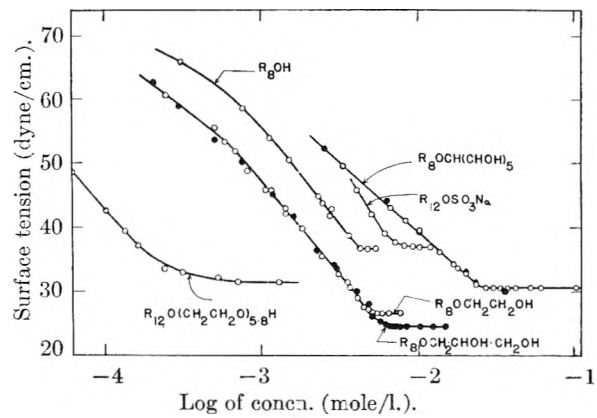

Fig. 1.—The surface tension–log concentration curves of octanol, octyl glycol ether, α-octyl glyceryl ether and octyl glucoside.

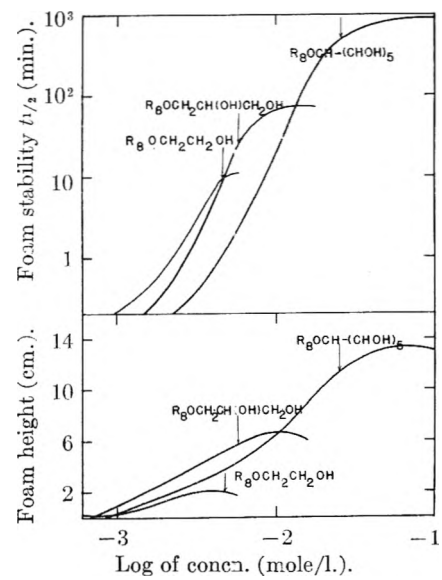

Fig. 2.—The foaminess and foam stability as a function of the log concentration of octyl glycol ether, octyl glyceryl ether and octyl glucoside. Arrows indicate the c.m.c.

Discussion

(1) The c.m.c. values of the ionic surfactants, potassium octanoate and octylpyridinium chloride,[1] are, respectively, 0.2 and 0.23 mole/l.; whereas those of non-ionic polyol ethers containing the same hydrocarbon chain are of the order of 0.005–0.025 mole/l., *i.e.*, the c.m.c. values of ionic surfactants are 10–40 times larger than those of non-ionic surfactants. Accordingly, the electrical repulsion of an ionic surfactant, to which no salt has been added, is about 2.3–3.7kT.[13,14] This value

(8) W. D. Harkins and F. E. Brown, *J. Am. Chem. Soc.*, **41**, 519 (1919).

(9) W. M. Sawyer and F. M. Fowkes, THIS JOURNAL, **62**, 159 (1958).

(10) M. Nakagaki and K. Shinoda, *Bull. Chem. Soc. Japan*, **27**, 367 (1954).

(11) G. Nilsson, THIS JOURNAL, **61**, 1135 (1957).

(12) A. Wilson, M. B. Epstein and J. Ross, *J. Coll. Sci.*, **12**, 345 (1957).

is in good agreement with the $2.9kT$ estimated by another approach.[15]

(2) The c.m.c. values of sodium dodecyl sulfate and sulfonate, 0.0081 and 0.0095 mole/l., are close to those of non-ionic surfactants containing a C_8 hydrocarbon chain. Thus, the surface activity of non-ionic surfactants with octyl as the hydrophobic group is similar to that of ionic surfactants with dodecyl as the hydrophobic group, provided that the hydrophilic groups of the non-ionic surfactants are not very large.

(3) The c.m.c. value of octyl glucoside (0.025 mole/l.) is about 100 times larger than that of polyoxyethylene dodecyl ether (0.00025 mole/l.), although the hydrophilic groups are nearly the same size. Therefore, the energy required to transfer one methylene group from a hydrocarbon medium to water is estimated as about $1.15kT$.[13]

(4) Figure 2 shows that foaminess and foam stability increase remarkably with the size of the hydrophilic moiety of the molecule; for example, the foam stability of octyl glucoside is about 100 times greater than that of octyl glycol. The so-called hydrophilic–lyophilic balance seems to bear a close relationship to these properties.

(5) The surface tension–log concentration curves of pure surfactants exhibit sharp inflections, while the commercial surfactants in many cases exhibit a gradual decrease in surface tension over a large concentration range. $R_{12}O(CH_2CH_2O)_{5.3}H$,[2] which was purified by molecular distillation, shows no sharp inflection, a finding which suggests that the surface tension measurements were affected by time or that the material was impure.

We wish to thank Mr. S. Hirota for the synthesis of octyl glycol ether, and Mr. S. Hayashi and Mr. S. Tamba for carrying out preliminary experiments.

(13) K. Shinoda, *Bull. Chem. Soc. Japan*, **26**, 101 (1953).

(14) J. Th. G. Overbeek and D. Stigter, *Rec. trav. chim.*, **75**, 1263 (1956).

(15) K. Shinoda, THIS JOURNAL, **60**, 1439 (1956).

A STUDY ON MICELLE FORMATION IN COLLOIDAL ELECTROLYTE SOLUTIONS

BY C. BOTRÉ, V. L. CRESCENZI AND A. MELE

Laboratorio Ricerche sulla Struttura e l'Attività di Composti chimici, Istituto di Chimica Farmaceutica, Università, Roma, Italy

Received July 10, 1958

Membrane electrodes of both negative and positive type have been used to determine the activity of counterions in aqueous solutions of cationic and anionic detergents. The method has been found to be a useful tool to determine the critical concentration for micelle formation. An evaluation of the degree of association between micelles and counterions from the experimental activity coefficients has indicated that the strong electrostatic field of the charged micelles tends to bind a large fraction of counterions. A simple treatment of soap micelles as polymeric electrolytes has been considered.

Introduction

Results of several investigations on colloidal electrolytes have shown that the properties of aqueous solutions of this class of compounds, of which detergents are typical examples, exhibit a more or less abrupt change at a critical value of the concentration. This value marks almost a transition from the ideal behavior to the markedly abnormal behavior observed at low and high concentration, respectively. A process of formation of aggregates is the accepted explanation for the existence of a critical concentration.

It is generally agreed that amphiphilic molecules arrange themselves to build a micelle so that the hydrocarbon chains orient themselves away from the water while their polar groups are distributed on the surface.[1–3] The aggregation of single molecules containing polar groups to form micelles, obviously causes a new situation regarding the distribution of their counterions in solution. The ionic heads forming a charged layer on the external surface of the micelles may be expected to exert a high electrostatic field in the neighborhood of the micelles, and therefore to affect the distribution of the counterions around them. The consequent interaction between micelles and counterions leads to the lowering of the free charges of the former because of an extensive binding of counterions. This fact may offer a very significant contribution to the growth and stability of the micelles.

In our opinion, useful information about the complex phenomena of micelle formation in ionic detergent solutions might be gathered from a detailed knowledge of the above effects, as may be inferred, for instance, from a study on the activity of counterions in these solutions.

The present work reports some data on the activity coefficients of three typical ionic detergents, *i.e.*, sodium lauryl sulfate, sodium laurate and laurylamine hydrochloride. The activity of counterions has been determined by means of membrane electrodes both of negative and positive type, and the investigation has been extended to a wide range of detergent concentrations. An attempt to treat theoretically micelles as polymeric electrolytes also will be reported.

Experimental

Material.—Sodium lauryl sulfate (NaLS) was prepared following a procedure described by Dreger.[4] The product

(1) G. S. Hartley, "Aqueous Solutions of Paraffin Chain Salts," Actualités Scientifiques et Industrielles n° 387, Herman et Cie., Paris 1936; *Kolloid Z.*, **38**, 22 (1939).

(2) J. W. McBain, "Colloid Science," D. C. Heath and Co., Boston, Mass., 1950.

(3) P. Debye and E. W. Anacker, THIS JOURNAL, **55**, 644 (1951).

(4) E. E. Dreger, G. I. Keim, G. A. Miles, L. Shedlovsky and J. Ross, *Ind. Eng. Chem.*, **36**, 610 (1944).

was purified by repeated crystallization from ethyl alcohol and extraction with ether for 36 hours. Sodium laurate (NaL) was obtained by neutralizing pure grade lauric acid with standardized sodium hydroxide.

Laurylamine hydrochloride (LAH) was obtained by dissolving laurylamine (pure grade) in ethyl alcohol and adding concentrated HCl. Precipitation of the product occurred on standing. The crystalline material thus obtained was purified by several crystallizations from ethyl alcohol.

Membrane Potential Determinations. Apparatus.—Figure 1 shows schematically the apparatus for the potentiometric titrations, which is basically the same as that used in a previous investigation.[5]

The agar bridges of the usual type employed in our previous work were replaced by mixed agar–liquid bridges as shown in Fig. 1. It was found, in fact, that precipitation of the detergent occurred at the tip of the agar bridges, causing an interruption of the electrical circuit.

Cation selective membranes were prepared according to the procedure already described.[5] Anion selective membranes, A-10 Permaplex, were supplied by United Water Softener Ltd., London. The standardization of the membranes was performed always before their use, by titrating a standard NaCl solution against the same NaCl solution. The results of these titrations confirmed their high selectivity. The slopes of the straight lines obtained by plotting the e.m.f. *versus* the logarithm of the activity, according to Nernst's equation, were found to be 56–57 mv. for negative membranes and 53–54 mv. for positive membranes.

Procedure.—A solution of detergent was placed into one half cell and a standard solution of NaCl into the other (see Fig. 1). The membrane potential determinations were carried out either by diluting stepwise a concentrated solution of detergent with water or *vice versa* by concentrating a diluted solution of detergent. Readings of the potentials were recorded at each step. The activity of counterions was calculated from Nernst's equation at each concentration of detergent and has been expressed as $\gamma_+ = a_+/c$ for anionic detergent and $\gamma_- = a_-/c$ for cationic detergent.

Conductivity Measurements.—A Philips a.c. bridge was used. A stock solution of detergent contained in a 100-ml. cell was diluted progressively with water and readings were taken at each stage.

The values of the c.m.c. were obtained by plotting in each case the specific conductivity against the square root of the concentration.[6]

Results and Discussion

Determination of the C.m.c.—In Fig. 2 typical plots of the activity coefficients of Na^+ ions against the molar concentration of NaLS are reported. The upper curve is relative to NaLS in the absence of extraneous ions, and the lower curve to NaLS in the presence of added NaCl (0.02 *M*).

In Fig. 3 analogous plots are shown for NaL and for LAH. As may be seen from the curves reported, a rather sharp break occurs for all the compounds at a certain concentration of detergent. These breaks have been identified with the critical micelle concentration in each case. The values of the c.m.c.

TABLE I

Compd.	Conductivity: Our results	Conductivity: Lit.	Dye[d]	Membrane potential
NaL	0.032	0.034[a]	0.024	0.035
NaLS	.008	.008[b]	.0061	.008
LAH	.014	.0138[c]	.0131	.014

[a] E. Gonick, *J. Am. Chem. Soc.*, 67, 1191 (1945). [b] Reference 6. [c] A. W. Ralston and C. W. Hoerr, *J. Am. Chem. Soc.*, 64, 772 (1942). [d] W. D. Harkins "The Physical Chemistry of Surface Films," Reinhold Publ. Corp., New York, N. Y., 1957, p. 304.

(5) C. Botré, V. L. Crescenzi and A. Mele, "Proc. International Symposium Coordination Compounds, Rome 1957," suppl. *Ricerca Sci.*, **28**, 369 (1958).

(6) R. J. Williams, J. N. Phillips and K. J. Mysels, *Trans. Faraday Soc.*, **51**, 728 (1955).

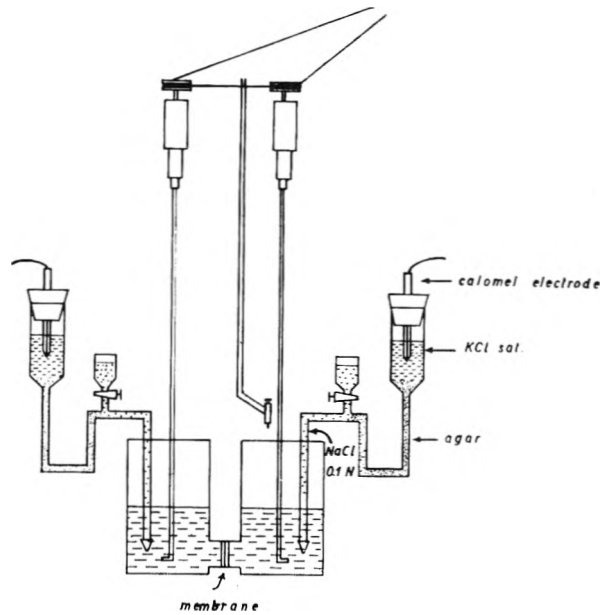

Fig. 1.—Apparatus.

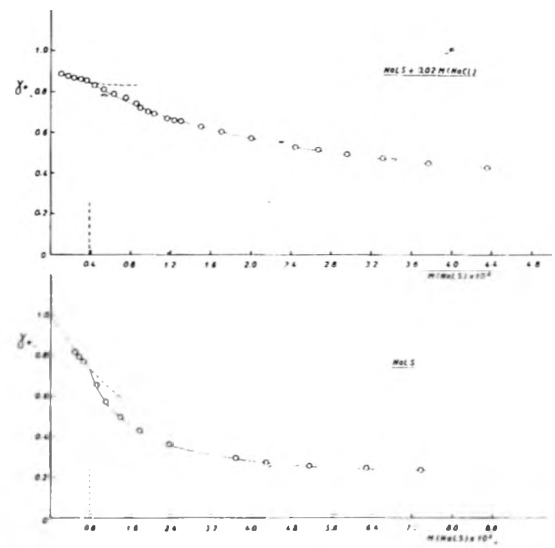

Fig. 2.—Experimental activity coefficient γ_{ex} as a function of the molarity of sodium lauryl sulfate (NaLS).

interpolated from the curves of Figs. 2 and 3, are reported in the fourth column of Table I.

From these results it appears that membrane electrodes may offer a new useful technique to determine the c.m.c. in detergent solutions. A qualitative approach to this method was outlined by Kolthoff, *et al.*,[7] some years ago, but to the best of our knowledge no further work has been carried out along this line.

As mentioned in the experimental part, the membrane potential determinations were carried out following two alternative procedures. While the two methods have provided equivalent results regarding the values of the c.m.c., the general trend of the γ-concentration curves below the c.m.c. was found to be dependent markedly upon the procedure followed. Lower values of the activity coefficients were obtained by using the dilution method.

(7) C. W. Carr, W. F. Johnson and I. M. Kolthoff, THIS JOURNAL, **52**, 636 (1948).

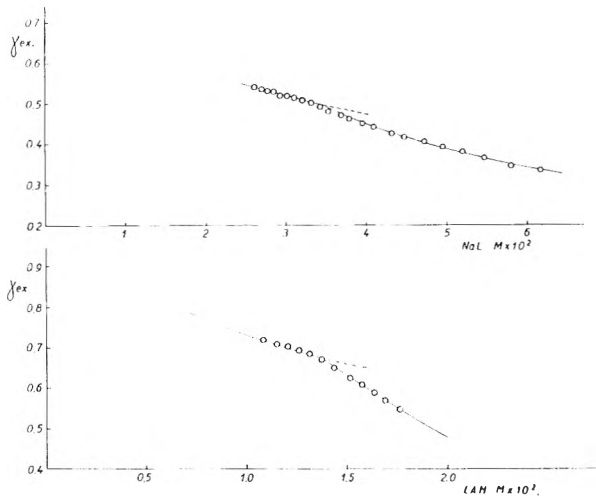

Fig. 3.—Experimental activity coefficient γ_{ex} as a function of the molarity of sodium laurate (NaL) and laurylamine hydrochloride (LAH).

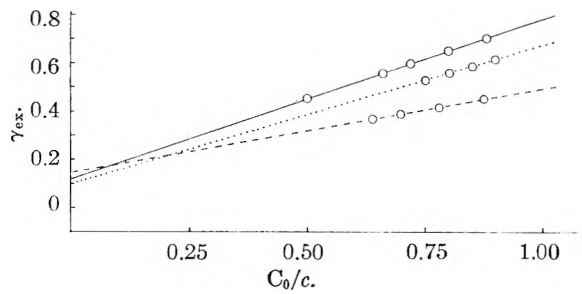

Fig. 4.—Experimental activity coefficient γ_{ex} as a function of C_0/C according equation 2: ———, sodium lauryl sulfate (NaLS); – – –, sodium laurate (NaL); . . . . laurylamine hydrochloride (LAH).

Thus far, no satisfactory explanation may be adduced. False equilibria and formation of small clusters of detergent molecules may account for this peculiar effect. These hypotheses can only be convalidated by a further and more careful study.

Binding of Counterions in Micelle Solutions.—With regard to the change of the activity coefficient with concentration, it may be observed that below the c.m.c. the behavior of detergent molecules is not very different from that typical of uni-univalent electrolytes. The departure from the behavior which might be predicted by direct application of the Debye–Hückel theory can be ascribed to the tendency of detergent molecules to give small aggregates below the c.m.c. Actually in the case of sodium lauryl sulfate, dimerization is claimed to occur up to 50% at the critical micelle concentration[8]; perhaps for sodium laurate and laurylamine hydrochloride the situation is similar.

Immediately above the c.m.c., the γ-concentration curves show a steep decrease which is clearly consistent with the assumed nature of the micelles in solution. The high charge density on the surface of micelles exerts a strong electric field on the counterions, which therefore are attracted strongly.

Using our experimental data, we have made an attempt to evaluate the extent of the binding of counterions by micelles. For this purpose we have assumed, in agreement with generally accepted views, that above the c.m.c. any addition of detergent merely increases the number of micelles. Both the concentration of monomers and the number of monomers per micelle are considered constant.

With these conditions and by formal separation of the contribution of the unmicellized and micellized molecules, the experimental activity of counterions may be expressed as

$$a = \gamma(C_0 + \alpha C_m) \qquad (1)$$

where

C_0 = c.m.c.
$C_m = \dfrac{C - C_0}{n}$ = micelle concn.
α = degree of dissociation of micelles
γ = activity coefficient of counterions
n = number of monomers
C = concn. of detergent

It follows from (1) that the experimental value of the activity coefficient is

$$\gamma_{ex} = \alpha\gamma + \gamma[C_0/C(1 - \alpha)] \qquad (2)$$

In Fig. 4 a plot of γ_{ex} against C_0/C is shown for the three detergents studied. In each case, a linear relationship is obtained indicating that both γ and α may be considered practically constant in the range of concentration investigated. By extrapolating $C_0/C = 0$, the values of $\alpha\gamma$ have been obtained (see first column of Table II), and in turn assuming γ to be equal to the experimental value at the critical micelle concentration (second column of Table II) approximate values of α have been calculated for each case (third column of Table II).

From the number n of monomers per micelle and the value of α, the number of charges z, per micelle has been calculated (fourth column of Table II). In the last column of the same table, the values of the degree of dissociation α evaluated from the data given in the literature (light scattering and electrophoresis) also are shown.

TABLE II

Compd.	$\alpha\gamma$	γ at c.m.c.	α	n	z[c]	α, lit.
NaLS	0.124	0.76	0.16	80[a]	13	0.18[a]
NaL	.16	.51	.31	..	..	..
LAH	.10	.67	.15	133[b]	20	0.11[b]

[a] J. N. Phillips and K. J. Mysels, THIS JOURNAL, 59, 325 (1955). [b] M. E. McBain and E. Hutchinson, "Solubilization," Academic Press, Inc., New York, N. Y., pp. 232–235. [c] $z = \alpha n$.

The agreement is very satisfactory, particularly in view of the approximations in the above treatment and of the many restrictive hypotheses made in order to estimate the z values from light scattering and electrophoresis.

The high binding properties toward their own counterions and the practical invariance of the degree of binding shown by micelles in detergent solutions has been suggested to compare micelles with polymeric electrolytes. It is apparent from the results of this investigation that micelles and the coiled macroions which are present in solution of polyelectrolytes, show many common features. Micelles, in fact, may be considered as spheres with a charge distribution on the surface, comparable in size and shape—though to a smaller degree—with coiled polyelectrolytes.

(8) P. Mukerjee, Abstracts of the Meeting of the American Chem. Soc., Miami, April, 1957.

A convenient approach to the problem of binding by micelles will be considered here on the basis of a simple theory that has been proved already to be successful when applied to other polyelectrolytes.[9]

For this purpose, a simplified picture of micelle solutions was assumed. Micelles were considered as spheres covered with n ionizable groups (n = number of monomers per micelle) of radius a corresponding to the hydrocarbon chain length of the monomers. The monomers present in solution at a practically constant concentration (c.m.c.) were assumed to play the role of "added salt." Both radius and number of ionizable groups per micelle were considered independent of micelle concentration. Therefore, an evaluation of the binding of counterions by micelles has been made by means of the relation

$$\ln \frac{1-\alpha}{\alpha + mk'\phi} = \ln \frac{\phi}{1-\phi} + \alpha p(1-\phi^{1/3}) \quad (3)$$

proposed by Oosawa for spherical polyelectrolytes,[10] where m is the number of added ions. The parameter p is related to the charge n on the spherical ion and its dimension a according to e is the

$$p = \frac{ne^2}{DkTa} \quad (4)$$

charge, D the dielectric constant and k and T have the usual meaning. ϕ is the volume fraction of the micelles and it is proportional to the micelle concentration according to

$$\phi \frac{4}{3} \pi a^3 \frac{N}{V} C_m = \frac{C_m}{k'} \quad (5)$$

N = Avogadro number
V = total volume
a and n have the meaning as in (4)

Equation (3) has been applied to NaLS, a compound of well defined properties and structure.

Values of α have been calculated for NaLS in the absence of extraneous ions (m = c.m.c.) and for NaLS in the presence of NaCl 0.02 M (m = c.m.c. + 0.02). The parameters introduced in (3) are listed in Table III and the linear plots obtained are shown in Fig. 5.

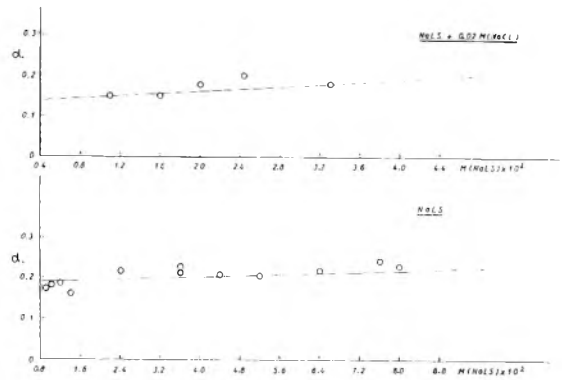

Fig. 5.—Degree of dissociation α *versus* the molarity of sodium lauryl sulfate as calculated according to equation 3. The points represent the values of α from the γ_{ez}'s.

TABLE III

Compd.	a, Å.	n	$m^c \times 10^2$	p
NaLS[a]	18.5	80	0.80	32.0
NaLS–NaCl, 0.02 M[b]	21.0	94	2.39	33.1

[a] J. N. Phillips and W. J. Mysels, THIS JOURNAL, 59, 325 (1955). [b] D. Stigter and W. J. Mysels, *ibid.*, 59, 45 (1955). [c] m in the absence of added NaCl is assumed equal to the concentration of detergent at the c.m.c.

The points on the curves represent the value of α as obtained according to relation 2 from the experimental data. The agreement between theory and experiments is quite satisfactory; furthermore, the effect due to the addition of NaCl on the degree of dissociation is correctly verified by the theory.

Acknowledgments.—The authors are greatly indebted to Prof. A. M. Liquori for helpful suggestions and stimulating discussions. This work was sponsored and financially supported by Colgate-Palmolive Company, New York, which is gratefully acknowledged.

(9) F. Ascoli, C. Botré, V. L. Crescenzi, A. M. Liquori and A. Mele, to be published.

(10) F. Oosawa *J. Polymer Sci.*, **23**, 421 (1957).

A MODEL OF ACTIVE CARBON[1]

BY W. F. WOLFF

Research Department, Standard Oil Company (Indiana), Whiting, Indiana

Received July 14, 1958

A model for the structure of active carbon and a mechanism for the formation of such a structure is proposed. According to this view, the micropore structure of conventional active carbons is formed by a random oxidative attack on individual graphitic planes. A mathematical treatment based on this model defines a structure consistent with the available experimental data.

Introduction

Two steps common to the preparation of active carbons are carbonization and activation.[2] In the first step, organic matter is pyrolyzed to give a carbonaceous residue, or "char." In the activation step, a gaseous oxidant is commonly used to develop a pore structure in the char. Carbons used for gas adsorption are activated by steam through the endothermic water-gas reaction.

Gas-adsorbent carbons apparently have a layer structure,[3] with a micropore system consisting of molecular-size fissures[4] developed during the activation step. Typically, about half of the carbon is consumed during this step. The size and

(1) Presented in part before the Division of Physical and Inorganic Chemistry at the 133rd meeting of the American Chemical Society, San Francisco, California, April, 1958.

(2) J. J. Kipling, *Quart. Revs.*, **10**, 1 (1956).

(3) P. H. Emmett, *Chem. Revs.*, **43**, 69 (1948).

(4) W. F. Wolff, THIS JOURNAL, **62**, 829 (1958).

shape of these pores, and the amount of carbon consumed, suggest that they are formed by the burning out of layer segments from stacks of graphitic planes.

This hypothesis has been developed in the form of a general model for the structure of active carbon and a mechanism for the formation of such a structure. Many elements of the model are modifications of previously developed views.[2-6] The assumption that the activating agent randomly attacks the planes allows the model to be treated quantitatively. A mathematical treatment gives relationships between the surface area and density of carbon that can be checked experimentally.

Formation of Active Carbon.—Steam-activated and similar carbons are hypothesized to be formed in the following manner. In the carbonization step, pyrolysis of organic matter leads to the formation of polynuclear aromatic systems similar to, but much smaller than, those found in graphite. These small graphitic-like planes tend to be stacked one on the other[7] to form more or less impervious particles, of which the external surfaces provide the surface area of the char. The planes are bounded by hydrogen, hydrocarbon radicals or other functional groups. Carbonization is completed in the activation step with the removal, cracking or cyclization of the less-stable edge groups. Thus, the complexity of the edge groups is reduced in proportion to the severity of the activation conditions.

The activating agent also attacks the individual planes. Once the oxidation has been initiated at the periphery of any one of them, further attack on the same plane is favored over another initiation step. The oxidation continues until the edge atoms in the attacked plane attain a structure, or structures, that resists oxidation as much as the edge atoms in the unattacked planes. Thus, activation proceeds with the removal of large segments of individual planes. The remaining fissures, only a few ångstroms wide, make up the micropores of the active carbon. Because the initiation step occurs in a random fashion, some micropores with widths corresponding to the removal of two or more adjacent planes are formed. The macropores are not formed during the activation step but are the interstices between graphitic particles; they have dimensions many orders of magnitude greater than the micropores.

Indirect support for the activation mechanism is given by data from other studies. In the oxidation of carbon blacks, the porosity obtained in partially oxidized particles has been attributed to a preferential attack on the edge atoms of graphitic planes.[8]

Studies with graphite crystals[9,10] show that gaseous oxidants preferentially attack the carbon along a graphite plane and leave hexagonal open areas, with visible step-like discontinuities at the edges. These observations support the view that the burning out of graphitic planes is terminated by the formation of a particularly stable configuration of edge atoms or functional groups.

Mathematical Model.—The changes in the carbon structure called for by the preceding hypothesis should be predictable on a probability basis. An attempt has been made to develop a mathematical system capable of predicting them as a function of the degree of activation.

A mathematical model was set up in which the char is considered to be formed of small graphitic cubes equal in size. The size of each cube is determined by the number of planes and the interplanar distance. Activation involves the random removal of entire planes from the cube. Except when planes are removed from the top or bottom of the stack, removal of planes leaves fissures in the cube.

In order to relate the surface areas calculated by this model to experimental values determined by nitrogen adsorption,[11] restrictions must be placed on the surface areas assigned to the fissures. Those formed by the removal of two or more adjacent planes are assigned an internal area equal to the areas of the tops and bottoms of the fissures; those resulting from the removal of a single plane are assigned only half as much area. In this manner, account is taken of the fact that only a single layer of nitrogen molecules can fit into the smallest crevices.

From such a model, the surface area, density, pore-size distribution and similar parameters are obtained as functions of the number of planes removed, and thus of the degree of activation. The density value most readily obtained from the mathematical model corresponds to the density of the regions that contain only micropores and can be defined as the micropore density.

The relations that give the surface area A in square meters per gram and the micropore density d in grams per cubic centimeter as functions of the degree of activation are

$$A = \frac{2618(3 - 2f)}{L(1 - f)} + \frac{1309f(L - fL - 1)(L + fL - 2)}{L(L - 1)(1 - f)} \qquad (I)$$

and

$$d = \frac{d_c[L(1 - f)^2 + (1 - f)]}{(L + 1) - (L + 2)f} \qquad (II)$$

where f is the fraction of the planes removed during activation, L is the number of graphitic layers in an unactivated particle, and d_c is the micropore density of the unactivated char in grams per cubic centimeter. Derivations of these and subsequent equations from the mathematical model are given in the Appendices.

Under the restrictive assumptions that the graphitic particles in the char are very large and have the density of graphite, eqs. I and II reduce to

$$A = 1309f(1 + f) \qquad (III)$$

(5) J. C. Arnell and W. M. Barss, *Can. J. Research*, **26A**, 236 (1948).

(6) J. W. Hassler, "Active Carbon," Chemical Publishing Co., 1951, p. 25.

(7) H. L. Riley, *Quart. Revs.*, **1**, 59 (1947).

(8) W. R. Smith and M. H. Polley, THIS JOURNAL, **60**, 689 (1956).

(9) G. R. Hennig, "Properties of Graphite Compounds," presented at the Second Conference on Carbon, Buffalo N. Y., June, 1955.

(10) G. R. Hennig, "Catalytic Oxidation of Graphite," presented at the Third Biennial Carbon Conference, Buffalo, N. Y., June, 1957.

(11) S. Brunauer, "The Adsorption of Gases and Vapors. Vol. I. Physical Adsorption," Princeton Univ. Press, Princeton, N. J., 1943, pp. 285-299.

TABLE I

SURFACE-AREA AND MICROPORE-DENSITY VALUES

Carbon	Probable carbon source	Ref.	B.E.T. surface area (m.²/g.)	Gas employed in surface area measurement	$1/d$	Method used in computing $1/d$ values
Fineman A	Coconut	12	644	N_2	0.759	[a]
Fineman B	Coconut	12	749	N_2	.762	[a]
Guest B	Coconut	13	792	N_2	.762	[a]
Fineman C	Coconut	12	895	N_2	.848	[a]
Fineman E	Coconut	12	1070	N_2	.907	[a]
Fineman F	Coconut	12	1136	N_2	.977	[a]
Fineman G	Wood	12	1840	N_2	1.525	[a]
Drake, Columbia	Coconut	14	1397	N_2	0.982	[b]
Drake, Darco	(?)	14	560	N_2	.681	[b]
Wiig, PN208	(Coal Char)	15	162	N_2	.714	[b]
Wiig, PN94	Coal	15	404	N_2	.661	[b]
Wiig, PN98	Coal	15	591	N_2	.696	[b]
Wiig, PN102	Coal	15	754	N_2	.745	[b]
Wiig, PN110	Coal	15	1056	N_2	.873	[b]
Wiig, PN112	Coal	15	1105	N_2	.950	[b]
Sargent	Coconut		1035	N_2	.87	[c]
Burrell	Coconut		1143	N_2	1.02	[c]
Fisher	Coconut		1092	N_2	.98	[c]
Wood charcoal	Wood		745	N_2	1.01	[c]
Sucrose	Sucrose		314	N_2	0.61	[c]
HNO_3 Leached	Coconut		1126	N_2	1.03	[c]
Columbia	Coconut		1457	N_2	1.12	[d]
Columbia	Coconut		1430	N_2	1.15	[d]
Pittsburgh	Coal		854	N_2	0.83	[d]
Emmett, CWSN-19	Wood	3	1227	C_6H_6	1.05	[d]
Dubinin, Carbon 1	(?)	16	386	H_2O(?)	0.59	[e]
Dubinin, Carbon 1	(?)	16	547	H_2O(?)	.59	[e]
Everett, 90%	Coconut	17	512	C_6H_6	.67	[f]
Everett, 78%	Coconut	17	551	C_6H_6	.70	[f]
Everett, 44%	Coconut	17	1159	C_6H_6	1.01	[f]
Everett, 19%	Coconut	17	999	C_6H_6	0.93	[f]
Davies A	Nutshell	18	1303	C_6H_6	.99	[f]
Davies B	Nutshell	18	1002	C_6H_6	.87	[f]
Davies C	Nutshell	18	870	C_6H_6	.84	[f]
Davies D	Nutshell	18	677	C_6H_6	.74	[f]
Davies I	Nutshell	18	1418	C_6H_6	1.30	[f]
Davies J	Nutshell	18	936	C_6H_6	.87	[f]
Davies K	Wood	18	1969	C_6H_6	1.53	[f]
Davies E	Coal	18	1237	C_6H_6	1.09	[g]
Davies F	Coal	18	996	C_6H_6	0.92	[g]
Davies G	Coal	18	774	C_6H_6	.80	[g]
Davies H	Coal	18	566	C_6H_6	.70	[g]
Davies L	Lignite	18	635	C_6H_6	1.22	[g]
Davies M	Coal	18	611	C_6H_6	0.70	[g]

[a] $1/d = \frac{1}{\text{apparent density in } H_2O}$ + volume H_2O adsorbed at $P/P_0 = 1$. [b] $1/d = \frac{1}{\text{apparent density in Hg}} - V_{\text{macro}}$. Macropore volume, V_{macro}, determined from volume of mercury forced into pores at known pressures. [c] $1/d \cong 0.44$ + volume N_2 adsorbed at $P/P_0 = 1$. [d] $1/d \cong 0.43$ + volume N_2 adsorbed at $P/P_0 = 1$. [e] $1/d \cong 0.44$ + micropore volume. [f] $1/d \cong 0.44$ + volume C_6H_6 adsorbed at $P/P_0 = 1$. [g] $1/d \cong 0.43$ + volume C_6H_6 adsorbed at $P/P_0 = 1$.

and

$$d = 2.26(1 - f) \qquad \text{(IV)}$$

Under the same restrictions, the calculation of theoretical pore distributions becomes equally simple

$$F_W' = f^{W-1}(1 - f) \qquad \text{(V)}$$

$$A_W = 1309f(1 - f), \text{ for } W = 1 \qquad \text{(VI)}$$

and

$$A_W = 2618f^W(1 - f), \text{ for } W > 1 \qquad \text{(VII)}$$

where F_W' is the fraction of pores formed by the removal of W adjacent planes when a certain fraction f of the total number of planes is removed at ran-

(12) M. N. Fineman, R. M. Guest and R. McIntosh, *Can. J. Research*, **24B**, 109 (1946).

(13) R. M. Guest, R. McIntosh and A. P. Stuart, *ibid.*, **24B**, 124 (1946).

(14) L. C. Drake and H. L. Ritter, *Ind. Eng. Chem., Anal. Ed.*, **17**, 787 (1945).

(15) E. O. Wiig and S. B. Smith, THIS JOURNAL, **55**, 27 (1951).

(16) M. M. Dubinin, *Quart. Revs.*, **9**, 101 (1955).

(17) D. H. Everett and W. I. Whitton, *Proc. Roy. Soc. (London)*, **A230**, 91 (1955).

(18) R. G. Davies, *Chemistry and Industry*, 160 (1952).

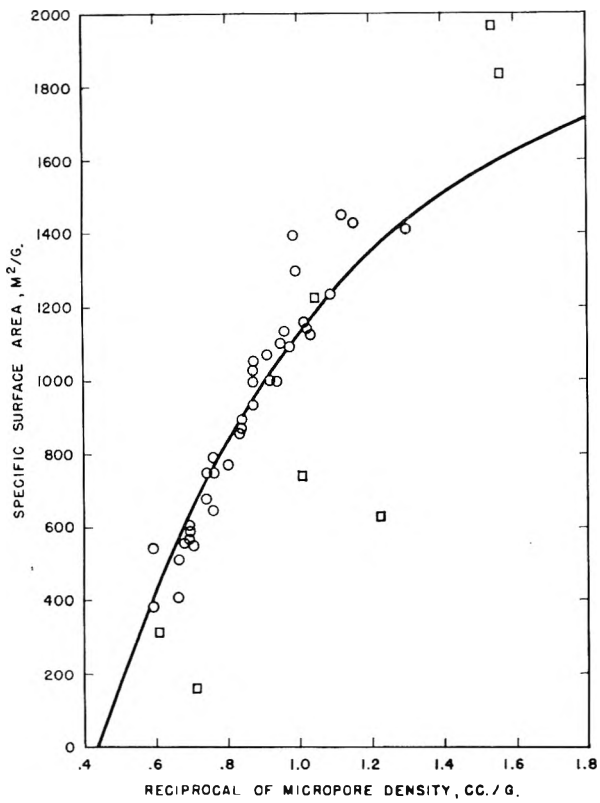

Fig. 1.—$A(d)$ plotted against all available data.

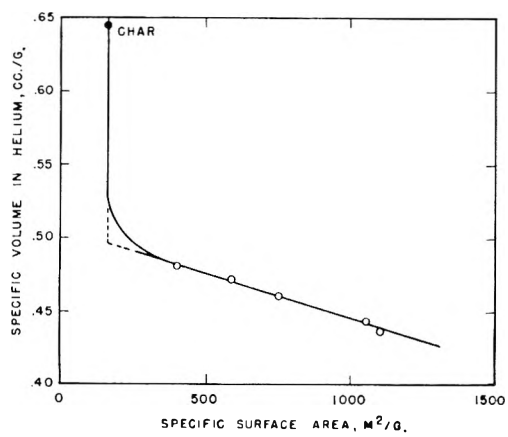

Fig. 2.—Specific volume as a function of surface area in the activation of a coal-based char.

dom; and A_W is the surface area in square meters per gram furnished by any given type of pore. More complicated forms that are not restricted with regard to crystallite size and density are given in Appendix A.

Application of the Model.—To test the validity of the quantitative treatment and thus, indirectly, of the proposed model, an attempt was made to check the agreement of the equations with experimental data. Because of the lack of adequate data on pore distribution, only eq. I through IV can be tested. A general function, $A(d)$, relating surface area to micropore density, obtained by eliminating f between equations III and IV, has been compared with all available experimental values. The less-restricted relationship, $A(d/d_c,L)$, obtained by combining eq. I and II, has been checked with data for a coal-based carbon and a coconut charcoal.

Check of $A(d)$.—To check the function $A(d)$, experimental values for the surface areas and micropore densities of representative carbons were used. All readily available data from which these values could be determined, or estimated, are compiled in Table I; all types of active carbons and chars are included. These data are superimposed on a plot of $A(d)$ in Fig. 1. Values for the active carbons from nutshells and coal are indicated as circles; values for other materials, by squares. The good agreement between experimental and predicted values gives strong support to the proposed mathematical model, despite the approximations made in developing it.

Check of $A(d/d_c,L)$ with a Coal-based Carbon.—To check the validity of these approximations, the more rigorous function, $A(d/d_c,L)$, has been tested with published data for a coal-based char and steam-activated carbons prepared from this char.[15] In order to use the function, two properties of the char must be determined. One is the density d_c of the graphitic regions. The other is the average number L of graphitic planes in a stack.

The value of d_c can be calculated from data given for the apparent densities of the carbons measured in helium. The reciprocals of these densities—the specific volumes in helium—for the char and the active carbons are plotted in Fig. 2 against their surface areas. An essentially linear relationship holds for all points representing the active carbons. The regular and gradual change in specific volume with surface area probably is due to concentration of the inorganic content in the active carbon, the formation of isolated graphitic planes and possibly further graphitization. On the other hand, the abrupt change in specific volume noted when the char is first activated may be due to removal of hydrocarbon material bounding the graphitic particles.

By extrapolating the linear portion of the curve back to the surface area of the char, the specific volume in helium of the unactivated graphitic regions, $1/d_c$, is obtained. The corresponding density value, 2.01 g./cc., differs substantially from the 2.26 g./cc. of graphite, assumed in the derivation of equation IV.

The theoretical external surface area E of the graphitic particles is given by the first term in eq. I

$$E = \frac{2618(3 - 2f)}{L(1 - f)} \qquad \text{(VIII)}$$

Upon substituting the surface area of the char for E and setting f equal to zero, one can solve for L, the number of planes in an unactivated graphitic stack. A value of 49 is obtained.

This value and the extrapolated d_c value can be used to relate the surface area of the carbon to the micropore density through the function $A(d/d_c,L)$. Figure 3 shows the resulting relationship, $A(d/2.01, 49)$ and the experimentally determined points for the active carbons. Good agreement is obtained between experiment and theory.

Check of $A(d/d_c,L)$ with a Coconut Charcoal.—Equations I and II were also tested with data[12] on the steam activation of a coconut char. Although

data for the unactivated char were not given, apparent densities in helium for varying degrees of activation were included. The corresponding specific volumes in helium were plotted against surface area. Just as in the case of the coal-based char, a linear relationship was obtained, although slope and intercepts were different.

The apparent density of the char in helium d_c is obtained with little error from the extrapolated intercept. Substituting this value, $d_c = 1.89$ g./cc., into equation II gives an equation that, with eq. I, produces a family of curves relating surface area to micropore density as a function of L. When $L = 40$, good agreement between experiment and theory is obtained, as shown in Fig. 4.

Opportunity to check the validity of these results is afforded by an estimate[17] that the coconut-based carbons were activated from "an 80%-yield to a 50%-yield charcoal." Assuming that the fraction of carbon consumed and the fraction of planes removed are equivalent, these "yields" correspond to values of $f = 0.2$ for the least-activated carbon and $f = 0.5$ for the most activated material. The f values calculated by eq. I, from the surface area and the above L and d_c values, are $f = 0.27$ and $f = 0.48$, respectively. The agreement seems satisfactory.

Discussion

The values of L calculated for both the coal- and coconut-based carbons correspond to stacks of graphitic layers about 150 Å. in height. If the heights and widths of the stacks are equal, the plane diameter, the average distance across the layers, will also be about 150 Å. On the other hand, plane diameters estimated for active carbons by X-ray techniques and from carbon:hydrogen ratios generally range from 20 to 50 Å.[4] The apparent discrepancy can be resolved by assuming that the large particle sizes calculated from the surface areas of chars correspond to aggregated stacks of planes. A heterogeneous particle of this type would not be expected to behave much differently than a homogeneous stack.

The mathematical treatment presented doesn't make allowances for the presence of ash or the distribution of particle sizes and shapes. Corrections for the ash content can be made by modifying the value for the density of the char. On the other hand, such a mathematical model probably cannot be applied to extreme activations, where most of the particle is eaten away and mechanical collapse occurs.

The success of the model in fitting the experimental evidence is a necessary but not a sufficient condition for establishing the validity of the activation mechanism. Other mathematical models based on a random distribution of pore sizes might also give satisfactory correlations between surface area and density. Such has been found to be the case for models with a Gaussian distribution of pore widths in a layer-type structure. These models are less satisfactory, however, in that they require the use of arbitrary constants and are not as consistent with experimental evidence.

Acknowledgment.—The author is grateful to G. S. John for helpful comments and suggestions on the development of the mathematical aspects of this work.

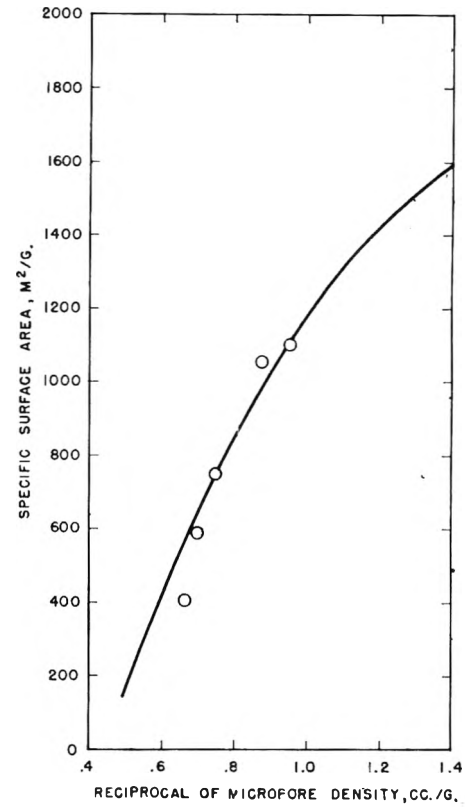

Fig. 3.—$A(d/2.01, 49)$ plotted against literature data.

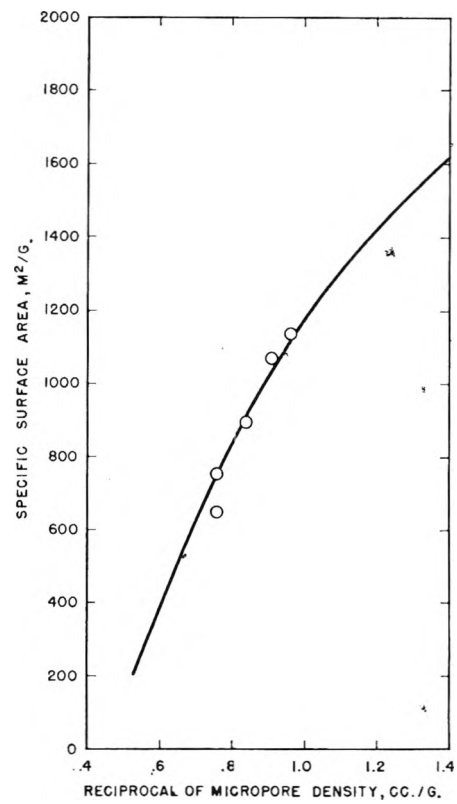

Fig. 4.—$A(d/1.89, 40)$ plotted against literature data.

Appendix A

Derivation of Equation I.—Assume the unacti-

vated char is made up of graphitic cubes containing L planes each and with an interplanar distance of h_c (in ångströms). Each cube has a surface area, furnished by the faces of the cube, of

$$a_{EC} = 6(h_cL)^2 \quad \text{(A1)}$$

With activation, however, this external surface area

$$F_1' = \frac{(L-2)!}{(fL-1)!}\left[\frac{1}{\frac{(L-2)!}{(fL-1)!} + \frac{(L-3)!}{(fL-2)!} + \cdots + \frac{(L-fL)!}{1!} + \frac{(L-fL-1)!}{1}}\right] \quad \text{(A18)}$$

varies with the fraction f of planes removed

$$a_{EC} = 2(h_cL)^2 + (1-f)4(h_cL)^2 \quad \text{(A2)}$$
$$= 2(h_cL)^2(3-2f) \quad \text{(A3)}$$

The number X of planes removed is

$$X = Lf \quad \text{(A4)}$$

On random removal of X planes from a stack of L planes, the fraction of planes removed that contribute to the formation of crevices W planes wide is

$$F_W = \frac{W(L-W-1)!(L-X)(L-X-1)(X-1)!}{L!(X-W)!} \quad \text{(A5)}$$

for $L > X > W > 0$, and

$$F_0 = \frac{2}{L-X+1} \quad \text{(A6)}$$

for $L > X > W = 0$.

If F_W' is the fraction of all crevices W planes wide

$$F_W' = \frac{(L-W-1)!}{(X-W)!}\left[\frac{1}{\frac{(L-2)!}{(X-1)!} + \frac{(L-3)!}{(X-2)!} + \cdots + \frac{(L-X)!}{1!} + \frac{(L-X-1)!}{1}}\right] \quad \text{(A7)}$$

The number of pores P_1 in the graphite cube that are only one plane wide is

$$P_1 = F_1 \times X \quad \text{(A8)}$$

or

$$P_1 = F_1Lf \quad \text{(A9)}$$

Combining (A4) and (A5) and solving for $W = 1$, gives

$$F_1 = \frac{(1-f)(L-fL-1)}{(L-1)} \quad \text{(A10)}$$

and combining (A10) and (A9), yields

$$P_1 = \frac{fL(1-f)(L-fL-1)}{(L-1)} \quad \text{(A11)}$$

The number of pores, $P > 1$, more than one plane wide is

$$P_{>1} = P_T - P_1 \quad \text{(A12)}$$

where P_T is the total number of pores formed. However

$$P_T = \frac{P_1}{F_1'} \quad \text{(A13)}$$

therefore

$$P_{>1} = \frac{P_1}{F_1'} - P_1 \quad \text{(A14)}$$

or

$$P_{>1} = P_1\left(\frac{1}{F_1'} - 1\right) \quad \text{(A15)}$$

The contribution of the pores in the cube to its total surface area is

$$a_{PC} = (h_cL)^2P_1 + 2(h_cL)^2P_{>1} \quad \text{(A16)}$$

because the smallest pores can only accept one layer of adsorbate molecules. Combining (A15) and (A16)

$$a_{PC} = (h_cL)^2P_1\left[1 + 2\left(\frac{1}{F_1'} - 1\right)\right] \quad \text{(A17)}$$

Combining (A4) and (A7) and setting $W = 1$

and

$$1/F_1' = 1 + \frac{fL-1}{L-2} + \frac{(fL-1)(fL-2)}{(L-2)(L-3)} + \frac{(fL-1)(fL-2)(fL-3)}{(L-2)(L-3)(L-4)} + \cdots \quad \text{(A19)}$$

which combined with (A17) gives

$$a_{PC} = (h_cL)^2P_1\left\{1 + 2\left[\frac{fL-1}{L-2} + \frac{(fL-1)(fL-2)}{(L-2)(L-3)} + \frac{(fL-1)(fL-2)(fL-3)}{(L-2)(L-3)(L-4)} + \cdots\right]\right\} \quad \text{(A20)}$$

However

$$\frac{fL-1}{L-fL} = \frac{fL-1}{L-2} + \frac{(fL-1)(fL-2)}{(L-2)(L-3)} + \frac{(fL-1)(fL-2)(fL-3)}{(L-2)(L-3)(L-4)} + \cdots \quad \text{(A21)}$$

Equation A21 combined with (A20) gives

$$a_{PC} = (h_cL)^2P_1\left[\frac{L+fL-2}{L(1-f)}\right] \quad \text{(A22)}$$

or, when combined with (A11)

$$a_{PC} = \frac{(h_cL)^2f(L-fL-1)(L+fL-2)}{L-1} \quad \text{(A23)}$$

The total surface area of the cube a_c will be

$$a_C = a_{EC} = a_{PC} \quad \text{(A24)}$$

or

$$a_C = 2(h_cL)^2(3-2f) + \frac{(h_cL)^2f(L-fL-1)(L+fL-2)}{L-1} \quad \text{(A25)}$$

combining eq. A23 and A24. The area in square meters is

$$a_C = \frac{2(h_cL)^2(3-2f)}{10^{20}} + \frac{(h_cL)^2f(L-fL-1)(L+fL-2)}{(L-1)(10^{20})} \quad \text{(A26)}$$

The interplanar distance h_c in the original graphitic cube is inversely proportional to its density d_c. Relating these values to the corresponding values for graphite

$$\frac{h_c}{3.38} = \frac{2.26}{d_c} \quad \text{(A27)}$$

The weight, in grams, of the graphitic cube after activation is

$$W_n = d_c(1-f)(h_cL)^3 \times 10^{-24} \quad \text{(A28)}$$

and the specific surface area of the cube A is given by

$$A = \frac{A_c}{W_p} \quad \text{(A29)}$$

By combining (A26) and (A28) with (A29), the specific surface area A in square meters per gram, is obtained

$$A = \frac{2(3 - 2f) \times 10^4}{d_c h_c L(1 - f)} + \frac{f(L - fL - 1)(L + fL - 2) \times 10^4}{d_c h_c L(L - 1)(1 - f)} \quad \text{(A30)}$$

or, when combined with (A27)

$$A = \frac{2618(3 - 2f)}{L(1 - f)} + \frac{1309f(L - fL - 1)(L + fL - 2)}{L(L - 1)(1 - f)} \quad \text{(I)}$$

Appendix B

Derivation of Equation II.—On removing a certain number X of planes from the graphite cube, a certain fraction F_0 of those removed will be removed from the top and bottom of the cube and thus will decrease the volume of the cube. Then the height H_X of the reduced cube will be

$$H_X = \frac{L - F_0 X}{L}(h_c L) \quad \text{(B1)}$$

or, when combined with (A4) and (A6)

$$H_X = \left(L - \frac{2Lf}{L - Lf - 1}\right) h_c \quad \text{(B2)}$$

The volume of the cube will be

$$V_{CR} = \left(L - \frac{2Lf}{L - Lf + 1}\right) h_c^3 L^2 \quad \text{(B3)}$$

or, in cc.

$$V_{CR} = \left(L - \frac{2Lf}{L - Lf + 1}\right) h_c^3 L^2 \times 10^{-24} \quad \text{(B4)}$$

The density of this cube will be

$$d = \frac{W_p}{V_{CR}} \quad \text{(B5)}$$

Upon combining (A28) and (B4) with (B5)

$$d = \frac{d_c(1 - f)}{1 - \frac{2f}{L - Lf + 1}} \quad \text{(B6)}$$

which reduces to the form

$$d = \frac{d_c[L(1 - f)^2 + (1 - f)]}{(L + 1) - (L + 2)f} \quad \text{(II)}$$

Appendix C

Derivation of Equations III, IV and V.—Equation III is obtained by calculation of the limit, as L approaches infinity, of eq. I.

Equation IV is similarly obtained from eq. II, with the additional substitution of the density of graphite for d_c.

In deriving eq. V, eq. A7 is solved for $W = 1, 2, 3$, etc. The limit as L approaches infinity is determined in each case, to obtain

$$\text{Lim } F_1' = 1 - f \quad \text{(C1)}$$
$$\text{Lim } F_2' = f(1 - f) \quad \text{(C2)}$$
$$\text{Lim } F_3' = f^2(1 - f) \quad \text{(C3)}$$

or, in general

$$F_W' = \lim_{L \to \infty} F_W' = F^{W-1}(1 - f) \quad \text{(V)}$$

SALTING EFFECTS IN THE SOLVENT EXTRACTION BEHAVIOR OF INORGANIC COMPOUNDS[1]

By R. M. Diamond[2]

Department of Chemistry and Laboratory for Nuclear Studies, Cornell University, Ithaca, New York

Received July 9, 1958

The variation in the distribution ratio for tracer indium(III) distributing between an oxygenated organic solvent[3] and aqueous solutions of hydrochloric acid in which the concentration of HCl was varied while keeping the initial ionic strength constant with various chloride salts[4] was studied as a model system for the extraction behavior of ionic species under these conditions. It is seen that the extraction of acid species plays a somewhat unique role due to the special ability of the hydronium ion to hydrogen-bond water molecules in first shell solvation and to enhance further coördination with the solvent molecules. In such acid extractions, the coördinating ability of the organic solvent, determined by its basicity and the steric availability of the donor atom, and not the solvent's dielectric constant, is of paramount importance. In contrast, the extraction of large, relatively unhydrated salt species, such as $N(C_2H_5)_4{}^+InCl_4{}^-$, depends primarily on the dielectric constant of the organic solvent and not on its coördinating ability. With solvents of high dielectric constant, *i.e.*, nitrobenzene, the extraction of ionic species increases with increasing size of the ions. With solvents of low dielectric constant but good coördinating ability, such as diethyl ether, the extraction of hydrated cations decreases with increasing crystallographic size, exactly the reverse order. The variations in the extraction of the indium tracer with replacement of the aqueous HCl by the different salt chlorides are explained on the basis of (1) the creation of new extracting species involving an added ion and the ion of interest; (2) the creation of new extracting species not involving the ion of interest, but repressing the latter's extraction; (3) a change in the relative proportion of the extractable species in the aqueous phase; (4) a change in the nature of the aqueous phase with changing water activity and dielectric constant.

The use of "salting" agents in solvent extraction is now a well established practice[5-8] and, with the proper choice of salt and conditions, may greatly enhance the extraction. The present paper is an attempt to study the factors involved in such extraction of inorganic species and to explain the dif-

(1) Work supported in part by the U. S. Atomic Energy Commission.

(2) Radiation Laboratory, University of California, Berkeley 4, California.

(3) Solvents used were diethyl, butyl ethyl and β,β'-dichlorodiethyl ethers, methyl isobutyl and diisobutyl ketones, dibutyl phthalate, tributyl phosphate, methyl benzoate, methyl salicylate, *o*- and *m*-nitrotoluenes, nitrobenzene and 2-ethylhexanol.

(4) Salts used were lithium, sodium, potassium, ammonium, cesium, tetramethyl and tetraethyl ammonium chloride.

(5) (a) F. Hecht and A. Grünwald, *Mikrochemie ver. Mikrochim. Acta*, **30**, 279 (1942); (b) N. H. Furman, R. J. Mundy and G. H. Morrison, U. S. Atomic Energy Commission Report, AECD-2938.

(6) R. Bock and E. Bock, *Z. anorg. Chem.*, **263**, 146 (1950).

(7) G. H. Morrison and [illegible] (1950).

(8) L. Garwin and A. N. Hixson, *Ind. Eng. Chem.*, **41**, 2303 (1949).

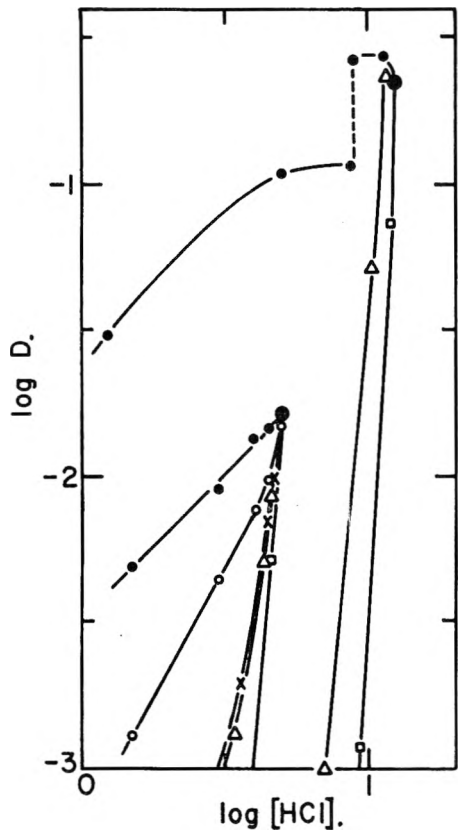

Fig. 1.—Log D *vs.* log [HCl] for diethyl ether, the chloride ion concentration held constant with: LiCl●—●; NaCl, ○—○; KCl, ▲—▲; NH_4Cl, ■—■; CsCl, □—□; $N(CH_3)_4Cl$, △—△; $N(C_2H_5)_4Cl$, X—X. Initially, 10 ml. of ether to 5 ml. of aqueous solution.

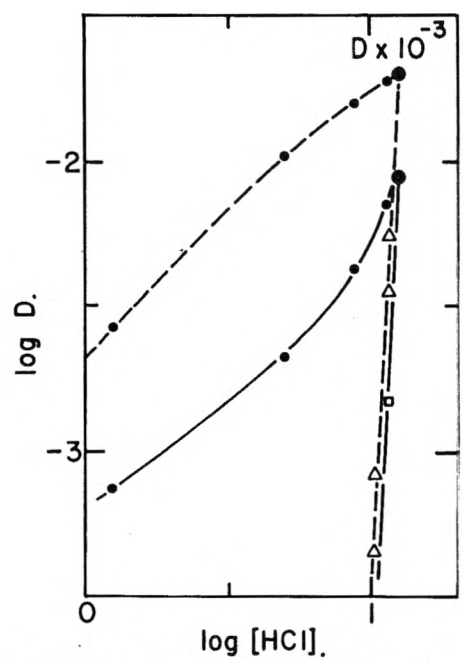

Fig. 2.—Log D *vs.* log [HCl] for butyl ethyl ether ———; log $D \times 10^{-3}$ *vs.* log [HCl] for dibutyl ether using Fe(III) tracer – – – –. Symbols have same meaning as in Fig. 1.

ferent types of behavior. The addition of the salting agent may act in several ways, *i.e.*, (1) create a new extracting species involving the added ion and the ion of interest; (2) create a new extracting species not involving the ion of interest, but repressing the latter's extraction; (3) change the relative proportion of extractable species in the aqueous phase; (4) change the nature of the aqueous phase by changing the water activity and the dielectric constant of that phase.

Since all four factors may be involved when replacing hydrogen ion with some other cation in a halometallic acid extraction system, one such family of systems, indium(III) chloride–aqueous HCl–organic solvent, was studied in detail. Fragmentary work with iron(III) chloride and molybdenum(VI) chloride gave the same results and strongly indicated that the behavior to be described, and the explanations, hold for all the halometallic acid extraction systems, and the similar thiocyanate salt systems.[9] The first two factors mentioned above are treated explicitly in the general equations derived earlier (Case 4, paper II[10]) and given below, but the last two factors cannot be so readily handled and must be considered as causing a variation, predictable as to direction, in the concentration "constants" of the equations.

Experimental

Tracer and Reagents.—The radioactive indium tracer used, 49 day In^{114m}, was obtained from Union Carbide Nuclear Co., Oak Ridge, Tennessee. Counting was done with a well-type NaI scintillation counter whose pulses were selectively discriminated by a single channel analyzer. No radioactive impurity in the tracer could be detected during the course of the work.

Reagent grade diethyl ether and C.P. butyl ethyl and dibutyl ethers, methyl isobutyl ketone, dibutyl phthalate, methyl benzoate, methyl salicylate, *o*- and *m*-nitrotoluenes, nitrobenzene, *o*-dichlorobenzene and practical grade 2-ethylhexanol and diisobutyl ketone were used without further treatment. C.P. β,β'-dichlorodiethyl ether was distilled under reduced pressure and a colorless, two-degree cut taken. C.P. tributyl phosphate had low-boiling impurities steam distilled off, was washed with sodium hydroxide, water, and then dried over $MgSO_4$.[11] Reagent grade hydrochloric acid, lithium chloride, sodium chloride, ammonium chloride and potassium chloride were used without further purification, except filtering, as were 99+% pure cesium chloride, tetramethylammonium and tetraethylammonium chloride.

Procedure.—The procedure for the distribution experiments was the same as described previously in paper III.[12] The measurements were performed at 21 ± 1° with initially equal volumes of organic and aqueous solutions.[13] Duplicate trials showed that when D was in the range 0.001 to 100, reproducibility was usually 10% or better; exceptional cases showed differences as large as 30%. When D was less than 0.001, the reproducibility was correspondingly poorer. Centrifugation was used to speed up phase separation with the nitrobenzene, *o*- and *m*-nitrotoluene, methyl benzoate, methyl salicylate and β,β'-dichlorodiethyl ether systems.

Results and Discussion

For indium(III) chloride extractions from aqueous hydrochloric acid solutions containing another univalent cation, symbolized by A^+, the following species must be considered. Aqueous phase: In^{+++}, $InCl^{++}$, $InCl_2^+$, $InCl_3$, $InCl_4^-$, H^+, A^+, Cl^-,

(9) A discussion of one such thiocyanate system, the cobalt thiocyanate system, is to be published by R. Watkins, G. Welt and R. M. Diamond.

(10) R. M. Diamond, THIS JOURNAL, **61**, 69 (1957).

(11) The author wishes to thank Dr. D. G. Tuck for the purified tributyl phosphate.

(12) R. M. Diamond, THIS JOURNAL, **61**, 75 (1957).

(13) When using diethyl ether, two volumes were taken per volume of aqueous solution because of the solubility of the ether in the aqueous acid.

Organic phase: $InCl_4^-$, H^+, A^+, Cl^-, $H^+InCl_4^-$, H^+Cl^-, A^+Cl^-, and still larger ion associations.[14] $H^+InCl_4^-$, $A^+InCl_4^-$, H^+Cl^- and A^+Cl^- represent ion-pairs in the organic solvent, and also true molecular species if they exist, *i.e.*, HCl.

The extraction behavior of a substance is most easily measured in terms of the distribution ratio

$$D = \frac{\text{concn. of substance in organic phase}}{\text{concn. of substance in aqueous phase}}$$

In the present case

$$D = \frac{(InCl_4)_0 + (HInCl_4)_0 + (AInCl_4)_0}{(In) + (InCl) + (InCl_2) - (InCl_3) + (InCl_4)} \quad (1)$$

where $(\ )_0$ and $(\ )$ represent the concentrations of the enclosed species in the organic and aqueous phases, respectively, and charges have been omitted for simplicity. By means of equilibrium relations given in paper II,[15] and for the case where indium is present in only trace amounts, this becomes

$$D = \frac{\frac{\alpha_{HInCl_4}}{\sqrt{\alpha_{HCl}}}(InCl_4)\sqrt{\frac{\alpha_{HCl}(H) + \alpha_{ACl}(A)}{\alpha_{HCl}(Cl)}} + \alpha_{HInCl_4}\delta_{HInCl_4}(H)(InCl_4) + \alpha_{AInCl_4}\delta_{AInCl_4}(A)(InCl_4)}{\sum_{i=0}^{4}(InCl_i)} \quad (1')$$

Since the experimental data are most easily presented in plots of log D *vs.* log [HCl], with [HCl] = (H) in the mixed acid–salt solution of constant ionic strength, the logarithmic derivative of equation 1′, subject to the condition (H) + (A) = (Cl) = constant, yields

$$\frac{d\log D}{d\log [HCl]} = \frac{\partial \log D}{\partial \log (H)} - \frac{(H)}{(A)}\frac{\partial \log D}{\partial \log (A)} = \frac{1}{2}f^{\circ}_{InCl_4}\frac{\alpha_{ACl}(H) - \alpha_{HCl}(H)}{\alpha_{HCl}(H) + \alpha_{ACl}(A)} + f^{\circ}_{HInCl_4} - \frac{(H)}{(A)}f^{\circ}_{AInCl_4} \quad (2)$$

where f° represents the fraction of indium in the organic phase in the form of the indicated species.

The experimental results are given in Figs. 1–10 as plots of log D *vs.* log [HCl] for initial ionic strengths of 2.0, 5.0 and 12.6 *m*.[16] The value of [HCl] was varied from that of the total ionic strength (pure acid) down to about 10–20% of the ionic strength by replacement with various alkali and substituted ammonium chlorides. Three features stand out from these (and related) experiments. They are: (1) the special ease of extraction of acid species compared to the corresponding alkali metal salts; (2) the order of extraction from mixed acid–alkali chloride solutions into basic oxygenated solvents decreases from lithium to cesium chloride; (3) that with weakly basic, high dielectric constant solvents, extraction increases from CsCl, NMe_4Cl and NEt_4Cl solutions in that order, and the value of D may become much larger than with the pure HCl solution alone.

The special extractability of (strong) acid species is reflected in the fact that HCl and the complex metal acids extract much better (by orders of magnitude) into most oxygenated (basic) solvents from aqueous solutions than do the corresponding alkali at the same concentration. Even when a mixed aqueous acid–salt solution is predominantly the latter, the extracting species is almost exclusively the acid. The origin of the difference in extractability of the hydrogen ion and of the alkali cations is likely a difference in the structure of the hydrated species. Because water molecules are so much smaller than the organic solvent molecules involved, more water dipoles than organic molecules can pack around a cation to form its primary[17] solvation shell. Each water–ion interaction is also usually stronger than an ion–organic molecule interaction, and so the energy of first shell solvation by water is greater than that with the oxygenated organic solvents. This means that to extract into the solvent without great loss of solvation energy, the cation must carry its primary water shell with it, and then in the organic phase undergo further solvation of this hydrated species by the organic molecules. Evidence is increasing that the H_3O^+ ion in water has three water molecules hydrogen-bonded to it as a primary hydration shell[18–21] of pyramidal structure, *i.e.*

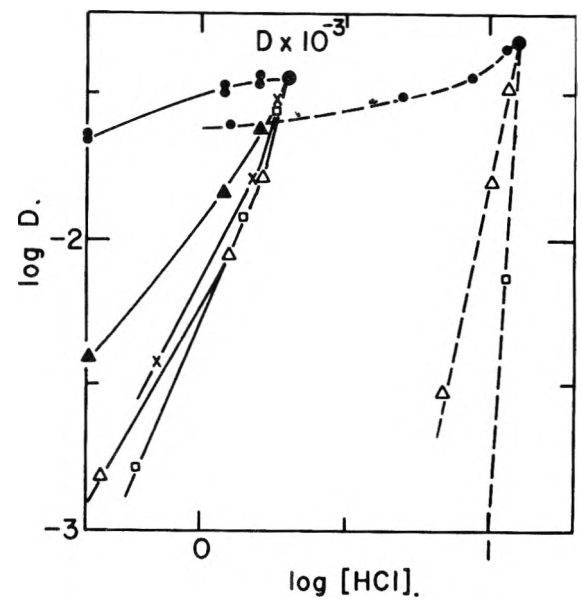

Fig. 3.—Log $D \times 10^{-3}$ *vs.* log [HCl] for tributyl phosphate ———; log d *vs.* log [HCl] for dibutyl phthalate – – – –. See Fig. 1 for meaning of symbols.

(14) Larger ion associations involving more than one $InCl_4^-$ ion were most unlikely in the present study as the indium concentration was $\sim 3 \times 10^{-6}$ *M*.

(15) The necessary equations are: $\alpha_{HCl}(H)(Cl) = (H)_0(Cl)_0$, $\alpha_{HInCl_4}(H)(InCl_4) = (H)_0(InCl_4)_0$, $\alpha_{ACl}(A)(Cl) = (A)_0(Cl)_0$, $\alpha_{AInCl_4}(A)(InCl_4) = (A)_0(InCl_4)_0$, $\delta_{HInCl_4}(H)(InCl_4)_0 = (HInCl_4)_0$, $\delta_{AInCl_4}(A)_0(InCl_4)_0 = (AInCl_4)_0$, and $(A)_0 + (H)_0 = (Cl)_0 + (InCl_4)_0$.

(16) The concentrated CsCl solution used was 10.0 *m*, so that the experiments done with it were not at a constant initial ionic strength.

(17) In this paper, primary solvation means coördinative solvation, that is, solvation involving bonding, directly to the ion, and secondary solvation means that involving bonding to this primary unit and nonspecific, electrostatic solvation, that from orienting and polarizing solvent molecules not bonded to the charged species.

(18) E. Glueckauf, *Trans. Faraday Soc.*, **51**, 1235 (1955).

(19) K. N. Bascombe and R. P. Bell, *Disc. Faraday Soc.*, **24**, 158 (1957).

(20) E. Wicke, M. Eigen and T. Ackermann, *Z. physik. Chem.*, **1**, 340 (1954).

(21) D. G. Tuck and R. M. Diamond, *Proc. Chem. Soc.*, 236 (1958).

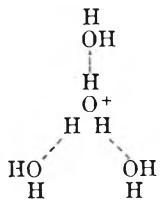

These waters are bound more strongly than might be expected from the size of the hydronium ion (similar to potassium ion), because the positive charge of the H_3O^+ is not distributed over the surface of the ion, but is concentrated on the three hydrogens, making for strong hydrogen-bonds to the three water molecules. This hydrated structure is further

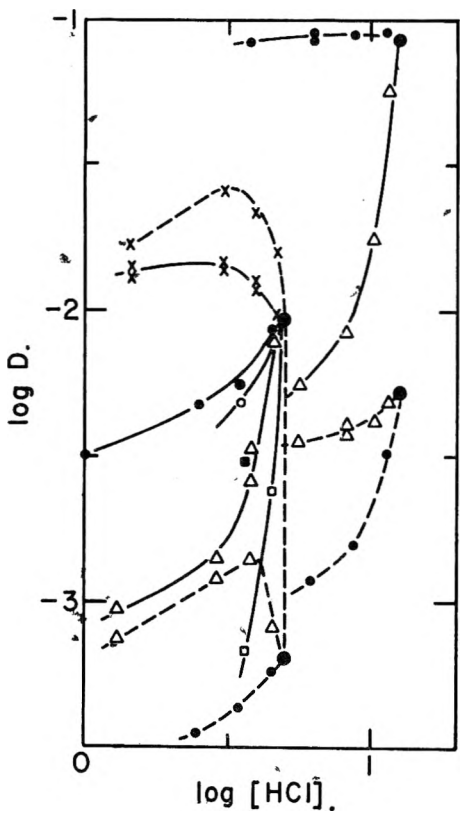

Fig. 4.—Log D *vs.* log [HCl] for methyl benzoate ———; for methyl salicylate – – – –. See Fig. 1 for meaning of symbols.

solvated either by more water molecules or by the basic organic molecules, the oxygen (or nitrogen) of the solvent molecule bonding to the first shell water molecule through one of the latter's hydrogens.[22] This secondary solvation is more favorable for H_3O^+ than for any other small cation, since the

(22) Extraction of either the complex metal acids or of simple mineral acids is negligible without a basic oxygen or nitrogen in the solvent molecule, that is, without an electron donating group. And actual coördination must be involved rather than a dipole interaction of the solvent, as *o*-dichlorobenzene (dielectric constant = 9.93 at 25°), shows negligible acid extraction compared to diethyl ether (dielectric constant = 4.34 at 25°). Furthermore, there is a poor correlation between the degree of extraction of an acid and the dielectric constant of the solvent, except in a series of similar solvents of a particular class, such as the aliphatic ethers, methyl ketones, etc., but a better one with combined basicity and steric availability of the donor group. With very basic solvents and only moderately strong acids, the solvent may displace water from the first hydration shell, *cf.* ref. 21.

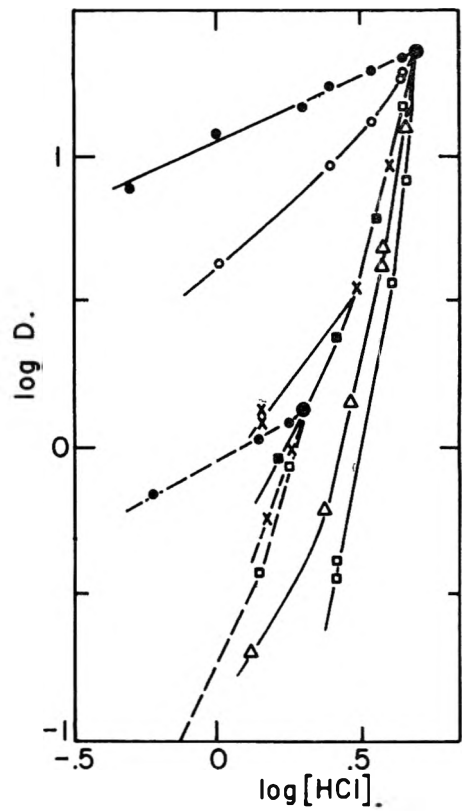

Fig. 5.—Log D *vs.* log [HCl] for methyl isobutyl ketone at 5.0 m ionic strength ———, at 2.0 m ionic strength – – – –. See Fig. 1 for meaning of symbols.

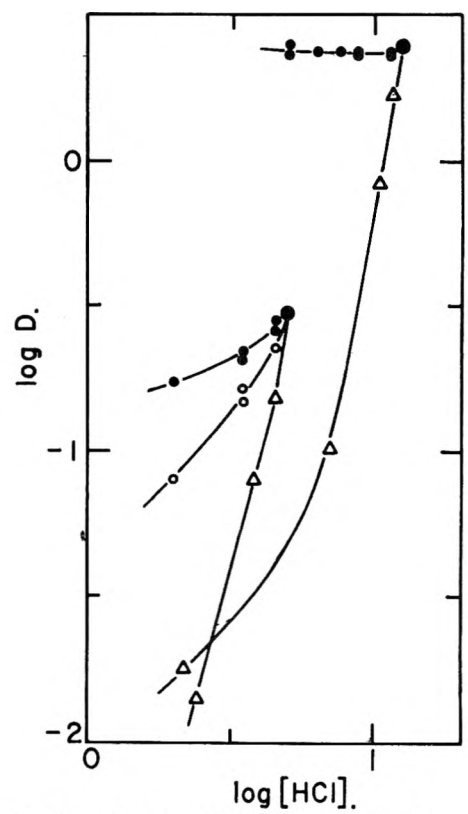

Fig. 6.—Log D *vs.* log [HCl] for diisobutyl ketone, the chloride ion concentration held constant with: LiCl, ●—●; NaCl, ○—○; KCl, ▲—▲; NH_4Cl, ■—■; CsCl, □—□; $N(CH_3)_4Cl$, △—△; $N(C_2H_5)_4Cl$, X—X.

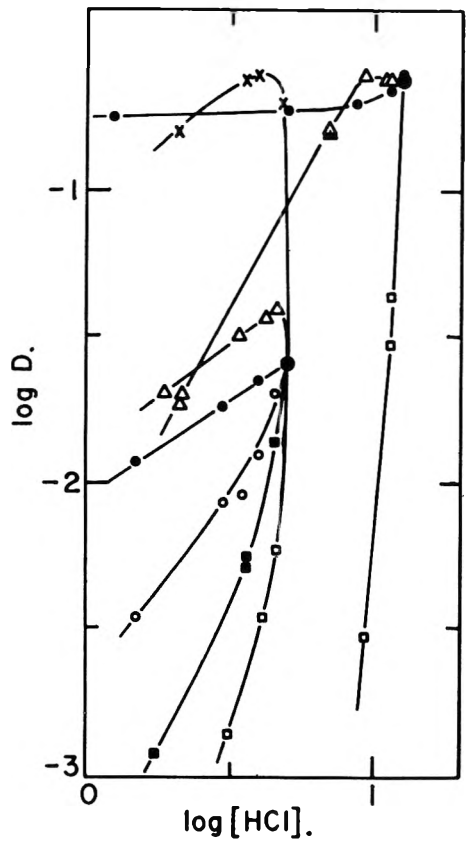

Fig. 7.—Log D *vs.* log [HCl] for β,β'-dichlorodiethyl ether See Fig. 6 for meanir g of symbols.

positive charge concentrated on the (inner) hydronium hydrogens can shift to the (outer) hydration water hydrogens by the vibration jump mechanism responsible for the high equivalent conductivity of H_3O^+ in water.[23] That is, one of the inner protons can jump over to one of the hydration shell waters, leading to a structure

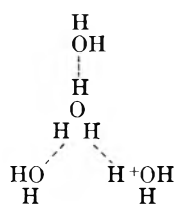

in which the hydration shell water becomes, temporarily, the hydronium ion, and now the hydrogens of this molecule, carrying a partial positive charge, can hydrogen-bond more strongly the basic oxygen of the solvent molecule than the less polarized water molecule in the hydration shell of, say, a lithium cation. The structure shown above is, of course, only one of three equivalent forms with the positive charge concentrated in turn on each of the hydration shell waters. This proton jump mechanism obviously cannot occur with the alkali or other cations, and so is unique with the H_3O^+ ion and its hydration shell. Along with the stronger first shell hydration already mentioned, this stronger solvent binding should contribute to a larger solvation energy in the organic phase for the

(23) (a) E. Hückel, *Z. Elektrochem.*, **34**, 546 (1928); (b) J. D. Bernal and R. H. Fowler, *J. Chem. Phys.*, **1**, 515 (1933).

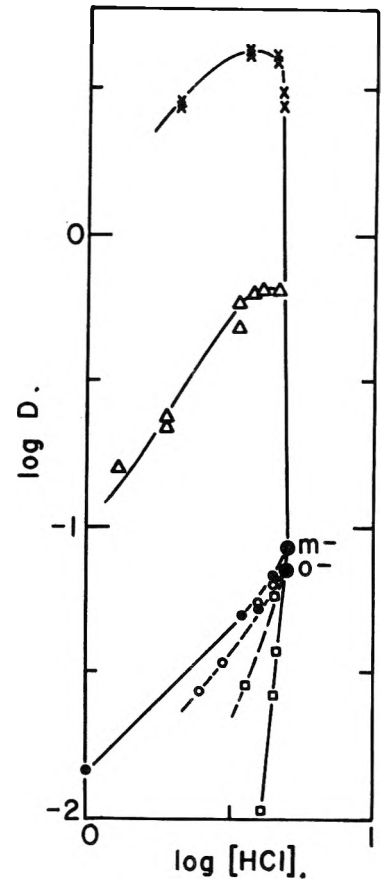

Fig. 8.—Log D *vs.* log [HCl] for *m*-nitrotoluene ———, for *o*-nitrotoluene – – – –. The curve for *m*-nitrotoluene and NaCl–HCl is the same as that for *o*-nitrotoluene and LiCl–HCl except that the value of D in 5.0 *m* HCl is somewhat higher for the *meta* than for the *ortho* isomer. With the same proviso, the curves for the alkyl ammonium salts appear to be the same for the two isomers. See Fig. 6 for meaning of symbols.

acids than for salts of the same anion. It is suggested that these are the reasons for the much larger extractability of the acids (of the complex metal anions, as well as of the simpler anions such as Cl^-, Br^-, ClO_4^-, etc.) than of the corresponding alkali metal salts.[24]

Since for most of the solvents used in this work, the alkali metal cations have a negligible distribution ratio compared to that of the hydronium ion, the substitution of alkali chloride for aqueous HCl, at constant ionic strength, should decrease the value of D for any strong acid present and, in particular, for trace amounts of $HInCl_4$. That is, in eq. 1 the third term is negligible and the second decreases with decreasing H^+. But Figs. 1–10 show that there is considerable variation in the amount of decrease in D, depending upon the nature of the alkali salt. This is mainly due to a variation in the aqueous phase structure and water activity (factor 4). For the different cations tie up in hydration differing amounts of water, and the smaller the degree of hydration of the salt, the higher the dielectric constant and the water activity of the solution, and the lower the concentration of the solute, effec-

(24) The situation can be somewhat different with very basic solvents, such as tributyl phosphate, which under certain conditions can displace a primary shell water molecule.

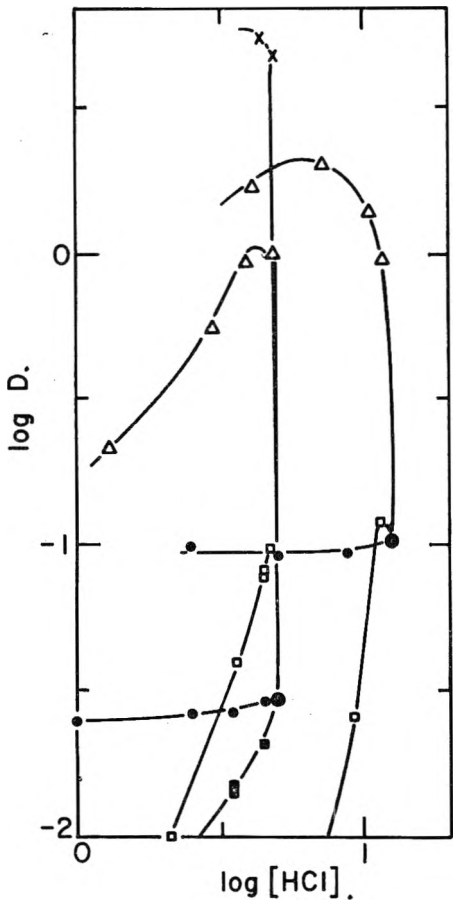

Fig. 9.—Log D *vs.* log [HCl] for nitrobenzene. See Fig. 6 for meaning of symbols.

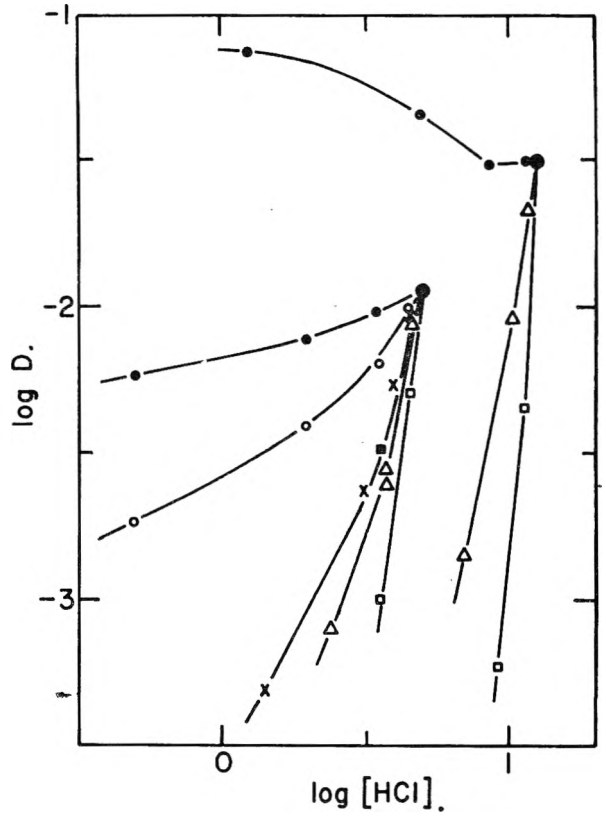

Fig. 10.—Log D *vs.* log [HCl] for 2-ethylhexanol. See Fig. 6 for meaning of symbols.

tively. Hence, due to the possibility of more complete solvation, the more inviting the aqueous solution becomes for the trace ionic species, and so the smaller the tendency to transfer into the organic phase and the lower the value of the distribution ratio. The order of hydration for the alkali cations is $(H_3O^+) \approx Li^+ > Na^+ > K^+ \approx NH_4^+ > Cs^+$, as is indicated by the water activity of the halide salts, and by the limiting equivalent conductivities of the ions.[25] Thus, the salting in, the lowering of the distribution ratio of the species of interest ($HInCl_4$ in the present paper) should increase as one goes from lithium to cesium chloride, and should increase with the amount of salt replacing the acid,[26] just as is observed in Figs. 1–10. Actually, the salting in cannot be due solely to the change in water activity, as then the limiting case would be the replacement of acid solution by pure water. That is, replacement of acid by an alkali salt should always lead to a value of D higher than that from a pure acid solution containing the same concentration of acid as the mixed acid–salt solution, and this is not true experimentally. For example, extraction into diethyl ether from 3.5 m HCl–1.5 m CsCl gives a distribution ratio for $HInCl_4$ about one-tenth as large as from 3.5 m HCl alone. The presence of the CsCl represses the extraction, and this must be an aqueous phase effect as the same species, $HInCl_4$, extracts in either case, and this behavior is observed with most of the solvents used. Such salting in by large univalent ions is well known as a salt effect in the distribution of non-electrolytes.[27] It must depend upon the changes in the water structure caused by the large ions, and possibly upon a quasi-lattice structure of the ions themselves in such concentrated solutions, but a satisfactory explanation has not been given.

In the extraction of metal complex ions, the nature of the cation present in macro amounts also has an effect through its influence on the formation of the complex. Since the latter process consists of the replacement of first shell water molecules by anions, the increased water activity in going from lithium to cesium solutions hinders the formation of the complex and so tends to lower D in that order for complex extracting species. This should be most important at the lower chloride concentrations where formation of the complex is least complete.

There is also an effect due to the dielectric constant of the solvent. With low dielectric constant solvents, ion-paired indium(III) species predominate so that the $(InCl_4^-)_o$ term in eq. 1 becomes vanishingly small, and d log D/d log [HCl] $\approx +1$. But with solvents of higher dielectric constant, such

(25) R. A. Robinson and R. H. Stokes, "Electrolyte Solutions," Appendices 6.1 and 8.10, Butterworths Scientific Publications, London, 1955.

(26) The activity coefficient of HCl in alkali chloride–hydrochloric acid mixtures behaves in this fashion; it is essentially constant in LiCl–HCl mixtures (slight increase with LiCl at ionic strengths above 3 M), and decreases with decreasing HCl in NaCl–HCl, KCl–HCl and CsCl–HCl mixtures at constant ionic strength, the decrease becoming more marked in that salt order, *cf.* J. E. Hawkins, *J. Am. Chem. Soc.*, **54**, 4480 (1932), and H. S. Harned and O. E. Schupp, *ibid.*, **52**, 3892 (1930).

(27) F. A. Long and W. F. McDevit, *Chem. Revs.*, **51**, 119 (1952).

as methyl isobutyl and diisobutyl ketones, ion-paired species in the organic phase may partly dissociate, and then the first term must be kept. For the non-extracting alkali salts, eq. 2 simplifies to d log D/d log [HCl] $\approx$ $^1/_2$ $f°_{InCl_4^-}$ + $f°_{HInCl_4}$. Because of the presence of the term for $InCl_4^-$ which decreases with decreasing [HCl] as [HCl]$^{1/2}$, the plots of log D *vs.* log [HCl] for the ketones should show smaller slopes than the corresponding ones for the ethers, and they do, compare Figs. 1 and 2 with Figs. 3 and 4. Note particularly the plots for LiCl–HCl.

There are, however, conditions under which the substitution of an alkali salt for the corresponding acid increases the distribution ratio of the species of interest rather than decreasing it. For example, this will be true with very basic solvents which extract and coördinate with the acid, but not with the salts, so readily as to reduce the "free" solvent concentration significantly. The progressive replacement of acid by alkali salt in the aqueous phase, at constant ionic strength, decreases the acid concentration in the organic phase and frees solvent molecules, resulting in an increase in D for non-acidic, but solvent coördinating species. This is certainly a major factor in the increased extraction of $UO_2(NO_3)_2$ into tributyl phosphate from mixed $LiNO_3$–HNO_3 solutions over that from HNO_3 alone,[28] and is probably an important factor in the salting out of $UO_2(NO_3)_2$[5] and $Th(NO_3)_4$[6] into diethyl ether from HNO_3 solutions by nitrate salts.[29] This is probably also a reason why the extraction of $HInCl_4$ from mixed HCl–LiCl solutions at high (12.6 m) aqueous ionic strength remains essentially constant down to [HCl] $\approx$ 3 m into methyl benzoate (Fig. 4) and diisobutyl ketone (Fig. 6), and even increases at first, into 2-ethylhexanol (Fig. 10).

A related type of effect may occur with small basic solvent molecules which can dissolve readily in the aqueous phase. For example, the great solubility of the diethyl ether molecule (and to a lesser extent, that of diisopropyl ether) in concentrated aqueous hydrohalic acids so dilutes the aqueous phase that the equilibrium acid concentration there does not increase with increasing initial acid concentration above about 7 M. As a result, the extraction of a metal complex acid present as a micro-component passes through a maximum and then decreases beyond a certain initial acid concentration.[30,31] The use of mixed salt–acid solutions, such as LiCl–HCl, decreases markedly the solubility of ether in the aqueous phase (another example of the better coördination of the hydrated hydrogen ion than of lithium ion with basic organic solvents), increasing the aqueous phase concentration (and ether phase volume), and leads to increasing, sometimes to quite high, values of the distribution ratio of the species of interest with increasing salt substitution. An illustration is the extraction of $HInCl_4$ into diethyl ether from LiCl–HCl solutions at 12.6 m ionic strength, Fig. 1. With the acid alone, (10 M) the greater part of the ether dissolves in the aqueous phase. This reduces the aqueous HCl molarity almost by half, while, concurrently, the ether phase becomes so concentrated in HCl that the extraction of other species is repressed by the proportion of solvent molecules already coördinated. Upon substituting LiCl for HCl, the ether is forced back out of the aqueous phase, increasing the ionic concentration there, and so the value of D shows an actual increase with initial substitution by LiCl, until the formation of a second ether phase at 30% LiCl–70% HCl.

The situation is somewhat different when considering extraction from aqueous HCl solutions as the hydrogen ion is replaced by a large, relatively unhydrated cation such as a tetra-substituted ammonium cation. Such cations have small hydration energies; they do not have a primary (coördinated) hydration shell, and their large bulk displaces a considerable volume of hydrogen-bonded water. This leads to a tendency to be squeezed out of the water structure. The limiting case would be an uncharged non-hydrogen-bonding molecule such as $C(CH_3)_4$ which forms a separate immiscible phase so as to maximize the water–water bonding. When considering increasingly large and relatively unhydrated ions such as $N(CH_3)_4^+$, $N(C_2H_5)_4^+$, etc., this behavior becomes important, and salts of these ions are more soluble in the organic solvents than the corresponding alkali salts. Van der Waals (dispersion) interactions between the hydrocarbon parts of the ions and the organic solvent molecules also help to contribute to the extractability of these ions. This affects the distribution of $InCl_4^-$ (or other anion of interest) by the creation of a new organic phase salt species containing that ion, *i.e.*, either dissociated or ion-paired $AInCl_4$. In the expressions for D and d log D/d log [HCl], equations 1′ and 2, a term involving A^+ becomes important, and may, in fact, dominate the expression. Furthermore, since the origin of such salt extraction is due primarily to an aqueous phase phenomenon, the disturbance of the water structure, and not to coördination with organic phase molecules, the extraction of such large relatively unhydrated ions should be much less dependent on the coördinating ability of the oxygenated solvent than is the extraction of acid species. In fact, extraction of the substituted ammonium salts should also occur with non-basic (non-oxygenated) solvents, in contrast to the case of the acids, and this may be illustrated by comparing the values of D for indium(III) extraction into *o*-dichlorobenzene from 5 m HCl, $D < 0.0004$, and from 5 m $N(C_2H_5)_4Cl$; $D = 0.008$.

(28) E. Hesford and H. A. C. McKay, *Trans. Faraday Soc.*, **54**, 573 (1958).

(29) Most likely the anomalous order Bock and Bock found for the salting out of $Th(NO_3)_4$ into diethyl ether with various alkali metal and alkaline earth nitrates is due to the fact that they used saturated solutions of the different nitrates and so had very different nitrate molalities in each system. If the values of D for thorium nitrate extraction from the different nitrate solutions would be compared at the same nitrate molality, they very likely would show a regular decrease in the order Li > Na > K > Rb > Cs and Mg > Ca > Sr > Br, for the reasons given above.

(30) (a) D. E. Metzler and R. J. Meyers, *J. Am. Chem. Soc.*, **72**, 3776 (1950); (b) D. E. Campbell, Ph.D. Dissertation, Rensselaer Polytechnic Institute, 1952; (c) I. Nelidow and R. M. Diamond, THIS JOURNAL, **59**, 710 (1955).

(31) The maximum comes at a higher HCl concentration with the larger, less soluble diisopropyl ether molecules. With HBr, and even more so with HI, the maximum occurs earlier than with HCl for both of the ethers, *cf.* H. M. Irving and F. J. C. Rossotti, *Analyst*, **77**, 801 (1952).

On the other hand, the extraction of large unhydrated ions shows a better correlation with the dielectric constant of the solvent. Such behavior is most reasonable, as with the large ions there is no primary solvation, so that the secondary electrostatic (orientation) solvation energy, which depends mainly upon the dielectric constant, (*cf.* the Born equation) becomes dominant. For the large ions, low dielectric constant media provide the least (electrostatic) solvation energy, and the loss in transferring from water with its high dielectric constant to the solvent can only partly be compensated for by the electrostatic energy of ion-pairing. Thus, the value of the distribution ratio for such species should increase with the dielectric constant of the solvent. Furthermore, this effect should become more important, the larger the ion, as then the greater is the portion of its solvation energy due to the secondary electrostatic solvation.

These effects are exactly what is observed experimentally. Extraction of the tetramethyl and tetraethyl salts of $InCl_4^-$ into the diethyl, butyl ethyl and dibutyl ethers of low dielectric constant (4.34 at 20° and 3.06 at 25° for diethyl and dibutyl ethers,[32] respectively) is very low, and so for this reason and because the substituted ammonium salt solutions have higher water activities than the acid solutions, the replacement of H^+ by the ammonium cation leads to a marked lowering in the value of the distribution ratio of indium(III), Figs. 1 and 2.[33]

But with methyl benzoate and methyl salicylate, solvents of somewhat higher dielectric constant and of considerably less basic nature, the extraction of the metal acid species is much poorer to start with, and extraction of the substituted ammonium salts may become quite important. In fact, for extraction from 5.0 *m* $N(C_2H_5)_5Cl$–HCl mixtures into these esters, the value of D not only does not decrease with initially decreasing acid concentration, but rises above that from 5.0 *m* HCl alone, Fig. 4.

Methyl benzoate and methyl salicylate also furnish interesting examples of the relative importance of the coördinating power (combination of basicity and steric availability of the basic oxygen or nitrogen) and of the dielectric constant of the solvent in determining the extraction efficiency of the solvent toward acid and salt species. Methyl salicylate has the higher dielectric constant, 9.41 at 30° compared to 6.59 at 20° for methyl benzoate,[32] but the carbonyl oxygen of the former is blocked by internal chelation by the ortho phenol group. As a result, methyl salicylate cannot coördinate as well as the benzoate with the $H_3O(H_2O)_3^+$ ion, and so the extraction of $H_3O(H_2O)_3^+InCl_4^-$ (or other acid[30c]) is poorer with it than with methyl benzoate (by a factor of 10–50 for indium), and this will also be true for extraction of $HInCl_4$ from the mixed acid chloride–alkali chloride solutions which show values of D decreasing in the expected order, LiCl to CsCl, for both solvents. But use of the mixed alkyl ammonium chloride–HCl solutions leads to the extraction of salt species; *i.e.*, $N(C_2H_5)_4^+InCl_4^-$, which do not involve actual solvent coördination. The blocked or unblocked carbonyl group is not important except that its presence in the molecule furnishes a polar group and contributes to the dielectric constant of the solvent. In fact, extraction should be better into methyl salicylate with its higher dielectric constant than into methyl benzoate. And Fig. 4 shows that this is indeed true for extraction from $N(C_2H_5)_4Cl$–HCl solutions. The replacement of only 10% of the acid by the tetraethyl ammonium salt increases the value of D with methyl salicylate about 30 times. In contrast, methyl benzoate, whose D for indium from 5.0 *m* HCl is almost 20 times larger than that of the salicylate, shows an increase in D of only a few per cent. with 10% replacement of the acid by $N(C_2H_5)_4Cl$. In this case, the extraction of the salt, $N(C_2H_5)_4InCl_4$, is almost balanced by the decreased extraction of the solvent coördinated acid, $HInCl_4$.

The ester tributyl phosphate does not show high extractions with the substituted ammonium salts, Fig. 3, and this is primarily due to its superior coördinating ability with the hydrated hydrogen ion. This solvent is the best acid extractant used in the present work; the value of D even at 2.0 *m* HCl is greater than unity. Partly this is due to the basicity of the P→O group, partly to the steric availability of the oxygen of the group.

The ketones, methyl isobutyl and diisobutyl, have somewhat higher dielectric constants than the esters, but, like TBP, they coördinate with hydrated cations, particularly H^+, too well to show any increase in D with replacement of HCl by a tetraalkyl ammonium salt. Again, this can be explained as due to a steric factor. The carbonyl oxygen juts out and so is more available sterically than the ether oxygen for the large $H_3O(H_2O)_3^+$ species, while the greater basicity of the ethers shows up in coördination with smaller molecules such as HCl, D_2O or CH_3OD.[34] This makes the ketonic solvents more advantageous than perhaps has been generally realized for the extraction of complex metal acids.[35]

With β,β'-dichlorodiethyl ether, a solvent of still higher dielectric constant, 21.2 at 20°,[32] and poorer coördinating ability, the extraction of $HInCl_4$ from mixed acid–tetra-substituted ammonium salt solutions gives values of D higher than for extraction from pure HCl itself. The terms involving A^+ in equations 1 and 2 have become dominant, and the latter equation simplifies to

$$\text{d log } D/\text{d log [HCl]} \approx -1/2 \frac{\alpha_{ACl}(H)}{\alpha_{HCl}(H) + \alpha_{ACl}(A)}$$

With initial replacement of acid by alkyl ammonium salt, a large increase in D can be predicted (d log D/d log [HCl] $\approx -\alpha_{ACl}/2\alpha_{HCl}$, initially, with $\alpha_{ACl} > \alpha_{HCl}$). At 5.0 *m* ionic strength, the value of D with 20% $N(C_2H_5)_4Cl$–80% HCl is just 10 times that of 5.0 *m* HCl alone and the plot does, indeed, show a very steep initial increase. With further replacement of HCl by the alkyl ammonium salt, the

(32) A. A. Maryott and E. R. Smith, "Table of Dielectric Constants of Pure Liquids," National Bureau of Standards Circular 514, 1951.

(33) The values of D for indium(III) with dibutyl ether are too small to be measured accurately, so $HFeCl_4$ was used as the distributing metal complex acid.

(34) W. Gordy and S. C. Stanford, *J. Chem. Phys.*, **9**, 204 (1941); **9**, 215 (1941).

(35) V. I. Kuznetsov, *J. Gen. Chem.* (*U.S.S.R.*), **17**, 175 (1947); *cf.*, *C. A.*, **42**, 18e (1948).

value of D drops due to the increasing water activity of the aqueous phase (or decreasing activity coefficients of the aqueous ionic species) on substituting the relatively unhydrated salt for the highly hydrated acid. At 12.6 *m* ionic strength, water activity effects are much greater, and so the rapid increase in water activity with the replacement of HCl by $N(CH_3)_4Cl$ compensates for, or prevents, any marked initial increase in D, as occurs at 5.0 *m*.

With *o*- and *m*-nitrotoluenes, Fig. 8, the still higher dielectric constants 27.4 and 23.8 at 20°,[32] respectively, help the extraction of the non-coördinating alkyl ammonium ions still more relative to that of the solvent coördinating $H_3O(H_2O)_3^+$, so that from a 20% $N(C_2H_5)_4Cl$–80% HCl solution of 5.0 *m* ionic strength there is a 50-fold increase in D over that from 5.0 *m* HCl. This yields a respectable extraction of indium(III). The use of $N(CH_3)_4Cl$ gives a smaller initial increase in D, about a factor of 7, due to its smaller size, hence smaller disturbance of the water structure.

With nitrobenzene, of still higher dielectric constant, 34.8 at 30°,[32] the extraction of large ionic salt species is still further enhanced, Fig. 9. In fact, with nitrobenzene there is even an increase in D over the value in pure HCl solution upon the initial replacement of HCl by CsCl at both 5.0 and 12.6 *m* ionic strengths. Apparently even a pair of ions as small as $Cs^+InCl_4^-$ can achieve sufficient electrostatic solvation in nitrobenzene to be squeezed out of the aqueous phase in preference to $H_3O(H_2O)_3^+$-$InCl_4^-$, a feat which is helped by the weak basicity of nitrobenzene. It is the least basic of the solvents used,[34] even appreciably less so than the nitrotoluenes, and this is reflected in its lower value of D for extraction of $HInCl_4$ from 5.0 *m* HCl than that of the nitrotoluenes. With an unstructured and non-coördinating (non-basic) solvent of high dielectric constant, presumably all the alkali cations would show extraction in the order of increasing (crystallographic) size, the reverse of the order found with the low to moderate dielectric constant solvents studied in this work. That is, since their relative extraction order would be due to their increasing water structure displacement and decreasing loss of first shell and secondary solvation, it would be in the order $Cs^+ > NH_4^+ > K^+ > Na^+ > Li^+$. This is, in fact, the order found for the extraction of the alkali perrhenates and reineckates[36] and of the alkali polyiodides[37] from their own dilute aqueous solutions into nitromethane, giving an almost complete reversal of the order of salt extraction from the quite basic, low dielectric constant ethers to the not so basic but high dielectric constant nitromethane. The reason this reversal in cation order does not show up completely with the $InCl_4^-$ extraction into nitrobenzene may well be the partial dissociation of the complex anion into non-extracting species in the other salt solutions (Factor 3), and is being studied further.

The last solvent studied, 2-ethylhexanol, is representative of the extraction behavior of ionic species into alcohols. The latter are a special class of solvents compared to those already described. For they are hydroxylated solvents with a polar group most similar to that of water; this group can coördinately solvate either cations or anions, that is, the oxygen can coördinate with cations and the hydrogen can hydrogen-bond to anions. All the other classes of solvents used can do only the former, so that anions receive only secondary electrostatic solvation. Since the anion of interest, $InCl_4^-$, has little primary solvation even in water, the ability of 2-ethylhexanol to coördinate (hydrogen-bond) with anions would seem of little direct importance. But for smaller anions, such as Cl^-, which extract relatively poorly into the other classes of solvents, the solvation possible in the alcohol phase leads to higher extraction, relative to large anion species, than with other classes of solvents. As a result, the extraction of $HInCl_4$, or of any other solvent-coordinating species, from HCl solutions into 2-ethylhexanol (or other alcohol), Fig. 10, is much lower than might have been expected for such a basic solvent, because the HCl ties up an appreciable portion of the alcohol molecules and thus decreases their availability for other extracting species. (Also, the hydrogen-bonded alcohol structure, though less complete than that of water, works against the extraction of large ions, cations or anion, in just the same way that the water structure helps squeeze larger ions out into unstructured solvents.) With 12.6 *m* HCl, so much acid extracts and coördinates solvent, that upon replacement of the aqueous HCl by LiCl, the freeing of solvent molecules more than compensates for the mass-action decrease in the value of D for $HInCl_4$, and so the D increases with increasing replacement of HCl by LiCl, at least up to 90% LiCl–10% HCl. Eventually it must, and does, decrease when only $LiInCl_4$ is left to extract, as the salt extracts more poorly than the acid. Similarly, the fact that HCl extracts much better than $CaCl_2$ into 2-octanol, tying up more of the alcohol and decreasing the amount of free solvent, is most likely the explanation for the tapering off in the value of D for $CoCl_2$ extracting from HCl solutions of increasing acid concentration, compared to the continued increase in D for similar $CoCl_2$ extraction from $CaCl_2$ solutions into 2-octanol, as noted by Garwin and Hixson.[8]

(36) H. L. Friedman and G. R. Haugen, *J. Am. Chem. Soc.*, **76**, 2060 (1954).

(37) R. Bock and T. Hoppe, *Anal. Chim. Acta*, **16**, 406 (1957).

THERMODYNAMIC PROPERTIES OF MOLTEN AND SOLID SOLUTIONS OF SILVER CHLORIDE AND LITHIUM CHLORIDE

By M. B. Panish, R. F. Newton, W. R. Grimes and F. F. Blankenship

Chemistry Division, Oak Ridge National Laboratory,[1] *Oak Ridge, Tennessee*

Received August 18, 1958

Free energy data and related thermodynamic quantities have been obtained for solid and liquid solutions of AgCl and LiCl between 300 and 900° from galvanic cells of the type Ag/AgCl, LiCl/Cl_2. Appreciable positive deviations from Raoult's law were observed for the liquid solutions. The effect of composition on the activity of AgCl in the solid solutions suggested that the electrolyte was metastable with respect to separation into two solid phases over a wide range of concentrations.

Introduction

The thermodynamic properties of the AgCl–NaCl system between 300 and 900°, as determined from electrometric measurements, were presented in a previous paper.[2] Due to the mobility of the Ag^+ ion, solid solutions containing AgCl have sufficient electrolytic conductance to be studied at temperatures well below the solidification point.[3] Hence, activity measurements were extended to the solid solution region with the result that evidence of metastable phase behavior was found. For purposes of comparison, a similar investigation of the AgCl–LiCl system was undertaken.

As with AgCl–NaCl, AgCl–LiCl appears to form a continuous series of solid solutions throughout the entire composition range,[4,5] however, there is an earlier phase diagram in which a region of immiscibility is indicated.[6]

Electrometric measurements of the activity of silver chloride in molten AgCl–LiCl have been made previously by Salstrom[7] over a rather small temperature range, the upper limit of which was near 600°. The investigation described here extends the measurements in the liquid range to almost 900°. The two sets of measurements are in very good agreement over the common temperature range.

Experimental

The apparatus and the procedure were the same as used for the AgCl–NaCl system[2] except that additional precautions were taken to avoid contact between LiCl and atmospheric moisture.

Results and Discussion

Liquid Region.—The effect of temperature and of composition on the e.m.f. of the cell Ag/AgCl, LiCl/Cl_2 in the liquid range is shown in Table I. The estimated uncertainty in the e.m.f. values is ±0.5 mv. The cell potentials are linear with temperature and the temperature coefficient increases with increasing concentration of AgCl.

Computed thermodynamic data for AgCl obtained from the electromotive force and its temperature coefficient are given in Table II. Free energies of formation are given by $\Delta F_1 = -23.07E$, where the subscript 1 designates silver chloride, and E is the cell e.m.f. The partial molal free energy of mixing $\bar{F}_1 = \Delta F_1 - \Delta F_1^0$, where the superscript refers to pure silver chloride, is equal to $RT \ln a_1$; thus the activities are based on pure liquid as the standard state. Figure 1 shows the variation of the activity of AgCl with composition at 800°, and includes for comparison a curve for the corresponding behavior in the silver chloride–sodium chloride system. Another comparison between the two systems is provided by the excess free energy of mixing of silver chloride, $\bar{F}_1^E = \bar{F}_1 - RT \ln N_1$,

Table I

Variation of E.M.F. (volts) with Temperature for the Cell

Ag|AgCl (X_1), LiCl|Cl_2
Molten

N_1 = mole fraction of AgCl

T (°C.)	E.m.f. (obsd.)	T (°C.)	E.m.f. (obsd.)	T (°C.)	E.m.f. (obsd.)
N_1 = 1.00		N_1 = 0.815		N_1 = 0.191	
482.0	0.9028	834.0	0.8212	817.0	0.9060
484.0	.9043	830.0	.8236	758.0	.9131
498.8	.8972	543.0	.8993	662.0	.9242
504.0	.8982			658.5	.9256
517.5	.8935	N_1 = 0.585		612.5	.9327
534.5	.8882				
551.6	.8823	887.0	0.8260	N_1 = 0.105	
553.0	.8819	881.0	.8364		
566.0	.8796	780.5	.8552	808.5	0.9439
567.6	.8793	705.0	.8705	774.0	.9498
591.7	.8700	605.0	.8957	768.0	.9505
610.5	.8652	506.0	.9202	758.5	.9514
654.0	.8532			722.5	.9536
659.7	.8532	N_1 = 0.252		720.5	.9538
688.0	.8446			653.5	.9592
695.0	.8422	865.5	0.8838		
698.0	.8417	864.0	.8843	N_1 = 0.0286	
723.6	.8358	765.0	.8970		
744.2	.8298	693.0	.9092	883.5	1.0647
757.0	.8253	633.5	.9174	880.5	1.0648
795.0	.8151	589.5	.9255	855.0	1.0613
800.5	.8148			83[illegible].5	1.0590
		N_1 = 0.238		765.5	1.0542
N_1 = 0.905				715.0	1.0508
		790.5	0.8982	639.5	1.0475
842.0	0.8107	650.5	0.9183		
703.0	.8443				
602.0	.8756				
571.0	.8892				
489.5	.9136				

(1) Operated for the United States Atomic Energy Commission by the Union Carbide Corporation.

(2) M. B. Panish, R. F. Newton, W. R. Grimes and F. F. Blankenship, This Journal, **62**, 1325 (1958).

(3) A. Wachter, *J. Am. Chem. Soc.*, **54**, 919 (1932).

(4) D. S. Lesnykh and A. G. Bergman, *Zhur. Phys. Chem. U.S.S.R.*, **30**, 1959 (1956).

(5) D. S. Lesnykh and A. G. Bergman, *Zhur. Ob. Chem. U.S.S.R.*, **23**, 4 (1953).

(6) "Landolt-Börnstein," Vol. 5 [1], p. 612.

(7) E. J. Salstrom, T. J. Kew and T. M. Powell, *J. Am. Chem. Soc.*, **58**, 1848 (1936).

TABLE II

THERMODYNAMIC PROPERTIES[a] OF MOLTEN SILVER CHLORIDE DILUTED WITH LITHIUM CHLORIDE

N_1 (AgCl)	0.0286	0.105	0.191	0.238	0.252	0.585	0.815	0.905	1.000
$dE/dt \times 10^6$	+68	−87	−133	−143	−147	−223	−265	−289	−289
$\Delta\bar{S}_1$, cal./°C.	+1.57	−2.01	−3.07	−3.30	−3.39	−5.14	−6.11	−6.65	−6.65
$\bar{S}_1$, cal./°C.	8.22	4.64	3.58	3.35	3.26	1.51	0.54	0.0	0.00
$\Delta\bar{H}_1$, cal.	−22720	−24010	−24230	−24230	−24250	−25170	−25740	26080	−25910
$\bar{H}_1$, cal.	3190	1900	1680	1680	1660	740	170	0	0
T, °C.									
600 E (v.)	1.0442	0.9640	0.9338	0.9258	0.9222	0.8970	0.8845	0.8792	0.8700
600 $\Delta\bar{F}_1$ (cal.)	−24100	−22240	−21550	−21358	−21280	−20700	−20410	−20290	−20070
600 F_1	−4020	−2170	−1480	−1290	−1210	−630	−340	−220	0
600 a_1	0.100	0.286	0.427	0.476	0.498	0.697	0.823	0.882	1.00
600 γ_1	3.50	2.72	2.24	2.00	1.97	1.19	1.01	0.98	1.00
700 E	1.0510	0.9555	0.9205	0.9112	0.9078	0.8741	0.8578	0.8500	0.8419
700 ΔF_1	−24250	−22050	−21240	−21020	−20950	−20170	−19790	−19610	−19430
700 $\bar{F}_1$	−4820	−2620	−1810	−1590	−1520	−740	−360	−180	0
700 a_1	0.083	0.258	0.392	0.439	0.456	0.682	0.830	0.909	1.00
700 γ_1	2.90	2.45	2.05	1.84	1.81	1.16	1.02	1.00	1.00
800 E	1.0580	0.9471	0.9072	0.8971	0.8932	0.8520	0.8310	0.8910	0.8138
800 ΔF_1	−24410	−21850	−20930	−20700	−20610	−19660	−19170	−18940	−18780
800 $\bar{F}_1$	−5630	−3070	−2150	−1920	−1830	−900	−390	−164	0
800 a_1	0.072	0.236	0.367	0.407	0.424	0.656	0.830	0.926	1.00
800 γ_1	2.55	2.25	1.92	1.71	1.68	1.12	1.02	1.02	1.00
900 E	1.0646	0.9380	0.8939	0.8830	0.8780	0.8300	0.8050	0.7925	0.7859
900 ΔF_1	−24560	−21640	−20630	−20370	−20260	−19151	−18575	−18290	−18130
900 $\bar{F}_1$	−6430	−3510	−2500	−2240	−2130	−1020	−440	−160	0
900 $\bar{F}_1^C$	1856	1744	1358	1105	1082	230	30	70	0
900 a_1	0.063	0.222	0.343	0.382	0.401	0.645	0.826	0.935	1.00
900 γ_1	2.23	2.11	1.80	1.60	1.59	1.10	1.02	1.02	1.00

[a] Subscript 1 indicates AgCl. E = e.m.f. (estimated error ±0.5 mv.). $\Delta F_1 = -23.07E$ (estimated error ±25 cal.). $\bar{F}_1 = \Delta F_1 - \Delta F_1^0 = RT \ln a_1$ (estimated error ±50). $\bar{F}_1^E = F_1^0 - RT \ln N_1$. $\Delta S_1 = 23.07\, dE/dt$. $\bar{S}_1 = \Delta S_1 - \Delta S_1^0$. a_1 = activity based on pure AgCl (estimated error ±0.45). $\gamma_1 = a_1/N_1$ (estimated error ±0.02).

where N_1 is mole fraction; this quantity as a function of composition at 900° for the two systems is plotted in Fig. 2. Other tabulated quantities are $\Delta S_1 = n\mathfrak{F}dE/dT$, the partial molal entropy of mixing $\bar{S}_1 = \Delta S_1 - \Delta S_0$, also the corresponding heat quantities ΔH_1 and $\bar{H}_1$, and the activity coefficient $\gamma = a/N_1$.

The greater positive deviations of AgCl in LiCl than in NaCl mixtures are consistent with the behavior found by Hildebrand and Salstrom[8] in the AgBr–LiBr and AgBr–NaBr systems at lower temperatures. A tendency toward positive deviations arises from the effect of the electrostatic field of the alkali cations in diminishing the partly covalent character of the Ag–Cl bond. The smaller Li^+ ion is more effective than the Na^+ ion. An alternative viewpoint, suggested by Forland,[9] regards the relatively small volume change on melting of AgCl, compared with alkali chlorides, as an indication of different liquid structures for the pure components; mixing the liquid structures results in an increase in energy content tending to positive deviations. By contrast, an opposing tendency toward negative deviations, expected with cations that differ in size and polarizing properties, predominates in the AgBr–KBr and AgBr–RbBr systems.[8]

Solid Solution Region.—An electrometric determination of the activity of AgCl in AgCl–NaCl solid solutions at 150 and 200° by Wachter[10] gave a smooth continuous curve for activity as a function of composition showing positive deviations at low AgCl concentrations and negative deviations at high AgCl concentrations. In between, there was a region in which the activity of AgCl de-

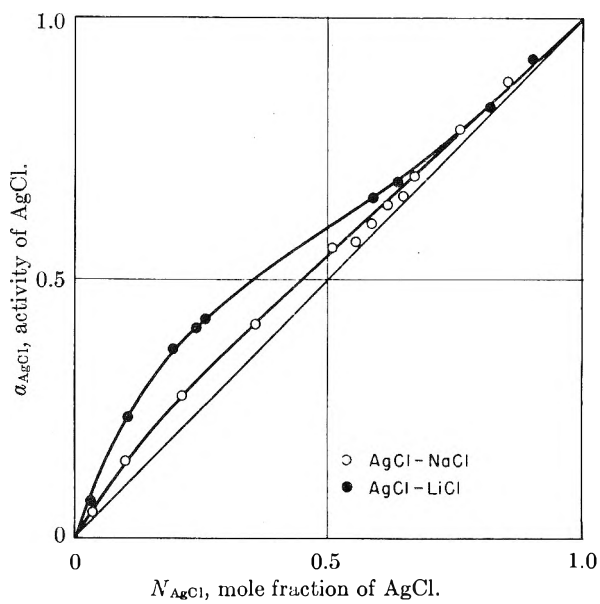

Fig. 1.—The activity of AgCl in AgCl–LiCl and AgCl–NaCl solutions at 800°.

(8) J. H. Hildebrand and E. J. Salstrom, *J. Am. Chem. Soc.*, **54**, 4257 (1932).

(9) T. Forland, Pennsylvania State University, ONR Report No. 69, June 1956.

(10) A. Wachter, *J. Am. Chem. Soc.*, **54**, 919 (1932).

TABLE III

VARIATION OF E.M.F. (VOLTS) WITH TEMPERATURE FOR THE CELLS

Ag|AgCl, LiCl|Cl_2
Solid

N_1 = mole fraction of AgCl

T (°C.)	E.m.f. (obsd.)	T (°C.)	E.m.f. (obsd.)	T (°C.)	E.m.f. (obsd.)	T (°C.)	E.m.f. (obsd.)
N_1 = 1.00		N_1 = 0.191		N_1 = 0.252		N_1 = 0.895	
454.0	0.9232	460.0	0.9368	448.0	0.9532	398.5	0.9681
400.0	.9554	452.5	.9411	441.0	.9542	393.5	.9707
361.0	.9768	440.0	.9473	437.0	.9568	362.0	.9909
318.2	1.003	428.5	.9554	425.0	.9643	330.5	1.010
309.0	1.006	414.5	.9646	399.5	.9764	299.0	1.024
265.3	1.027	409.5	.9631	378.5	.9837		
265.2	1.024	396.5	.9703	356.0	.9948	N_1 = 0.905	
264.3	1.029	394.5	.9735	344.0	.9963		
		392.0	.9721	315.5	1.006	402.5	0.9836
N_1 = 0.105		383.5	.9775	312.0	1.011	401.0	0.9799
		381.5	.9785	283.5	1.019	365.5	1.008
480.0	0.9303	373.5	.9788			349.5	1.015
479.0	.9308	360.0	.9874	N_1 = 0.585		326.5	1.0265
476.0	.9285	358.5	.9884			324.0	1.0250
440.5	.9421	341.5	.9940	421.5	0.9616	322.5	1.0235
434.5	.9449	330.5	1.001	386.5	.9812	301.5	1.0269
419.5	.9506	327.0	0.9973	369.0	.9897		
415.5	.9527	322.0	1.005	343.0	1.001	N_1 = 0.915	
415.0	.9549	321.5	1.001	331.5	1.006		
411.5	.9561	314.5	1.004	307.0	1.013	403.5	0.9564
371.0	.9779	311.5	1.003	302.5	1.014	374.5	.9744
368.0	.9804	304.0	1.013			350.0	.9905
357.5	.9804	290.5	1.011	N_1 = 0.815		319.5	1.006
355.0	.9816					301.0	1.015
340.5	.9891	N_1 = 0.238		407.0	0.9672		
338.5	.9893			403.0	.9672	N_1 = 0.955	
336.5	.9900	433.0	0.9572	397.0	.9706		
		404.0	.9715	373.0	.9836	440.0	0.9377
		389.5	.9727	349.0	.9920	399.0	.9647
		372.0	.9859	347.0	.9935	365.0	.9845
		327.5	1.003	345.5	.9978	342.0	.9929
		299.5	1.013	341.5	.9990	316.0	1.008
						303.5	1.0146

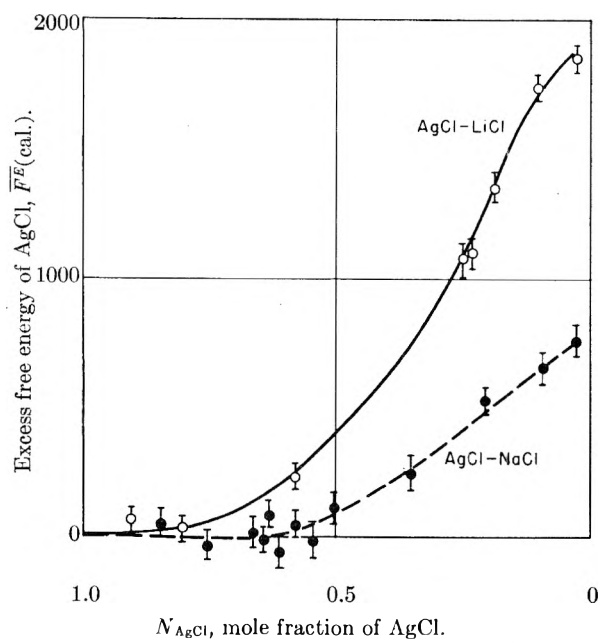

Fig. 2.—The excess free energy of AgCl in AgCl–LiCl and AgCl–NaCl solutions at 900°.

creased with increasing concentration; this was regarded as a demonstration of the freezing in of supersaturated solid solutions which persisted indefinitely although they were metastable with respect to separation into two phases.

When the AgCl–NaCl system was examined in this Laboratory[2] the results for the solid region indicated that the upper consolute temperature for the immiscibility gap was at about 450°. Below the consolute temperature, at 300 and 400°, positive deviations resembling those found by Wachter were obtained but in the region of the immiscibility gap the activity values were too scattered to permit conclusions regarding a continuous decrease in activity with increasing concentration. These considerations led to an interest in the activity of AgCl in AgCl–LiCl solid solutions.

The solid solutions were obtained from liquid solutions by quenching the cell in water. Unmixing of the metastable phases was evidently prevented by the difficulty of nucleation and by the slowness of diffusion in the solid solutions.

The variation of e.m.f. with temperature for the cell

TABLE IV

THERMODYNAMIC PROPERTIES[a] OF SOLID SILVER CHLORIDE DILUTED WITH LITHIUM CHLORIDE

N_1	0.105	0.191	0.238	0.252	0.585	0.815	0.895	0.905	0.915	0.955	1.00
300°											
E	1.008	1.012	1.012	1.015	1.015	1.014	1.022	1.027	1.015	1.015	1.010
ΔF_1	−23250	−23350	−23350	−23420	−23420	−23400	−23580	−23690	−23420	−23420	−23300
$\bar{F}_1$	0	−50	−50	−120	−120	−100	−280	−390	−120	−120	0
a_1	1.0	0.96	0.96	0.90	0.90	0.92	0.78	0.71	0.90	0.90	1.00
400°											
E	0.9161	0.970	0.973	0.975	0.975	0.970	0.967	0.983	0.964	0.964	0.954
ΔF_1	−22170	−22380	−22450	−22490	−22490	−22380	−22310	−22680	−22150	−22240	−22010
$\bar{F}_1$	−160	−370	−440	−480	−480	−370	−300	−670	−140	−140	0
a_1	0.89	0.76	0.72	0.70	0.70	0.76	0.80	0.61	0.91	0.91	1.00

[a] Symbols have the same meaning as in Table II.

$$Ag\left|\begin{matrix}AgCl,\ LiCl\\(solid\ soln.)\end{matrix}\right|Cl_2$$

is shown in Table III. The estimated error in e.m.f. is ±1–3 mv. Data are not given for solid solutions containing less than 10 mole % AgCl because the cell voltage drifted steadily in the direction of increasing AgCl activity. In general the potentials for the solid solutions differed but little from the value for pure AgCl. Consequently the free energies of mixing and the activities in Table IV were not very accurately determined, but are of interest as an approximate representation of the solid solution behavior.

The region in which the measured activities of AgCl resemble those expected for a supersaturated solid solution is more extensive with LiCl than with NaCl. Moreover, one portion of the composition range of the AgCl–LiCl solid solutions appears to provide an example of a decreasing activity of AgCl with increasing concentration.

Greater positive deviations in LiCl rich solid solutions than with NaCl at the same concentration are consistent with the smaller lattice size of LiCl and the view that the positive deviations result from lattice strain.

AQUEOUS SOLUTIONS OF POLYVINYLSULFONIC ACID: PHASE SEPARATION AND SPECIFIC INTERACTION WITH IONS, VISCOSITY, CONDUCTANCE AND POTENTIOMETRY[1]

BY H. EISENBERG[2] AND G. RAM MOHAN

The Weizmann Institute of Science, Rehovot, Israel

Received September 2, 1958

Aqueous solutions of polyvinylsulfonic acid and its salts with various monovalent cations, separate into two liquid phases at high concentrations of added monovalent electrolytes. The phase separation has been studied as a function of temperature, polymer and added electrolyte concentration. The phenomenon is highly specific with respect to the monovalent electrolytes investigated. In the alkali halide series the order of specificity is NaCl < KCl > RbCl and KI > KBr > KCl; no phase separation occurs under similar conditions with HCl, LiCl, CsCl and NH_4Cl. Partial separation of K^+ from Na^+, K^+ from NH_4^+, Rb^+ from NH_4^+ and Na^+ from H^+ in mixtures containing the chlorides of both respective cations has been achieved. From potentiometric and conductimetric titrations polyvinylsulfonic acid is shown to behave as a fully ionized polyelectrolyte. Specific effects with alkali cations are shown, from viscosity and conductivity measurements, to exist also in dilute solutions of the polymer, both in the absence and in the presence of added monovalent electrolytes; they are correlated to the order of specificity of the same cations in phase separation.

Introduction

An investigation of some solution properties of polyvinylsulfonic acid (PVSA) and its salts with metallic monovalent cations led to the discovery of liquid–liquid phase separation phenomena (coacervation)[3] at high concentrations of added monovalent electrolyte. The phase separation depends upon (a) added electrolyte concentration, (b) polymer concentration, (c) temperature, and (d) is highly specific with respect to the monovalent cations and anions investigated.

(a) At a given temperature and polymer concentration there exists a lower and an upper limit of added electrolyte concentration between which phase separation occurs.

(b) At a given temperature and added electrolyte concentration there exists also a lower and an upper limit of polymer concentration between which phase separation occurs.

(c) With increase in temperature phase separa-

(1) Presented at the 134th ACS Meeting, Chicago, September 7–12, 1958.

(2) Mellon Institute, Pittsburgh, Pa. (on leave of absence from Weizmann Institute of Science).

(3) For a discussion of various cases of phase separation in colloid and polyelectrolyte solutions see references 4–7.

(4) M. J. Voorn, *Rec. trav. chim.*, **75**, 317, 405, 427, 925, 1021 (1956).

(5) J. Th. G. Overbeek and M. J. Voorn, *J. Cell. Comp. Physiol.*, **49**, Suppl. 1, 7 (1957).

(6) I. Michaeli, J. Th. G. Overbeek and M. J. Voorn, *J. Polymer Sci.*, **23**, 443 (1957).

(7) H. Thiele and L. Langmaack, *Z. physik. Chem. (Leipzig)*, **206**, 394 (1956).

tion in a given system completely disappears upon mixing the two phases. For each polymer-added electrolyte system there exists a temperature T_p at which phase separation occurs; above T_p the system is homogeneous, whereas below T_p two phases in thermodynamic equilibrium coexist. The plots of T_p against added electrolyte concentration (at constant polymer concentration), and of T_p against polymer concentration (at constant added electrolyte concentration) exhibit distinct maxima in all cases investigated.

(d) With the electrolytes HCl, LiCl, CsCl and NH_4Cl no phase separation occurs down to the freezing points of the solutions. The maximum in the T_p against added electrolyte concentration plots for NaCl and RbCl is at room temperature whereas for KCl it is about 50°. Sulfate and nitrate anions lower the T_p's, whereas bromide and iodide increase them in that order of chloride. The shift in the T_p curves has been used for defining suitable conditions for the partial separation of K^+ from Na^+, K^+ from NH_4^+, Rb^+ from NH_4^+ and Na^+ from H^+ in mixtures containing the chlorides of both respective cations.

The problem of specific interactions with ions in polyelectrolyte solutions and gels is of major interest for an understanding of polyelectrolyte systems; valid criteria are required to determine whether such peculiarities as, for instance, low activity coefficients, low mobilities and many other equilibrium and transport phenomena, may be unequivocally attributed to the non-specific action of the large electrostatic potential (on the multiply charged polyelectrolyte molecule); or whether such phenomena are, in part, or wholly, due to specific binding. We have recently been able to show[8] that no specific interactions with K^+, Na^+ and Li^+ may be inferred from conductance measurements on dilute aqueous solutions of partially ionized polymethacrylic (PMA) and polyacrylic (PAA) acids.[9] These polymeric acids in the fully ionized state are shown below not to exhibit the phenomenon of phase separation with metallic monovalent ions. On the other hand viscosity and conductance measurements on dilute solutions of PVSA and its neutral salts (with and without added electrolyte) indicate that, to some extent, specific interactions responsible for the phase separation phenomena in PVSA, are also reflected in the dilute solution properties of this polymer.

Vinylsulfonic acid (VSA) may be polymerized and conveniently transposed into its well defined salts by neutralization with a suitable base, to yield polymer solutions, the viscosity, conductance and *p*H of which are stable over long periods of time. It will be shown below from both conductance and potentiometric measurements that PVSA constitutes a typical ionophoric[12] polyelectrolyte, entirely analogous in its neutralization behavior to such "strong acids" as HCl for instance, apart from the low activity coefficients of the protons, which appears to be due to the electrostatic potential of the macromolecule.

Vinylsulfonic acid and its salts have first been prepared by Kohler[13] and the early literature on their preparation, polymerization and uses has been summarized in Schildknecht's monograph.[14] More recently Breslow and co-workers[15-17] have given a new synthesis of vinylsulfonic acid and its sodium salt and have studied polymerization, copolymerization and viscosities of the polymers. Dialer and Kerber[18] have studied the viscosity of the Na^+ salts of PVSA and Kern and co-workers[19,20] have studied polymerization, viscosity and potentiometry, and have indicated the importance of the polymer in the catalysis of hydrolytic reactions in peptides and proteins. The monomer used in this investigation has been prepared according to Kohler[13] and was polymerized by ultraviolet radiation in the cold, in concentrated aqueous solution. A polydisperse, unfractionated sample of PVSA (mol. wt. = $(3.5 \pm 0.5) \times 10^4$) was used.

Experimental

Polymerization of VSA, Purification and Molecular Weight (Mol. Wt.) of PVSA.—Fifteen ml. of VSA[13] was distilled *in vacuo* (b.p. 110° at 0.4 mm.) into a quartz flask containing 5 ml. of water, cooled in ice. The 75% clear, colorless, solution of VSA in water was polymerized *in vacuo* in the quartz receiver, in the cold room (at about 4°), by exposure for 16 hours to the light of an AH4 ultraviolet lamp, at about 40 cm. distance. The monomer polymerized to yield a clear gel. It was removed from the polymerization vessel by dissolving in a small amount of water, and dialyzed against conductivity water until no more acidity (from monomer and low polymers diffusing through the dialysis membrane) could be detected in the equilibrating water. During dialysis the volume of the polymer solution increased appreciably because of transport of water into the concentrated polyelectrolyte phase; the polymer solution was periodically concentrated in the dialysis bag by evaporation across the membrane. This was achieved by simultaneous exposure of the dialysis bag to the action of a fan (to evaporate the liquid on the surface of the membrane) and an infrared lamp (to provide enough heat to the evaporating solution to keep it at about room temperature). Finally 80 ml. of a 0.82 eq./l., very viscous solution of PVSA was obtained (corresponding to about 7.1 g. of PVSA). This solution was stored at 4° and was used for all subsequent measurements.

The polymer solution did not absorb bromine and very little ultraviolet absorption could be detected (down to a wave length of 2100 Å.) in the Beckman U.V. spectrophotometer. For elementary analysis the hygroscopic polymer was dried for 5 days *in vacuo* at room temperature, over P_2O_5. The equivalent weight, from titration of solutions of the dried material with standard base, was found to be 120 (theor. 108). Assuming $^2/_3$ molecules of residual water per monomer unit (eq. weight 120) elementary analysis gave: C, found 19.9% (theor. 20%) H, found 4.6% (theor. 4.45); S, found 24.5% (theor. 26.6).

No attempt at fractionation was made in this work. It is likely though that some of the low mol. wt. material was

(8) H. Eisenberg, "International Symposium on Macromolecular Chemistry," Prague, September 1957; *J. Polymer Sci.*, **30**, 47 (1958).

(9) It should be mentioned though that specific effects have been reported for PMA and PAA by Gregor and co-workers[10,11] in solutions of alkali halides and with bulky quaternary ammonium counterions.

(10) H. P. Gregor and M. Frederick, *J. Polymer Sci.*, **23**, 451 (1957).

(11) H. P. Gregor, D. H. Gold and M. Frederick, *ibid.*, **23**, 467 (1957).

(12) R. M. Fuoss, *J. Chem. Ed.*, **32**, 527 (1957).

(13) E. P. Kohler, *Amer. Chem. J.*, **17**, 728 (1897); **20**, 680 (1898).

(14) C. E. Schildknecht, "Vinyl and Related Polymers," John Wiley and Sons, Inc., New York, N. Y., 1952, p. 645.

(15) D. S. Breslow and G. E. Hulse, *J. Am. Chem. Soc.*, **76**, 6399 (1954).

(16) D. S. Breslow, R. R. Hough and J. T. Fairclough, *ibid.*, **76**, 5361 (1954).

(17) D. S. Breslow and A. Kutner, *J. Polymer Sci.*, **27**, 295 (1958).

(18) K. Dialer and R. Kerber, *Makromol. Chem.*, **17**, 56 (1956).

(19) W. Kern, W. Herold and B. Scherhag, *ibid.*, **17**, 231 (1956).

(20) W. Kern and R. C. Schulz, *Angew. Chem.*, **69**, 153 (1957).

removed in the dialysis procedure. The mol. wt. of the dialyzed stock material was estimated by light scattering in 0.5 mole/l. NaCl at λ 4360 Å. and found to be (3.5 ± 0.5) × 10^4 using dn/dc = 0.172 ml./g. (determined in aqueous solution at the Na wave length λ 5890 Å.).

Phase Separation Experiments.—Solutions of PVSA and their neutral salts were made up with concentrated solutions of HCl, LiCl, NaCl, KCl, RbCl, CsCl, NH_4Cl, KI, KBr, $NaNO_3$, KNO_3 and Na_2SO_4 (analytical reagents) and in some cases directly by adding the dry salt (and calculating concentration in moles/l.[21]). The polyelectrolyte–electrolyte solutions were heated with mixing above the phase separation temperature (T_p) to yield clear solutions. On gradually lowering the temperature strong turbidity sharply occurred at T_p and was visually observed; T'_p was reproducible to ±0.2° independently whether approached from a high or a low temperature. Below T_p the solutions almost immediately separated into two liquid phases which were completely clear when the system was kept at a constant temperature for a few hours. The two layers were thoroughly mixed and allowed to separate again to ensure thermodynamic equilibrium; they were then carefully separated with capillary pipets (leaving a small amount around the interphase boundary undisturbed) and samples for analysis were removed from each phase with suitable micropipets (0.025 to 0.100 ml.). The over-all accuracy of the phase separation experiments is estimated to be ±3%.

Analytical Procedures in the Phase Separation Experiments.—Chloride was determined potentiometrically in aqueous 80% acetone, in HNO_3 medium, using $AgNO_3$ standard solution.

For the sulfate analyses known volumes of the polymer solutions were dehydrated over P_2O_5 in Pt boats. The dry samples were combusted in a stream of O_2 at about 700°; SO_2 was absorbed in H_2O_2 solution and titrated with $BaClO_4$, using Thorin as indicator. In the presence of added electrolytes non-volatile sulfates formed in the Pt combustion boats during combustion. In all such cases the residues after combustion were digested with H_2O_2 and titrated as before, after removal of H_2O_2 by boiling.

Ammonium was determined by distillation over NaOH into boric acid and titration of the complex with standard HCl to *p*H 5.2 (mixed methylene blue–methyl red indicator).

The alkali metal cations were determined by flame photometry using a Beckman Model B Flame Spectrophotometer. Potassium was determined at 7680 Å. and Na^+ at 5890 Å. in the concentration range from 10^{-3} to 10^{-4} mole/l. Calibration curves were constructed for K^+ and for Na^+ at constant concentration of 10^{-2} mole/l. of NaCl and KCl, respectively. Also, when analyzing for K^+ in mixed polyelectrolyte–electrolyte solutions (containing both K^+ and Na^+ ions in unknown amounts), these solutions were made 10^{-2} mole/l. with respect to NaCl and *vice versa*. It was found by this procedure that interference due to the presence of the polymer (activity factors, viscosity, sulfonate anion) and foreign alkali cations (in cations distribution experiments) were eliminated and analytical results (±2%) could be obtained.

Viscosity Measurements.—Viscosity measurements were performed at 25° in a modified Ostwald–Fenske capillary viscometer standardized according to ASTM D 445 (Series 50, r = 0.0215 cm., flow time (for 10 ml. H_2O) 245.3 sec., Kroepelin average rate of shear, for H_2O, $\bar{G}$ = 1100 $sec.^{-1}$). Concentrations of PVSA in this work were expressed in equiv./l. of SO_3^- groups and may be transformed into g./ml. by multiplying with 0.108; η_{sp}/c and $[\eta]$ are given in l./equiv. and may be transformed in ml./g. by dividing by 0.108. Viscosities were checked in a Couette viscometer,[22] at a rate of shear G = 1 $sec.^{-1}$, indicating no shear dependence, even in pure aqueous solutions; it should be noted that with the relative low mol. wt. of the polyelectrolyte this result is not surprising.

Special care was taken in the determination of the viscosity of the various PVSA salts in the absence of added electrolyte. These values are very sensitive to slight ionic impurities and the measurements were performed by directly adding concentrated base solution into the viscometer

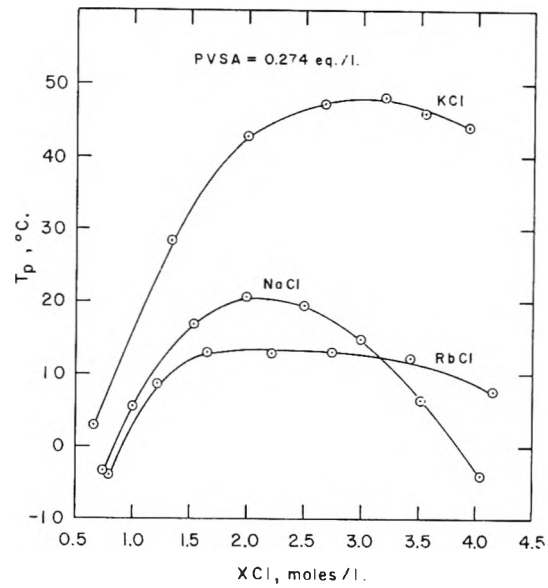

Fig. 1.—Phase separation temperatures T_p at constant concentration of PVSA, with various electrolytes XCl (X = Na, Rb, K).

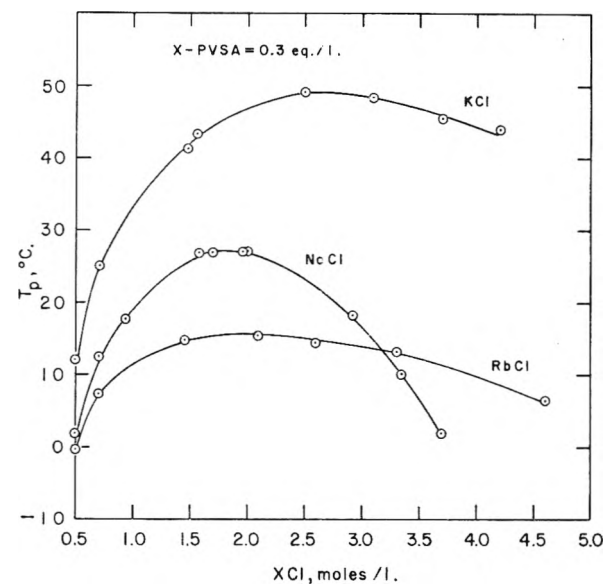

Fig. 2.—Phase separation temperatures T_p, at constant concentration of X-PVSA, with various electrolytes XCl (X = Na, Rb, K).

with an Agla Micrometer Syringe (Manufactured by Burroughs Welcome and Co. London). This all-glass buret delivers a total of 0.5 ml., the smallest graduation corresponding to 0.0002 ml.; a polyethylene capillary tube was used for introducing the titrant directly into the viscometer. The same device also was used for addition of concentrated electrolyte, respectively, polyelectrolyte solution, for all the viscosity conductance and potentiometric measurements.

Conductance Measurements.—Conductance measurements were performed at 2000 cycles per second at 25° using a twin cell compensated for electrode polarization in a circuit recently described.[8] Conductance data were expressed in terms of equivalent conductance $\Lambda = 10^3 \kappa/c$ where κ is the specific conductance of the solution and c the equivalent concentration of ionophoric groups. No frequency effect was observed between 30 and 30000 cycles per second. Carbon dioxide-free water (specific resistance ~ 10^6 ohms) was used throughout and a solvent correction applied. The same water also was used in all the other experiments.

Potentiometric Titration.—Potentiometric titration and *p*H measurements were performed at 25° with a Beckman

(21) H. S. Harned and B. B. Owen, "The Physical Chemistry of Electrolytic Solutions," Reinhold Publ. Corp., New York, N. Y., 1950, p. 556, Table (12-1-1A).

(22) E. H. Frei, D. Treves and H. Eisenberg, *J. Polymer Sci.*, **25**, 273 (1957).

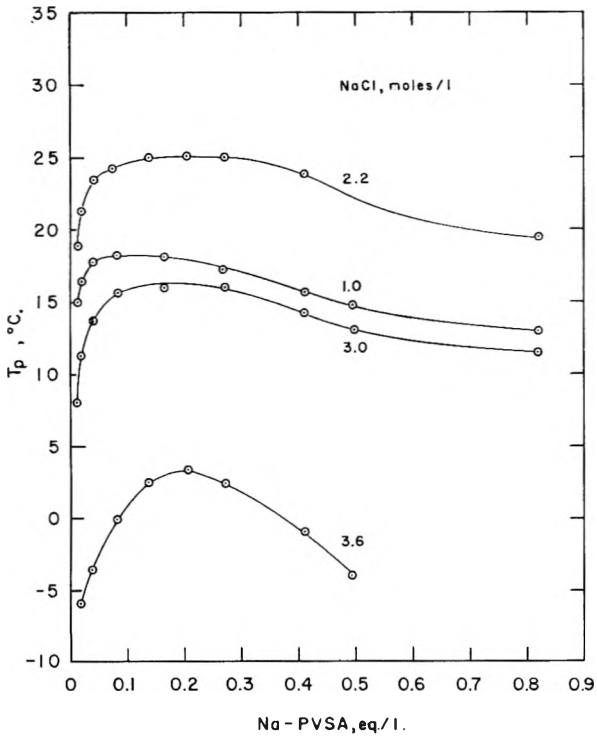

Fig. 3.—Phase separation temperatures T_p, at constant concentrations of NaCl, as a function of Na–PVSA concentration.

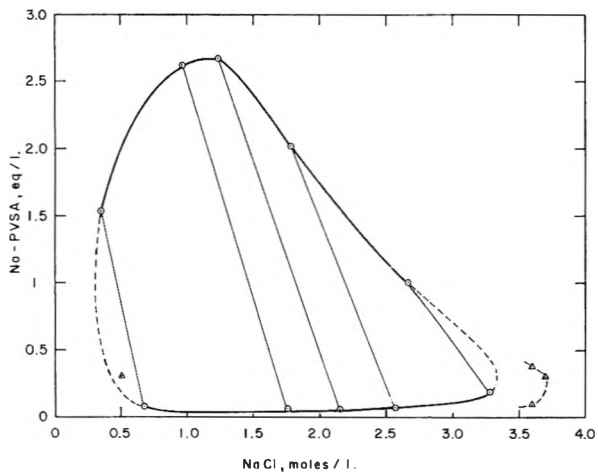

Fig. 4.—Phase diagram of Na–PVSA with NaCl at 0°.

Model G vacuum tube potentiometer using a glass electrode in conjunction with a calomel, saturated KCl, electrode. The readings were standardized with HCl 10^{-1} mole/l. (*p*H 1.085), K-biphthalate 0.05 mole/l. (*p*H 4.01) and Na-borate 0.05 mole/l. (*p*H 9.18).

Results and Discussion

I. Phase Separation Studies. Phase Separation Temperatures.—The phase separation temperatures T_p have been plotted against NaCl, KCl and RbCl concentration for PVSA in Fig. 1 and for PVSA neutralized with the respective bases in Fig. 2. No phase separation occurs in both cases with HCl, LiCl, CsCl and NH_4Cl down to the freezing points of the solution. An examination of Figs. 1 and 2 reveals that, at the low added electrolyte concentration side, the curves seem to be converging (as specific effects are likely to become less pronounced at low electrolyte concentrations); at high concentrations of added electrolyte specific effects predominate and the curves diverge markedly. All curves exhibit a distinct maximum, showing that the two phases recombine, at constant temperature, with excess electrolyte. The curves for PVSA in Fig. 1 are lower than the corresponding curves for its neutral salts in Fig. 2; this is due to the fact that the H^+ ions lower T_p (no coacervation for HCl). At high concentration of added electrolytes, though, when the mole fraction of H^+ decreases because of the high concentration of neutral salt, the curves for PVSA converge with the curves for X–PVSA (where X represents Na, K and Rb, respectively) as can be easily seen by superimposing Figs. 1 and 2. The effect on T_p of change of polymer concentration (Na–PVSA) at constant NaCl concentrations is shown in Fig. 3.

The remarkable feature of both Figs. 1 and 2 is the order of the cations with respect to phase separation. We choose to define order of specificity with respect to phase separation in a certain cation series in terms of the order in which substitution of one cation by another produces an increase in T_p at corresponding ionic strength. Considering the alkali metal cations we find the following order: $(Li^+) < Na^+ < K^+ > Rb^+ > (Cs^+)$. Phase separation thus does not follow the order of the hydrated ionic radii. This is further exemplified by the observation that no phase separation occurs with NH_4Cl in spite of the fact that both NH_4^+ and K^+ are known to have nearly identical ionic radii in aqueous solution.

A series of measurements were performed to determine the influence of the anions in the phase separation experiments. Thus it was found that no phase separation occurs with Na_2SO_4 whereas with K_2SO_4 the maximum of the T_p against salt concentration curve is around 9° (at about 0.5 mole/l. of K_2SO_4); sulfate anion thus lowers T_p as compared with Cl^-. The maximum in the curve for KNO_3 also lies at about 9° (at about 1.4 moles/l. of KNO_3). In the halogen ion series the maximum for KBr lies at 69° (at about 4 moles/l. of KBr) and for KI no maximum was observed as T_p is above the boiling point of the solutions, from 1.4 moles/l. KI concentration. The order for phase separation is thus $I^- > Br^- > Cl^-$ in this series.

Phase Diagrams at Constant Temperature.—The phase separation of a solution of Na–PVSA with NaCl may be represented by a three dimensional surface in the rectangular coördinate system NaCl–NaPVSA–temperature. Above this surface no phase separation occurs whereas below this surface two phases coexist; at the surface $t = T_p$ and at the apex of the surface $t = T_c$, the critical phase separation temperature for this sample of Na–PVSA in solutions of NaCl. Figure 2 represents a section through this surface at constant Na–PVSA and Fig. 3 a number of sections at constant NaCl concentrations. An isothermal section through the surface represents the miscibility gaps in terms of the two components Na–PVSA and NaCl. While it is, in principle, possible to construct the isothermal sections from a study of the phase separation temperatures T_p, no information on the tie-lines, *i.e.*, the lines connecting conjugate phases in

TABLE I

PHASE SEPARATION DATA FOR Na–PVSA WITH NaCl, AT 0°

Concentrations are in equiv./l. of ions.

No.		Cl^-	SO_3^-	Na^+	$\frac{(SO_3^-)_{co}}{(SO_3^-)_{eq}}$	$\frac{(Na \times Cl)_{co}}{(Na \times Cl)_{eq}}$
1	Equil. liq.	0.67	0.073	0.75	20.9	1.34
	Coacervate	0.355	1.53	1.88		
2	Equil. liq.	1.75	0.063	1.81	41.6	1.07
	Coacervate	0.96	2.62	3.58		
3	Equil. liq.	2.15	0.054	2.20	50.0	1.04
	Coacervate	1.23	2.66	3.90		
4	Equil. liq.	2.57	0.063	2.63	31.9	1.02
	Coacervate	1.79	2.01	3.80		
5	Equil. liq.	3.28	0.183	3.46	5.5	0.86
	Coacervate	2.66	1.00	3.66		

thermodynamic equilibrium, may be obtained by this procedure. To obtain the tie-lines it is necessary to lower the temperature below T_p and to study the composition of the two coexisting phases in thermodynamic equilibrium. Using this procedure for a number of NaCl and polymer concentrations at the same temperature (0°), a set of points, connected by tie-lines in pairs, were obtained. The closed curve described by these points (the circles in Fig. 4) represents an isothermal cut through the phase surface, in the two coördinates Na–PVSA (based on the analytical data for SO_3^-) and NaCl (based on the analytical data for Cl^-). The position of the dotted portions of the curve is uncertain.

The analytical results for the phase separation diagram in Fig. 4 are tabulated in Table I. We have tabulated the ratios of the polymer concentrations $(SO_3^-)_{co}/(SO_3^-)_{eq}$ of the coacervate (co) to equilibrium (eq) phases, and the ratios of the mass products of NaCl in the two phases. The latter $(Na \times Cl)_{co}/(Na \times Cl)_{eq}$ may be identified with the ratios of the corresponding activity coefficients, this constituting a statement of the Donnan equilibrium between the two phases.

Effect of Polymer Polydispersity on Phase Separation.—It already has been stated above that it is, in principle, possible to construct the phase surface and to obtain the isothermal sections from a study of the phase separation temperatures T_p. The intersections in Fig. 2 of the NaCl curve for Na–PVSA = 0.3 equiv./l. with $t = 0°$ and the intersection in Fig. 3 of the curve for NaCl = 3.6 moles/l. with $t = 0°$ have been plotted (triangles) in Fig. 4. For a monodisperse polymer the data obtained by both procedures should lie on the same curve. For a polydisperse polymer the phase diagram in Fig. 4 represents an "apparent" phase diagram only, in which the polydispersity of the polymer has not been taken into consideration. Polymer fractionation may occur in the polydisperse polymer solution, in the experiments involving separation into two phases (below T_p) and is likely to shift the points on the "apparent" phase diagram in a way dependent on the polymer mol. wt. distribution curve.

Polymer fractionation was indeed observed in the phase separation experiments. A solution of Na–PVSA = 0.8 equiv./l. in 0.53 mole/l. NaCl was cooled to 0° ($T_p = 2.5°$) and the supernatant and coacervate phases, which were nearly equal in volume, were analyzed for SO_3^-; the polymer concentrations were found to be in the ratio of 1:7. Aliquots from the supernatant and coacervate solutions were made up to NaCl = 0.5 mole/l. and the limiting viscosity numbers $[\eta]$ were determined in this solvent. It was found that $[\eta]$ in the supernatant was 2.37 l./equiv. and in the coacervate phase 4.6 l./equiv. This is to be compared to $[\eta] = 3.8$ l./equiv. (see Fig. 13 below) for the original polymer, before phase separation. It is planned to study the fractionation effect and the influence of mol. wt. on T_p, polymer and salt distribution in a subsequent work.

Preliminary Observations on Other Polyelectrolyte Systems.—The question arises whether the phenomenon of phase separation of fully ionized polyelectrolytes (having a high fixed charge density) with monovalent ions is a general phenomenon or is restricted to a few selected systems in which phase separation is brought about by specific action of certain cations and anion pairs only. With *Na metapolyphosphate* liquid–liquid phase separation was achieved in NaCl and KCl solution but here the T_p's for NaCl were much higher than those for KCl, in distinct contrast to PVSA. No phase separation was achieved with LiCl, RbCl and CsCl. *Polyvinylpyridonium butyl bromide* precipitated in a gel phase with NaCl, KCl and KBr when the solution was heated and redissolved upon *cooling;* the interesting observation for polyvinylpyridonium butyl bromide is the negative temperature coefficient of phase separation which leads to precipitation when heat is supplied to the system. A similar effect was observed[23] in a non-ionized polymer system (polymethacrylic acid in methanol–ether mixture) when polymer fractions were precipitated by heating the solution and redissolved by cooling the system. Aqueous solutions of slightly ionized PMA were also shown by Silberberg, Eliassaf and Katchalsky[24] to separate into two phases with increase in temperature whereas no phase separation was observed in the case of PAA; similar observations also were reported by these authors with respect to gelation of the polymer solutions.

Fully neutralized polymethacrylic and polyacrylic acids did not show phase separation with monovalent ions in aqueous solution. When a drop of

(23) A. Katchalsky and H. Eisenberg, *J. Polymer Sci.*, **6**, 145 (1951).

(24) A. Silberberg, J. Eliassaf and A. Katchalsky, *ibid.*, **23**, 259 (1957).

TABLE II

PHASE SEPARATION DATA FOR PVSA WITH NaCl, AT 0°

Concentrations are in equiv./l. of ions.

No.		Cl^-	SO_3^-	H^+	Na^+	$\frac{(SO_3^-)_{co}}{(SO_3^-)_{eq}}$	$\frac{(Na \times Cl)_{co}}{(Na \times Cl)_{eq}}$	$\frac{(H \times Cl)_{co}}{(H \times Cl)_{eq}}$	$\frac{(Na^+/H^+)_{co}}{(Na^+/H^+)_{eq}}$
1	Equil. liq.	1.06	0.084	0.278	0.87	19.5	1.41	0.72	1.98
	Coacervate	0.66	1.63	0.320	1.97				
2	Equil. liq.	1.41	0.030	0.278	1.16	67.5	1.36	0.62	2.22
	Coacervate	0.86	2.02	0.281	2.60				
3	Equil. liq.	2.09	0.030	0.278	1.84	67.8	0.91	0.49	1.88
	Coacervate	1.18	2.04	0.239	2.97				
4	Equil. liq.	2.61	0.047	0.278	2.37	44.2	0.90	0.51	1.76
	Coacervate	1.62	2.05	0.229	3.44				
5	Equil. liq.	3.08	0.064	0.278	2.87	26.2	0.88	0.56	1.57
	Coacervate	2.16	1.68	0.224	3.61				
6	Equil. liq.	3.68	0.13	0.280	3.53	8.5	0.79	0.58	1.37
	Coacervate	2.78	1.10	0.213	3.67				

methanol was added to a solution in NaCl the polymers precipitated in the form of a sticky gel and in the case of KCl in the form of fine powders. The precipitates redissolved upon heating the systems and reprecipitated upon cooling; attempts to remove the methanol by repeated washing of the precipitates with concentrated salt solutions, solution and precipitation by heating and cooling, did not alter this phenomenon. It appears thus that addition of a small amount of methanol to these polymeric acids (which had not been exposed to any organic solvents during their preparation) irreversibly changes the nature of their behavior toward phase separation with monomeric ions; specific, irreversible solvation with methanol in preference to water is suspected to be responsible for this behavior.

No phase separation was observed with a sample of *Na polyvinyl phosphate* with either NaCl and KCl. *Sodium polystyrene sulfonate* flocculated with NaCl and KCl and was redissolved by increasing the temperature. Butler, Robins and Shooter[25] fractionated polystyrenesulfonic acid by precipitation with concentrated HCl and Mock and Marshall[26] used KI for the same purpose.

It was reported recently by Schachat and Morawetz[27] that dialysis equilibrium measurements of carrageenin, an acidic polysaccharide with half-ester sulfate groups, gave no evidence of a selective affinity for K^+ over Na^+, although this polymer precipitates with K^+ salts but not with Na^+ salts at similar concentrations.

Unequal Distribution of Ions by Phase Separation in Mixed Electrolyte Systems.—In mixed electrolyte systems, unequal distribution of cations (and probably also of anions) may be achieved under suitable conditions. Phase separation at 0° of a solution of PVSA = 0.274 equiv./l. in the presence of varying amounts of NaCl has been studied and the results are listed in Table II; the selectivity coefficients $(Na^+/H^+)_{co}/(Na^+/H^+)_{eq}$ are shown in the last volume of Table II and are seen to depend on NaCl concentration. An examination of Tables I and II shows that the ratios $(SO_3^-)_{co}/(SO_3^-)_{eq}$ exhibit a pronounced maximum at intermediate concentration of NaCl; the ratios $(Na \times Cl)_{co}/(Na \times Cl)_{eq}$ monotonously decrease from values larger than unity at low NaCl concentrations to values lower than unity with increase in NaCl concentration; the values of $(H \times Cl)_{co}/(H \times Cl)_{eq}$ in Table II were always lower than unity and exhibit a significant minimum at intermediate NaCl concentrations. The individual activity coefficients of the components in the separate phases and in the polyelectrolyte solutions before phase separation occurs have not been determined at this stage.

Phase separation experiments for the study of the distribution of the cations from mixtures of KCl and NaCl, KCl and NH_4Cl, and RbCl and NH_4Cl are summarized in Table III. Phase separation was studied at temperatures intermediate between the T_p's of the respective cations at a given ionic strength. It was found that the concentration of the cation for which separation occurs at a higher temperature is selectively higher in the coacervate phase. For example, in the cases examined, $(K^+/Na^+)_{co}/(K^+/Na^+)_{eq} = 1.28$ and $(K^+/NH_4^+)_{co}/(K^+/NH_4^+)_{eq} = 1.56$, and $(Rb^+/NH_4^+)_{co}/(Rb^+/NH_4^+)_{eq} = 1.25$. Complete separation of ions could probably be achieved by means of a suitable counter current systems.

II. Solution Properties. Potentiometric Titration.—In potentiometric titration PVSA behaves as a typical ionophoric electrolyte and titration with base involves straightforward displacement of H^+ by alkali cations; potentiometric titration measures the water formation reaction $H^+ + OH^- \rightleftarrows H_2O$ and changes in pH values may be related within the limits of their formal definition, to changes in the negative logarithms of the activities of the protons in the polyelectrolyte solution. The upper curve in Fig. 5 represents the titration of PVSA with NaOH in aqueous solution (in the absence of extraneous electrolyte). The lower points have been obtained by the same titration in 0.1 mole/l. LiCl, NaCl and KCl; the lower curve represents the titration of HCl at the same concentration and it is seen that all points determined in the polyelectrolyte titration in the presence of 0.1 mole/

(25) J. A. V. Butler, A. B. Robins and K. V. Shooter, *Proc. Roy. Soc.* (*London*), **A241**, 299 (1957).

(26) P. A. Mock and C. A. Marshall, *J. Polymer Sci.*, **17**, 591 (1955).

(27) R. E. Schachat and H. Morawetz, THIS JOURNAL, **61**, 1177 (1957).

TABLE III

PHASE SEPARATION DATA FOR SEPARATION OF CATIONS FROM MIXED ELECTROLYTES WITH COMMON ANION (Cl^-)

(a) K^+/Na^+

	t, °C.	Cl^-	SO_3^-	Na^+	K^+	K^+/Na^+	$\frac{(K^+/Na^+)_{co}}{(K^+/Na^+)_{eq}}$	$\frac{(K \times Cl)_{co}}{(K \times Cl)_{eq}}$	$\frac{(Na \times Cl)_{co}}{(Na \times Cl)_{eq}}$
Orig. soln.		1.04	0.62	0.81	0.81	1.00			
Equil. liq.	25	1.10	0.14	0.68	0.61	0.90	1.28	1.64	1.28
Coacervate		0.70	2.32	1.37	1.57	1.15			

(b) K^+/NH_4^+

	t, °C.	Cl^-	SO_3^-	NH_4^+	K^+	K^+/NH_4^+	$\frac{(K^+/NH_4^+)_{co}}{(K^+/NH_4^+)_{eq}}$	$\frac{(K \times Cl)_{co}}{(K \times Cl)_{eq}}$	$\frac{(NH_4 \times Cl)_{co}}{(NH_4 \times Cl)_{eq}}$
Orig. soln.		1.02	0.62	0.83	0.81	1.03			
Equil. liq.	25	1.06	0.21	0.73	0.56	0.76	1.56	1.82	1.16
Coacervate		0.76	1.82	1.19	1.42	1.19			

(c) Rb^+/NH_4^+

	t, °C.	Cl^-	SO_3^-	NH_4^+	Rb^+	Rb^+/NH_4^+	$\frac{(Rb^+/NH_4^+)_{co}}{(Rb^+/NH_4^+)_{eq}}$	$\frac{(Rb \times Cl)_{co}}{(Rb \times Cl)_{eq}}$	$\frac{(NH_4 \times Cl)_{co}}{(NH_4 \times Cl)_{eq}}$
Orig. soln.		1.53	0.79	0.89	1.42	1.60			
Equil. liq.	0	1.72	0.29	0.80	1.19	1.49	1.25	1.31	1.05
Coacervate		1.34	1.74	1.08	2.01	1.86			

l. added salts lie on the HCl titration curve. The difference between the two titration curves in Fig. 5

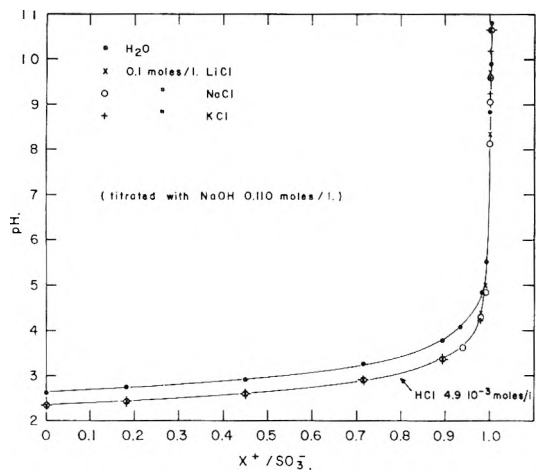

Fig. 5.—Potentiometric titrations of PVSA: $c_{PVSA} = 4.92\ 10^{-3}$ eq./l.

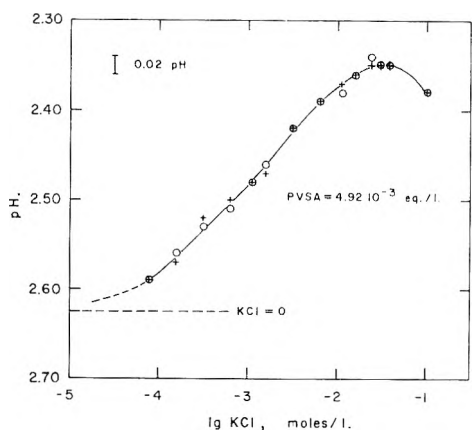

Fig. 6.—pH of PVSA as a function of KCl concentration.

equals 0.26 pH unit and is constant along the whole titration curve. This parallel shift is characteristic of ionophoric polyelectrolytes[28] and reflects the

(28) See A. R. Peacocke and S. Lifson (*Bioch. Bioph. Acta*, **22**, 191 (1956)) for a discussion of a parallel shift in the titration curves in the much more complicated case of deoxyribonucleic acid.

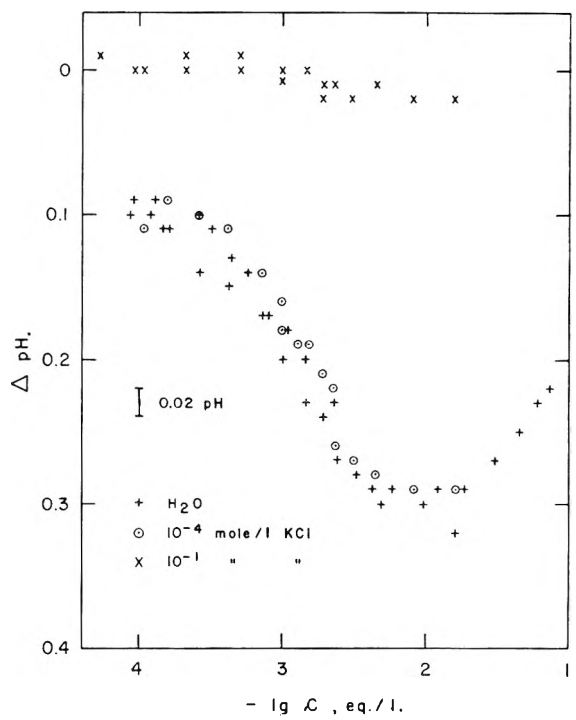

Fig. 7.—Potentiometric dilution titrations of PVSA (ΔpH is the difference between the pH of the PVSA solution and the pH of a solution of HCl at the same concentration of KCl).

fact that the electrostatic potential, which determines the activity coefficients,[29] does not change in dilute solutions along the titration curve by substitution of one cation by another. Upon addition of 0.1 mole/l. neutral salt, the large electrostatic potential is screened off and the pH values decrease to those encountered in monomeric electrolytes (lower curve in Fig. 5). The pH values (within the limits of the accuracy of the experiments) are not sensitive to specific interactions of the ions with the polyelectrolyte molecule. In Fig. 6 we have plotted pH of a PVSA solution (4.92×10^{-3} equiv./

(29) For a calculation of activity coefficients using polyelectrolyte models see references 30 and 31.

(30) A. Katchalsky and S. Lifson, *J. Polymer Sci.*, **11**, 409 (1953).

(31) R. A. Marcus, *J. Chem. Phys.*, **23**, 1057 (1955).

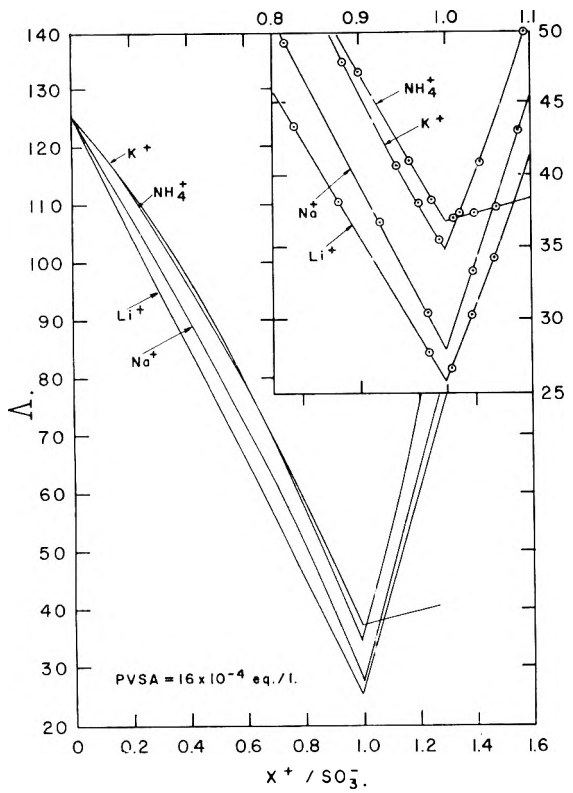

Fig. 8.—Conductimetric titrations of PVSA with LiOH, NaOH, KOH and NH_4OH, at 25°.

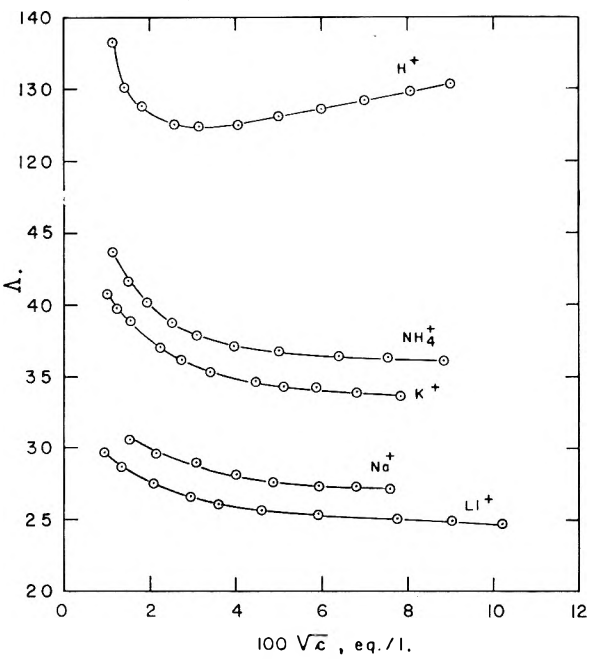

Fig. 9.—Equivalent conductances Λ of solutions of PVSA and its Li, Na, K, and NH_4 salts; t = 25°.

l.) as a function of the logarithm of KCl concentration over the range for KCl = 0 to KCl = 0.1 mole/l.

It is interesting to compare the difference in the behavior of PVSA in Figs. 5 and 6 with the titration behavior of a typical ionogenic[12] polyelectrolyte, PMA,[32] which already has been discussed by

(32) A. Katchalsky, N. Shavit and H. Eisenberg, *J. Polymer Sci.*, **13**, 69 (1954).

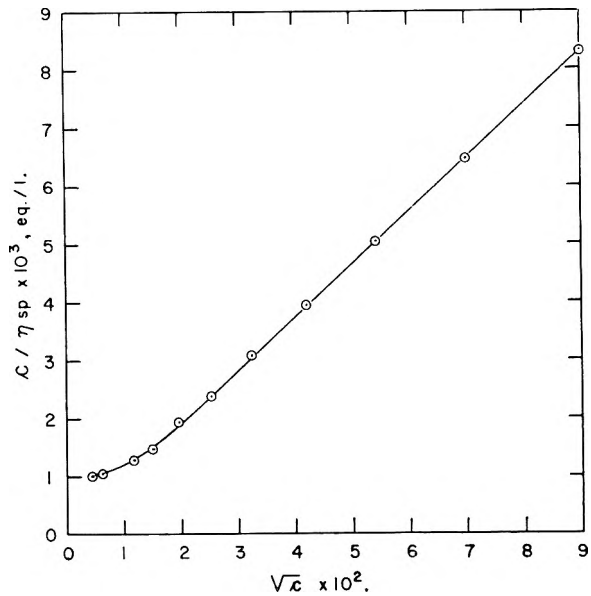

Fig. 10.—Reciprocal viscosity numbers c/η_{sp} of aqueous solutions of PVSA at 25°.

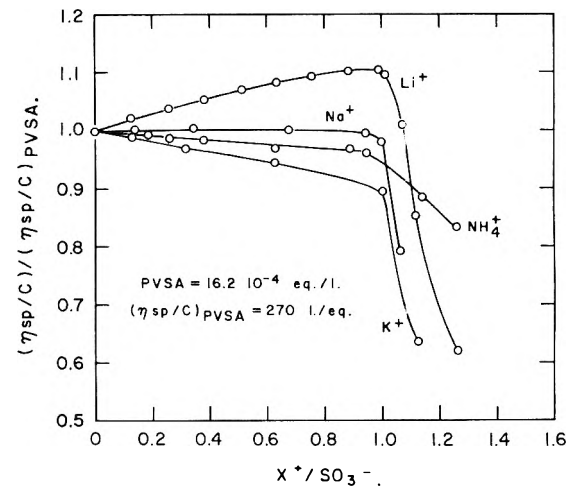

Fig. 11.—Viscometric titrations of PVSA with various bases XOH (X = Li, Na, K and NH_4); t = 25°.

Kern and Schulz.[20] Whereas in PMA, at half neutralization, the pH may change by a few pH units[32] upon increasing the ionic strength, the maximum change in the pH observed in the case of PVSA is of the orders of a few tenths of a pH unit. This is due to the fact that, whereas in an ionogenic polyelectrolyte the electrostatic potential participates in the dissociation equilibrium of the polymeric acid and effectively reduces the availability of protons in solution by the chemical reaction $COO^- + H^+ \rightleftarrows COOH$, in the case of PVSA only the activity coefficients of the protons are influenced by the electrostatic potential, and not their concentrations.

In Fig. 7 we have plotted ΔpH (pH of the PVSA solution minus pH of an HCl solution at the same concentration of acid and of KCl) of PVSA solutions as a function of concentration of PVSA. It is seen that (a) ΔpH is practically identical in aqueous and 10^{-4} mole/l. KCl solutions over the whole concentration range, (b) ΔpH in these solutions increases with decreasing concentration and then decreases with further decrease in concentra-

tion and (c) ΔpH in 10^{-1} mole/l. KCl is practically equal to zero and very slightly increases at higher concentrations.

Conductance Measurements in the Absence of Added Electrolytes.—In Fig. 8 we have plotted conductivity titrations of PVSA with LiOH, NaOH, KOH and NH_3 at 25°, which again bring out the essential features of the titration of a "strong" acid with three "strong" and one "weak" (NH_3) bases. The equivalent conductances Λ, though, are much lower than in simple ionophoric electrolytes and the titration curves exhibit a slight curvature.

In Fig. 9 the values of Λ of PVSA, and its neutral salts, have been plotted (for convenience) against $\sqrt{c}$. It is seen that while the equivalent conductances of the neutral salts show the familiar increase with decrease in concentration as observed in ionophoric polyelectrolyte systems,[33] the equivalent conductance of PVSA goes through a minimum with decrease in concentration. Also, while it was found[8] that for PMA the changes in Λ for pairs of the three counterions (K^+, Na^+ and Li^+) could be represented by the difference in the limiting equivalent counterion conductance $\lambda^0_{X^+} - \lambda^0_{Y^+}$ multiplied by a constant ϕ smaller than unity (ϕ is independent of the concentration and of the nature of the counterion), no such regularity exists in the case of PVSA. Indeed the conductance of NH_4–PVSA is significantly higher than that of K–PVSA although $\lambda^0_{NH_4^+} - \lambda^0_{K^+} \sim 0$; an examination of Table IV in which

$$\phi = (\Lambda_{X-PVSA} - \Lambda_{Y-PVSA})/(\lambda^0_{X^+} - \lambda^0_{Y^+})$$

is shown for the ion pairs investigated ($c = 16 \times 10^{-4}$ equiv./l.), brings out clear effects of specific interactions. The irregularity in the values in Table IV is due to the fact that the curves in Fig. 9 for K^+ and Na^+ (ions for which specific interactions are expected) are shifted to lower values of Λ with respect to the curves for H^+, NH_4^+ and Li^+ (ions for which no evidence of specific interactions has been detected).

TABLE IV

ϕ VALUES FROM CONDUCTANCE MEASUREMENTS OF PVSA, WITH VARIOUS CATIONS, IN SALT-FREE SOLUTIONS[a]

	—NH_4^+	—K^+	—Na^+	—Li^+
H^+	0.319	0.326	0.324	0.313
NH_4^+		Very large	0.382	0.323
		K^+	0.294	0.264
			Na^+	0.202

[a] $c_{PVSA} = 16 \times 10^{-4}$ equiv./l. $\Lambda_{PVSA} = 125.0$; $\Lambda_{NH_4-PVSA} = 36.9$; $\Lambda_{K-PVSA} = 34.9$. $\Lambda_{Na-PVSA} = 28.0$; $\Lambda_{Li-PVSA} = 25.7$.

Viscosity Measurements.—The viscosity numbers of PVSA in water increase with decreasing concentration in a manner similar to all polyelectrolytes; no maximum in the curve has been found down to the lowest concentrations investigated (2×10^{-5} equiv./l.). The reciprocal viscosity numbers have been plotted against $\sqrt{c}$ in Fig. 10 in the familiar Fuoss plot.[34] The plot is linear over a wide range of concentrations and shows upward curvature below 4×10^{-4} equiv./l. The values of η_{sp}/c, particularly at low polymer concentrations, are much larger than would correspond to non-interacting, stretched rods. Quantitative discussion is postponed until data on discrete polymer fractions will be available.

In Fig. 11 viscometric titrations of aqueous solutions of PVSA with a number of bases have been plotted. With LiOH the viscosity increases up to the equivalence point and sharply drops with further addition of base (screening effect due to extraneous electrolyte). With NaOH the viscosity is nearly

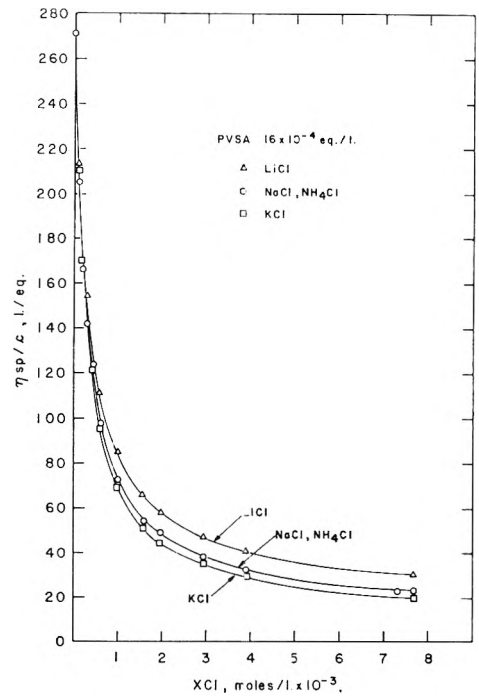

Fig. 12.—Viscosity numbers η_{sp}/c of solutions of PVSA as a function of concentration of added electrolyte XCl (X = Li, Na, K and NH_4): $t = 25°$.

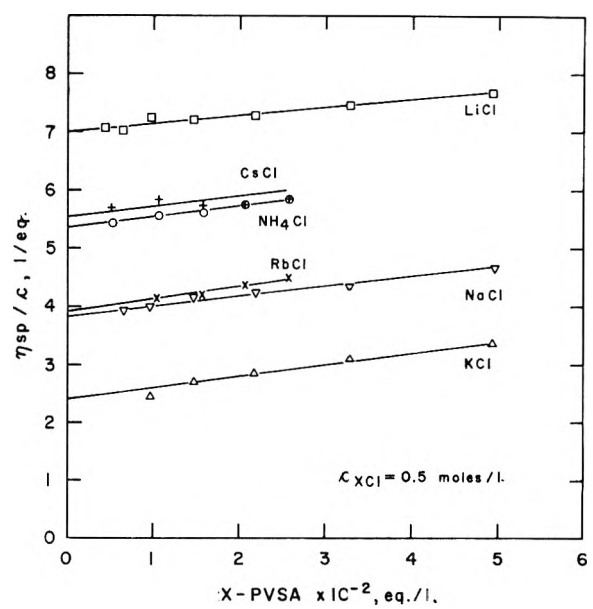

Fig. 13.—Viscosity numbers η_{sp}/c of solutions of X–PVSA at 0.5 mole/l. of added electrolytes XCl (X = Li, Na, K, Rb, Cs and NH_4); $t = 25°$.

(33) R. MacFarlane, Jr., and R. M. Fuoss, *J. Polymer Sci.*, **23**, 103 (1957).

(34) R. M. Fuoss, *Disc. Faraday Soc.*, **11**, 125 (1957).

constant over the whole neutralization range, a slight drop is registered over the same range with NH_3, and a pronounced decrease with KOH.

The influence of added electrolytes on the viscosity has been tested by addition of various electrolytes to a solution of PVSA (Fig. 12); the viscosity drops sharply with increase in added electrolyte concentration. The order of viscosities in the various electrolyte solutions is LiCl > NaCl, NH_4Cl > KCl.

Clear cut evidence of specific interactions is shown in Fig. 13 where η_{sp}/c of salts of PVSA with various cations has been plotted against polymer concentration, in the presence of 0.5 mole/l. added electrolyte concentrations. The order of the viscosities exactly follows the pattern exhibited in the phase separation experiments. In the presence of LiCl, $[\eta]$ is highest and decreases by a factor of 3 for KCl, NaCl being intermediate. With RbCl the viscosity is higher than for KCl, being nearly identical with the solutions in NaCl. In CsCl there is a further increase in viscosity and about the same values are obtained for NH_4Cl. Figure 13 may be interpreted in a straightforward manner. The phenomenon of phase separation has been shown to be due to specific interactions of the polyelectrolyte ion with various counter and co-ions. It may be assumed that solutions of electrolytes (such as LiCl, CsCl and NH_4Cl) in which no phase separation occurs are better solvents than solutions of electrolytes (such as RbCl, NaCl and particularly KCl) in which phase separation does occur. It is known from non-ionic polymers[35] that in good solvents more extended configurations of the macromolecules are favored, leading to higher values of η_{sp}/c and $[\eta]$. In poor solvents, and particularly near the phase separation point, the polymeric coils assume a more compact shape, corresponding to their "unperturbed"[35] dimensions. This is exactly the result exemplified in Fig. 13 in which the viscosities are shown to follow the order LiCl > NaCl > KCl < RbCl < CsCl, NH_4Cl, in direct correlation to the order in which phase separation occurs with the same electrolytes.

We have also measured $[\eta]$ of Na–PVSA in 1.0 and 0.5 mole/l. of Na_2SO_4; it was found that the two values were identical $[\eta]$ = 4.0 l./equiv. At 0.1 mole/l. of $NaSO_4$ $[\eta]$ = 6.0 l./equiv.

Acknowledgments.—The sulfur and chloride determination were performed by Mr. E. Meyer, Head of the Microchemical Laboratory at the Weizmann Institute, to which we express our sincerest thanks for his work. We also gratefully acknowledge the help of Dr. K. Schallinger of the Israeli Government Agricultural Station in Rehovot, for the flame photometry measurements.

(35) R. J. Flory, "Principles of Polymer Chemistry," Cornell University Press, Ithaca, N. Y., 1953.

THE INTERACTION OF KRYPTON WITH METALS. AN APPRAISAL OF SEVERAL INTERACTION THEORIES[1]

BY R. A. PIEROTTI[2] AND G. D. HALSEY, JR.

Department of Chemistry, University of Washington, Seattle, Wash.

Received September 2, 1958

Adsorption data for the interaction of krypton with evaporated films of iron, copper, sodium and tungsten at 75°K. have been obtained. Krypton isotherms on sodium films treated with oxygen and water vapor are reported. Interaction energies are determined and compared with those predicted by several dispersion force theories. It is found that the Kirkwood–Muller equation is the most suitable of the theories considered and that it yields semi-quantitative agreement with experiment for both metallic and non-metallic adsorbents. It is possible to predict the general form of isotherms of the rare gases on homogeneous surfaces by using Kirkwood–Muller energies in an isotherm equation developed by Singleton and Halsey.

I. Introduction

Metallic Interaction Theories.—Lennard-Jones[3] assumed a metal to be ideally polarizable and derived for the interaction of a rare gas atom with a metal surface the expression

$$E^*_{LJ} = \frac{mc^2\chi}{2} \times \frac{1}{R^4} \qquad (1)$$

where m is the mass of an electron, c is the velocity of light, R is the distance between the surface and the gas atom, and χ is the diamagnetic susceptibility of the gas.

Bardeen[4] modified the Lennard-Jones theory to take into account the interaction of the electrons in the metal. He obtained the expression

$$E^*_B = \frac{\alpha_0 I}{8} \times \frac{Ke^2/2rI}{1 + Ke^2/2rI} \times \frac{1}{R^3} \qquad (2)$$

where e is the charge of an electron, K is a numerical constant approximately equal to 2.5, r is the radius of a sphere in the metal containing one conduction electron, α_0 is the atomic polarizability and I is the ionization potential of the gas.

Margenau and Pollard[5] showed that a metal could not be considered ideally polarizable when interacting with a system whose resonant frequency was in the far-ultraviolet. They assume the conduction electrons in the metal to be "free" and

(1) This research was supported in part by the United States Air Force through the Air Force Office of Scientific Research of the Air Research and Development Command under contract No. AF 18(600)-987.

(2) Presented in partial fulfillment of the requirements for the degree of Doctor of Philosophy.

(3) J. E. Lennard-Jones, *Trans. Faraday Soc.*, **28**, 333 (1932).

(4) J. Bardeen, *Phys. Rev.*, **58**, 727 (1940).

(5) H. Margenau and W. G. Pollard, *ibid.*, **60**, 128 (1941).

hence, the metal behaves as though it were negatively polarizable. They derive the expression

$$E^*_{MP} = \frac{e^2\alpha_0}{16}\left(\frac{K}{r} - \frac{hn_0}{\pi m\nu_0}\right) \times \frac{1}{R^3} \qquad (3)$$

where h is Planck's constant, n_0 is the number of conduction electrons per cc. of the metal, and ν_0 is the resonant frequency of the gas.

Non-metallic Interaction Theories.—Polanyi[6] showed that the dispersion interaction energy of a rare gas with a solid surface was

$$E^* = \frac{\pi NC}{6} \times \frac{1}{R^3} \qquad (4)$$

where N is the number of atoms per cc. of the solid, R is the perpendicular distance of the gas atom from the surface of the solid, and C is a proportionality constant. The constant C has been approximated theoretically by several workers. Those theories considered in this work are due to London,[7] Slater and Kirkwood,[7] and Kirkwood and Muller.[8,9]

London derived for C the expression

$$C_L = \frac{3}{2} \times \frac{I_1I_2}{I_1 + I_2} \times \alpha_1\alpha_2 \qquad (5)$$

where the I's and α's are the ionization potentials and the polarizabilities of the atoms.

Slater and Kirkwood obtained for C the expression

$$C_{SK} = \frac{3}{4\pi} \times \frac{eh}{m^{1/2}} \times \frac{\alpha_1\alpha_2}{\left(\frac{\alpha_1}{n_1}\right)^{1/2} + \left(\frac{\alpha_2}{n_2}\right)^{1/2}} \qquad (6)$$

where the n's are the numbers of electrons in the outer shells of the atoms.

Kirkwood and Muller modified the Slater–Kirkwood expression to remove the quantity n. They used the atomic property of diamagnetic susceptibility and obtained

$$C_{KM} = 6mc^2 \frac{\alpha_1\alpha_2}{\frac{\alpha_1}{\chi_1} + \frac{\alpha_2}{\chi_2}} \qquad (7)$$

where the χ's are the diamagnetic susceptibilities of the atoms. Note that throughout this paper positive energies denote attraction.

The Adsorption Isotherm Equation.—Singleton and Halsey[10] have derived the equation

$$\ln \frac{p}{p_0} = -\frac{E_1}{n^3kT} + \frac{w}{kT}(1 - g) \qquad (8)$$

for adsorption of a crystalline adsorbate. Here p is the pressure of the adsorbate in equilibrium with the adsorbed layers, p_0 is the saturation vapor pressure of the adsorbate at the temperature (T) of the isotherm, n is the number of adsorbed layers, k is the Boltzmann constant, E_1 is the interaction energy in the first layer exclusive of the short range forces, w is the lateral interaction energy and g is a "compatibility factor."[10]

To obtain a continuous isotherm, the integral number n can be replaced by the continuous variable θ, the fraction of the surface covered. This yields the equation

$$\ln \frac{p}{p_0} = -\frac{E_1}{\theta^3kT} + \frac{w}{kT}(1 - g) \qquad (9)$$

II. Experimental

Dosage Measurement.—The dosage measuring system was composed of two parts: a thermostated gas buret and a high precision mercury McLeod gauge.

The mercury menisci of the McLeod gauge were illuminated from behind with soft lighting and were observed with a cathetometer which could be read to 0.01 mm. All measurements were corrected for the density of mercury and for the compression effect. Pressure measurements from 0.0010 ± 0.0005 mm. to 2.000 ± 0.001 mm. could easily be made and were reproducible. This gauge used in conjunction with the gas buret permitted measurements of gas volumes as small as 0.050 ± 0.005 microliter (STP).

Pressure Measurement.—Rosenberg[11] has described a precise manometer utilizing a thermistor as the sensing element. His circuitry has been used in this work with almost no modification. The thermistor bead, suitably mounted in a lead glass capsule, was obtained from Western Electric (catalog number D-176255). The capsule was joined to the Pyrex system through a graded seal. The gauge and all its electrical contacts were maintained at 27.40 ± 0.02° in a constant-temperature oil-bath. The potential measurements were made with a Leeds and Northrop type K-2 potentiometer along with a Leeds and Northrop type R galvanometer.

The gauge was calibrated by comparison with the precision McLeod gauge. It was found to give highly reproducible pressure–voltage curves and the measured pressures were precise to better than 0.5% from 10^{-2} to 1 mm. and better than 1 to 2% from 10^{-4} to 10^{-2} mm.

The saturation vapor pressures of krypton were measured with a small McLeod gauge, especially constructed for pressures from 0.1 to 1.0 mm. The mercury menisci were illuminated from behind and observed with a cathetometer. Pressures could be read to ±0.003 mm.

Saturation vapor pressures of argon were measured with a standard U-tube manometer constructed from twelve millimeter Pyrex tubing. The menisci were read with a cathetometer.

The Adsorption Cell.—The cell was similar to that used by Kington and Holmes[12] except that it was cylindrical instead of spherical. The bulb was constructed from Pyrex tubing; the tungsten leads were brought through uranium glass seals. The volumes of the cells were usually about 8 or 9 cc.

Evaporations were made from either a hairpin filament of the parent metal or from a tungsten helical filament on which the metal was previously vacuum melted. The second method was necessary to deposit heavy copper films.

The cell and filament were first baked at 450° for at least ten hours under vacuum. It then was placed in a dewar containing either an ice–water mixture or liquid nitrogen and the filament heated to the temperature of the evaporation. It was found that a large amount of gas was evolved from the filament, therefore it was necessary to continue pumping through the first part of the evaporation. The evaporation rate was kept low, so that the filament should be thoroughly degassed at the evaporation temperature. When the pressure in the system during the evaporation became less than 10^{-5} mm., the adsorption system was isolated from the pumps and the evaporation continued.

The sodium films were produced by distilling sodium metal into the adsorption cell and then sealing off the distillation pot. The sodium was triply distilled *in vacuo* before distilling it into the cell.

The sodium oxide film was prepared by oxidizing a sodium film with oxygen. The sodium hydroxide film was prepared by permitting the sodium oxide film to react with water vapor. The water vapor was supplied by the dehydration of a quantity of $BaCl_2 \cdot 2H_2O$ which had been introduced into the system.

The Cryostat.—The cryostat was of the usual design.[13] The temperature was maintained by an argon vapor pres-

(6) M. Polanyi, *Trans. Faraday Soc.*, **28**, 316 (1932).
(7) H. Margenau, *Rev. Modern Phys.*, **11**, 1 (1939).
(8) J. G. Kirkwood, *Z. Physik*, **33**, 57 (1932).
(9) A. Muller, *Proc. Roy. Soc.* (*London*), **A154**, 624 (1936).
(10) J. H. Singleton and G. D. Halsey, Jr., *Can. J. Chem.*, **33**, 184 (1954).
(11) A. J. Rosenberg, *J. Am. Chem. Soc.*, **78**, 2929 (1956).
(12) G. L. Kington and J. M. Holmes, *Trans. Faraday Soc.*, **49**, 417 (1953).
(13) W. J. C. Orr, *Proc. Roy. Soc.* (*London*), **A173**, 349 (1939).

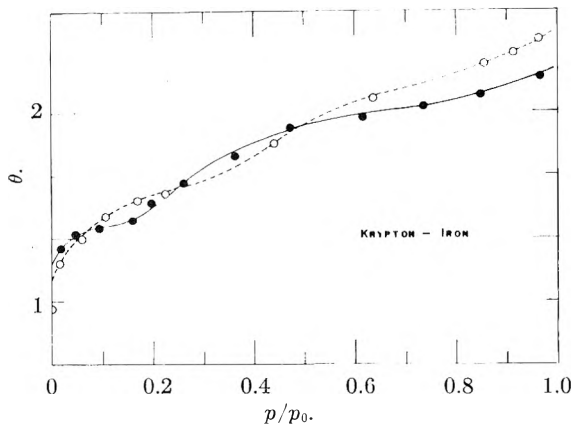

Fig. 1.—Krypton–iron adsorption isotherms determined at 75°K. for films annealed at 70° (open circles) and at 480° (filled circles).

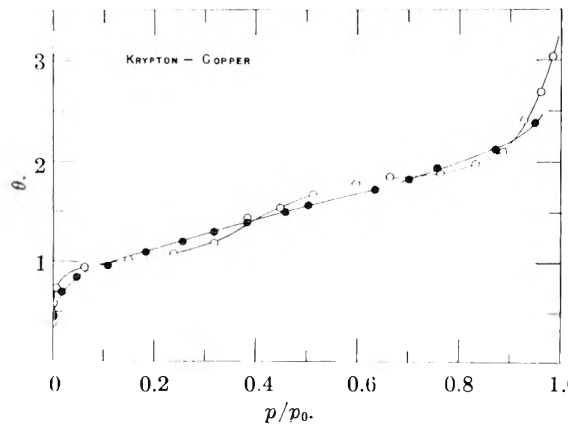

Fig. 2.—Krypton–copper adsorption isotherms determined at 75°K. for films annealed at −195° (filled circles) and at 25° (open circles).

sure thermometer which actuated a relay-controlled valve. When this valve was open a mechanical oil pump pumped on the liquid nitrogen causing the bath to cool.

The temperatures were measured with either an argon vapor pressure thermometer using the vapor pressure data of Clark, Din and Robb[14] or with a krypton vapor pressure thermometer using the data of Fisher and McMillan.[15] Temperatures were maintained to ±0.05°K. at 74.90 and 68.80°K. As a precaution to avoid errors caused by temperature fluctuations, measurements of p_0 were made simultaneously with measurements of p.

Materials.—One-millimeter thin-walled capillary tubing was used in the adsorption system to keep the dead space at room temperature to a minimum. Two very small traps were placed in the system and were kept at Dry Ice–acetone temperature.

Spectroscopically pure gases obtained from Air Reduction Sales Company in Pyrex flasks were used without further purification. Spectroscopically pure iron and copper wire obtained from Johnson, Matthey and Co., Limited, London, England, were used.

Dead Space Determination.—The dead space of the system was made in two parts: first the dead space of the traps, gauge and connecting tubing was determined and then the volume of the cell was determined.

Krypton interacts quite strongly with glass at liquid nitrogen temperature making it impossible to use this gas to determine the dead space. Krypton was used to determine the volume of the cell at the ice-point from which the dead space factors for the temperatures of the experiments were calculated.

The thermal transpiration corrections were made with the equation proposed by Bennett and Tompkins.[16]

Adsorption on Glass.—Krypton isotherms were determined on the glass cell prior to the evaporation of the metal. These isotherms along with estimates of the fraction of the cell uncovered by the film after the evaporation were used to correct for the amount of gas adsorbed on the glass. These corrections are about 20% of the amount of gas adsorbed on the metal in the case of the thin films of iron and copper; they are relatively small for the heavy copper and tungsten films and for the sodium films.

Test of Apparatus.—In order to determine whether or not measurements made with this apparatus on very small surface area samples in a large dead space were consistent with measurements of large surface area samples in a relatively small dead space, a separate test was performed. A sample of P-33 carbon black having a total surface area of about 50 sq. cm. or about one-quarter that of the lowest surface area film used in this work was placed in a typical adsorption cell and a krypton isotherm determined. This isotherm did not differ by more than about 5% at the most difficult part of the isotherm, that is, at high coverages, from the isotherm of krypton on a gram sample of P-33 made by Singleton and Halsey.[17]

III. Results

Iron Experiments.—Three iron films were produced. In each case the cell was kept in an ice-bath during the evaporation. The first film weighed 2.0 mg. and krypton isotherms were determined on it as a function of the annealing temperature. The BET area of the film annealed at 0° was 700 sq. cm. or 4.7 times the BET area of the glass cell before the deposition; the film annealed at 70° was 3.5 times that of the cell and the film annealed at 480° was 1.1 times that of the cell. Figure 1 shows the isotherms are plotted as a function of the fraction of the surface covered. Notice that the isotherm for the sintered film has developed a step-like structure, which is an indication of increasing homogeneity.

The second film was sintered at 480° immediately after deposition. This film weighed 3.4 mg. and had a BET area 1.2 times that of the glass. The third film, which was treated exactly as the second, weighed 3.4 mg. and had a BET area 1.2 times that of the glass cell.

The interaction energy, E_1/kT, was determined from the position of the steps passing through the values of θ equal to 1.5 and 2.5. The average value was 8.7 ± 0.5; the compatibility factor, g, was 0.96.

Haul and Swart[18] found step-formation in the isotherm of krypton on iron crystals which they formed by the reduction of the oxide with hydrogen. Their data treated with equation 9 gave E_1/kT equal to 7.8. They observed two-dimensional condensation at 77°K. while in the present work no evidence of it was found even at 69°K. They observed no hysteresis in their work indicating that they had a non-porous solid. The slightly porous films used in this work may have introduced enough heterogeneity to suppress the two-dimensional condensation.

Copper Experiments.—Three copper films were deposited. The first weighed 2.9 mg., had a BET area 1.2 times that of the cell and was evaporated while the cell was in an ice-bath. This film had a step-like structure and showed a little desorption hysteresis.

A second film weighing 93.7 mg. was deposited while the cell was immersed in liquid nitrogen. A krypton isotherm was determined immediately, then the film was allowed to warm to room temperature and the isotherm repeated. The unsintered film had an area one hundred times that of the sintered film, which in turn had an area 3.5 times that of the glass cell. The isotherms, plotted as a function of the fraction of the surface covered, are shown in Fig. 2.

The third copper film weighed 3.7 mg., was deposited at 78°K. and immediately sintered by warming it to room temperature. The krypton BET area of this film was 1.5 times that of the cell. Argon isotherms were determined up to p/p_0 of 0.02 (Fig. 3). Neither krypton nor argon showed signs of a two-dimensional phase change.

(14) A. M. Clark, F. Din and J. Robb, *Physica*, **17**, 876 (1951).

(15) B. B. Fisher and W. G. McMillan, THIS JOURNAL, **62**, 494 (1957).

(16) M. J. Bennett and F. C. Tompkins, *Trans. Faraday Soc.*, **53**, 185 (1957).

(17) J. H. Singleton and G. D. Halsey, Jr., THIS JOURNAL, **59**, 1011 (1954).

(18) R. A. W. Haul and E. R. Swart, *Z. Elektrochem.*, **61**, 380 (1957).

E_1/kT determined for the krypton was 9.4 ± 0.4; the compatibility factor was 0.96. E_1/kT was estimated for argon to be about 7.5; no estimate of q could be made.

Sodium Experiments.—Two sodium films were deposited. In each case the cell was at room temperature. The film weights were not determined. Krypton isotherms are shown in Fig. 4. No adsorption was found within the experimental error of these investigations. No estimate of the interaction energy (other than it appears to be negative) could be made.

The second sodium film was oxidized at room temperature using pure oxygen. The film immediately lost its luster which indicated that a reaction had taken place. Krypton was not adsorbed on the sodium oxide film (see Fig. 5).

The sodium oxide was then treated with water vapor at room temperature. A krypton isotherm determined immediately after the reaction showed a slight hump at its very beginning, but this hump disappeared when the film was annealed at 70°. The hump probably was due to a small amount of water which remained on the surface. The isotherm for the annealed film is shown in Fig. 5.

E_1/kT for krypton on NaOH was 1.0; the compatibility factor was 0.99.

Tungsten Experiments.—A tungsten film was deposited at 0°. It weighed 20.3 mg. and had a BET area 30 times that of the glass cell. The film was annealed at 450°, but this was insufficient to sinter the film. The krypton isotherm shows faint indications of step formation but not sufficient to warrant the use of equations 8 or 9. E_1/kT was estimated to be around 15 (see Fig. 6).

IV. Discussion

Physical Properties of Substances.—To make the calculations which follow, it was necessary to compile a list of the appropriate physical properties of the substances to be considered. In certain cases where no experimentally determined values were available, estimations based upon either observed related properties or theoretically calculated properties were made.

In those cases where the diamagnetic susceptibility was not available but where the index of refraction or the polarizability was, the Kirkwood formula[8]

$$\chi = \frac{e^2 N a_0}{4mc^2} (n\alpha_0)^{1/2} \qquad (10)$$

was used, where χ is the diamagnetic susceptibility e and m are the charge and mass of an electron, c is the velocity of light, n is the number of electrons, a_0 is the Bohr radius and α_0 is the atomic polarizability. Fisher and McMillan[19] and these authors, have found equation 11 to be quite satisfactory in the case of spherically symmetrical atoms or molecules. The expression was used to calculate the diamagnetic susceptibility of iron, tungsten and oxygen. These were the only cases where better estimates could not be found in the literature.

Sodium metal is feebly paramagnetic. In this case the diamagnetic susceptibility of sodium ion, which has been determined experimentally, was used.

Copper metal is diamagnetic, but the measured susceptibility cannot be used as the diamagnetic susceptibility of copper atoms. Copper is diamagnetic because of the diamagnetic contribution due to the filling of the d shell is greater than the paramagnetic contribution of the free electrons. The susceptibility listed in Table I was obtained from the theoretical estimate for copper ion.

The polarizabilities of copper, iron and tungsten were calculated from the index of refraction of the metals at long wave lengths.

(19) B. B. Fisher and W. G. McMillan, *J. Chem. Phys.*, **28**, 562 (1958).

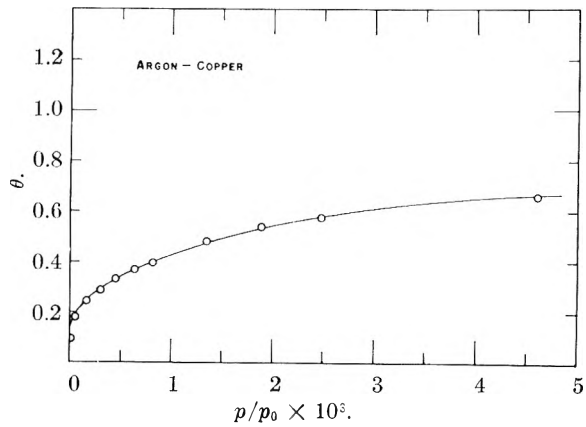

Fig. 3.—Argon–copper adsorption isotherm determined at 69°K. on film annealed at 25°.

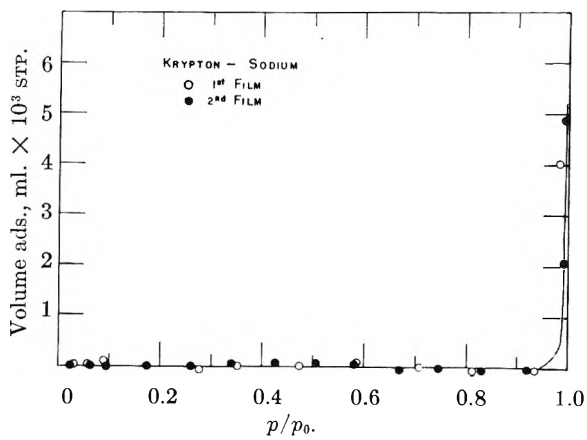

Fig. 4.—Krypton–sodium adsorption isotherms determined at 75°K.

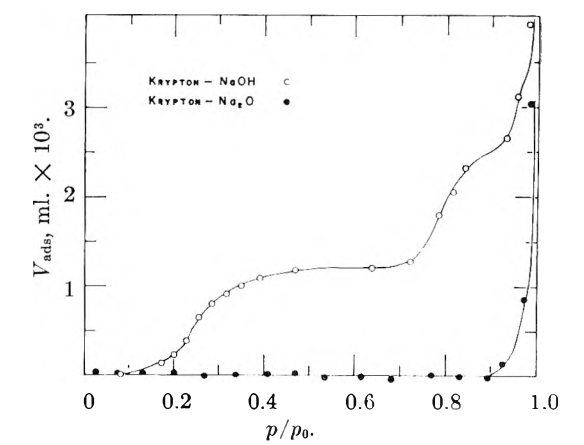

Fig. 5.—Krypton–Na_2O (filled circles) and krypton–NaOH (open circles) adsorption isotherms determined at 75°K.

Self-interaction Energies.—Equations 1 to 7 yield the energy of interaction E^* between an adsorbed atom and a solid. When the calculated interaction energy is divided by kT, a dimensionless quantity is obtained which may be compared with the experimentally determined E_1/kT from equations 8 and 9 if it is first modified to account for the other atoms in the adsorbed phase. Because the equilibrium pressure over the adsorbent p is divided by the reference-state pressure p_0, E_1 repre-

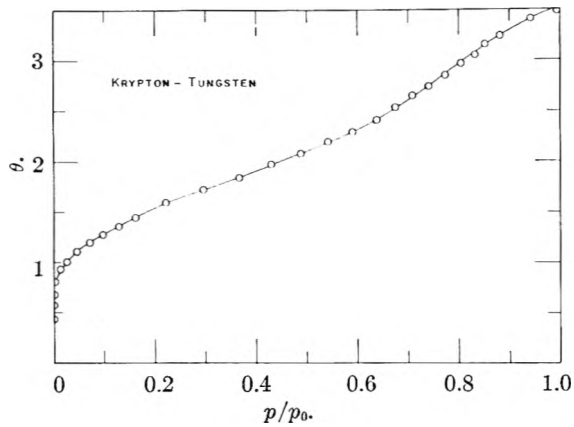

Fig. 6.—Krypton–tungsten adsorption isotherms determined at 69°K. on film annealed at 450°.

TABLE I

PHYSICAL PROPERTIES OF SUBSTANCES

Molecule	Density (g./cc.)	Polarizability ($\times 10^{24}$)	Susceptibility ($\times -10^{29}$)	Ionization potential (e.v.)
Ne	1.20[a]	0.39[b]	1.17[c]	25.7[b]
Ar	1.65[h]	1.63[b]	3.24[i]	17.5[b]
Kr	2.99[h]	2.46[b]	4.65[i]	14.7[b]
Xe	3.56[h]	4.00[b]	7.04[i]	12.2[b]
N_2	0.81[f]	1.74[b]	2.00[c]	15.8[b]
O_2	1.14[f]	1.57[b]	2.57[k]	13.6[b]
CH_4	0.41[f]	2.58[b]	6.67[f]	14.1[b]
Na	0.97[e]	29.7[b]	0.90[m]	2.08[b]
Cu	8.92[d]	2.14[a]	2.17[n]	7.68[f]
Fe	7.86[d]	1.13[a]	2.79[r]	7.83[f]
W	19.3[e]	3.00[g]	7.63[r]	8.1[f]
C	2.24[d]	1.02[d]	3.79[d]	11.2[f]
Na_2O	2.27[d]	2.71[f]	3.83[p]	
NaOH	2.13[d]	1.65[f]	3.93[f]	
NaBr	3.21[d]	4.60[f]	8.06[f]	
AgI	5.67[d]	9.28[d]	13.6[d]	
CaF_2	3.18[d]	2.53[f]	4.68[d]	
KCl	1.98[f]	4.32[f]	6.40[f]	

[a] "The American Institute of Physics Handbook," McGraw-Hill Book Company, Inc., New York, N. Y., 1957. [b] H. Margenau, *Rev. Modern Phys.*, 11, 1 (1939). [c] E. C. Stoner, "Magnetism," Methuen and Co., Ltd., London, 1948, p. 38. [d] "International Critical Tables," Vol. I and IV, McGraw-Hill Book Co., Inc., New York, N. Y., 1926–28. [e] "Handbook of Chemistry," 6th ed., Handbook Publishers, Inc., Sandusky, Ohio, 1946. [f] "Handbook of Chemistry and Physics," Chemical Rubber Publishing Co., Cleveland, Ohio, 1949. [g] J. W. Mellor, "A Comprehensive Treatise on Inorganic and Theoretical Chemistry," Longmans, Green and Co., New York, N. Y., 1939, Vol. XI. [h] J. R. Partington, "An Advanced Treatise in Physical Chemistry," Vol. III, Longmans, Green and Co., Inc., New York, N. Y., 1952, p. 149. [i] K. E. Mann, *Z. Physik*, 98, 548 (1936). [j] J. H. Van Vleck, "The Theory of Electric and Magnetic Susceptibilities," Oxford University Press, London, 1932, p. 225. [k] J. G. Kirkwood, *Physik. Z.*, 33, 57 (1932). [m] Approximated by the value of Na ion from *c*. [n] Approximated by the value of Cu ion from *j*. [p] Calculated from the Pascal summing rule from *c*. [r] Calculated from the polarizability using the Kirkwood formula from *k*. All polarizabilities except from reference *b* are calculated from the refractive indices.

sents the energy in excess of that which would cause the condensation of the adsorbate. This excess energy arises from the presence of a semi-infinite thickness of adsorbent. By introducing the adsorbent, a semi-infinite thickness of adsorbate had to be removed. E_1, therefore, will be given by subtracting the energy of self-interaction E^s from the energy of interaction E^*.[10]

The London expression for the self-interaction energy is

$$E^s{}_L = \frac{\pi N_2}{8D^3} \times I_2\alpha_2 \qquad (11)$$

where N_2, I_2 and α_2 are the number of atoms per cc. in the bulk adsorbate, the ionization potential and the atomic polarizability of the adsorbate, respectively. D is the distance the atom is from the surface. The subscript 2 will refer to the adsorbate and 1 will refer to the adsorbent.

The Slater–Kirkwood self-interaction energy is

$$E^s{}_{SK} = \frac{ehN_2}{16m^{1/2}D^3}\,\alpha_2{}^{1/2}n_2{}^{1/2} \qquad (12)$$

where h is Planck's constant and n_2 is the number of electrons in the outer shell of the adsorbate atom.

The Kirkwood–Muller equation yields

$$E^s{}_{KM} = \frac{\pi mc^2N_2}{2D^3}\,\alpha_2\chi_2 \qquad (13)$$

where c is the velocity of light and χ_2 is the diamagnetic susceptibility of the adsorbate.

Before the above equations may be used, the distance D must be evaluated. Equation 8 refers to atoms at large distances from the surface. This distance will be very nearly equal to some multiple of the distance separating adjacent parallel planes of atoms in the bulk adsorbate.[10] D is, therefore, the distance between the adjacent parallel planes which for close-packed crystals is equal to the square-root of two-thirds times the lattice parameter.

Table II lists the calculated energies of self-interaction for various gases. The self-interaction energy should be approximately one-half the heat of condensation. Notice that only the Kirkwood–Muller energies are comparable to those to be expected. Fisher and McMillan[19] found that the Kirkwood–Muller expression gave better energies for the interaction of pairs of atoms than did the London expression.

TABLE II

SELF-INTERACTION ENERGIES (E^*/kT)[a]

Gas	London	Slater–Kirkwood	Kirkwood–Müller	$\frac{1}{2}(\Delta H/RT)$[b]
Neon	0.4	0.7	0.9	1.4[c]
Argon	2.3	3.0	5.3	6.1[d]
Krypton	3.1	4.1	8.4	8.4[d]
Xenon	1.9	2.4	5.8	5.6[d]
Methane	2.3	3.0	9.2	7.3[d]
Nitrogen	2.9	1.3	4.3	4.4[c]
Oxygen	2.4	5.6	6.5	5.4[c]

[a] All values are for 75°K. except those of xenon which are for 160°K. [b] Obtained from the "American Institute of Physics Handbook," McGraw-Hill Book Co., Inc., New York, N. Y., 1957. [c] From the heat of vaporization. [d] From the heat of sublimation.

Interaction of Metals.—In Table III under the column headed Lennard-Jones (a) the energies were calculated using

$$\frac{E_1}{kT} = \frac{mc^2\chi_2}{2D^3kT} - \frac{E^s{}_{KM}}{kT} \qquad (14)$$

where $E^s{}_{KM}$ was obtained from the Kirkwood–Muller expression. The first term is due to Len-

nard-Jones. The use of the diamagnetic susceptibility yields energies that are too high by a factor of four.

The column labeled Lennard-Jones (b) was calculated using

$$\frac{E_1}{kT} = \frac{\alpha_2 I_2}{8D^3kT} - \frac{E^s_{KM}}{kT} \qquad (15)$$

The first term is the image force potential derived by Lennard-Jones but using polarizabilities and ionization energies instead of the diamagnetic susceptibilities. This expression was used by Bardeen.[4] Equations 14 and 15 give interaction energies that are independent of the nature of the metal.

The fourth column, headed Margenau and Pollard was calculated with the expression

$$\frac{E_1}{kT} = \frac{e^2\alpha_0}{16D^3kT}\left(\frac{K}{r} - \frac{h\nu_0}{\pi m \nu_0}\right) - \frac{E^s_{KM}}{kT} \qquad (16)$$

This expression gives energies that are too low by a factor of about three or four. Notice, however, that the nature of the metal has been taken into consideration; sodium has about one-third the interaction energy as those of the other metals.

The Bardeen energies, column five, were calculated with the equation

$$\frac{E_1}{kT} = \frac{\alpha_2 I_2}{8D^3kT} \times \frac{Ke^2/2rI_2}{1 + Ke^2/2rI_2} - \frac{E^s_{KM}}{kT} \qquad (17)$$

This treatment distinguishes between the various metals, but yields values of E_1/kT that are too low by a factor of six or seven. It predicts that krypton is energetically incompatible with sodium, but does so also for oxygen on carbon.

The sixth column lists the energies calculated with the Kirkwood–Muller expression

$$\frac{E_1}{kT} = \frac{\pi mc^2 N_1}{D^3kT} \times \frac{\alpha_1\alpha_2}{\left(\frac{\alpha_1}{\chi_1}\right) + \left(\frac{\alpha_2}{\chi_2}\right)} - \frac{E^s_{KM}}{kT} \qquad (18)$$

where N_1 is the number of atoms per cc. of the adsorbent. This equation correctly predicts the energetic incompatibility of the krypton–sodium system; it places all the metals and carbon in the correct order of interaction strength; and it is within about 20 or 30% of the experimentally determined E_1/kT's.

The London values, column seven, were calculated with the expression

$$\frac{E_1}{kT} = \frac{\pi N_1}{4D^3kT} \times \alpha_1\alpha_2 \times \frac{I_1 I_2}{I_1 + I_2} - \frac{E^s_L}{kT} \qquad (19)$$

The Slater–Kirkwood values, column eight, were calculated with

$$\frac{E_1}{kT} = \frac{ehN_1}{8m^{1/2}D^3kT} \times \frac{\alpha_1\alpha_2}{\left(\frac{\alpha_1}{n_1}\right)^{1/2} + \left(\frac{\alpha_2}{n_2}\right)^{1/2}} - \frac{E^s_{SK}}{kT} \qquad (20)$$

Notice that in equations 19 and 20 the self-interaction terms were obtained from their respective treatments. These treatments give better agreement with experiment than do either the Lennard-Jones, the Bardeen or the Margenau and Pollard treatments. They are not as satisfactory as the Kirkwood–Muller treatment.

It is apparent that metals cannot be distinguished as a class from non-metals by means of physical adsorption. Theories developed especially to account for metallic properties fail to agree with experiment; those developed to account for simple interactions between atom pairs succeed or at least give better agreement with experiment than do the others.

Because metals behave as though they were made up of isolated atoms, a comparison of the London, the Slater–Kirkwood and the Kirkwood–Muller treatments should be possible. Examination of the last four columns of Table III clearly shows the superiority of the Kirkwood–Muller expression for the calculation of physical adsorption energies. Since the London expression was derived using perturbation theory, it should give energies that are too low. The Slater–Kirkwood expression derived using variation theory should give the upper limit of the energy, while the Kirkwood–Muller expression, a modification of the Slater–Kirkwood expression, should give, because of the use of diamagnetic susceptibilities, even higher energies. In all three expressions only the dipole–dipole interactions are considered, while interactions due to quadrupoles and higher symmetries are not included. Dipole–quadrupole interactions contribute up to a quarter or a half of the dipole–dipole interactions.[7] The London and Slater–Kirkwood equations are usually thought of as giving approximate adsorption energies because it is assumed that the repulsive forces counterbalance the forces due to the higher term attractive interactions. Because the repulsive term drops off more rapidly with distance than the other terms, it would be expected that at moderate distances from the surface (as obtained from equations 8 and 9), the quadrupole interactions still contribute to the adsorption energy while the repulsive term has become negligible. Thus, a theory which yields more or less correct values for the dipole–dipole interactions will yield adsorption energies that are too low. The Kirkwood–Muller expression, which is too large to account for the dipole–dipole interactions, fortuitously gives approximate or semi-quantitative agreement with experiment for the adsorption energy at high coverages.

Interaction of Non-metals.—Table IV summarizes several investigations of rare gases adsorbed on non-metals. Notice that krypton on sodium oxide and xenon on calcium fluoride are predicted to be energetically incompatible, whereas they are found to exhibit a type III isotherm. The isotherm of xenon on calcium fluoride is the usual type III isotherm with adsorption starting at low p/p_0, but not showing very much adsorption until p/p_0 equal to about 0.50. The krypton–sodium oxide isotherm, however, is a very severe type III isotherm showing no adsorption until p/p_0 equal to about 0.9. In either case the onset of adsorption could be the result of heterogeneity, capillarity or an entropy effect. The calculated values of E_1/kT obtained from the Kirkwood–Muller formula for the rare gases on non-metals, including these containing more than on atomic species is in general very satisfactory.

Table V compares the calculated and observed values of E_1/kT for polyatomic adsorbates. The calculated values for liquid nitrogen and liquid oxygen on ionic substrates are always low. This

TABLE III

GAS–METAL INTERACTION ENERGIES (E_1/kT)

System	Lennard-Jones[a]	Lennard-Jones[b]	Margenau–Pollard	Bardeen	Kirkwood–Müller	London	Slater–Kirkwood	Exptl.[c]
Na–Kr	41.6	10.7	1.1	−1.2	−4.6	3.4	6.7	−?
Cu–Kr	41.6	10.7	2.9	0.5	11.5	5.7	5.6	9.4
Fe–Kr	41.6	10.7	2.1	1.6	8.6	1.7	2.1	8.7
W–Kr	41.6	10.7	2.9	1.1	25.7	6.5	5.0	15.0
C–Kr	41.6	10.7	2.9	0.9	14.4	4.0	4.4	8.0
Cu–Ar	38.0	12.7	4.3	2.3	10.6	3.9	5.2	7.5[d]
C–Ar	38.0	12.7	5.0	2.7	13.3	2.6	5.1	11.0
C–N_2	18.4	11.0	4.5	0.9	8.3	1.6	6.6	6.8
C–O_2	28.5	7.0	2.0	−4.0	10.4	1.7	2.7	11.0

[a] Using diamagnetic susceptibility in the image force expression. [b] Using polarizability and ionization energy data in the image force expression. [c] Determined using either equation 8 or 9. [d] Determined using $(E_1/kT) = -\ln(P/P_0)$ evaluated at $\theta = 1/2$ in the first layer.

might be expected because diatomic molecules have permanent electric quadrupoles. Drain[20] calculated that the quadrupole interaction of N_2 with KCl would be of the order of 800 cal./mole. This correction added to the Kirkwood–Muller energy would make the predicted E_1/kT equal to 4.0 as compared to the experimental value of 5.3. No values of the quadrupole interactions for the other systems in Table V were available.

TABLE IV

RARE GAS–NON-METAL INTERACTION ENERGIES (E_1/kT)

System	Kirkwood–Muller	Exptl.[a]
Na_2O–Kr	−0.4	0.05
NaOH–Kr	0.9	1.0
NaBr–Kr	4.7	2.8[b]
AgI–Ar	9.7	11.0[c]
Xe–Ar	2.6	1.2[c]
KCl–Ar	2.5	2.5[d]
CaF_2–Ar	2.5	2.2[e]
CaF_2–Xe	−0.2	0.1[e]

[a] Determined using either equation 1.12 or 1.13. [b] From the data of Fisher and McMillan, *J. Chem. Phys.*, **28**, 562 (1958). [c] From the data of Singleton and Halsey, *Can. J. Chem.*, **33**, 184 (1955). [d] From the data of W. J. C. Orr, *Proc. Roy. Soc.* (*London*), **A173**, 349 (1939). [e] From the data of Edelhoch and Taylor, THIS JOURNAL, **58**, 344 (1954).

Prediction of the Form of the Isotherm.—When one considers the drastic approximations that go into Kirkwood–Muller expression and the rather crude isotherm equation employed, the agreement with experiment is satisfactory. The general availability of polarizability and susceptibility data and the simplicity of the calculations make this method useful in obtaining an idea of the approximate form of the adsorption isotherm of the rare gases on metallic or non-metallic surfaces. This may be done by calculating E_1/kT from equation 18 and setting it equal to $-\ln p/p_0$ (this equation assumes that the crystal structure of the adsorbed layers is compatible with that of the bulk adsorbate, that is $g = 1$). Table VI compares the calculated and observed position of the steps in several isotherms.

(20) L. E. Drain, *Trans. Faraday Soc.*, **49**, 650 (1953).

For krypton on sodium and on sodium oxide and for xenon on calcium fluoride, it is predicted that no adsorption would take place or at most a type III isotherm might be observed. It is found that sodium does not adsorb krypton and that Kr–Na_2O and Xe–CaF_2 give type III isotherms. For argon on AgI, copper and carbon and for krypton on copper, iron, tungsten and carbon the predicted first step is at very low p/p_0 and this is found experimentally. It should be mentioned that because the self-interaction energy of water (ice) is extremely high owing to hydrogen bonding, the above theory would predict that water would not be adsorbed by any solid to which it could not at least

TABLE V

INTERACTION ENERGIES (E_1/kT) OF POLYATOMIC ADSORBATES WITH NON-METALS

System	Kirkwood–Muller	Exptl.[a]
CaF_2–N_2	1.2	8.0[b]
NaBr–N_2	3.2	6.3[c]
KCl–N_2	1.3	5.3[d]
NaBr–CH_4	6.7	5.8[c]
CaF_2–O_2	−0.2	3.0[b]

[a] Determined using equation 1.12. [b] From the data of Edelhoch and Taylor, THIS JOURNAL, **58**, 344 (1954). [c] From the data of Fisher and McMillan, *J. Chem. Phys.*, **28**, 562 (1958). [d] From the data of W. J. C. Orr, *Proc. Roy. Soc.* (*London*), **A173**, 349 (1939).

TABLE VI

THE PREDICTED POSITION OF STEPS

System	Predicted p/p_0	Exptl. p/p_0
NaOH–Kr[a]	0.41	0.27
NaBr–Kr[a]	.01	.07
KCl–Ar[a]	.08	.08
CaF_2–Ar[a]	.08	.06
NaBr–CH_4[a]	.001	.003
NaOH–Kr[b]	.89	.81
NaOH–Kr[c]	.97	.95

[a] For the first step in the isotherm. [b] For the second step in the isotherm. [c] For the third step in the isotherm.

hydrogen bond. This has been confirmed in the case of water on silver iodide by the work of Karasz, Champion and Halsey.[21]

(21) F. E. Karasz, W. M. Champion and G. D. Halsey, Jr., THIS JOURNAL, **60**, 376 (1956).

MEDIUM EFFECTS IN THE RACEMIZATION OF A BIPHENYL HAVING A CATIONIC BARRIER GROUP

BY JOHN E. LEFFLER AND W. H. GRAHAM[1]

Contribution from the Department of Chemistry, Florida State University, Tallahassee, Fla.

Received September 10, 1958

The racemization of a biphenyl is subject to effects due to specific interactions of the biphenyl with adjacent solvent molecules. Changes in the solvent change both the activation enthalpy and the activation entropy, but the relation between these is not simple unless the solvents belong to a closely related series. Rate ratios up to a factor of five and ranges in activation enthalpy and entropy of about 3 kcal./mole and 9 cal./mole degree are reported. The solvent effects are highly specific and do not correlate with those observed for other reactions or with any of the macroscopic physical properties of the solvent.

The rate of a reaction in solution depends on two types of solute–solvent interaction. One of these, the electrostatic interaction of the solute with the non-adjacent or bulk part of the solvent, is well understood and can be described in terms of the electrical properties of the solute molecule and the macroscopic electrical properties of the solvent. However, the intimate interaction of solute molecules with adjacent solvent molecules is less well understood and is undoubtedly highly specific, correlating poorly or not at all with solvent parameters such as the macroscopic dielectric constant of the medium.

The racemization of optically active biphenyls, which is relatively free from mechanistic uncertainties, is almost an ideal reaction for the study of such specific medium effects. Because the reaction involves little or no redistribution of charge, the ground and transition states will be virtually identical from the standpoint of remotely situated solvent molecules. The observed medium effects will therefore represent differences in the specific interactions of the ground and transition states with their adjacent solvent molecules. For example, the rate would not be correlated with the solubility, because the non-specific or long range solvent effects important in the latter (especially for ions) will cancel out in the transition state.

The transition state for the racemization of an optically active biphenyl such as I

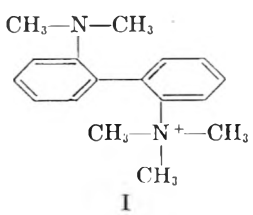

I

is a set of energy levels which the two enantiomorphs have in common. In the energy levels of the ground state, the barrier groups (occupying the 2,2′-positions) have a considerable freedom of rotation relative to their benzene rings; on the other hand, the benzene rings themselves are restricted in their relative motions to a range of orientations in which the planes of the ring are nearly perpendicular. In the energy levels of the transition state, the relative torsion of the two benzene rings increases in amplitude to include and pass the coplanar orientation, but this increase in rotational freedom is achieved only at the expense of an even greater decrease in the rotational freedom of the barrier groups relative to their benzene rings. The net effect is that the energy levels of the transition state are less densely spaced than those of the ground state, and the entropy of activation is negative. The main reason for the considerable activation energy in a biphenyl racemization is the steric repulsion of the groups during their passage through the eclipsed positions. This repulsion energy has been shown to be of the right order of magnitude by the calculations of Westheimer and Mayer.[2] Because of the 25 kcal. or so of vibrational activation energy the transition state molecules should be visualized as undergoing a motion which is much more violent as well as qualitatively different from that of the ground state molecules. The vibrationally excited nature of the transition state tends to make its solvation weaker and less intimate than that of the ground state. In the present example, it is possible to explain all of the observed solvent effects at least qualitatively in terms of the desolvation of the ground state during the activation process, ignoring the solvation of the transition state.[3]

The enthalpy and entropy increments for the desolvation of the ground state will, of course, depend not only on the forces and constraints experienced by molecules in the solvation shells but also on the forces and constraints in the macroscopic solvent, hence on the quasi-crystalline nature of the solvent.

In this paper we report the rates and activation parameters for the racemization of the biphenyl ion I at 79.4 and 100.0° in some seventy-seven different media. The biphenyl is one first prepared by Shaw and Turner[4] and investigated by Cook and Turner,[5] who first showed that the racemization rates do indeed depend upon the solvent.

Discussion of Results

The racemization is first order or nearly[6] first

(1) Based on the doctoral dissertation of W. H. Graham. Presented in part at the Symposium on "Solvent Effects and Reaction Mechanisms," Queen Mary College, London, July, 1957.

(2) F. H. Westheimer and J. E. Mayer, *J. Chem. Phys.*, **14**, 733 (1946).

(3) This simplification is not always possible, perhaps because a large part of the excess energy of the transition state in some biphenyl racemizations is potential rather than kinetic. When the transition state is relatively static and coplanar, its solvation, especially by π-complexing solvent components, cannot be neglected: J. E. Leffler and B. M. Graybill, unpublished work.

(4) F. R. Shaw and E. E. Turner, *J. Chem. Soc.*, 135 (1933).

(5) D. E. Cook and E. E. Turner, *ibid.*, 88 (1937).

(6) In certain solvents, notably the alcohols and aqueous-organic mixtures, there is a slight downward drift in the first-order rate con-

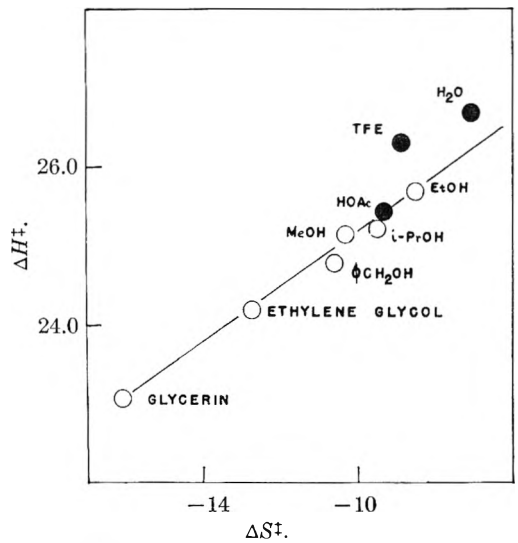

Fig. 1.—$(CH_3)_2NC_6H_4C_6H_4N^+(CH_3)_3$ camphorsulfonate in hydroxylic solvents.

order in all the media studied. The rate constant in water depends on the initial concentration of the run, being higher at higher concentrations (Table I). The concentration dependence appears to vanish in solutions more dilute than 0.02 *N*. We have chosen 0.02 *N* as a standard concentration for all of our runs unless otherwise specified. The anion may be assumed to be *d*-camphorsulfonate unless otherwise specified.

TABLE I

THE CONCENTRATION EFFECT IN WATER AT 100.0°

Initial concn., moles/l.	Rate constant, sec.$^{-1}$ × 10^5	Initial concn., moles/l.	Rate constant, sec.$^{-1}$ × 10^5
0.008	4.92	0.033	5.18
.009	5.06	.036	5.17
.018	4.94	.070	5.40
.020	4.93	.106	5.95
.026	4.98		

Single-component Solvents.—In Table II are recorded the activation parameters for the 80–100° temperature range for various pure solvents. It is found that the range of reaction rates in *single component* solvents is about a factor of four to four and a half depending on the temperature, trifluoroethanol being the slowest and dimethyl sulfoxide the fastest.[7] The slow reaction in trifluoroethanol can be attributed to hydrogen bonding.

The activation parameters show a considerably greater spread than might have been expected from the range in rate constants, the usual cancelling effect being operative to some extent. The range in activation enthalpy for the single-component solvents is about 3 kcal./mole and the range in entropy about 9 cal./mole degree.

If attention is restricted to the alcohols (glycerol, ethylene glycol, benzyl alcohol, methanol, isopropyl alcohol and ethanol), it is found that a graph of the enthalpy of activation against the entropy (Fig. 1) consists of a single isokinetic[8] line. If a single isokinetic line represents a qualitatively uniform solvation mechanism, we may conclude that water and trifluoroethanol act differently from the alcohols, since the corresponding points are not on the line.[9]

In contrast to the simple relationship between the activation parameters for the alcohol series, the enthalpy–entropy relationship for the entire set of solvents, representing, a much wider variety of chemical structures, is a scatter diagram. This lack of a smooth relationship indicates the highly specific nature of intimate solvation and its dependence on the chemical structure of the solvent.

A further indication of the specificity of intimate solvation in this reaction is the complete lack of correlation (for any wide selection of solvents) of either the rates or the activation parameters with any physical property of the solvent or even with the rate of any other reaction in the same solvent. Solvent parameters which have been compared with our data include the dielectric constant, the viscosity, Y[10] and Z.[11]

However, in spite of the high specificity of the solvation effects, the racemization rate of *d-o*-(2-dimethylaminophenyl)-phenyltrimethylammonium benzenesulfonate is nearly the same in D- and L-2-methyl-1-butanols even though the solvated species are diastereoisomeric. The near equivalence of these rates was determined indirectly from an experiment which compares the rates of the *d*- and *l*-biphenyls in D-2-methyl-1-butanol: a fresh solution of the *dl*-biphenyl is only slightly more levorotatory than a solution which has been heated to ensure equilibrium between the diastereoisomeric solvates. It also was found that the increase in rotation caused by heating a solution of the *l*-salt in this solvent is only slightly greater than the decrease in rotation caused by heating a solution of the *d*-salt. Of course the D- and L-2-methyl-1-butanols must be very much alike from the point of view of a solute interacting mainly with the hydroxyl group, and the enantiomorphs of a more highly asymmetrical solvent would probably show a greater difference. It has been shown, for example, that the equilibrium of *dl*-8-nitro-N-benzenesulfonyl-N-(2-hydroxyethyl)-1-naphthylamine is shifted in ethyl (+)-tartrate as solvent.[12]

Two-component Solvents.—Table III contains the activation parameters for the racemization in

stant as the reaction progresses. This drift, which amounts to about 4% in the rate constant, is absent in water itself and in non-hydroxylic organic solvents. In order to minimize the effect of the drift on the comparison of the rate constants, these have been compared at the same extent of reaction, corresponding to a rotation (due to the cation) about 1/2.73 of the initial value. In order to determine whether association with the optically active anion is responsible for the drift, benzenesulfonate was substituted for the *d*-camphorsulfonate. Since this change made no difference, we are inclined to attribute the drift to a stereospecific interaction between the positive ions.

(7) The racemization without solvent in the solid state at 100° is immeasurably slow.

(8) J. E. Leffler, *J. Org. Chem.*, **20**, 1202 (1955).

(9) It is not unusual for water to differ from the alcohols in its effect on activation parameters. For example, the enthalpies and entropies of activation for the solvolysis of methyl tosylate in a series of alcohols form an isokinetic line, but the line does not pass near the point for water: J. B. Hyne and R. E. Robertson, *Can. J. Chem.*, **34**, 863 (1956).

(10) E. Grunwald and S. Winstein, *J. Am. Chem. Soc.*, **70**, 846 (1948); A. H. Fainberg and S. Winstein, *ibid.*, **78**, 2770 (1956).

(11) E. M. Kosower, *ibid.*, **80**, 3253 (1958).

(12) J. Glazer, M. M. Harris and E. E. Turner, *J. Chem. Soc.*, 1753 (1950).

TABLE II

PURE SOLVENTS

Solvent	k, sec.$^{-1}$ × 10^5 79.4°[a]	k, sec.$^{-1}$ × 10^5 100.0°[a]	$\Delta H^{\ddagger}$, kcal./mole[c]	$\Delta S^{\ddagger}$, cal./mole deg.[c]
Trifluoroethanol	0.41	3.46	26.31 ± 0.11	− 8.87 ± 0.31
Deuterium oxide	.56	4.74	26.39 ± .06	− 8.04 + .18
Water	.57	4.93	26.71 ± .06	− 7.11 ± .15
Methanol	1.03	7.87	25.17 ± .04	−10.30 ± .10
Acetic acid	1.08	8.56	25.47 ± .01	− 9.34 ± .02
Glycerol	1.10	7.18	23.08 ± .26	−16.08 ± .73
Acetonitrile	1.18	9.14	25.24 ± .16	− 9.83 ± .44
Ethanol	1.18	9.50	25.70 ± .08	− 8.51 ± .22
Ethylene glycol	1.20	8.51	24.19 ± .02	−12.77 ± .06
Nitrobenzene	1.29	10.05	25.36 ± .10	− 9.31 ± .27
Isopropyl alcohol	1.42	10.90	25.22 ± .07	− 9.52 ± .20
Benzyl alcohol	1.52	11.32	24.79 ± .06	−10.61 ± .16
Chloroform[b]	1.53	12.24	25.69 ± .17	− 8.03 ± .47
Dimethylformamide	1.62	12.49	25.19 ± .14	− 9.32 ± .40
Dimethyl sulfoxide	1.82	13.39	24.66 ± .06	−10.62 ± .16

[a] These are mean rate constants. The individual values have been adjusted in those cases where the temperature was actually a fraction of a degree different from 79.4 or 100.0°. [b] It was necessary to use chloroform stabilized by a trace of ethanol. [c] The significance of the numbers indicating the precision is discussed in the experimental section.

TABLE III

TWO-COMPONENT SOLVENTS

Solvent, wt. % of first component	k, sec.$^{-1}$ × 10^5 79.4°[a]	k, sec.$^{-1}$ × 10^5 100.0°[a]	$\Delta H^{\ddagger}$,[b] kcal./mole	$\Delta S^{\ddagger}$,[b] cal./mole deg.
Methanol–water				
0	0.57	4.93	26.71 ± 0.06	− 7.11 ± 0.15
3.8	.62	5.33	26.55 ± .09	− 7.39 ± .24
16.5	.72	6.12	26.46 ± .11	− 7.35 ± .30
20.8	.74	6.19	26.17 ± .02	− 8.10 ± .06
44.2	.90	7.19	25.62 ± .08	− 9.27 ± .21
70.2	1.02	7.80	24.16 ± .06	−10.34 ± .15
94.0	1.02	7.87	25.21 ± .05	−10.19 ± .15
100.0	1.03	7.87	25.17 ± .04	−10.30 ± .10
Ethanol–water				
3.8	0.64	5.33	26.24 ± 0.08	− 8.20 ± 0.23
20.8	0.93	7.33	25.50 ± .15	− 9.56 ± .42
44.1	1.10	8.38	24.99 ± .06	−10.67 ± .17
48.7	1.16	8.92	24.91 ± .07	−10.80 ± .20
63.5	1.22	9.28	25.07 ± .06	−10.26 ± .18
75.9	1.25	9.46	24.98 ± .12	−10.45 ± .33
96.0	1.23	9.52	25.18 ± .04	− 9.89 ± .11
98.0	1.19	9.69	25.87 ± .05	− 8.01 ± .13
100.0	1.18	9.50	25.70 ± .08	− 8.51 ± .22
Isopropyl alcohol–water				
20.7	1.02	7.94	25.31 ± 0.06	− 9.93 ± 0.18
43.9	1.26	9.41	24.87 ± .05	−10.76 ± .14
60.9	1.37	10.10	24.64 ± .05	−11.24 ± .13
79.7	1.41	10.49	24.81 ± .02	−10.70 ± .05
100.0	1.42	10.90	25.22 ± .07	− 9.52 ± .20
***t*-Butyl alcohol–water**				
7.2	0.75	6.21	26.05 ± 0.05	− 8.41 ± 0.13
23.9	1.16	8.75	24.96 ± .06	−10.67 ± .18
43.9	1.33	9.71	24.52 ± .02	−11.64 ± .05
66.1	1.43	10.43	24.47 ± .06	−11.63 ± .17
91.4 (Solubility limit)	1.60	11.82	24.70 ± .13	−10.77 ± .35
Ethylene glycol–water				
18.0	0.69	5.74	26.17 ± 0.06	− 8.24 ± 0.15
46.7	0.86	6.83	25.60 ± .05	− 9.44 ± .13
84.5	1.09	8.26	25.02 ± .08	−10.61 ± .22
100.0	1.20	8.50	24.19 ± .02	−12.77 ± .06
β-Trifluoroethanol–water				
5.2	0.63	5.30	26.23 ± 0.13	− 8.25 ± 0.35
18.7	.67	5.63	26.15 ± .07	− 8.34 ± .20
35.6	.63	5.31	26.23 ± .13	− 8.25 ± .35
73.4	.52	4.52	26.63 ± .09	− 7.52 ± .25
100.0	.41	3.46	26.31 ± .11	− 8.87 ± .31
Acetone–water				
20.9	0.95	7.38	25.26 ± 0.04	−10.20 ± 0.12
44.2	1.19	8.65	24.49 ± .09	−11.94 ± .25
66.5	1.37	9.45	23.85 ± .12	−13.47 ± .32
95.2 (Solubility limit)	1.54	11.46	24.73 ± .12	−10.75 ± .32
Dioxane–water				
29.3	1.07	8.08	24.94 ± 0.06	−10.86 ± 0.16
40.9	1.27	9.34	24.62 ± .09	−11.43 ± .25
50.9	1.37	9.57	23.92 ± .09	−13.26 ± .24
72.2	1.63	11.41	24.03 ± .05	−12.70 ± .13
83.8	1.87	13.10	23.98 ± .03	−12.48 ± .10
92.6 (Solubility limit)	2.11	14.72	23.93 ± .07	−12.39 ± .18
Dimethyl sulfoxide–water				
15.5	0.76	6.22	26.03 ± 0.05	− 8.46 ± 0.15
52.4	1.14	8.90	25.31 ± .02	− 9.69 ± .06
76.7	1.48	10.93	24.69 ± .05	−10.93 ± .15
86.8	1.64	12.16	24.71 ± .02	−10.67 ± .05
100.0	1.82	13.39	24.65 ± .06	−10.62 ± .20
Acetic acid–water				
4.0	0.40	4.00	28.41 ± 0.29	− 3.00 ± 0.79
17.2	.42	4.29	29.11 ± .41	− 0.93 ± 1.14
34.3	.54	5.20	28.01 ± .12	− 3.51 ± 0.35
51.2	.62	5.50	27.03 ± .06	− 6.03 ± .16
72.4	.78	6.70	26.54 ± .14	− 6.96 ± .38
100.0 (Solubility limit)	1.08	8.56	25.47 ± .01	− 9.34 ± .02
Acetic acid–benzene				
2.2	1.92	14.13	24.55 ± 0.09	−10.79 ± 0.24
19.3	1.68	12.33	24.57 ± .06	−11.02 ± .18
37.4	1.55	11.50	24.70 ± .07	−10.79 ± .18
54.4	1.48	11.00	24.70 ± .09	−10.89 ± .23
78.2	1.31	10.00	25.00 ± .09	−10.30 ± .25
100.0 (Solubility limit)	1.08	8.56	25.47 ± .01	− 9.34 ± .02
Methanol–benzene				
8.3	1.62	12.80	25.52 ± 0.06	− 8.41 ± 0.17
47.4	1.27	9.75	25.20 ± .06	− 9.79 ± .17
64.3	1.19	9.06	25.04 ± .15	−10.37 ± .42
73.0	1.15	8.85	25.23 ± .04	− 9.89 ± .11
81.8	1.07	8.67	25.83 ± .08	− 8.35 ± .22
91.8	1.07	8.47	25.50 ± .03	− 9.28 ± .08
95.7	1.03	8.00	25.26 ± .03	−10.03 ± .08
100.0	1.03	7.87	25.17 ± .04	−10.30 ± .10

[a] These are mean rate constants. The individual values have been adjusted in those cases where the temperature was actually a fraction of a degree different from 79.4 or 100.0°. [b] The significance of the numbers indicating the precision is discussed in the Experimental section.

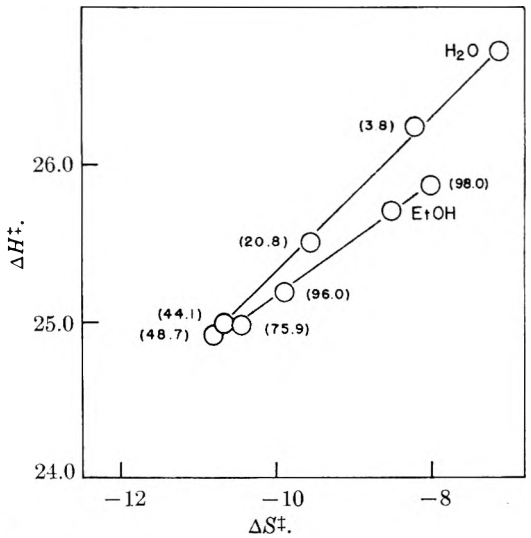

Fig. 2.—$(CH_3)_2NC_6H_4C_6H_4N^+(CH_3)_3$ camphorsulfonate in aqueous ethanol (wt. %).

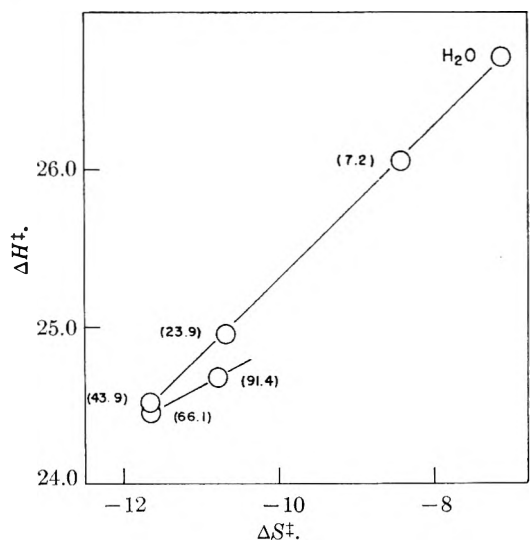

Fig. 3.—$(CH_3)_2NC_6H_4C_6H_4N^+(CH_3)_3$ camphorsulfonate in aqueous *t*-butyl alcohol (wt. %).

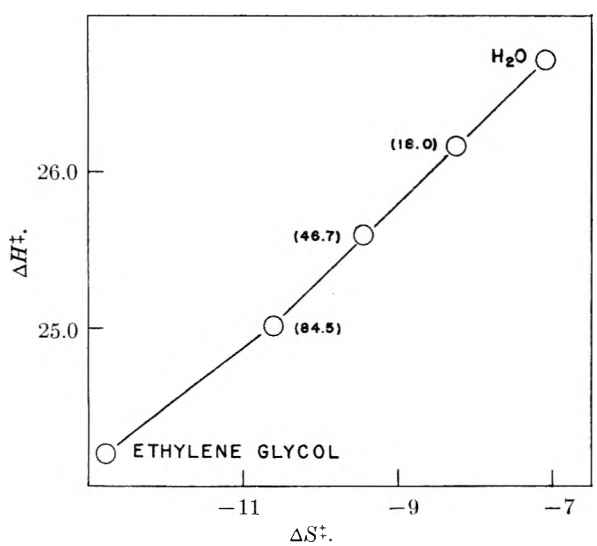

Fig. 4.—$(CH_3)_2NC_6H_4C_6H_4N^+(CH_3)_3$ camphorsulfonate in aqueous ethylene glycol (wt. %).

a few of the sixty-one two-component solvent mixtures.

The behavior of alcohol–water mixtures is about what might have been expected in view of the fact that the point for water does not fall on the isokinetic line for the series of pure alcohols. The activation parameter for the mixtures of water with various alcohols shows a linear enthalpy *versus* entropy relationship from zero up to about fifty or more weight per cent. of the alcohol. Beyond this point the line breaks sharply, in most cases doubling back nearly upon itself. Figures 2 and 3 for aqueous ethanol and aqueous *t*-butyl alcohol are given as examples.[13] In the series of monohydric alcohols the values of the enthalpy and entropy at which the line breaks are in the order methanol > ethanol > isopropyl alcohol > *t*-butyl alcohol, *i.e.*, in the order of increasing molecular volume rather than the order in which the points fall on the isokinetic line for the pure alcohols.

The somewhat different behavior of aqueous ethylene glycol is shown in Fig. 4.

Although the enthalpy–entropy diagram for the monohydric alcohol–water mixture shows sharp breaks, we prefer to interpret the results in terms of a gradual change in the solvation mechanism rather than in terms of an abrupt change. One reason for this preference is that the graphs of enthalpy and entropy against weight per cent. of the alcohol are smooth, the minimum found in these curves in most cases being very broad. The relationship is shown in Fig. 5 for the isopropyl alcohol–water system. The minima in the activation parameters can be rationalized by simply assuming that the activation process involves considerable desolvation and release of solvent molecules to the bulk solvent structure. For methanol and ethanol it is known that the excess enthalpies and entropies of mixing with water pass through a minimum.[14] If this is general for the monohydric alcohols of our series it affords a sufficient explanation for the minima in the activation enthalpy and entropy.

The enthalpy–entropy relationship for the β-trifluoroethanol–water mixture is much more complicated than that for the unsubstituted alcohols. It has both a maximum and a minimum in the enthalpy and entropy, and a single maximum in the rate. On the other hand, the enthalpy–entropy relationship for the acetone–water mixtures is very much like those of the alcohol–water mixtures except that the single minimum occurs at a considerably lower value of the enthalpy and a more negative value of the entropy.

The activation parameters for the dioxane–water and dimethyl sulfoxide–water mixtures resemble each other. In both cases the enthalpy of activation decreases as a linear function of the entropy up to about 70% (by weight) of the organic component. Above this composition, however, there is a sharp break. The enthalpy of activation remains almost constant, but the entropy increases, causing the rate

(13) For the even more complicated pattern of the solvolysis reaction (S_N1-type) in mixed solvents the reader should refer to the excellent paper by S. Winstein and A. H. Fainberg, *J. Am. Chem. Soc.*, **79**, 5937 (1957).

(14) A. G. Mitchell and W. F. K. Wynne-Jones, *Disc. Faraday Soc.*, **15**, 161 (1953).

to continue to rise. The rates in 92.6% dioxane–water mixtures were the fastest observed for any medium, being 5.15 times as fast as for trifluoroethanol at 79.4° and 4.26 times as fast at 100.0°.

In aqueous acetic acid the dimethylamino groups are protonated to a considerable extent, as can be seen from the low value of the specific rotation. In aqueous hydrochloric acid the specific rotation is also low and the rate of racemization is too slow to measure. The latter result presumably means that the repulsion of the two positive charges, which should accelerate the racemization, is of lesser importance than the increased solvation of the protonated dimethylamino group and the change in hybridization.

Although the low specific rotation reduces the accuracy of the results for aqueous acetic acid mixtures, there is no doubt about the direction of the effects. The addition of very small amounts of acetic acid to water drastically reduces the rate, but slightly larger additions of acetic acid increase the rate. The enthalpy–entropy relationship (Fig. 6) is V-shaped, but with a maximum rather than the minimum encountered in the aqueous alcohol mixtures. Since our experiment with hydrochloric acid shows that the protonated form does not racemize at all, the activation parameters in aqueous acetic acid include contributions from the deprotonation as well as the desolvation of the biphenyl.

The addition of benzene to acetic acid results in a steady increase in rate. The enthalpy and entropy decrease as benzene is added and maintain their linear relationship with each other until a proportion of about 50% benzene is reached. At about that composition, there is a sharp break in the linear relationship and there appear to be at least two minima and one maximum in the curve before the solubility limit is reached near 98% benzene.

The addition of benzene to methanol also causes a steady increase in rate and the plot of enthalpy against entropy of activation is N-shaped, with breaks at 50 and 80% methanol. The initial increase in enthalpy and entropy of activation on adding benzene to methanol cannot be due to increased solvation of the biphenyl, since the rate actually increases. It could, on the other hand, be attributed to a change in the nature of the solvent structure to which the molecules of the solvation shell are returned during the desolvation which accompanies the activation process. Relative to pure methanol, the desolvation in a solvent containing a little benzene is more endothermic and also involves a greater decrease in the constraint of the solvent molecules. This seems to be in the wrong direction if the effect is due merely to the presence of benzene instead of methanol in the solvation shell, but could be due to a change in the structure of the bulk solvent. The required change is that solvent molecules are less tightly associated with each other in the solvent mixture than they are in pure methanol. Hence the differences in enthalpy and entropy between solvent and solvation shell are greater for the mixture than for the pure alcohol. Miller and Fuoss have suggested that benzene added to methanol breaks down the

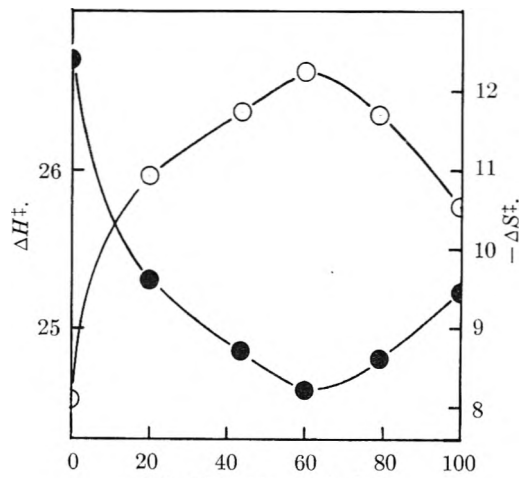

Fig. 5.—$(CH_3)_2NC_6H_4C_6H_4N^+(CH_3)_3$ camphorsulfonate in aqueous isopropyl alcohol. The filled circles represent $\Delta H^{\ddagger}$, the open circles represent $\Delta S^{\ddagger}$.

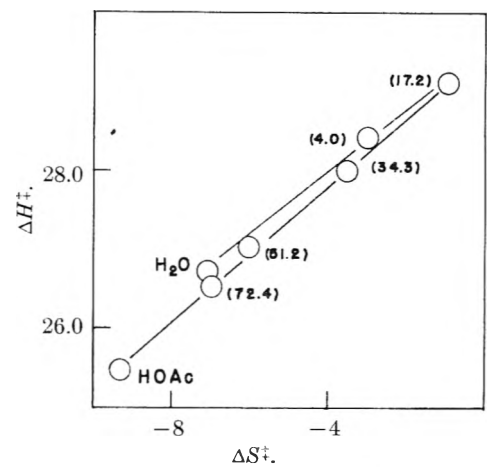

Fig. 6.—$(CH_3)_2NC_6H_4C_6H_4N^-(CH_3)_3$ camphorsulfonate in aqueous acetic acid (wt. %).

polymeric structure of the solvent and increases the amount of monomeric methanol.[15]

Experimental and Mathematical Procedures

2,2′-Bisdimethylaminobiphenyl.—2,2′-Dinitrobiphenyl was made by means of a modified Ullmann reaction[16] using pretreated copper bronze.[17] The reduction to the diamine with iron filings proved to be erratic and most of the reduction was carried out by a catalytic procedure similar to that of Blood and Noller.[18] The methylation was done by the procedure of Shaw and Turner.[4]

***dl-o*-(2-Dimethylaminophenyl)-phenyltrimethylammonium Iodide.**—The following procedure is easier than the sealed tube method of Shaw and Turner. One equivalent of 2,2′-bisdimethylaminobiphenyl is refluxed for several hours in anhydrous acetone containing several equivalents of methyl iodide. The white solid product is filtered off, more methyl iodide is added, and the refluxing is continued, producing a second crop of solid product. The product needs no recrystallization, melts at 184–185°, and is obtained in quantitative yield. It is essential that the acetone be dry or the product will be contaminated with its hydriodide salt.

***d-o*-(2-Dimethylaminophenyl)-phenyltrimethylammonium *d*-Camphorsulfonate.**—This substance was prepared by the method of Shaw and Turner,[4] m.p. 184–185°, $[\alpha]^{25}D$ 48.6 in water at 1.32 g./100 cc.

(15) R. C. Miller and R. M. Fuoss, *J. Am. Chem. Soc.*, **75**, 3076 (1953).

(16) N. Kornblum and D. L. Kendall, *ibid.*, **74**, 5782 (1952).

(17) E. C. Kleiderer and R. Adams, *ibid.*, **55**, 4225 (1933).

(18) A. E. Blood and C. R. Noller, *J. Org. Chem.*, **22**, 711 (1957).

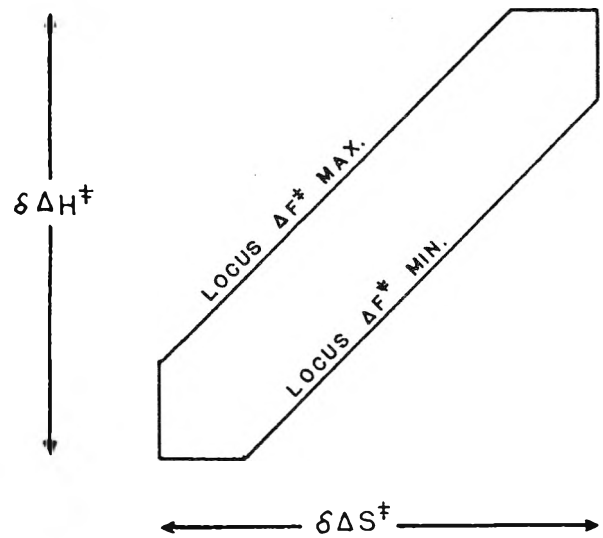

Fig. 7.

dl-o-(2-Dimethylaminophenyl)-phenyltrimethylammonium Benzenesulfonate.—The racemic benzenesulfonate is prepared by warming a solution of silver benzenesulfonate in acetone–ethanol with an equivalent amount of the *dl-o*-(2-dimethylaminophenyl)-phenyltrimethylammonium iodide. Silver iodide is removed by centrifugation and the solution is diluted with heptane which causes the racemic salt to crystallize.

d-o-(2-Dimethylaminophenyl)-phenyltrimethylammonium Iodide.—This compound, prepared by the method previously reported,[4] was recrystallized from chloroform–hexane; m.p. 181–182° dec.

d-o-(2-Dimethylaminophenyl)-phenyltrimethylammonium benzenesulfonate[6] was crystallized from acetone–hexane, m.p. 124–125°, $[\alpha]^{25}D$ 43.5 in H_2O at 0.84 g./100 cc.

l-o-(2-Dimethylaminophenyl)-phenyltrimethylammonium Benzenesulfonate.—The *l*-iodide is obtained by adding sodium iodide to the mother liquor from the crystallization of the *d-o*-(2-dimethylaminophenyl)-trimethylammonium *d*-camphorsulfonate, and crystallizing the product by adding hexane; $[\alpha]^{25}D$ −40.0, m.p. 124–125°.

Solvents.—Unless otherwise noted, all solvents were carefully dried and purified by distillation and/or fractional crystallization. Dimethyl sulfoxide (99.9%) was used as supplied by the Stephan Chemical Co., Chicago. "Spectro grade" chloroform, containing a trace of ethanol, was used without further purification since it was found that pure chloroform tended to produce phosgene during the runs.

Absolute ethanol and methanol were prepared by the methods described by Fieser.[19] Reagent grade benzene and analytical reagent grade glycerol were used without purification. Dioxane was purified by refluxing over sodium hydroxide for several days and then refluxing and distilling over sodium. "Spectro grade" acetone was used directly. Since all acetone solutions used were aqueous mixtures, traces of water were unimportant. D-2-Methyl-1-butanol, $[\alpha]^{22.4}D$ −5.79, was supplied by the Dow Chemical Company.

Investigation of Side Reactions.—Equimolecular amounts of methyl iodide and 2,2′-bisdimethylaminobiphenyl heated in chloroform for eight hours gave the quaternary iodide in only 2.18% yield as determined by Volhard titration. When *dl-o*-(2-dimethylaminophenyl)-phenyltrimethylammonium iodide was heated in chloroform, however, the back reaction to 2,2′-bisdimethylaminobiphenyl was almost complete after a few hours. The racemization of the quaternary ammonium biphenyl can therefore not be measured in the presence of iodide ion. The corresponding reactions involving methyl camphor sulfonate do not take place. The infrared spectra of *o*-(2-dimethylaminophenyl)-phenyltrimethylammonium *d*-camphorsulfonate before and after mutarotation in chloroform are identical. Furthermore, the spectra of a chloroform solution of methyl *d*-camphorsulfonate and bis-dimethylaminobiphenyl before and after heating at the usual racemization temperature are identical, indicating that the reverse reaction does not take place. Demethylation by water would produce hydrogen ion; none is liberated, as shown by titration to a phenolphthalein endpoint, when the *d*-camphorsulfonate is heated in water for several hours. Disproportionation to a doubly quaternary salt and 2,2′-bisdimethylaminobiphenyl can be ruled out as a side mechanism in view of the fact that a large excess of a much more nucleophilic substance, dimethylaniline, produces only a 10% increase in racemization rate in ethanol and a 4% increase in chloroform, probably medium effects. An *intramolecular* methylation of the dimethylamino group by the trimethylammonium group would not lead to racemization in any case.

Kinetics.—Samples in nitrogen-filled ampules were placed in thermostats of conventional design with a temperature control of ±0.02°. Absolute values of the temperature, known to within 0.1°, were obtained from N.B.S. calibrated thermometers. The ampules were quenched by immersion in ice-water, opened, and the contents placed in the polarimeter tube. The Bellingham and Stanley polarimeter, equipped with a sodium vapor light source, was read in a darkened room whose temperature was controlled to ±2°. For most points a total of sixteen readings, eight each with the tube turned in opposite directions, were taken. Generally four to six points, in addition to an initial and final point, were taken for each run. These points were clustered in that part of the curve which gives maximum accuracy for the rate constant.

A standard concentration of 0.02 *N* was used in most of the experiments. This concentration was chosen for maximum conservation of material consistent with adequate rotation.

The concentration of the *d-o*-(2-dimethylaminophenyl)-phenyltrimethylammonium *d*-camphorsulfonate had little effect on its specific rotation

Normality	$[\alpha]^{22}D$ in H_2O, degree
0.01025	48.8
.02726	48.6
.05126	48.6

It was also observed that variations in room temperature had no detectable effect on the specific rotations in the ordinary solvents. However, in experiments using D-2-methyl-1-butanol as solvent, it was necessary to control the temperature to ±0.2° because the specific rotation of the solvent changed appreciably with temperature, about 0.01° per degree.

Asymmetrical Environment Experiments.—The optical rotations of solutions of *d* and *l* and *dl-o*-(2-dimethylaminophenyl)-phenyltrimethylammonium benzenesulfonate in D-2-methyl-1-butanol were measured before and after heating in sealed ampules. The concentration of the *dl*-salt was

	Angle, before heating	Conditions	Angle, after heating	Δα
d-salt	168.035°	16 hr. at 100°	167.151°	0.884
l-salt	166.268°	11 days at 80°	167.170°	.912
dl-salt	167.341°	16 hr. at 100°	167.370°	.029

different from that of the others, but the concentrations of the *d*- and *l*-salts were nearly equal. The error expected in the Δα due to the fluctuation of the rotation of the solvent with the temperature at which it is read, is about 0.004.

Racemization in the Solid State.—A sample of *d-o*-(2-dimethylaminophenyl)-phenyltrimethylammonium *d*-camphorsulfonate was sealed in an ampule under nitrogen and left in a steam-bath for 55 days. The specific rotation in aqueous solution before heating was 47.9°, after heating, 47.8°.

The Calculation of Rate Constants. Activation Parameters and their Errors.—The rate constant is given by the equation

$$k = \frac{2.303}{2t} \log \frac{\alpha_0}{\alpha}$$

where t is the elapsed time, α_0 the initial rotation of the solution, and α the rotation at time t. The rotations are corrected for that due to the camphorsulfonate. The method of least squares was used to calculate the best values of the

(19) L. F. Fieser, "Experiments in Organic Chemistry," 3rd ed., D. C. Heath and Co., Boston, Mass., p. 281.

activation parameters for the experimental temperature range, fitting the equation

$$\log \frac{k}{T} = \log \frac{\bar{k}}{h} + \frac{\Delta S^{\ddagger}}{2.303R} - \frac{\Delta H^{\ddagger}}{2.303R}\frac{1}{T}$$

The calculations were performed on a desk calculator and checked with an I.B.M. model 650 digital computer, using a program for which we are indebted to Prof. H. C. Griffith of the F.S.U. mathematics department.

The expected maximum errors in $\Delta H^{\ddagger}$ and $\Delta S^{\ddagger}$ are about ± 0.14 kcal./mole in the enthalpy of activation and about ± 0.40 cal./mole degree in the entropy of activation, based on a conservative estimate of $\pm 0.002°$ as the maximum error in the average of the sixteen readings of α for each point. The calculation of the least-squares activation parameters gives us a measure of their precision as a by-product. These numbers indicated as precision measures in the tables have the form of probable errors, 0.6745 times the standard deviations. It should be remarked that these numbers are not, in fact, probable errors, because the statistical sample of points for each solvent is too small, some of the reported error quantities no doubt being fortuitously small. On the other hand, the mean of the error figures for a large number of related solvents very likely is a measure of the probable error of the activation parameter for that series.

In the graphs of activation enthalpy *versus* entropy, the experimental points are represented by small circles. These circles are not probable error contours. The actual probable error contour is a narrow ellipse[20] whose major axis has a slope numerically equal to the mean experimental temperature in degrees Kelvin. The reason for the elliptical shape of the probable error contour is that the precision with which log k, or the free energy of activation, is known is such that if $\Delta H^{\ddagger}$ has the largest value permitted by its probable error, then $\Delta S^{\ddagger}$ must also have nearly its largest permitted value. That is to say, the *largest* value for the enthalpy within its probable error and the *lowest* value for the entropy within its probable error, are a combination which would correspond to an extremely improbable value for the rate constant.

The effect of this restriction on the probable error contour is shown in Fig. 7.

The practical consequence of the sloping elliptical error contour is that points having relative positions like those for 44.1 and 75.9% alcohol in Fig. 2 are more likely to differ significantly than points having relative positions like those for 44.1 and 48.7% alcohol.

Acknowledgments.—This investigation was aided by the Office of Ordnance Research, U. S. Army, through a research contract and by a National Science Predoctoral Fellowship (held by W. H. G., 1957–1958). We also wish to thank Professors E. Grunwald and F. H. Westheimer for helpful discussions.

(20) J. Mandel and F. J. Linnig, *Anal. Chem.*, **29**, 743 (1957).

KINETICS OF THE STEAM–CARBON REACTION

BY GEORGE BLYHOLDER[1] AND HENRY EYRING

Department of Chemistry, University of Utah, Salt Lake City, Utah

Received September 11, 1958

The data for the steam–graphite reaction from 900 to 1300° and in the 5 to 100 μ pressure range are presented as a function of both pressure and temperature. The rate-determining processes are the adsorption of water vapor and the desorption of molecular hydrogen from the surface. Absolute rate theory calculations lead to the conclusion that the adsorbed species have a limited mobility upon the surface.

Introduction

There have appeared a large number of papers on the steam–carbon reaction. It is generally agreed that the reaction may be represented by the equation

$$C_{(s)} + H_2O_{(g)} \longrightarrow CO_{(g)} + H_{2(g)}$$

Beyond the agreement that CO and H_2 are the primary products of the reaction at one atmosphere or less of H_2O pressure, there is little agreement on the activation energy, order of the reaction and the magnitude of rate constants. A number of experimental conditions which have not been met by previously reported data are deemed necessary if the resultant data are to be suitable for kinetic interpretation. The amount of H_2O vapor decomposed should be small to avoid the retarding effect of H_2 on the reaction. This condition also makes interpretation of the order of the reaction unambiguous. The H_2O vapor and the carbon surface should be at the same temperature. If this is not done the temperature of the activated complex in the reaction is not clearly defined. The nature of the carbon should be adequately defined. In this study we are interested in the reaction of graphite with water vapor so the carbon samples are from a spectroscopic graphite electrode. It is to be expected that natural graphites which contain impurities and carbonized filaments which are not 100% graphitized would react differently from pure graphite.

With these conditions in mind an apparatus was designed in this Laboratory to study the reactions of graphite with oxidizing gases between 900 and 1300° and in the 5 to 100 μ pressure range. The apparatus is a flow system in which water is admitted through a capillary before the furnace and the flow is maintained by a mercury diffusion pump after the furnace. The furnace is such that a four inch long zone is maintained at $\pm 2°$. The incoming vapor is heated on alumina chips in the central region of the furnace. The graphite samples, which were cut from a 1/4 inch diameter spectroscopic electrode (National Carbon Company), are suspended by means of a platinum wire in the constant temperature zone of the furnace. The rate of the reaction was followed by measuring the rate of pressure build up of CO and H_2 after the H_2O was trapped out. Results with this apparatus have appeared in an earlier publication.[2] Unfortunately, it has recently been discovered that, due to the high flow rate of vapor (over 1000 cm./sec.) through the furnace and an unfortunate choice of location of the thermocouple gage used to determine pressure, the pressures of water vapor in the furnace at the sam-

(1) Presently a Research Associate at the Johns Hopkins University, Baltimore 18, Maryland.

(2) J. S. Binford, Jr., and H. Eyring, THIS JOURNAL, **60**, 486 (1956).

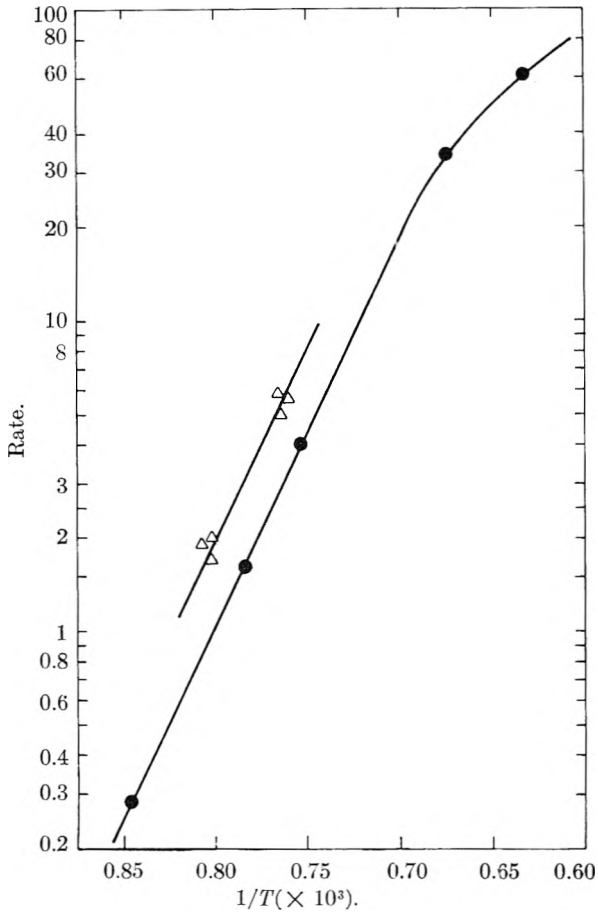

Fig. 1.—Temperature dependence.

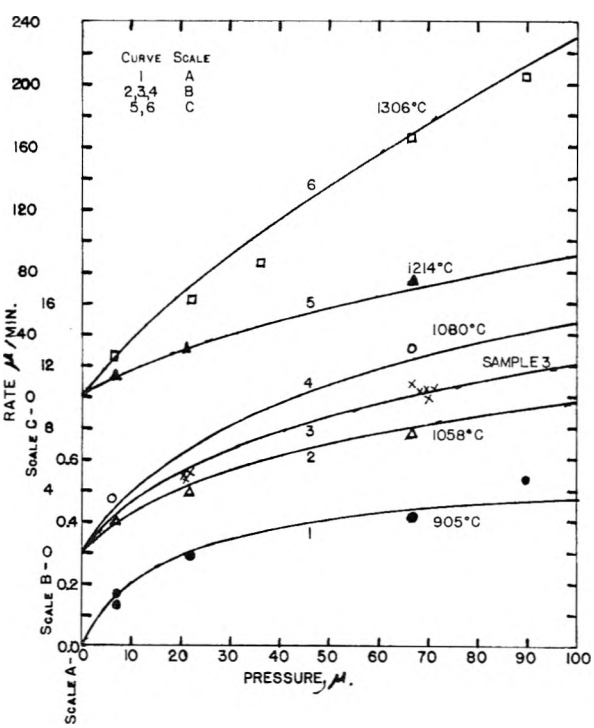

Fig. 2.—Pressure dependence.

ple were given incorrectly in that publication. In order to obtain the correct pressure at the sample two thermocouple gages were placed immediatelv down stream on a tube which is a straight line extension of the tube furnace. Due to the high linear flow rate a pressure drop due to flow is found between these gages. A linear extrapolation is used to obtain the pressure at the sample. In all other respects the apparatus and experimental procedure are those previously reported. Since the pressure dependence of the reaction is of such fundamental importance a complete new set of data was obtained. These data, which for the first time give the steam–graphite reaction free from secondary reactions, will now be presented.

Experimental

The first sample used consisted of a rod of spectrographic graphite two inches long and $^1/_4$ inch in diameter. It had a geometric surface area of 10.75 cm.^{2} and a volume of 1.61 cm.^{3}. In Fig. 1, the experimental points for the temperature dependance of the reaction at 22 μ H_2O pressure are given by the solid circles. The rate is given in terms of the original measurements which are the rate of pressure build up in μ per minute in a 3.35-l. volume. The pressure increase is due to an equimolar mixture of CO + H_2. A pressure build up of 1 μ/min. is equivalent to 0.92 × 10^{15} molecule of carbon per second reacting.

The pressure dependence of the reaction on this sample at 905, 1058, 1080, 1214 and 1306° is shown in Fig. 2. In this figure the experimental points are given. The lines are drawn from a kinetic expression which will be explained later. It is observed from this figure that the pressure dependence of the reaction changes with temperature. They also show that the form of the temperature dependence curve is a function of the pressure chosen.

It has been demonstrated[3] that diffusion of the reacting gas into the pores of graphite of the type used in these experiments may affect the observed kinetics. The first experiment tried to determine whether or not pore diffusion affected the reaction was to use a sample in which the volume to area ratio was radically different from that of the first sample. Sample 2 had an area of 16 sq. cm. and a volume of about 0.7 cm.^{3}. The sample was about 0.9 mm. thick. No exact measurement of the sample thickness was made but this value is within 10% of the exact value. The reaction with this sample had the same pressure dependence as sample 1 at 1014°. At this temperature the ratio of the rate on sample 1 to that on sample 2 at the same pressure is 2.5. The area ratio for the samples is 0.67 while the volume ratio is 2.3. It is seen, therefore, that the rate of the reaction is proportional to the volume of the sample and not to the area. This indicates that even on sample 1 the reaction is occurring throughout the entire volume of the sample. This leads to the conclusion that water vapor is effectively reaching all of the inner surface throughout the sample and so pore diffusion does not affect the reaction.

As a further check to make sure pore diffusion was not affecting the reaction, the reaction was investigated with samples 2 × 10^{-4} cm. thick. These were prepared by rubbing a spectrographic graphite rod against an inert ceramic support. This leaves a film of graphite much like a pencil mark on the support. This sample, number 3, had a surface area of 20.2 cm.^{2}. The pressure dependence on this sample at 1036° is shown in Fig. 2. The line is drawn using the same kinetic expression as was used to draw the lines in the other pressure dependence figures. The rate for sample 3 is in μ per minute into a 0.404 liter volume. It should be noted that if pore diffusion had been causing the change in pressure dependence with temperature for the sample 1 above 900° then the pressure dependence for this sample at 1036° should have been like that of the sample 1 at 900° instead of giving the norma pressure dependence of sample 1 at 1036°. The temperatur dependence of sample 3 at 21 μ is shown in Fig. 1 by the triangular marks. Again the rate for sample 3 is in μ per minute into a 0.404-liter volume. The temperature dependence of this sample is seen to be the same as that of sample 1. Again if pore diffusion were affecting the reaction the temperature dependence on the thin sample would have been different from that on the thick sample. The conclusion is drawn that pore

(3) G. Blyholder and H. Eyring, THIS JOURNAL, **61**, 682 (1957).

diffusion does not affect the reaction and that the data for sample 1 represent the true surface reaction.

Interpretation of Results.—Of the kinetic systems tried, these gave the best fit of the data.

$$H_2O + 2C_{(s)} \xrightarrow{k_1} OH_{(s)} + H_{(s)} \quad (1)$$

$$OH_{(s)} \longrightarrow O_{(s)} + H_{(s)} \quad (2)$$

$$2H_{(s)} \xrightarrow{k_{-2}} H_2\,(g) \quad (3)$$

$$O_{(s)} \longrightarrow CO_{(g)} \quad (4)$$

From the reaction of oxygen with graphite, the rate of equation 4 is known[3] to be much faster than the steam–graphite reaction. Thus the rate of equation 4 is fast and does not enter into the kinetic equation for the rate of the steam–graphite reaction. The rate of equation 2 is assumed to be fast. This assumption finds support in the work of Garten and Weiss,[4] who found that above 800° carbon activated with steam exhibited the characteristic of carbonyl oxygen rather than that of hydroxyl groups which were found to be a characteristic of activation of the carbon at 400°. From equations 1 and 3 we may now write

$$\frac{d\theta}{dt} = 2k_1 P(1 - \theta)^2 - 2k_{-2}\theta^2 \quad (5)$$

where

θ = fraction of the surface covered with H
P = pressure of H_2O

The rate at which H_2 comes off the surface which must also equal the rate of CO production is given by

$$R = k_{-2}\theta^2 \quad (6)$$

Making the steady-state assumption that $d\theta/dt = 0$, equation 5 may be solved for θ. Putting this result in equation 6 yields

$$R = \frac{k_1 P}{[1 + (k_0 P)^{1/2}]^2} \quad (7)$$

where

$$k_0 = \frac{k_1}{k_{-2}}$$

The temperature dependence of the rate constants necessary to fit the data is shown in Fig. 3. Values of the rate constants taken from Fig. 3 are used in equation 7 to produce the solid lines in Fig. 2. Equation 7 is seen to fit the pressure and temperature dependence of the reaction rate from 900 to 1300°. The activation energy for k_1, which is the rate constant for H_2O adsorbing on the surface, is 35.6 kcal. per mole from Fig. 3. From the temperature dependence of k_0 and k_1, the activation energy for k_{-2}, the rate constant for H_2 desorbing from the surface, is found to be 75 kcal. per mole. By adding the heat of chemisorption to the activation energy for adsorption of H_2 on graphite from work by Barrer[5] an activation energy for desorption of H_2 from graphite of 72 kcal. per mole is arrived at. This is in good agreement with the value herein arrived at from the kinetics of the steam–carbon reaction.

(4) V. A. Garten and D. E. Weiss, *Australian J. Chem.*, **8**, 68 (1955).

(5) R. M. Barrer, *J. Chem. Soc.*, 1256 (1936).

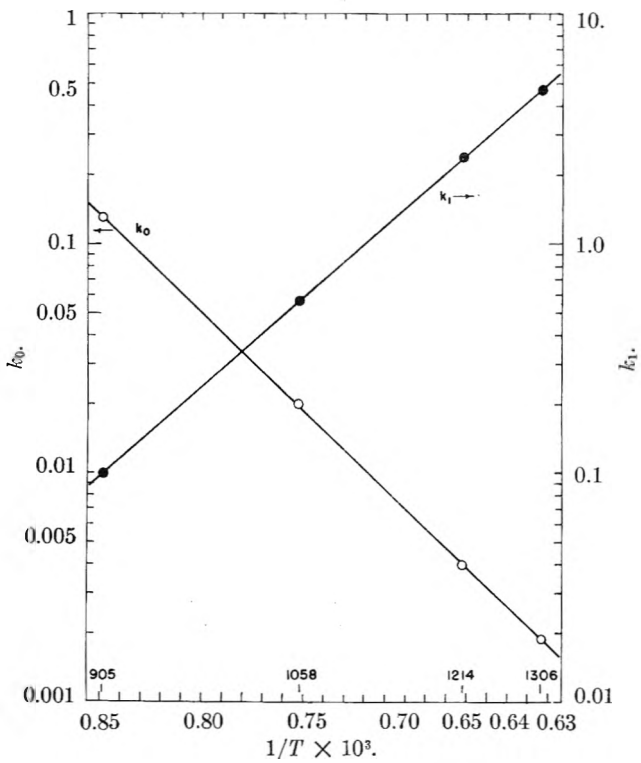

Fig. 3.—Temperature dependence of rate constants.

We may gain additional insight into the nature of the processes involved by calculating the rate constants k_1 and k_{-2} with the absolute rate theory of Eyring.[6] The rate of water going onto a bare surface is given by

$$v_1 = C_g C_s k' \quad (8)$$

where C_g = number of molecules per cm.^{3} of H_2O in the gas phase; C_s = surface sites per cm.^{2} taken as 10^{15} (the approximate number of carbon atoms per cm^2 of graphite lattice); k' = rate constant in sec.$^{-1}$. From absolute rate theory we have

$$k' = \kappa \frac{kT}{h} \frac{f^{\ddagger}}{f_i} e^{-E_0/kT} \quad (9)$$

where the symbols have their usual significance. It is assumed that the partition function for the activated complex involves only vibrational terms which to a good approximation may be replaced by unity. The partition function for the reactants is given by

$$f_i = f_{\text{vib.s}} f_{\text{vib. H}_2O} f_{\text{tr. H}_2O} f_{\text{rot. H}_2O}$$

Again the vibrational partition function for the surface and the water molecule are replaced by one. The translational and rotational partition functions are given by their usual terms.[6] The experimental activation energy is related to E_0 by

$$\frac{d \ln k}{dT} = \frac{E\,(\text{exp.})}{kT^2} \quad (10)$$

Application of equation 10 yields

$$E_0 = E\,(\text{exp.}) - 2RT$$

Putting numbers in for the terms in equation 8 yields at 1058° and 21 μ H_2O pressure

(6) S. Glasstone, K. J. Laidler and H. Eyring, "The Theory of Rate Processes," McGraw-Hill Book Co., Inc., New York, N. Y. 1941.

$$v_1 \text{ (calcd.)} = 0.34 \times 10^7 \text{ molecules/cm.}^2\text{-sec.} \quad (11)$$

We may also calculate the rate at which hydrogen comes off a completely covered surface. This is given by

$$v_2 = C_s k' \quad (12)$$

Here k' is given by equation 9. The process for which we wish to calculate k' is that for two hydrogen atoms on the surface reacting to form a hydrogen molecule. Since the activated complex is still part of the surface, if the hydrogen atoms are regarded as being most nearly characterized as immobile, then the partition function for the reactants and the activated state will involve only vibration terms which may be replaced by one. For this case k' reduces to

$$k' = \kappa \frac{KT}{h} e^{-E_0/kT} \quad (13)$$

Using equation 10 to find the relationship between the experimental activation energy and E_0 yields

$$E_0 = E \text{ (exp.)} - RT$$

We may now put numbers into equation 12 to yield at 1058°

$$v_2 \text{ (calcd.)} = 4 \times 10^{16} \text{ molecules/cm.}^2\text{-sec.}$$

The experimental values of v_1 and v_2 may be obtained from the data. The rate on sample 3 at 1058° and 21 μ H_2O pressure from Fig. 1 is found to be 7 μ/min. into a 0.404-l. volume. In more conventional units this is 7.8×10^{14} molecules/sec. for the total area of the sample. The geometric area of this sample is 20 cm.^{2} and the surface roughness may reasonably be taken[7] as 100. The resultant experimental rate is 3.9×10^{11} molecules/cm.^{2}-sec. From this value, equation 7, and k_0 from Fig. 3 is found

$$k_1 = 7 \times 10^{-3} \text{ cm./sec.}$$

and

$$k_{-2} = 2.5 \times 10^{12} \text{ molecules/cm.}^2\text{-sec.}$$

Since $v_1 = k_1 C_g$ and $v_2 = k_{-2}$ we have at 21 μ pressure

$$v_1 \text{ (exp.)} = 10.1 \times 10^{11} \text{ molecules/cm.}^2\text{-sec.}$$

and

$$v_2 \text{ (exp.)} = 2.5 \times 10^{12} \text{ molecules/cm.}^2\text{-sec.}$$

Comparison of the calculated and experimental values gives the interesting fact that the calculated value of v_1 is too small while the calculated value of v_2 is too large. In making the calculations for v_1 and v_2 it was assumed that all adsorbed species were immobile. At the temperatures of this work it would be reasonable to find at least limited mobility in the adsorbed species. If a limited mobility for adsorbed species is assumed the calculated rates are brought into agreement with the experimental ones. Until we have a more detailed knowledge of the species adsorbed on the surface this calculation can only be roughly approximated. It was therefore not deemed worthwhile carrying these calculations further at the present. It should be noted that the assumption of freely mobile adsorbed species gives rate constants which are in much poorer agreement than those obtained by the assumption of immobile species.

The kinetic treatment of the experimental data together with the calculations of absolute rate theory reveal the following picture for the steam–graphite reaction. Water is dissociatively adsorbed on the carbon surface. The evaporation of CO from the surface is rapid. The hydrogen comes off the surface more slowly than the CO. The pressure and temperature dependence of the reaction are explainable on the basis of the competition of the reactions of H_2O adsorption and H_2 desorption. The adsorbed species have limited mobility on the graphite surface. The above picture is in agreement with the strong inhibiting effect which hydrogen is found to[8] have on the steam–carbon reaction.

Acknowledgment.—The authors gratefully acknowledge the support of the United States Air Force under contract No. AF 33(038)20839.

(7) E. A. Gulbransen and K. F. Andrew, *Ind. Eng. Chem.*, **44**, 1034 1952).

(8) J. Gadsby, C. N. Hinshelwood and K. W. Sykes, *Proc. Roy. Soc. (London)*, **187A**, 129 (1946).

KINETICS OF THE REACTION BETWEEN URANIUM HEXAFLUORIDE AND SODIUM FLUORIDE.[1] II. SODIUM FLUORIDE PELLETS AND CRUSHED PELLETS[2]

BY F. E. MASSOTH[3] AND W. E. HENSEL, JR.[3]

Goodyear Atomic Corporation, Portsmouth, Ohio

Received October 1, 1958

A study of the kinetics of the reaction between uranium hexafluoride and sodium fluoride pellets and crushed pellets has been made over the temperature range 25 to 68°. Derivation of the logarithmic and parabolic laws for gas–solid reaction, involving a cubic particle, is presented. The reaction appears to proceed initially by a logarithmic mechanism and then by a parabolic mechanism. A blocking effect is advanced to explain the incomplete reaction with sodium fluoride pellets. A physical picture of the various steps of the reaction mechanism for the sodium fluoride–uranium hexafluoride reaction is presented.

Introduction

The factors which govern the kinetic laws for gas–solid reactions are: the chemical reactions at phase boundaries, the diffusion rates of reactants and the rates of nucleation and recrystallization. Usually the diffusion process is appreciably slower than the others and is rate determining. The mathematical form of the kinetic law describing this process is dependent upon the particle geometry. For spherical particles with constant surface concentration, the exact form of the diffusion equation involves a Fourier series expansion. Serrin and Ellickson[4] have shown that this exact solution can be approximated by the more general parabolic rate law, $dx/dt = k/x$. For spherical particles the integrated form is

$$k_g t = [1 - (1 - F)^{1/3}]^2 \qquad (1)$$

where F is the mole fraction converted at time t, and k_g is a constant. This parabolic law is equivalent to the Fourier expansion within 1% for values of F up to about 0.6.

Gaseous uranium hexafluoride reacts with sodium fluoride to form a solid addition complex of the formula $UF_6 \cdot 3NaF$.[5] Microscopy examination has shown that the particles of sodium fluoride are nearly cubic. Derivation of the parabolic law using the approach outlined by Farrar and Smith,[6] but based upon cubic particles, yields the integrated expression.

$$\left(\frac{k_c}{l_i^2}\right) t = 1/2 + 1/2(1 - F)^{2/3} - (1 - F)^{1/3} \qquad (2)$$

where

k_c is a rate constant
l_i is the initial particle edge
F is the fraction converted to product at time, t

If the particle dimensions are included in the reaction constant, equation 2 becomes

$$kt = 1/2 + 1/2(1 - F)^{2/3} - (1 - F)^{1/3} = f(B) \qquad (3)$$

where k is defined as the parabolic rate constant. Thus, a linear plot of $f(B)$ *versus* t is an indication of parabolic kinetics. Equation 3 is identical to equation 1 and hence is a good approximation of the the more rigorous Fourier expansion.

Another useful law correlating extent of reaction with time for gas–solid reactions, especially for thin films, is the logarithmic growth law. Although the logarithmic law has been well established experimentally, it seems to have little theoretical significance,[7] and is generally regarded as a useful empirical law for correlating rate data. This law states that the rate of build-up of film thickness of product with time is proportional to the exponential of x, or

$$\frac{dx}{dt} = ae^{-bx} \qquad (4)$$

where x is the film thickness of product at time t, and a and b are constants. Integration of equation 4, following the method of Farrar and Smith[6] and assuming cubic particles, gives

$$f(A) = c \log (gt + 1) \qquad (5)$$

where $f(A)$ is defined as $1 - (1 - F)^{1/3}$ and c and g are constants.

Other investigators[8,9] have used the integrated relationship

$$F = d \log (ht + 1) \qquad (6)$$

where d and h are constants.

Both equations 5 and 6 are derived from the basic law, equation 4. Equation 6 is for reaction on a plane surface, whereas equation 5 takes into account the geometry of the particles (spherical or cubic). Under conditions where gt is much greater than 1, equation 5 reduces to

$$f(A) = c \log t + c \log g \qquad (7)$$

Thus, a plot of $f(A)$ *versus* $\log t$ should approximate a straight line if the reaction follows logarithmic kinetics.

The fraction converted, F, can be determined experimentally from weight gain measurements taken during the reaction. Equation 8 expresses this relationship

$$F = \frac{W_t - W_0}{W_0(M_c/3M_0 - 1)} \qquad (8)$$

where

(1) This work was performed under Contract AT-(33-2)-1 with the United States Atomic Energy Commission.

(2) Part I, Sodium Fluoride Powder, appeared in THIS JOURNAL, **62**, 479 (1958).

(3) Southwest Research Institute, San Antonio, Texas.

(4) B. Serrin and R. T. Ellickson, *J. Chem. Phys.*, **9**, 742 (1941).

(5) F. E. Massoth and W. E. Hensel, Jr., THIS JOURNAL, **62**, 479 (1958).

(6) R. L. Farrar, Jr., and H. A. Smith, *ibid.*, **59**, 763 (1955).

(7) E. A. Gulbransen, *Trans. Electrochem. Soc.*, **91**, 573 (1947).

(8) U. R. Evans, *ibid.*, **83**, 335 (1943).

(9) N. F. Mott, *J. Inst. Metals*, **72**, 372 (1946); *Trans. Faraday Soc.*, **36**, 472 (1940).

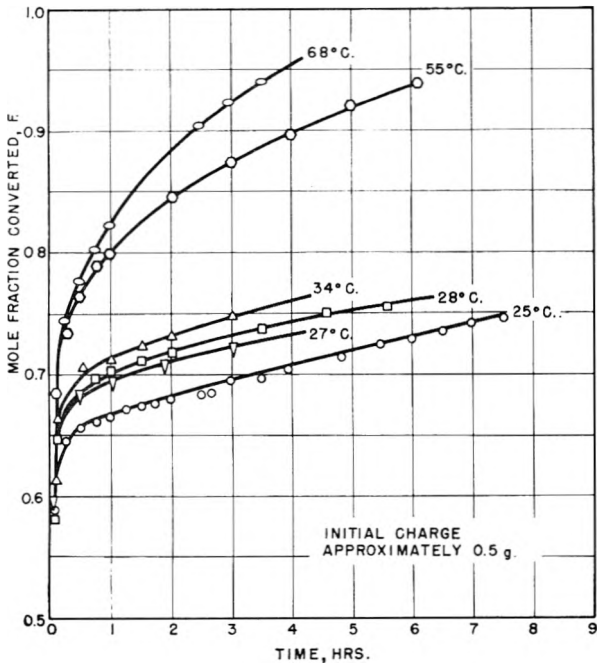

Fig. 1.—Mole fraction converted, F, *versus* time, crushed pellets.

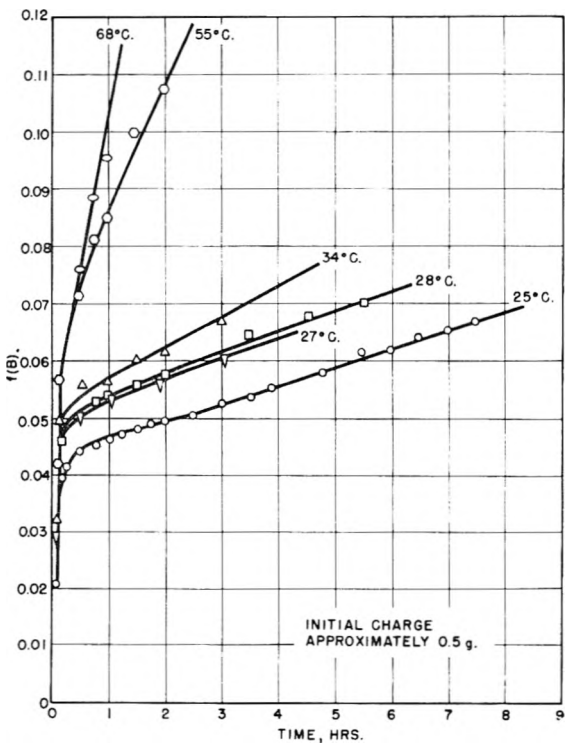

Fig. 2.—$f(B)$ *versus* time, crushed pellets.

W_t is the weight of sample at time t
W_0 is the initial weight of sodium fluoride
M_0 is the molecular weight of sodium fluoride
M_c is the molecular weight of the complex, $UF_6 \cdot 3NaF$

Experimental

Reagents.—One-eighth-inch cylindrical sodium fluoride pellets were obtained from the Harshaw Chemical Company. Crushed pellets were prepared by grinding pellets and screening through a 100-mesh sieve. Both materials were heated overnight at 275° to remove surface moisture and stored in a desiccator until used. Uranium hexafluoride was purified by several liquefaction and flashing cycles until the theoretical vapor pressure was attained.

The sodium fluoride powder referred to in this article is the same commercial product used in the study reported previously.[5]

Apparatus.—The apparatus used and the procedure followed are identical to those described previously.[5] The course of the reaction was followed by the increase in weight of sample with time under a constant uranium hexafluoride pressure of 90 mm. Both nickel and helix spring reactors were used.

Results

Crushed Pellets.—The results of a series of runs between uranium hexafluoride and sodium fluoride crushed pellets are graphically presented in Fig. 1. To determine whether the reaction followed parabolic kinetics, the data were plotted as $f(B)$ *versus* time in Fig. 2. The straight line obtained after a short initial period indicates conformance to parabolic kinetics. The slope of the straight line is the reaction rate constant k. The value of the slope at each temperature was obtained by a least squares analysis of the experimental points. Variation of the reaction rate constant with temperature is given in Fig. 3, where the logarithm of the slope is plotted against the reciprocal of the absolute temperature. From the least squares slope of this plot, the energy of activation for the reaction was calculated as 11.4 ± 0.5 kcal./mole of uranium hexafluoride. Hence, the reaction rate constant is given by the expression

$$k = 6.05 \times 10^5 e^{-11,400/RT} \text{ hr.}^{-1}$$

The steep initial slope, shown in Fig. 2, indicates that a faster reaction occurs initially than would be expected by the parabolic law. It was found that the reaction rate in this region can be characterized by a logarithmic growth law. In Fig. 4, a plot of log t *versus* $f(A)$ is given for the early period in the crushed pellet runs. The straight line portions obtained show by reference to equation 7, that the logarithmic rate law governs the early stages of the reaction. The time interval over which the logarithmic law is applicable is relatively short—about 300 seconds. On the other hand, the parabolic law predominates after approximately one-half hour. Hence, there appears to be a transition between the logarithmic and parabolic regions.

The logarithmic plot in Fig. 4 is not expected to hold at sufficiently low values of time. A better fit for the early period was obtained by use of equation 5. For one run, the resulting equation is

$$f(A_1) = 0.435 \log (0.0138t + 1)$$

In Fig. 5, the excellent agreement between the calculated curve (solid line) and the experimental points for this run is illustrated. Equally good results were obtained by this method for the other runs. Thus, the evidence indicates the initial reaction follows logarithmic kinetics.

Pellets.—The reaction of uranium hexafluoride with sodium fluoride pellets gave different results than reaction with the crushed pellets. The data, presented in Table I, show that the reaction apparently stopped at about 0.4 mole fraction converted. The extent of reaction was less for pellets than for crushed pellets at all times.

The initial portions of the curves obtained with pellets are similar to those obtained with crushed pellets. Runs with single pellets were made to study the initial reaction in detail. The results indicate that the initial reaction with pellets follows logarithmic kinetics. The logarithmic rates for pellets, single pellets, crushed pellets and sodium fluoride powder at room temperature are compared in Fig. 6. The logarithmic rates determined for pellets and for single pellets are comparable and are slightly lower than those obtained with crushed pellets. The results obtained previously with sodium fluoride powder show a considerably lower reaction rate than with either pellets or crushed pellets.

TABLE I

REACTION DATA FOR SODIUM FLUORIDE PELLETS

Temp., °C.	Time, hr.	F	Temp., °C.	Time, hr.	F
25	0.026	0.233	34	0.25	0.383
	.040	.261		1.25	.412
	.083	.309		3.25	.426
	.161	.356		67.25	.467
	.25	.371	34	1.00	.418
	.50	.392		2.00	.426
	1.00	.406		3.00	.430
	1.50	.412		19.70	.447
	2.00	.412	55	0.56	.384
	2.50	.413		1.20	.395
	3.50	.417		2.86	.404
	5.50	.419		4.86	.410
	6.50	.419	68	0.50	.336
				1.80	.346

The effect of pellet size upon the reaction rate was studied by using pellets which were cleaved and screened. The variation of extent of reaction with time for various sieve sizes is shown in Fig. 7. A general increase was noted in both extent and rate of reaction as the pellet size decreased. This agrees with the work of Cathers and Jolley.[10] Hence, there appears to be a macroscopic particle-size effect on the reaction.

Surface Area and Microscopy Studies.—Surface areas of sodium fluoride pellets, crushed pellets and reacted pellets were determined by both the B.E.T.[11] and a modified B.E.T. method.[12] In Table II, the surface area values are listed. The surface area per gram for pellets is of the same order of magnitude as that for crushed pellets, showing that the surface area is not appreciably affected by grinding. From the surface area value, the edge of an average cube was calculated to be 1.6 μ. After reaction, the surface area of the pellets was reduced markedly. Upon grinding, these same reacted pellets roughly doubled in surface area. Crushed pellets also exhibited a lower surface area after reaction. However, in this case it was necessary to grind the reacted material before determining the surface area since it fused into a hard mass.

(10) G. I. Cathers and R. L. Jolley, "Formation and Decomposition Reactions of the Complex UF_6·3NaF," paper presented at the American Chemical Society Meeting, Spring, 1957.

(11) S. Brunauer, P. H. Emmett and E. Teller, *J. Am. Chem. Soc.*, **60**, 309 (1938).

(12) F. W. Bloecher, Jr., "A New Surface Measurement Tool for Mineral Engineers," Massachusetts Institute of Technology, April 13, 1950, 5 p., Topical Report 6 (NYO-504).

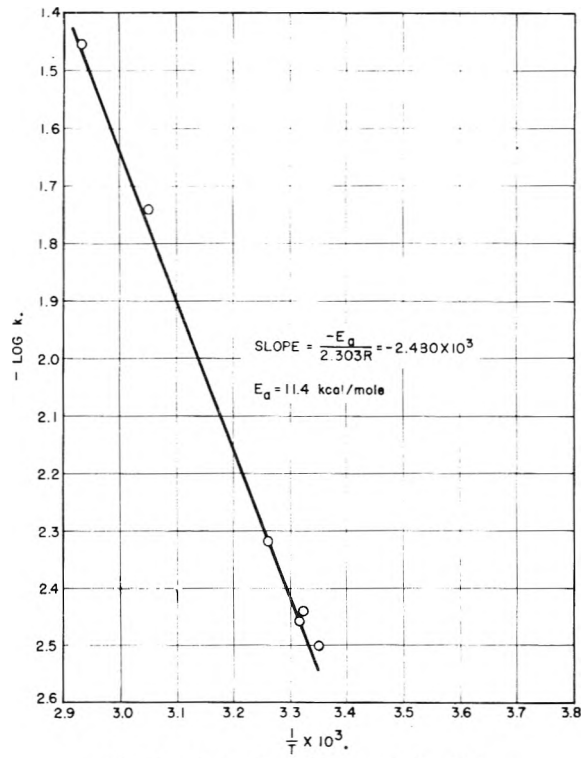

Fig. 3.—Arrhenius plot, crushed pellets.

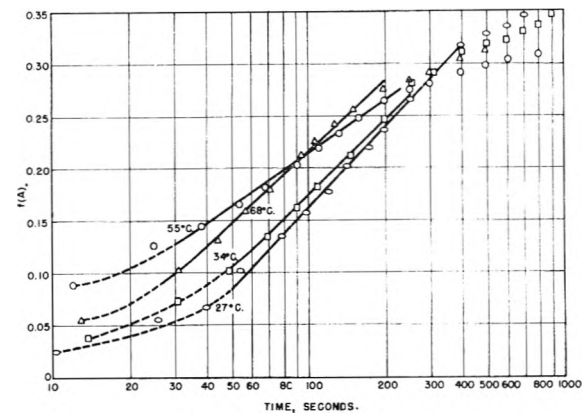

Fig. 4.—$f(A)$ *versus* logarithm of time, crushed pellets.

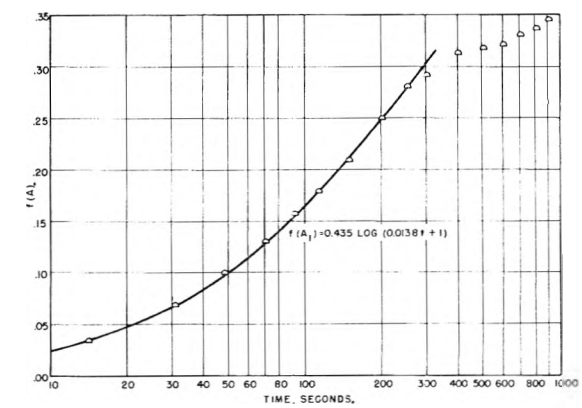

Fig. 5.—$f(A)$ *versus* logarithm of time for a typical crushed pellet run.

A limited particle size analysis,[13] of sodium fluo-

(13) R. A. Miller, "Observation on the Size and Shape of Sodium Fluoride Particles," Goodyear Atomic Corp., Oct. 17, 1957, 12 p., (GAT-L-419).

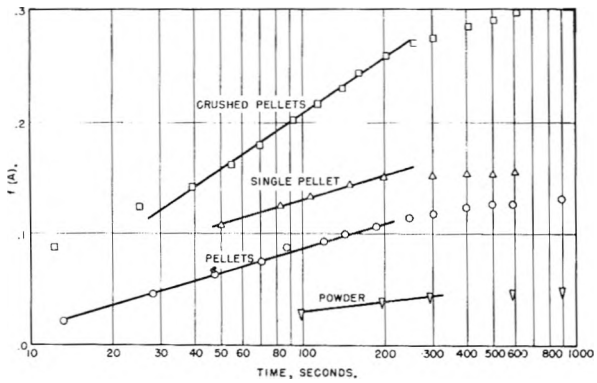

Fig. 6.—$f(A)$ *versus* logarithm of time for pellets, a single pellet, crushed pellets, and powder.

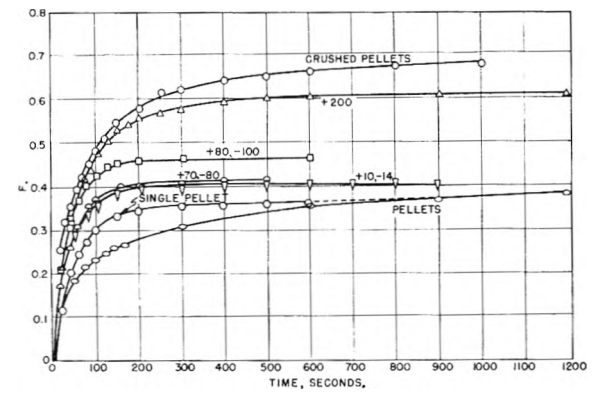

Fig. 7.—Mole fraction, F, *versus* time for various sieve sizes.

TABLE II

SURFACE AREA

	Surface area, m.²/g.[a]		
	Powder	Pellets	Crushed pellets
Unreacted	0.33	1.38(N)	1.48(N) 1.55(N)
Reacted	...	0.20(K)	...
Reacted and ground	...	0.36(K)	0.45(K) 0.52(N)

[a] N = nitrogen adsorption; K = krypton adsorption.

ride powder and crushed pellets, using light and electron microscopy techniques, showed a normal particle size distribution in both cases. The powdered particles exhibited nearly cubic shape while the individual particles in the crushed pellets were only roughly cubic. The median particle size for powder was 1.8 μ and for the crushed pellets 0.5 μ. These values are one-third to one-fourth those computed from the respective surface area determinations. This apparent discrepancy will be discussed later.

Discussion

Reaction of a gas and solid where only a solid product is formed proceeds at the interface between the two solids.[14] The over-all rate of reaction is generally the rate at which reactants can reach the interface. In the early stages, however, the rate at which new nuclei form by a direct reaction of the gas with unreacted solid may be important. Hence, two different mechanisms may be expected. The evidence accumulated in this investigation points to a dual reaction mechanism: namely, a fast initial reaction followed by a slower diffusion controlled reaction.

Our earlier work on sodium fluoride powder[5] showed that the over-all reaction kinetics followed a parabolic law after a brief but rapid initial reaction. Similar parabolic kinetics have been obtained in this investigation for crushed pellets. In the latter case, however, the extent of initial reaction was considerably greater. We would expect the rate, and therefore extent, of reaction to be proportional to the surface area. The greater extent of initial reaction observed for the crushed pellets as compared to the powder is in agreement with the larger surface area for the crushed pellets. In addition, a faster initial rate for crushed pellets might be expected since microscopic examination showed the cubic crystals to be more irregular, possessing more active sites for nucleation to take place.

The experimental results for pellets and crushed pellets suggest that the initial reaction follows the logarithmic growth law. Straight lines were obtained by a logarithmic plot of the data for pellets, single pellets, and sodium fluoride powder, as predicted by equation 7. In the case of crushed pellets, however, there is a curvature from the straight line at low times, but this was accounted for by use of the complete logarithmic law expression given by equation 5. Hence, it appears that in all cases, an initial logarithmic rate of reaction was obtained. Unfortunately, reproducibility between runs was not very good, although a satisfactory logarithmic fit for each run was obtained. Thus, duplicate runs gave logarithmic fits with different parameters. There seemed to be some consistency of slope between duplicate runs, but actual pick-up varied. The variation is probably due to non-uniformity of surface or differences in microscopic impurities between samples of duplicate runs. This phenomenon is not rare in gas–solid reactions; the effect of active surface sites and crystal imperfections can result in different initial paths of reaction under "identical" conditions.[14,15] Because of the inconsistency of duplicate runs it was not possible to evaluate quantitatively the effect of temperature upon the initial logarithmic rate.

There is a region between the initial logarithmic growth and the later parabolic growth which is of an indefinite character. It cannot be ascertained whether this is simply a natural transition region which links the logarithmic region with the parabolic and in which both rates coexist to varying degrees, or whether a separate mechanism prevails in this region. It extends over a longer time period than the logarithmic region but is shorter than the parabolic. On the other hand, in terms of actual material converted or reacted it has the smallest range.

The extent of reaction at the time when parabolic kinetics begin was considerably greater for crushed pellets than that found previously for powder. Since particle sizes for crushed pellets and powder

(14) S. J. Gregg, "Surface Chemistry of Solids," Reinhold Publ. Corp., New York, N. Y., 1951.

(15) P. H. Emmett, "Catalysis," Vol. I, Reinhold Publ. Corp., New York, N. Y., 1954, p. 87.

are different, it was considered interesting to compare the film thicknesses of the reaction product in the two cases. Comparison of the hypothetical film thickness at the time just preceding parabolic kinetics for crushed pellets and powder, indicates that the thickness is of the same order of magnitude in both cases.[16] Thus, the same mechanism is apparently followed for both materials, the parabolic law being obeyed only after a definite film thickness of product is formed.

The parabolic dependence for crushed pellets is in agreement with that found for powder. The activation energy for crushed pellets is 11.4 compared to 13.1 kcal./mole of uranium hexafluoride for powder. A statistical analysis of the data indicates that the difference in activation energies is slightly greater than the experimental error. Nevertheless, it is reasonable to assume that the same controlling factor is operative in both cases—namely, diffusion into the interior of the particle by a parabolic mechanism.

From the above discussion, it appears that the reaction proceeds initially by a logarithmic mechanism and then by a parabolic mechanism. For oxide films on metals, Cabrera and Mott[17] find that thin films generally obey a logarithmic growth while build-up of thick films follows parabolic kinetics. Riemen and Daniels[18] in a study of solid state reactions also propose a dual reaction mechanism to account for their data. On the other hand, the investigations of Gulbranson and co-workers[19,20] on oxidation of various metals show over-all parabolic kinetics with initial deviations. They do not state whether this is due to a separate mechanism or simply deviations at short times. Evans[21] discusses in considerable detail various mechanisms to account for this deviation. Jander[22] proposed that the initial deviation, in the case of reactions involving solids having low thermal conductivity, might be due to the heat liberated by the exothermic surface reaction. This would result in a more rapid initial reaction rate. Because of the small initial deviation, the kinetics obtained with sodium fluoride powder may be interpreted either by a separate initial mechanism or by deviation at low times. However, the large extent of reaction obtained for the crushed pellets before parabolic kinetics begin, almost certainly must indicate that a separate mechanism prevails in this region.

It is interesting to compare our results with those obtained at higher temperatures in a similar study by Worthington.[23] He has correlated his results by a logarithmic law throughout. Over the same extent of reaction, we found a logarithmic fit with crushed pellets. Upon further reaction we found a transition into parabolic kinetics while Worthington has not obtained data in this region. The fact that the reaction rates determined by Worthington are less at high temperatures than those obtained in this study at lower temperatures might be accounted for by a difference in particle size; *i.e.*, the powder used by Worthington may have a smaller surface area than the crushed pellets used in this investigation. Another factor to be considered is that since Worthington's investigation was conducted at a higher temperature, it is possible that there is a shift of the over-all parabolic mechanism to logarithmic in this temperature range. A shift of mechanism with temperature is quite common in gas–solid reactions.[24,25] Finally, in the temperature region of Worthington's study, the decomposition reaction becomes significant.[10] A small but appreciable back reaction might alter the nature of the forward reaction because of the paramount importance of the geometry of the particle.

It is indeed remarkable that the pellets exhibit completely different reaction characteristics than either powder or crushed pellets. They show a rapid initial pick-up which apparently stops abruptly below the theoretical conversion. The initial growth for pellets is slower than that for crushed pellets but faster than that for powder. This can be partially explained on the basis of surface area. Pellets have a larger surface area than powder and would be expected to react faster and to a greater extent initially. On the other hand, since pellets and crushed pellets have approximately the same surface area, they would be expected to react at comparable rates. That this is not found experimentally may be due to a physical blocking effect in the pellets which operates even at this low extent of conversion, reducing the available surface area.

It is necessary at this time to examine the structure of sodium fluoride. Light and electron micrographs revealed that sodium fluoride powder and crushed pellets consist of individual cubic crystals and clumps of these basic particles. The cubic crystals have a distribution of sizes, and a particle size analysis gives the median size of a basic cube. In the surface area measurements by nitrogen adsorption, the total areas of both basic cubes and clumps are determined. However, since the surface area determined by nitrogen adsorption is less than that calculated from microscopy measurements, the basic cubes in a clump must be partially fused. Electron micrographs of crushed sodium fluoride pellets supported this contention. Thus, nitrogen adsorption gives an average clump size whereas light microscopy gives an average cube size. This explains the apparent anomaly in particle size as determined by the two methods.

Reaction of powder and crushed pellets goes to completion. However, we must now explain incomplete reaction in the case of pellets. This can be

(16) It is assumed that x/l_i is proportional to $1 - (1 - F)^{1/3}$. The average values for F at the start of parabolic dependency for crushed pellets and powder are 0.67 and 0.22, respectively. Thus,

$$\frac{x_c}{(l_i)_c} \Big\backslash \frac{x_p}{(l_i)_p} \backsimeq 4$$

But from surface area measurements and light micrographs

$$(l_i)_p/(l_i)_c \backsimeq 4 \text{ and therefore } x_p/x_c \backsimeq 1$$

(17) N. Cabrera and N. F. Mott, *Repts. Progr. Phys.*, **12**, 163 (1949).

(18) W. P. Riemen and F. Daniels, THIS JOURNAL, **61**, 802 (1957).

(19) E. A. Gulbranson and K. F. Andrew, *J. Electrochem. Soc.*, **99**, 402 (1952); *J. Metals*, **2**, 586 (1950).

(20) E. A. Gulbransen, *Trans. Electrochem. Soc.*, **83**, 301 (1943).

(21) U. R. Evans, *ibid.*, **91**, 547 (1947).

(22) W. Jander, *Z. anorg. allgem. Chem.*, **166**, 3 (1927).

(23) R. E. Worthington, "The Reaction of Sodium Fluoride with Hex and Hydrogen Fluoride," Research and Development Branch, Copenhurst Works, Jan., 1957, 12 p. (CGR-R/CA-200).

(24) J. T. Waber, *et al.*, *J. Electrochem. Soc.*, **99**, 121 (1952).

(25) D. Cubicciotti, *J. Am. Chem. Soc.*, **74**, 1200 (1952).

accounted for by considering pellets to consist of aggregates of a large number of clumps. Since the surface areas of pellets and crushed pellets as determined by nitrogen adsorption are about the same, the clumps in the aggregate must be held loosely, probably by van der Waals forces, which permits almost complete adsorption of nitrogen on the individual clumps. Upon reaction with uranium hexafluoride, the aggregate surface and some of the interior clumps react rapidly. However, the addition compound formed results in a considerable swelling of the aggregate.[26] The swelling effectively closes off entry for uranium hexafluoride into the aggregate by formation of an impenetrable layer on the outside of the aggregate. This blocking effect does not occur with powder and crushed pellets because the clumps which are present are apparently not large enough to limit the reaction by blocking and complete reaction is obtained.

The impenetrable layer around each aggregate in the reacted pellets should be of considerable thickness, as is indicated by the appreciable extent of reaction obtained. This thick layer probably includes several layers of nearly completely reacted clumps (the inner clumps in an aggregate being only partially reacted). The apparent termination of reaction is accounted for by the thick layer of complex; *i.e.*, since the rate is inversely proportional to the layer thickness (parabolic law), the rate becomes negligibly small for very thick films. Presumably the reaction is continuing at an immeasurably slow rate. If the reacted aggregates are broken into clumps by grinding, new surfaces will be exposed so that upon further reaction with uranium hexafluoride, complete conversion should be attained. This is in accord with our results.

In the screening experiments, we reduce the overall size of the unreacted pellets, breaking down some of the aggregates into smaller aggregates and clumps. Since clumps are more reactive than aggregates, increased extent of reaction is expected with decreasing pellet size.

Mechanism of Reaction.—In any gas–solid reaction mechanism these general steps must be considered: initial reaction on the surface, adsorption of the gas on the product formed, transport of unreacted material to the reaction interface and chemical reaction at the interface. We will now attempt to present a physical picture of these various steps of the reaction mechanism for the sodium fluoride–uranium hexafluoride reaction.

Step I. Surface Reaction.—Diffusion of uranium hexafluoride through the gas phase is not considered a step in the reaction mechanism. When the uranium hexafluoride molecules strike the surface of the sodium fluoride, rapid chemical reaction takes place. This process probably occurs on active sites, *i.e.*, small areas of high potential energy.[15] From these nuclei, the interface spreads outward by surface diffusion until the entire surface is covered by a layer of product. At the same time there may be some inward penetration of the interface, but this rate is much slower than the lateral growth because of the retarding effect of the complex formed. Surface reaction is a relatively rapid process.

Step II. Adsorption of Uranium Hexafluoride on Complex.—After surface reaction is complete, uranium hexafluoride must be adsorbed on the complex in order for reaction to continue. This is generally a rapid process and in our case it is not rate controlling. If it were rate controlling, the rate of reaction would be expected to be proportional to the external surface area of the particle. Since there is a swelling of the particle upon reaction, an increase in surface area would be expected. Hence, the rate of adsorption should increase proportionally during reaction. However, the rate of reaction, experimentally observed, constantly decreased.

Step III. Build-up of Complex Film to a Definite Thickness.—The propagation of the interface inward is governed by a logarithmic law. Logarithmic growth is generally interpreted on the basis of recrystallization by repeated cracking and healing of the film, re-exposing fresh surfaces for reaction.[14] In most of this region the reaction is governed by logarithmic kinetics. However, near the end of the region the rate deviates from the logarithmic law. The deviation is attributed to a gradual shift of mechanism to parabolic kinetics with a period wherein both mechanisms coexist to varying degrees. When a definite film thickness is attained, then the reaction follows parabolic kinetics exclusively.

Step IV. Volume Diffusion through the Complex.—When a sufficient product film is built up as described in step III, the rate of reaction is controlled by a slow volume diffusion process through the film. The product film is stable and the rate of reaction is inversely proportional to the film thickness. If the film is not stable (*i.e.*, it cracks due to swelling or recrystallization, opening up grain boundary paths) linear kinetics would be obtained.[6] Evans[8] states that the parabolic law is followed in the case of oxide films on metals when the film is non-porous and possesses ionic and electronic conductivity. He describes the process as an outward ionic migration under a potential gradient associated with vacant sites in the cationic lattice. Gens[27] has found that fluorine atoms diffuse rapidly to the surface of sodium fluoride particles through defect sites. A similar type of mechanism may occur in our case.

Step V. Chemical Reaction at the Interface.—Little is known about this step except that it is fast compared to the parabolic diffusion. If this step were rate controlling, linear kinetics would be observed since availability of uranium hexafluoride to the unreacted surface would be independent of the film thickness of product. It is not known whether a sharp interface boundary is present here or a solid solution type of process takes place.

(26) Swelling would be expected because of the large atomic diameter of uranium compared to sodium and fluorine. Physical evidence of swelling was shown by the hardness of the complex after reaction. It was necessary to use a hammer to break up the product, since the original powder had become a solid, hard mass.

(27) T. A. Gens, "F^{18} Exchange between Fluorocarbons and Some Fluorine-Containing Compounds," Oak Ridge National Lab., Jan. 1957, 124 p. (ORNL-2363).

INTERMOLECULAR FORCES INVOLVING CHLOROFLUOROCARBONS

BY E. BRIAN SMITH, JOHN WALKLEY AND JOEL H. HILDEBRAND

Contribution from the Department of Chemistry, University of California, Berkeley, California

Received October 9, 1958

Solvent properties of chlorofluorocarbons have been studied in order to fill the long interval between hydrocarbons and fluorocarbons. The solubility of iodine in 2,2,3-$C_4Cl_3F_7$ is 0 1510 mole % at 25°. Between 0 and 35° it accords with the equation, $\log x_2 = 13.050 \log T - 35.075$ where x_2 is mole fraction. The relation of entropy of solution tc solubility previously found is again followed. In mixtures of 8.93 and 12.5 volume % of CCl_4 with C_7F_{16}, the solubilities of I_2 at 25° are 0.0388 and 0.0545 mole %, respectively. Partial molal volumes of Br_2 and I_2 have been determined in solvents ranging from C_7F_{14} to $CHBr_3$, including 3 chlorofluorocarbons, and in two mixed solvents, C_7F_{16}–CCl_4 and c-$C_4Cl_2F_6$–CCl_4. The data are evidence that contacts between halogen molecules and chlorine atoms in the solvents have much higher than random probability.

Fluorocarbons, by greatly extending the available range of internal forces,[1] have been of great service in providing stringent tests for theories of non-polar liquids and solution. However, the extension has been so great as to leave a considerable gap in solvent power for iodine between f-heptane and the poorest hydrocarbon solvent investigated, 2,2-dimethylbutane. The mole fraction of iodine in the latter at 25° is 26.3 times its value in the former.

We turned to chlorofluorocarbons to fill in this interval. Shinoda and Hildebrand[2a] determined the solubility of iodine in cyclodichlorohexafluorobutane, c-$C_4Cl_2F_6$, in $(C_3F_7COOCH_2)_4C$, and, to extend the range at the other end, in $CHBr_3$. We determined, also, the partial molal volume of iodine in a number of solvents,[2b] with the surprising result that in CCl_2FCClF_2 it is 67.7 cc., close to the value in many non-polar solvents, but rises to 81.2 cc. in c-$C_4Cl_2F_6$. Glew and Hildebrand[1c] had previously obtained the value of 100 cc. in perfluoroheptane. Because expansion contributes to the entropy of solution we have considered it important to look more closely into this factor.

Solubility of Iodine in 2,2,3-Trichloroheptafluorobutane, $C_4Cl_3F_7$.—We were so fortunate as to obtain a sample of this compound from Dr. T. M. Reed, and we determined the solubility of iodine therein in order to supplement other solubility data. The technique adopted was essentially that described by Glew and Hildebrand,[1c] but the apparatus was modified for use with a smaller volume of solvent, ~8 cc. The solution was stirred for 20 hours in the presence of excess iodine; temperatures were controlled to ±0.002°. The concentration of iodine was determined spectrophotometrically and checked by titration. The solutions obey Beer's law. The results are given in Table I. The figures in the last column have been calculated from the equation $\log x_2 = 13.050 \log T - 35.111$. The entropy of solution of solid iodine is 25.88. This places it on the straight line of Fig. I of ref. 2a, where the entropy of solution is plotted against the solubility expressed as $-R \ln x_2$. The solubility parameter of $C_4Cl_3F_7$ calculated from its molal volume, 166 cc., and the solubility parameter of iodine at 25° is 6.9, in excellent agreement with the value 6.92, obtained by Reed (private communication) from its heat of vaporization.

TABLE I

SOLUBILITY OF IODINE IN $C_4Cl_3F_7$, MOLE %, $100x_2$

t, °C.	0.00	14.80	19.36	25.00	35.30
Obsd.	0.0473	0.0961	0.1184	0.1510	0.2331
Calcd.	0.0479	0.0959	0.1181	0.1509	0.2347

The Solubility of Iodine in Mixtures of C_7F_{16} and CCl_4.—This was determined at 25° in two mixtures of different composition. The results are given in Table II.

TABLE II

SOLUBILITY OF IODINE IN MIXTURES OF C_7F_{16} WITH CCl_4 MOLE % AT 25°

Vol. % CCl_4	8.93	12.5
$100x_2$	0.0388	0.0545
δ_0 from x_2	6.0	6.3
δ_0 from eq. 1	6.1	6.2

δ_0 represents the solubility parameter of the mixed solvent calculated first, from x_2, second, by the equation

$$\delta_0 = \phi_1\delta_1 + \phi_3\delta_3 \qquad (1)$$

given by Hildebrand and Scott.[3] In this ϕ denotes volume fraction, and the subscripts 1 and 3, refer to C_7F_{16} and CCl_4; $\delta_1 = 6.0$ and $\delta_3 = 8.6$. The agreement is quite satisfactory.

Partial Molal Volumes.—We have determined the partial molal volume of iodine in 2,2,3-$C_4Cl_3F_7$, to add to those already at hand,[2b] but because the low solubility of iodine in fluorocarbons and fluorochlorocarbons makes it difficult to achieve the desired accuracy, we turned to bromine in order more easily to cover the solvents in this region. We used the rapid method employed in the earlier work, with all necessary precautions. The solvents were of high purity, dried as necessary over P_2O_5, distilled and run through a column of silica gel. Bromine was dried with P_2O_5 and distilled under reduced pressure. The mole fraction of halogen never exceeded 0.004, therefore the values given are virtually those of the partial molal volume of the halogen, $\bar{v}_2$, at infinite dilution. Duplicate determinations agreed within 0.4 cc. $mole^{-1}$. The results are given in Table III together with our earlier values for iodine.

TABLE III

PARTIAL MOLAL VOLUMES OF BROMINE AND IODINE AT 25° AND HIGH DILUTION, CC. $MOLE^{-1}$

Solvent	δ_1	Br_2	I_2
n-C_7F_{16}	6.0	71.7	100
c-$C_6H_{11}CF_3$	6.1	71.2	...
c-$C_4Cl_2F_6$	6.8	64.3	81.2
2,2,3-$C_4Cl_3F_7$	6.9	...	78.6
CCl_2FCClF_2	7.5	56.9	67.7
$SiCl_4$	7.6	54.9	67.1
CCl_4	8.6	54.1	66.7
$CHCl_3$	9.0	53.7	65.6
CS_2	10.0	49.9	62.3
$CHBr_3$	10.5	49.3	60.8
Br_2	11.5	51.5	...
I_2	14.1	...	59.0

The data are plotted in Fig. 1 against the solubility parameters of the solvents, δ_1. Noteworthy is the slow increase in $\bar{v}_2$ in the case of both halogens,

(1) (a) H. A. Benesi and J. H. Hildebrand, *J. Am. Chem. Soc.*, **70**, 3978 (1948); (b) J. H. Hildebrand, H. A. Benesi and L. M. Mower, *ibid.*, **72**, 1017 (1950); (c) D. N. Glew and J. H. Hildebrand, THIS JOURNAL, **60**, 616 (1956).

(2) (a) K. Shinoda and Joel H. Hildebrand, *ibid.*, **62**, 292 (1958); (b) **62**, 293 (1958).

(3) J. H. Hildebrand and R. L. Scott, "Solubility of Non-electrolytes," Reinhold Publ. Corp., 1950, eq. 11, p. 201.

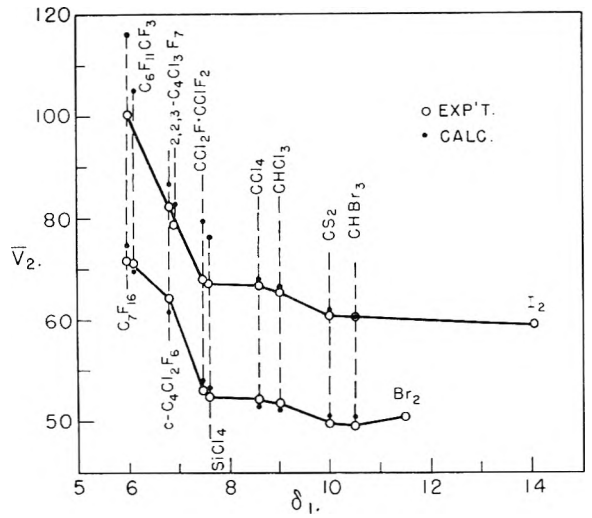

Fig. 1.

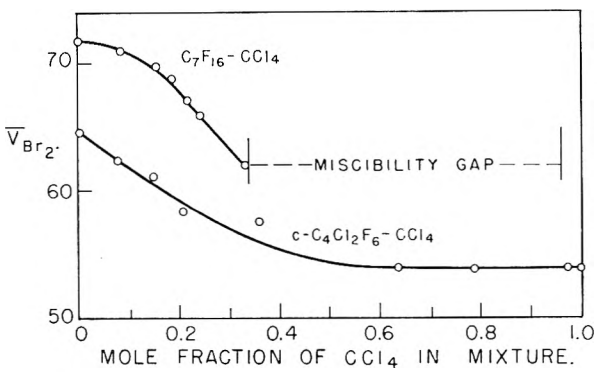

Fig. 2.

as δ_1 decreases all the way from $CHBr_3$ to CCl_2F-$CClF_2$, followed by rapid rise in both cases from the latter solvent to C_7F_{16}.

A smooth increase was to be expected on the basis of the relation[4]

$$\bar{v}_2 - v_2 = \beta_0 RT \ln \gamma_2 \qquad (2)$$

where β_0 is the compressibility of the solvent and γ_2 the activity coefficient of the solute. The points so calculated are shown in Fig. 1.

The sharp break in the experimental points, however, calls for further attention. We explain it as follows.

The major part of the surface area of a molecule of CCl_2FCClF_2 consists of chloride atoms. On the basis of a ratio of 1.33 for the van der Waals radii of chloride to fluoride, their cross-sections are in the ratio of 1.8, therefore approximately 64% of the surface area of this compound consists of chloride, and its behavior toward bromine and iodine with respect to both solvent power and partial molal volume is much closer to that of CCl_4 than to that of a pure fluorocarbon. However, in $C_4Cl_3F_7$ and $C_4Cl_2F_6$, chloride atoms, on the same basis, occupy 49 and 38%, respectively, and the halogen molecules are more frequently forced to be under the much weaker attractive potential of fluoride atoms.

We evidently have in these solutions molecules for which it is appropriate to recognize different attractive potentials in different parts of their surfaces, as was done years ago by Langmuir.[5] He assigned parameters for attractive potentials between molecules and groups present in molecules, and invoked the Boltzmann factor to give the probabilities of contacts of various energies.

We undertook to throw additional light upon this matter by determining the partial molal volume of bromine in two mixed solvents, permitting the ratio of chloride to fluoride areas to be varied continuously.

We used two mixtures, one, C_7F_{16} with CCl_4, which has a miscibility gap, the other, c-$C_4Cl_2F_6$ with CCl_4, whose composition can be varied through the entire range. The results are plotted in Fig. 2 against mole fraction of CCl_4 in the solvent. The striking feature is the rapid drop in $\bar{v}_2$ with increasing mole fraction of CCl_4. It is much steeper if plotted against volume fraction. Our interpretation is:

In the mixture C_7F_{16}-CCl_4, when only a little CCl_4 is present, it can have but little effect in lowering the value of $\bar{v}_g$ for Br_2, because contacts between them are rare, but as more CCl_4 is added, they increase rapidly, permitting $\bar{v}_2$ to drop rapidly toward its value in pure $\bar{v}_2$. Therefore $\bar{v}_2$ is less than an additive function of its values in the two pure solvents.

In the mixture, $C_4Cl_2F_6$–CCl_4, in which there is no gap, $\bar{v}_2$ again drops rapidly toward its value in pure CCl_4. This curve is not convex upward probably because chloride atoms are already present in large excess in the pure chlorofluorocarbon, and the further drop is roughly proportional to their increase. It seems more important to present the evidence for the concept qualitatively than, at this stage at least, to make a quantitative calculation by Langmuir's method. We remark only that these ternary solutions are obviously not strictly regular (we use "strictly" here in its proper, adjectival sense) but that preferred contacts occur with higher than purely random probability.

We are determining values of $(\partial P/\partial T)_V$ for these solvents in order to study the effects of expansion upon the entropy of solution.

We gratefully acknowledge the kindness of Dr. T. M. Reed in supplying the $C_4Cl_3F_7$, and the Atomic Energy Commission and National Science Foundation for the grants that have supported the work.

(4) *Cf.* ref. 3, p. 141.

(5) I. Langmuir, "Colloid Symposium Monograph," 1925, p. 48. See also, ref. 4, pp. 162–166.

KINETICS AND MECHANISM OF THE BASE-CATALYZED HYDRATION OF FUMARATE TO MALATE[1]

BY LUTHER E. ERICKSON AND ROBERT A. ALBERTY

Contribution from the Chemistry Department, University of Wisconsin

Received October 13, 1958

Thermodynamic and kinetic data are presented for the reversible, NaOH catalyzed hydration of fumarate to D,L-malate in H_2O in the temperature range 90–175°. The equilibrium constants are correlated with those obtained for the fumarase-catalyzed hydration of fumarate to L-malate at room temperature. The reaction follows a reversible first-order rate law in fumarate and malate. Rates are proportional to NaOH concentration at constant ionic strength. Proton magnetic resonance was used to show that the methylene protons of malate exchange with deuterons in D_2O more rapidly than the over-all reaction occurs. The racemization rate of L-malate catalyzed by NaOH is equal to the rate of dehydration of D,L-malate. A mechanism is presented which is consistent with these observations.

Introduction

The enzyme fumarase catalyzes the reversible hydration of fumarate to L-malate. Extensive studies of this reaction have been made.[2–4] The effect of *p*H on the kinetic constants indicates that acidic groups of the enzyme are involved in the catalytic process.[5] With the hope of getting a better understanding of the mechanism of the fumarase reaction, studies are being made of the catalysis of the hydration by strong acids[6] and bases. For the latter case,[7] the reaction may be written

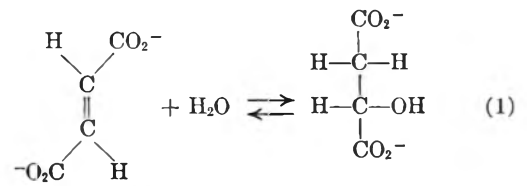

(1)

Experimental

Procedure.—Five-ml. samples of the reaction mixture were sealed in ten-ml. alkali resistant glass ampules supplied by Corning Glass Co., and heated to the desired temperature in an aluminum block thermostat with the temperature controlled to ±0.2°. Sodium hydroxide concentrations and temperatures were chosen so that the rates were slow enough so that errors due to the time lag in heating the samples to temperature were insignificant. Sodium chloride was used to control the ionic strength.

After being heated, the samples were cooled rapidly and analyzed, with a Beckman DU spectrophotometer, for fumarate. The absorbancy A at wave lengths from 270–300 mμ is proportional to the fumarate concentration, and malate does not absorb significantly in this region of the spectrum. It was, however, necessary to use a blank, *i.e.*, a solution of the same NaOH concentration, heated for the same time, with every sample, to correct for the absorbancy due to substances dissolved from the glass walls.

Equilibrium Quotient.—Representing sodium fumarate by F and sodium malate by M, reaction 1 can be written

$$F + H_2O \rightleftharpoons M \qquad (2)$$

for which the equilibrium constant is given by

$$K = \frac{a_M}{a_F a_{H_2O}} = Q\frac{y_M}{y_F a_{H_2O}} \qquad (3)$$

where a represents activity, Q, the equilibrium quotient, is the equilibrium molar concentration ratio of disodium malate to disodium fumarate, and y_M and y_F are the corresponding mean ionic activity coefficients. Experimentally, Q is determined from the absorbancies of a fumarate solution before reaction and after it has reached equilibrium, *i.e.*, $Q = (A_0 - A_\infty)/A_\infty$.

The following considerations show that fumarate and malate are the only substances present in the reaction mixture at significant concentrations at equilibrium. A synthetic "equilibrium" mixture, whose composition was based on the assumption that all the absorbancy is due to fumarate, showed no change in absorbancy when it was heated for several half-lives. If a third component were involved, the fumarate–malate ratio and the absorbancy of this mixture would have changed upon heating unless the absorbancy of the third component were just enough to compensate for the decrease in fumarate concentration. It is unlikely that it would exactly compensate at all wave lengths and temperatures studied.

However, samples of 2 *M* sodium malate in 4 *M* NaOH, heated for several days (approximately 100 times as long as necessary to reach within 1% of fumarate–malate equilibrium), showed significant yellow coloration. The yellow product was separated from fumaric and malic acids by partition chromatography using a celite column, 0.5 *N* HCl stationary phase and 65% CCl_3H, 35% butanol as the eluent.[8] The yellow product could be separated completely from fumaric acid with a 50 cm. column. Since it came off the column before fumaric acid, it is probably less polar than fumaric acid. The yellow compound can be titrated with NaOH; therefore, it contains an acidic group. The infrared spectrum showed strong absorption in the carboxyl region. Even under the extreme conditions required to produce significant color, the yellow product amounted to only 0.5% by weight of the initial fumarate. Therefore, no further attempt was made to complete the characterization.

Reaction Rate Constants.—The reaction obeys the rate law

$$-\frac{d(F)}{dt} = k'_h(F)(OH^-) - k'_d(M)(OH^-) = k_h(F) - k_d(M) \qquad (4)$$

where k_h is the first-order rate constant for the hydration reaction; k_d, the first-order rate constant for the dehydration reaction. Both k_h and k_d are proportional to the (OH^-) at constant ionic strength.

For this reversible, first-order reaction

$$-\log[(F)_t - (F)_{eq}] + \log[(F)_0 - (F)_{eq}] = \frac{k_h + k_d}{2.303}t \qquad (5)$$

where $(F)_0$, $(F)_t$ and $(F)_{eq}$ are the fumarate concentrations at time $t = 0$, $t = t$ and $t = \infty$. The rate constants were obtained by plotting $-\log(A_t - A_{eq})$ *vs.* t. Linear plots were obtained when either fumarate or malate was used as substrate. The individual first-order rate constants, k_h and k_d, for the hydration and dehydration reactions were determined by making use of the additional relation $Q = k_h/k_d$. Table I summarizes the rate and equilibrium quotient data.

Racemization Rate of L-Malate.—In order to compare the first-order rate constants for racemization k_r and de-

(1) This research was supported by the National Science Foundation and by the Research Committee of the University of Wisconsin from funds supplied by the Wisconsin Alumni Research Foundation.

(2) R. A. Alberty, W. G. Miller and H. F. Fisher, *J. Am. Chem. Soc.*, **79**, 3973 (1957).

(3) R. A. Alberty, *Advances in Enzymology*, **17**, 1 (1956).

(4) R. A. Alberty and B. M. Koerber, *J. Am. Chem. Soc.*, **79**, 6379 (1957) and earlier papers.

(5) R. A. Alberty, *J. Cell. Comp. Physiol.*, **47**, 245 (1956).

(6) L. T. Rozelle and R. A. Alberty, THIS JOURNAL, **61**, 1637 (1957).

(7) V. Loyde, *Ann.*, **192**, 80 (1878).

(8) W. G. Miller, Ph.D. thesis, University of Wisconsin, 1958.

TABLE I

RATE AND EQUILIBRIUM DATA FOR REACTION 1

T, °C.	Substrate concn., $M \times 10^2$	(NaOH) M	Ionic strength	Q	$k_h \times 10^6$, sec.$^{-1}$	$k_d \times 10^6$, sec.$^{-1}$	$\frac{k_h \times 10^6}{(OH^-)}$, M^{-1} sec.$^{-1}$	$\frac{k_d \times 10^6}{(OH^-)}$, M^{-1} sec.$^{-1}$
175	10	0.023	0.060	0.69	3.1	4.5	136	197
	10	.100	.130	.65	13.7	21	137	210
	10	.100	.330	.70	17.5	25	175	250
	10	.100	.330	.70	21	29	210	290
	10	.100	.530	.74	25	36	250	360
	10	.100	.530	.77	29	38	290	380
	10	.100	.530	.78	27	35	270	360
	10	.300	.530	.78	81	103	270	340
	10	.500	.530	.80	...	...	...	...
	~9	~ .090	~6.0	~1.65	...	...	...	...
150	2	0.108	0.117	0.88	3.4	3.8	31	35
	10	.100	.130	0.93	3.5	3.8	35	38
	10	.100	.330	1.00	3.7	3.7	37	37
	10	.100	.530	1.04	5.2	4.9	52	49
	2	.108	.546	1.03	6.1	5.6	57	51
	2	.150	.546	1.06	10.0	10.3	67	69
	2	.302	.546	1.06	...	...	...	...
	5	.480	.50	1.05	...	...	...	...
125	2	0.217	0.224	1.42	1.90	1.39	9.0	6.4
	2[a]	.217	.224	1.42	1.70	1.20	7.7	5.5
	2	.217	.546	1.49	2.8	1.9	12.8	8.7
	2[a]	.217	.546	1.49	2.8	1.9	12.8	8.7
	2	.536	.546	1.58	7.5	4.8	14.0	9.0
	2[a]	.536	.546	1.49	8.3	5.6	15.5	10.5
110	2000[a,b]	0.50	6.50	~10	147	13.9	294	27.8

[a] Indicates malate used as substrate; all others fumarate. [b] In D_2O.

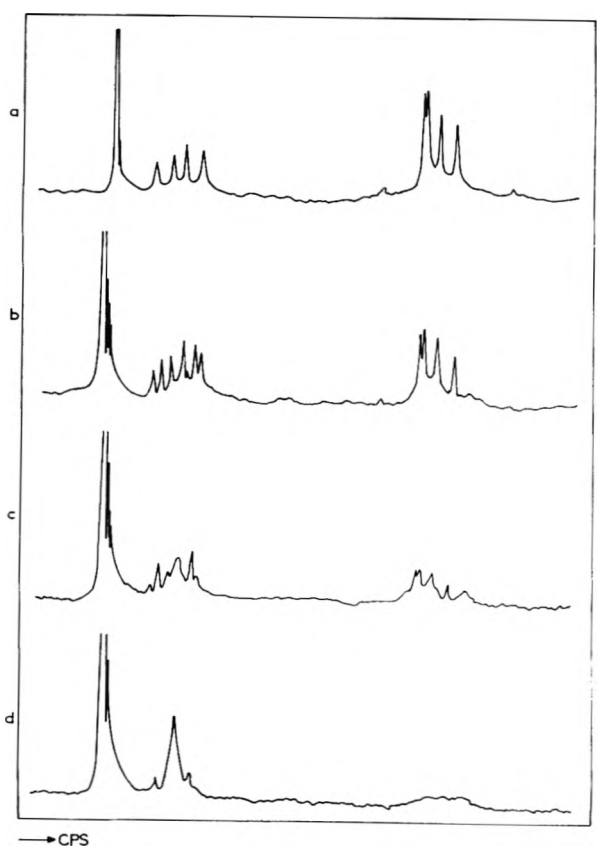

Fig. 1.—High resolution proton magnetic resonance spectra of 2 M disodium malate heated in 0.05 M NaOD, D_2O at 90° showing exchange of CH_2 protons: (a) unheated; (b) 1.2 hr.; (c) 5.0 hr.; (d) 18.9. hr.

hydration k_d, of L-malate, catalyzed by NaOH, both the absorbancy and optical rotation of L-malate solutions were measured as a function of time of heating. To increase sensitivity, a citrate, L-malate complex of molybdate was used to increase the small specific rotation of L-malate. Solutions for optical activity measurements were conveniently prepared by accurately pipetting into a flask 5.0 ml. of the L-malate solution to be analyzed, 5.0 ml. of 1 M trisodium citrate solution, 1.0 ml. of glacial acetic acid and 9.0 ml. of 29% (by weight) reagent quality ammonium molybdate solution.[9] The specific rotation $[\alpha]^{25}D$ of L-malate in this solution is about +1,400, over 500 times that of L-malate alone. Solutions 10 mM in L-malate gave optical rotations of +0.85 ± 0.02 at 25° using a 20 cm. cell and sodium lamp. The first-order rate constants for racemization at two temperatures are listed in Table II, along with k_d obtained from the same samples. The data show that the rates of racemization and of dehydration of L-malate, catalyzed by NaOH, are equal.

TABLE II

FIRST-ORDER RATE CONSTANTS FOR RACEMIZATION k_r AND DEHYDRATION k_d, OF L-MALATE, CATALYZED BY NaOH

T, °C.	(NaOH) M	Ionic strength	$k_d \times 10^6$, sec.$^{-1}$	$k_r \times 10^6$, sec.$^{-1}$
150	0.30	0.530	9.7	10.0
175	.10	.530	3.5	3.3

Proton Magnetic Resonance Studies.—Ten-ml. samples of 2.0 M sodium malate, 0.5 N in NaOH, were prepared and then frozen and sublimed to dryness under vacuum. The OH proton of the malate and the protons in the medium were exchanged out by adding 2–3 ml. portions of D_2O and subliming to dryness three times. The solution then was reconstituted with D_2O. The NaOD concentration was checked by neutralizing 1.0 ml. of the solution with excess standard HCl and back titrating with standard NaOH.

The solutions were placed in 0.5 mm. o.d. Pyrex tubes and heated for the desired time in an aluminum block thermostat. The spectra were observed at 40 megacycles using

(9) H. A. Krebs and L. V. Eggleston, *Biochem. J.*, **37**, 334 (1943).

a Varian V-4300 n.m.r. spectrometer equipped with superstabilizer.

The complete analysis of the proton magnetic resonance spectra of disodium malate in D_2O,[10] using the methods described in recent publications,[11,12] makes it possible for the chemical shift, δ_i, of particular protons and the spin-spin coupling constant, A_{ij}, between proton pairs to be calculated. From a knowledge of the chemical shifts of the three protons and of the three coupling constants for pairs of protons, the spectra of various partially deuterated malates can be predicted. Table III lists the resonance frequencies (relative to H_2O in a capillary) at 40 Mc. for the protons in dipotassium malate and three partially deuterated dipotassium malates.[13]

TABLE III

PROTON MAGNETIC RESONANCE FREQUENCIES (RELATIVE TO WATER) AT 40 MC. FOR DIPOTASSIUM MALATE AND PARTIALLY DEUTERATED MALATES IN D_2O

Compound Symbol	Structure	Frequencies of resonance (C.p.s.) Methine	Methylene
Na_2M	a	7.0, 11.8, 15.4, 19.6	62.9, 67.5, 77.8, 78.9, 81.5, 86.6, 93.6, 101.0
Na_2D_bM	b	11.9, 14.9	74.6, 77.6
Na_2D_cM	c	8.8, 18.2	81.5, 90.9
$Na_2D_bD_cM$	d	13.4	

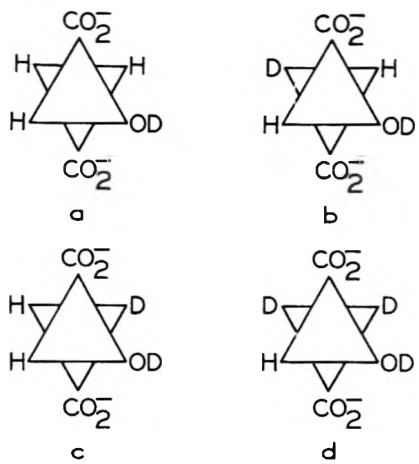

As shown in Fig. 1, when solutions of 2 M sodium malate in D_2O, containing 0.5 N NaOD, were heated to about 100°, the resonance lines associated with the methylene protons disappeared. In addition, while the spectrum in the methine region changed from a quadruplet to a singlet, its intensity remained virtually constant. This showed clearly that methylene protons were being replaced by deuterons from the medium. The spectrum of Na_2D_cM in both methylene and methine regions is evident in spectra (b) and (c). The Na_2D_bM lines are not resolved from those of Na_2M and $Na_2D_bD_cM$. Lack of resolution is partly a result of quadrupole broadening and the unresolved spin-spin splitting due to the deuterium. After prolonged heating, virtually all the methylene protons are exchanged and the spectrum of $Na_2D_bD_cM$ predominates.

If one assumes, as a first approximation, that the exchange of CH_2 protons in D_2O–NaOD is random and not affected by a deuterium on the same carbon, that the concentration of protons in the medium is negligible, and that there is no incorporation of deuterium through dehydration to fumarate and subsequent addition of D_2O, the rate of exchange of a methylene proton can be calculated. The exchange reaction then can be written

$$Na_2M \xrightarrow{k_4} (Na_2D_bM + Na_2D_cM) \xrightarrow{k_4} Na_2D_bD_cM \quad (6)$$

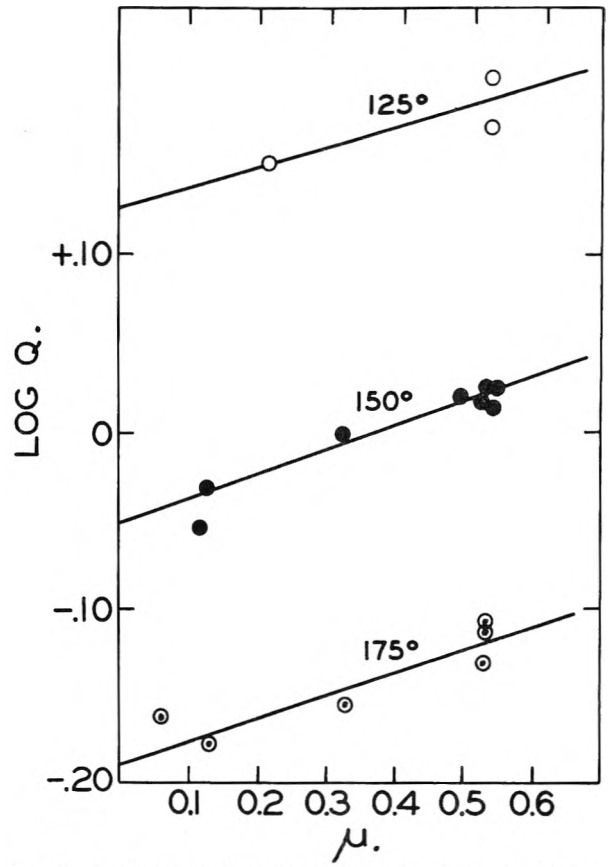

Fig. 2.—Ionic strength dependence of log Q for reaction 1.

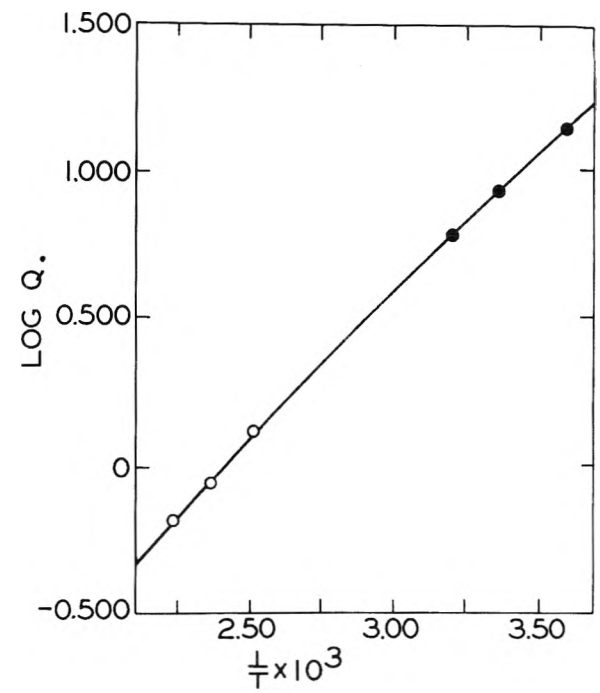

Fig. 3.—Temperature dependence of Q for reaction 1 at 0.10 ionic strength: ●, experimental points, fumarase catalysis; ○, experimental points, NaOH catalysis. Line given by $\log Q = 9.932 + 363/T - 4.127 \log T$.

(10) R. A. Alberty and P. Bender, *J. Am. Chem. Soc.*, **80**, 542 (1958).

(11) H. J. Bernstein, J. A. Pople and W. E. Schneider, *Canadian J. Chem.*, **35**, 65 (1957).

(12) H. S. Gutowsky, C. H. Holm, A. Saika and G. A. Williams, *J. Am. Chem. Soc.*, **79**, 4596 (1957).

(13) The proton resonance lines of disodium malate appear at slightly higher frequencies, relative to H_2O in a capillary, than the corresponding lines in the dipotassium malate spectrum.

For this system the concentration of Na_2D_bM + Na_2D_cM reaches a maximum at $t_{max} = 0.693/k_4$. The area under the peak (90.0 c.p.s.) which appears in methylene region of the n.m.r. spectrum of the heated samples (c) is a measure of the Na_2D_cM concentration. Comparison of spectra from a series of samples heated for different times makes it possible to calculate t_{max} and k_4 to within ±10%. Alternatively, the total area under the methylene proton peaks is a measure of the concentration of Na_2M + $^1/_2(Na_2D_bM$ + $Na_2D_cM)$. This area reaches half its original value at 1.70 half-lives, according to mechanism (6). Designating this time as t_a, $k_4 = 0.693 \times 1.70/t_a$. The values of k_4 at 90 and 110° determined by these approaches are 4.7×10^{-5} sec.$^{-1}$ and 27×10^{-6} sec.$^{-1}$, respectively.

Results and Discussion

Ionic Strength Dependence of Q.—The following considerations indicate that a linear dependence of log Q on ionic strength is expected at ionic strengths below 0.5. From (3)

$$\log Q = \log K + \log y_F - \log y_M + \log a_{H_2O} \quad (7)$$

A term linear in ionic strength often is added to the Debye–Hückel limiting law in order to represent the activity coefficient data of an electrolyte over a wider concentration range. With this modification, the mean ionic activity coefficient of a salt, $y_\pm$, is given by

$$\log y_\pm = \frac{Az_+ z_- \sqrt{\mu}}{1 + aB\sqrt{\mu}} + C\mu \quad (8)$$

where A and B are constants for a particular solvent and temperature, a and C are constants characteristic of the solute, z_+ and z_- are the ionic charges, and μ is the ionic strength. If a is assumed to be the same for fumarate and malate, the logarithm of their activity coefficient ratio is given by $(C_F - C_M)\mu$, and (7) becomes

$$\log Q = \log K + (C_F - C_M)\mu + \log a_{H_2O} \quad (9)$$

In the region where the activity of H_2O does not change significantly with electrolyte concentration, a plot of log Q *vs.* μ should be linear with slope $(C_F - C_M)$. For NaOH[14] and NaCl[15] solutions from zero to 0.6 ionic strength the activity of H_2O decreases from 1.00 to 0.98. Therefore, the log a_{H_2O} term in (9) contributes only about 0.01 to log Q at μ = 0.60 and would hardly be detectable in these measurements.

A plot of log Q *vs.* μ is shown in Fig. 2. The best straight lines drawn through the experimental points at 125, 150 and 175° all have a slope of 0.13 ± 0.02. Though no data are available on the activity coefficients of sodium fumarate or malate, C values at 25° for sodium formate (0.148) and sodium acetate (0.252)[16] indicate that 0.13 is a reasonable value for $C_F - C_M$.

The value of Q obtained by extrapolation to zero concentration is taken as K.

A comparison can be made of the ionic strength dependence of Q observed in these experiments and that obtained by Bock and Alberty for the fumarase-catalyzed reaction.[17] They obtained values of Q from 0.5 to 0.1 ionic strength which yield a slope of 0.12 for the log Q *vs.* μ plot, indicating that the ionic strength dependence of Q is essentially independent of temperature from 25 to 175°. Therefore, a plot of log Q *vs.* $1/T$ yields ΔH^0 for any series of determinations at constant ionic strength less than about 0.5.

Thermodynamic Functions.—From studies of the temperature dependence of Q for the reaction catalyzed by fumarase at μ = 0.10 and *p*H 7.3, between 5 and 40°, Bock and Alberty obtained $\Delta H^0 = -3960 \pm 100$ cal./mole.[17] Since these data were obtained at *p*H 7.3, where divalent fumarate and malate are the only significant species, the Q values can be compared directly with those obtained in this research. Figure 3 is a plot of log Q *vs.* $1/T$ including representative experimental points for the fumarase reaction. When the experimental values of Q for the enzymatic and non-enzymatic reactions are compared, the Q of the enzymatic reaction must be doubled since it is defined as (L—M)/(F) rather than [(L—M) + (D—M)]/(F). Over a limited temperature range, each set of data yields a straight line, but the slopes differ considerably. The data were fitted by the method of least squares, assuming $\Delta C^0_p = \bar{C}^0_{pM} - \bar{C}^0_{pF} - C_{pH_2O}$ is constant over the temperature range 5–175° and Q = 14.2 at 5°. This yields $\Delta C^0_p = -8.2$ cal. mole^{-1} deg.$^{-1}$ and the expression

$$\log Q = 9.932 + 363/T - 4.127 \log T \quad (10)$$

which is plotted in Fig. 3. No data are available on the heat capacities of aqueous fumarate and malate solutions. However, since for these dilute solutions C_{pH_2O} = 18 cal. mole^{-1} deg.$^{-1}$, $\bar{C}^0_{pM} = \bar{C}^0_{pF}$ = 10 cal. mole^{-1} deg^{-1}, which is reasonable.[18]

The values of K_{eq}, ΔH^0, ΔF^0 and ΔS^0 for the reaction are recorded in Table IV. The entropy decrease is probably to be expected in going from fumarate plus water to malate.

These results can be compared with the data for the corresponding acid-catalyzed reaction. For acid-catalyzed hydration of undissociated fumaric acid to malic acid, Rozelle and Alberty[6] obtained $\Delta S^0 = -16$ cal. mole^{-1} deg.$^{-1}$ and $\Delta H^0_a = -4900$ cal. mole^{-1} in the temperature range 125–200°. The ΔH^0 for the acid- and base-catalyzed reactions are not independent but are related through the enthalpies of ionization of fumaric and malic acids.[17] Recent determinations of ΔH_{M_1} and ΔH_{M_2}, the enthalpies of ionization of malic acid,[19] obtained from ionization constant measurements from 5 to 50°, allow us to calculate the enthalpy change for the acid catalyzed reaction from

$$\Delta H^0_a = \Delta H^0_b + (\Delta H_{F_1} + \Delta H_{F_2}) - (\Delta H_{M_1} + \Delta H_{M_2}) \quad (11)$$

where ΔH^0_a and ΔH^0_b represent the enthalpy changes for the acid- and base-catalyzed reactions, ΔH_{F_1} and ΔH_{F_2}, the enthalpies of ionization of fumaric acid.[20] At 25°, ΔH^0_a calculated from equation 11 is −5900 cal. mole^{-1} deg.$^{-1}$. From the difference in ΔH^0_a at 160 and 25°, ΔC^0_p for the acid-

(14) G. C. Akerlöf and G. Kegeles, *J. Am. Chem. Soc.*, **62**, 620 (1940).

(15) R. R. Robinson, *Trans. Proc. Roy. Soc. New Zeal.*, **75**, 203 (1945).

(16) E. A. Guggenheim, *Phil. Mag.*, [7] **22**, 322 (1936).

(17) R. Bock and R. A. Alberty, *J. Am. Chem. Soc.*, **75**, 1720 (1953).

(18) H. S. Harned and B. B. Owen, "The Physical Chemistry of Electrolytic Solutions," Reinhold Publ. Corp., New York, N. Y., 1950, p. 246.

(19) M. Eden and R. G. Bates, Chicago A.C.S. Meeting, September, 1958.

(20) E. J. Cohn and J. T. Edsall, "Proteins, Amino Acids and Peptides," Reinhold Publ. Corp., New York, N. Y., 1943, p. 82.

catalyzed reaction is $+7 \pm 3$ cal. mole^{-1} deg.$^{-1}$. The fact that ΔC^0_p for the acid-catalyzed reaction is $+7$ while ΔC^0_p for the base-catalyzed reaction is -8 probably reflects the increased rotational freedom of the undissociated malic acid as compared to the divalent malate anion.

Kinetic Data.—Both k_h and k_d, obtained at NaOH concentrations between 0.10 and 0.53 M and constant ionic strength, are nearly directly proportional to NaOH concentration. This is shown by the near constancy of $k_h/(OH^-)$ and $k_d/(OH^-)$ at a given ionic strength and temperature.

The activation energies for both forward and reverse reactions were evaluated by plotting log $k/(OH^-)$ *vs.* $1/T$ at constant ionic strength. Linear plots were obtained at $\mu = 0.54$ with data at 125, 150 and 175°. At the lower ionic strengths, data at only 125 and 175° were available for the plot. Values of the Arrhenius activation energy E were obtained from these plots; $\Delta H^\ddagger = E - RT$ and $\Delta S^\ddagger$, calculated from absolute rate theory, are listed in Table V. Values of $\Delta H^\ddagger$ and $\Delta S^\ddagger$ for the corresponding HCl catalyzed reaction are included for comparison.

TABLE IV

THERMODYNAMIC DATA FOR REACTION 1

T, °C.	K	ΔF^0, kcal. mole^{-1}	ΔH^0, kcal. mole^{-1}	ΔS^0, cal. deg.$^{-1}$ mole^{-1}
25	8.4	−1.26	−4.1	−9.5
125	1.34	−0.23	−4.9	−12
150	0.89	+0.10	−5.1	−12
175	0.65	+0.39	−5.3	−11

TABLE V

ENTHALPIES AND ENTROPIES OF ACTIVATION FOR REACTION 1

Catalyst	Ionic strength	ΔH_h^-, kcal. mole^{-1}	ΔH_d^-, kcal. mole^{-1}	ΔS_h^-, cal. deg.$^{-1}$ mole^{-1}	ΔS_d^-, cal. deg.$^{-1}$ mole^{-1}
NaOH	0.54	19	24	−34	−22
NaOH	.33	22	27	−28	−17
NaOH	.13	19	24	−35	−23
1 N HCl	1.0	22	27	−26	−10

Mechanism of the Reaction.—The results of these three types of experiments suggest the mechanism shown below

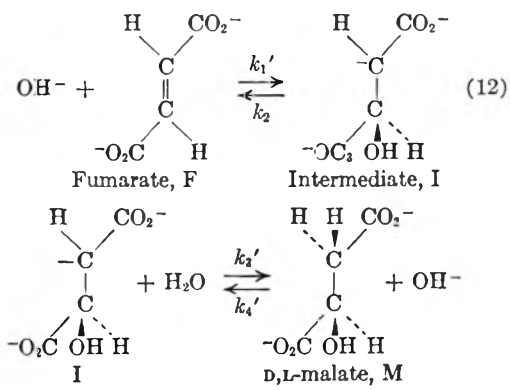

The mechanism provides for the fact that the hydration reaction is first order in fumarate, the dehydration, first order in malate, and that both k_h and k_d are proportional to (OH^-). In addition this mechanism provides for exchange of methylene hydrogens through the intermediate and does not permit racemization of L-malate except *via* fumarate.

Rate Constants for Mechanism 12.—If it is assumed that the intermediate is in a steady state, the relation between the four rate constants in this mechanism and the rate constants k_h and k_d, obtained spectrophotometrically, is given by

$$k_h = k_1k_3/(k_2 + k_3); \quad k_d = k_2k_4/(k_2 + k_3) \quad (13)$$

where $k_1 = k'_1(OH^-)$, $k_3 = k'_3(H_2O)$, and $k_4 = k'_4(OH^-)$.

Some idea of the relative magnitudes of k_1, k_2, k_3 and k_4 can be obtained from a comparison of the rate of exchange of methylene protons and k_h and k_d determined under the same conditions. Neglecting incorporation of deuterium into the methylene position of malate *via* dehydration to fumarate and subsequent addition of D_2O, the first-order rate constant for exchange calculated from n.m.r. studies is just k_4 in mechanism 12. With a sample of 2 M Na_2M, 0.5 N NaOD in D_2O at 110°, $k_4 = 27 \times 10^{-5}$ sec.$^{-1}$. Spectrophotometric analysis of the same samples yielded $k_h = 15 \times 10^{-5}$ sec.$^{-1}$ and $k_d = 1.5 \times 10^{-5}$ sec.$^{-1}$. From (13) $k_3/k_2 = k_4/k_d - 1 \cong 19$. Therefore, $k_1 = k_h(1 + k_2/k_3) \cong k_h$.

The magnitude of k_3 can be estimated by considering the first step in the dehydration of malate. The equilibrium constant for this step is given by

$$K = k_3/k_4 = (M)(OH^-)/(I) = K_w/K_a \quad (14)$$

where K_a is the acid dissociation constant of the methylene proton in malate. Pearson and Dillon suggest a value of $K_a = 10^{-24}$ for the methyl protons of acetate ion.[21] Their estimate is based on the rate of OD^- catalyzed exchange of methyl protons of acetate[22] and the assumption that the ratio of rates of removal of protons by H_2O and OH^- is the same as in acetone, as determined from bromination rate studies. The rate of exchange of methyl protons by acetate ion is within a power of 10 of the rate of exchange of methylene protons of malate at 100°, and both reactions have a activation energy of about 22 kcal. mole^{-1}. Since K_w[23] at 110° is 3×10^{-13}, $K_w/K_a = k_3/k_4 = 3 \times 10^{11}$. Hence $k_3 = 3 \times 10^{11} \times 27 \times 10^{-5}$ sec.$^{-1} \cong 10^8$ sec.$^{-1}$ and $k_2 = k_3/19 \cong 5 \times 10^6$ sec.$^{-1}$ at 110°. Thus, both k_2 and k_3 are much greater than either k_1 or k_4.

Acknowledgment.—The authors are indebted to Prof. P. Bender for assistance with the proton magnetic resonance experiments.

(21) R. G. Pearson and R. L. Dillon, *J. Am. Chem. Soc.*, **75**, 2439 (1953).

(22) K. F. Bonhoeffer, K. H. Greib and O. Reizt, *J. Chem. Phys.*, **1**, 664 (1939).

(23) H. S. Harned and B. B. Owen, *J. Am. Chem. Soc.*, **75**, 493 (1953).

GAS-KINETIC COLLISION DIAMETERS OF THE HALOMETHANES

BY GEORGE A. MILLER AND RICHARD B. BERNSTEIN

Contribution from the Chemistry Department, University of Michigan, Ann Arbor, Michigan

Received October 14, 1958

The Knudsen-gage radiometer technique has been used to measure gas-kinetic collision diameters for 17 halomethanes with a probable error of ±1% at 340, 415, 512 and 610°K. These results together with literature data for five additional halomethanes have been fitted with Lennard-Jones (12-6) potential constants using Hirschfelder's method. Calculated viscosities are listed for the 22 halomethanes at the four temperatures. The derived L-J force constants are found to be well correlated with the molecular polarizabilities. Necessary parameters are tabulated from which values of the collision diameters for the remaining 47 halomethanes may be predicted with an estimated uncertainty of less than ±2%.

Introduction

The correlation of molecular size with polarizability in terms of intermolecular potentials[1] has led to the present study of the halomethanes. The radiometer technique[2] was used to determine collision diameters. It has the advantage of being rapid and moderately accurate (±1%). The method makes use of the fact that the deflection of a Knudsen gage reaches a maximum when the mean free path of the gas equals a certain critical dimension of the gage.

Using the rigid sphere model of a gas molecule, Weber[3] has shown that the maximum deflection (θ_m) may be related to the mean free path (λ) and the number of molecules per unit volume (n) through the equation

$$\theta_m/\lambda n = C \qquad (1)$$

where C is a characteristic constant of the gage, $\lambda n = 1/\sqrt{2}\,\pi\,\sigma_{RS}^2$, and σ_{RS} is the rigid sphere diameter. Some minor qualifications must be made for effects like thermal accommodation and mechanical imperfections of the gage. For real molecules (with force fields) σ_{RS} is a decreasing function of temperature and, moreover, differs according to the particular transport property under consideration. Although the viscosity enters formally into Weber's theory, there is uncertainty as to the fundamental transport property involved in the region of the maximum deflection.

In the present work the Knudsen gage has been treated as an empirical instrument for determining σ_{RS}. The constant C was evaluated using gases of known σ_{RS}. For consistency all calibrations were based on values obtained from viscosity data. From the temperature dependence of σ_{RS} it is possible to estimate the Lennard-Jones (12-6) potential (L-J) force constants, σ and ϵ/k, by means of the proper viscosity formulas[4]

$$\eta \times 10^7 = 266.93\,\frac{\sqrt{MT}}{0.984\sigma_{RS}^2} = 266.93\,\frac{\sqrt{MT}}{\sigma^2\Omega^{(2,2)*}} \times f_\eta^{(3)} \qquad (2)$$

from which

$$\sigma_{RS}^2 = \sigma^2\left[\frac{\Omega^{(2,2)*}}{0.984 f_\eta^{(3)}}\right] \qquad (3)$$

The expression between brackets is a function of ϵ/k and the absolute temperature only. The symbols have the usual meaning (ref. 4), with σ, ϵ/k and η expressed in units of Å., °K. and g. cm.$^{-1}$ sec.$^{-1}$, respectively.

Experimental

The Knudsen gage was of the type described by Klumb and Schwarz.[5] It was constructed entirely of Vycor and quartz. A silver damping vane was sealed inside two quartz plates; a platinum mirror was made by baking a coat of "Liquid Bright Platinum" (Hanovia Chemical Co.) onto the inside surface of one of these plates. The gage was placed inside a vertical, cylindrical furnace provided with a window. A large permanent magnet for damping was located outside of the furnace. Stirring in the furnace was accomplished with a current of preheated air.

The pressure in the gage was increased stepwise by means of a gas pipet system until the point of maximum deflection had been passed. It was not necessary to know the pressure (*ca.* 10 μ(microns)) at the point of maximum deflection; only the value of θ_m was required.

The purity of all compounds used was greater than 98%. C.P. gases (Matheson Co.) were used without further purification. Other gases were examined mass-spectrometrically. Liquid samples were checked by measuring the index of refraction and/or vapor pressure.

Results

Five halomethanes served as primary standards[6] for the calibration of the Knudsen gage. Viscosity data from several sources were smoothed with the aid of the L-J potential. The force constants σ and ϵ/k obtained in this manner were thus consistent with the values of σ_{RS} calculated directly from the smoothed data. Good agreement was obtained with the values of σ_{RS} listed in Landolt-Börnstein[7] (derived from the same sources of data).

The maximum deflection of the Knudsen gage followed an equation slightly different from (1); it could be represented by the expression

$$\theta_m \times \sigma_{RS}^2 = a(T) + b\theta_m \qquad (4)$$

θ_m is in arbitrary scale units, $b = 2.78$, $a(T)$ is a temperature dependent gage constant, and T is the effective temperature of measurement defined as $(1/2)(T_h + T_c)$, where T_h and T_c are the temperatures of the hot and cold walls, respectively. The gage constant $a(T)$ (determined from the calibration data using eq. 4) showed a dependence on T at the four temperatures chosen for the present study

(1) See, for instance, W. Brandt, *J. Chem. Phys.*, **24**, 501 (1956).

(2) E. Weissmann, *Vakuum-Tech.*, **3**, 152 (1954).

(3) S. Weber, *Kgl. Danske Videnskab. Selskab, Mat.-fys. Medd.*, No. 24 (1947).

(4) J. O. Hirschfelder, C. F. Curtiss and R. B. Bird, "Molecular Theory of Gases and Liquids," John Wiley and Sons, Inc., New York, N. Y., 1954.

(5) H. Klumb and H. Schwarz, *Z. Physik*, **122**, 418 (1944).

(6) A number of other molecules (of known σ_{RS}) were measured as secondary standards. They served as a check on the characteristics of the gage.

(7) Landolt-Börnstein, "Zahlenwerte und Funktionen," Springer-Verlag, Berlin, 1950–51.

TABLE I

CALIBRATION STANDARDS (HALOMETHANES)

Molecule	Viscosity from lit., $\eta_{lit} \times 10^6$; σ_{RS} (Å.) from η_{lit}; σ_{RS} from eq. 4				L-J parameters fitted to η_{lit}	
	340°K.	415°K.	512°K.	610°K.	σ (Å.)	ϵ/k (°K.)
1. CH_3Cl[a]	122.1	149.3	183.4	216.5	4.05	412
	5.40	5.13	4.88	4.69		
	5.43	5.12	4.88	4.70		
2. CH_3Br[b]	154.2	189.3	233.4	273.0	4.16	434
	5.62	5.34	5.07	4.87		
	5.65	5.31	5.09	4.88		
3. CH_2Cl_2[a]	114.7	140.8	173.3	204.8	4.70	427
	6.34	6.02	5.71	5.49		
	6.31	5.96	5.68	5.47		
4. $CHCl_3$[a,c]	117.6	142 9	173.9	203.4	5.47	317
	6.82	6.50	6.22	6.01		
	6.88	6.56	6.21	6.00		
5. CCl_4[c,d]	113.0	137.9	168.1	197.0	5.83	339
	7.41	7.05	6.73	6.49		
	7.39	7.08	6.73	(decomp.)		

[a] H. Braune and R. Linke, *Z. physik. Chem.*, **A148**, 195 (1930). [b] T. Titani, *Bull. Chem. Soc., Japan*, **5**, 105 (1930). [c] T. Titani, *ibid.*, **8**, 255 (1933). [d] E. H. Sperry and E. Mack, Jr., *J. Am. Chem. Soc.*, **54**, 904 (1932).

T, °K.	340	415	512	610
$a(T)$	46.3	49.5	51.9	53.2

Table I summarizes the data on the five standard halomethanes and includes values of σ_{RS} back-calculated from the observed θ_m with equation 4 to indicate the accuracy of the calibration fit.

Table II gives the experimental results for seventeen other halomethanes. The L-J force constants obtained from the temperature dependence of σ_{RS} were used to calculate a second set of viscosities. It is seen that they reproduce the data within the precision of the measurements.

Correlation with Polarizability.—Over the temperature range studied it was found empirically that σ_{RS} may be expressed accurately ($\pm 1\%$) as a function of the polarizability, α(Å.^{3}), as

$$\text{Methyl halides: } \sigma_{RS} = G(T)\alpha^{0.22} \quad (5)$$

$$\text{All other halomethanes[8]: } \sigma_{RS} = F(T)\alpha^{1/3} \quad (6)$$

The temperature dependent constants were determined to have the values

T (°K.)	340	415	512	610
$F(T)$	3.39	3.23	3.08	2.97
$G(T)$	3.87	3.66	3.48	3.36

Equations 5 and 6, together with (2), permit a rapid calculation of viscosity (at four temperatures) for any halomethane, with an estimated uncertainty of 2 or 3%. They may also be useful for the estimation of collision numbers for application to chemical kinetics. However, for the purpose of extending the temperature range and for calculating other transport coefficients intermolecular potential constants would be more useful.

Although the L-J potential is intended only for application to spherical, non-polar molecules, it serves to correlate the present data over the range 340–610°K. within experimental error. Omitting consideration of the methyl halides, equation 6 implies an oversimplification for the remaining sixty-five halomethanes. The fact that σ_{RS} appears to be uniquely determined by α at each temperature is equivalent to a statement that the L-J force constants are single-valued functions of α. Actually, small deviations of σ_{RS} from equation 6 give rise to significant changes in σ and ϵ/k for any one compound. If log σ and log ϵ/k (from Tables I and II) are plotted against log α, three distinct pairs of lines are obtained corresponding to the three iso-electronic series (plus a fourth pair for the methyl halides). The ϵ/k plot, however, is rather scattered, due, in part, to the difficulty in determining this parameter accurately. A smoothed set of curves of log ϵ/k *vs.* log α were derived which are consistent with equations 5 and 6 and the values of σ from Tables I and II. Table III gives the final set of force constants expressed as a function of α for each iso-electronic series (here N is the number of electrons in the molecular valence shell).

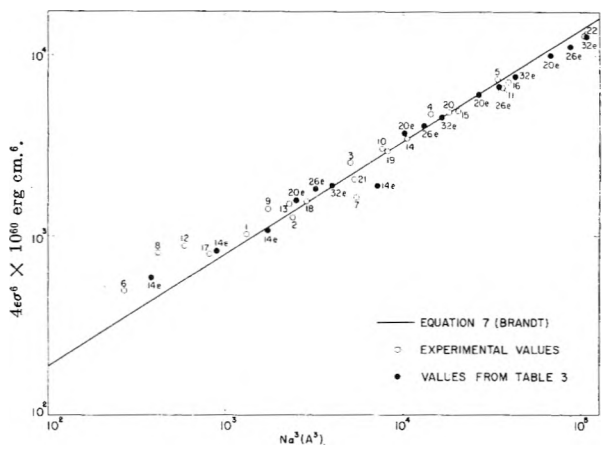

Fig. 1.—Brandt's modified dispersion formula (eq. 7) for 22 halomethanes. See Tables I and II for the numbering of the compounds. The solid circles are values calculated from Table III; they are labelled with the appropriate value of N (14e, 20e, 26e and 32e).

Table III has been used to calculate (with eq. 2) the viscosities of the twenty-two halomethanes used in this research. Comparison with viscosities

(8) With the exception of CH_2F_2, CHF_3 and CF_4; that is to say, for $\alpha < 3$.

TABLE II

RESULTS FOR 17 HALOMETHANES

Molecule	L-J (12-6) parameters σ (Å.)	ϵ/k (°K.)	σ_{RS} (Å.) from eq. 4; $\eta \times 10^6$ from σ_{RS}; $\eta \times 10^6$ from L-J parameters 340°K.	415°K.	512°K.	610°K.
6. CH_3F	3.73	333	4.72	4.47	4.30	4.17
			131	161.5	194	225
			131.5	160	195	228
7. CH_3I	4.23	519	6.03	5.72	5.38	5.15
			164	201.5	253	301
			166	204	252	300
8. CH_2F_2	4.08	318	5.12	4.85	4.61	4.49
			138	170	206	240
			139	169	205	240
9. CH_2FCl	4.48	318	5.62	5.33	5.08	4.94
			131	161	197	227
			132	160.5	195	228
10. CH_2ClBr	4.88	410	6.50	6.18	5.88	5.67
			135	165	202	237
			135	165	202.5	239
11. CH_2I_2	5.16	630	7.65	7.40	6.92	6.61
			140	165	210	251
			139.5	170	210	251.5
12. CHF_3	4.33	240	5.07	4.85	4.67	4.56
			163	197	236	270
			163	196	235	271
13. CHF_2Cl	4.68	261	5.63	5.33	5.13	5.03
			147	181	217	246
			149.5	180	217	251
14. $CHFClBr$	5.13	345	6.56	6.22	5.96	5.75
			141	173.5	210	246
			142	173	211	247.5
15. $CHCl_2Br$	5.25	427	7.07	6.74	6.46	(decom-
			128	156	192.5	posed)
			128	157	193	228
16. $CHBr_3$	5.33	559	7.70	7.36	6.92	6.60
			134	162	204	245
			134.5	164.5	204	243
17. CF_4	4.63	145	4.93	4.75	4.65	4.59
			193	230	266	298.5
			191	227	266	302
18. CF_3Cl	4.96	188	5.55	5.30	5.14	5.09
			166	201	239.5	264
			168	199	236	270
19. CF_2Cl_2	5.25	253	6.27	5.94	5.71	5.59
			140	172	207	236
			142.5	171	206	238
20. $CFCl_3$	5.44	334	6.90	6.54	6.27	6.04
			123	151.5	183	215
			124	151	184	215
21. CF_3Br	5.01	235	5.87	5.59	5.38	5.26
			177	216	259	295.5
			179	215	257.5	297
22. CBr_4	6.12	442	8.25	7.97	7.48	(decom-
			134	158.5	200	posed)
			132	161	199	235.5

listed in Tables I and II yields an average deviation of ±2%.

The L-J parameters are to be considered merely convenient aids in calculation when applied to polar and non-spherical molecules. Nevertheless, the fact that they can be correlated with polarizability does suggest a limited physical significance. It is of interest to see whether the separation of Table III into four iso-electronic series is reasonable in terms of the theory of dispersion energies. The Slater–Kirkwood formula leads to the relation[1] in terms of the L-J potential

$$4\epsilon\sigma^6 = B(N\alpha^2)^\beta \qquad (7)$$

where $B = 12.58 \times 10^{-60}$ erg cm.^{6}, and $\beta = 1/2$. It has been found by Brandt[1] in a survey of a number of non-polar and spherically symmetric molecules that, empirically, $B = 11.1 \times 10^{-60}$ erg cm.^{6} and $\beta = 0.62$. The straight line in Fig. 1 represents equation 7 using Brandt's constants.

TABLE III

SMOOTHED VALUES OF L-J PARAMETERS FOR THE HALOMETHANES AS A FUNCTION OF POLARIZABILITY

α	CH_2- (N = 14)		CH_2- (N = 20)		$CH-$ (N = 26)		$C-$ (N = 32)	
	σ	ϵ/k	σ	ϵ/k	σ	ϵ/k	σ	ϵ/k
(Å.^{3})	(Å.)	(°K.)	(Å.)	(°K.)	(Å.)	(°K.)	(Å.)	(°K.)
3	3.80	346						
4	3.95	388	4.37	304	4.59	245	4.88	170
5	4.06	428	4.52	352	4.75	286	5.06	206
6	4.16	461	4.66	398	4.90	324	5.21	239
7	4.24	490	4.78	440	5.02	360	5.36	269
8	4.32	519	4.89	482	5.13	394	5.47	297
9			4.98	520	5.22	426	5.59	324
10			5.07	558	5.32	458	5.69	350
12			5.22	628	5.48	518	5.86	396
14			5.35	696	5.62	574	6.03	434
16			5.47	760	5.73	628	6.15	466
18			5.57	820	5.85	678	6.28	490
20			5.66	880	5.95	730	6.40	514

Results for the twenty-two halomethanes are seen to follow this line, though with considerable scatter. Points calculated from Table III show more clearly that the iso-electronic series have retained some individual character (in particular, the methyl halide series, N = 14). This may reflect the polar, non-spherical character of the majority of the halomethanes studied.

The application of a three parameter potential function taking into account the permanent dipole moment (such as the Stockmayer potential) is not justified by the accuracy of the present results. Similarly, the introduction of a third parameter involving the moments of inertia is not warranted, although there is evidence that these molecules transfer rotational energy readily. However, even the two parameter L-J potential should probably be adequate to predict the correct dependence of σ_{RS} on the particular type of transport property.[9] Thus Table III could be used to estimate self-diffusion coefficients using the methods outlined in ref. 4.

Values of α for many of the sixty-nine halomethanes are known or may be derived from refraction data.[7,10] Most of these readily may be calculated to within ±2% using the bond polarizabilities (Å.^{3}): CH = 0.63, CF = 0.72, CCl = 2.52, CBr = 3.57 and CI = 5.35. Halomethanes for which data are known and for which α disagrees by more than ±2% with calculation based on the above bond values are

Compound	CH_2Cl	CHI_3	CBr_4
α (Å.^{3})	4.64	17.7	14.8

Note on Stannic Chloride.—An unusual set of force constants have been reported[11] for $SnCl_4$ (σ = 4.54, ϵ/k = 1550) presumably derived from viscosity data. It is of interest to attempt to estimate the L-J constants for this compound by applying Table III. Using a value of α = 13.8[1] and N = 32, force constants of σ = 6.01 and ϵ/k = 430 are predicted. A comparison of the fit of these constants to the original viscosity data is given in terms of σ_{RS}

T (°K.)	σ_{RS} (Å.) Obsd. (from η)	Calcd.
381	8.00	7.95
494	7.58	7.44
675	7.05	6.95
865	6.75	6.56

Acknowledgments.—The authors appreciate the support of this work by the U. S. Atomic Energy Commission, Division of Research, Contract AT-(11-1)-321, and the Alfred P. Sloan Foundation. Thanks also are due to Mr. J. N. Doshi for his assistance with some of the calculations.

(9) It should be pointed out, however, that the same two parameter fit is *not* expected to be satisfactory for the calculation of the second virial coefficient for a polar molecule. As pointed out in ref. 4 (Sec. 3.10b), there should be a strong dependence upon the dipole moment. To explore this point, sample calculations were carried out for five halomethanes using the two L-J parameters from Tables I and II, neglecting the dipole moment. The calculated values deviated appreciably from the known experimental values of the second virial coefficient.

(10) A. I. Vogel, *J. Chem. Soc.*, 636 (1943); J. M. Stevels, Thesis, 1937, Leiden.

(11) J. O. Hirschfelder, R. B. Bird and E. L. Spotz, *Trans. Am. Soc. Mech. Engrs.*, **71**, 921 (1949).

DIELECTRIC DISPERSION IN GASES AT 9400 MEGACYCLES[1]

BY JAMES E. BOGGS, JAMES E. WHITEFORD AND CAROL MAY THOMPSON

Electrical Engineering Research Laboratory and Department of Chemistry, The University of Texas, Austin, Texas

Received October 16, 1958

The dielectric constants of 25 gases have been measured at 9400 megacycles over a range of pressures and temperatures. Many of these gases show a lower orientation polarization at this frequency than at low frequencies. Although quantitative calculations are not possible for the asymmetric top molecules reported, the results are compared with previous observations where the dispersion has been connected with molecular inversion. Certain substances, notably those with C_{2v} molecular symmetry, do not exhibit dielectric dispersion of a measurable amount, although molecular inversion should be possible.

Recent papers from this Laboratory[2-4] have reported dielectric constant values for 21 gases measured at a frequency of 9400 megacycles. It has been shown that for many of these gases the orientation polarization at microwave frequencies is lower

(1) This work has been supported by Air Force Contract AF 33(616)-2842.

(2) J. E. Boggs, C. M. Crain and J. E. Whiteford, THIS JOURNAL, **61**, 482 (1957).

(3) J. E. Boggs, C. M. Thompson and C. M. Crain, *ibid.*, **61**, 1625 (1957).

(4) J. E. Boggs, *J. Am. Chem. Soc.*, **80**, 4235 (1958).

TABLE I

Gas	P_{30} (cc.) 9400 Mc.	P_{30} (cc.) "Static"	P_d (cc.) 9400 Mc.	P_d (cc.) "Static"	$\frac{P_0^s - P_0^{9400}}{P_0^s}$
C_2H_5Br	97.2	104.1[a]	23.3	21.2[a]	0.08
1-C_3H_7Br	104.9	119.0[b]	25.9	(23.7)[c]	.15
C_2H_5Cl	93.8	103.7[d]	19.1	20.9[d]	.12
1-C_3H_7Cl	101.2	109.7[d]	24.0	25.3[d]	.10
1-C_4H_9Cl	107.8	117.5[b]	26.9	28.6[e]	.11
2-C_3H_7Br	103.8	122.3[b]	26.5	(24.1)[c]	.19
2-C_3H_7Cl	96.9	115.8[b]	24.1	(21.1)[c]	.21
CH_3OH	62.7	66.1[f]	7.0	7.6[f]	.06
C_2H_5OH	66.2	71.1[g]	15.2	13.0[g]	.08
$C_2H_5OC_2H_5$	51.2	51.6[h]	26.9	26.0[h]	.01
CH_3OCH_2Cl	89.7	100.8[i]	19.6	(18.0)[c]	.14
$(C_2H_5)_3N$	40.9	41.8[j]	35.2	33.0[j]	?
COS	22.3	23.4[k]	12.9	14.4[k]	?
$CHBrCl_2$	39.7	...	27.1	(24.3)[c]	...
CH_2BrCl	68.2	...	16.6	(19.4)[c]	...
CH_2F_2	86.5	84.2[l]	7.5	(7.1)[c]	− .03
CH_2Cl_2	70.0	69.6[m]	20.6	20.0[m]	− .01
CH_2Br_2	64.5	64.7[m]	22.0	23.5[m]	.00
CCl_2F_2	25.5	25.4[n]	20.5	20.2[n]	?

[a] C. P. Smyth and K. B. McAlpine, *J. Chem. Phys.*, **2**, 499 (1934). [b] L. G. Groves and S. Sugden, *J. Chem. Soc.*, 158 (1937). [c] Molar refraction. P_d should be 5–10% larger. [d] R. Sanger, O. Steiger and K. Gächter, *Helv. Phys. Acta*, **5**, 200 (1932). [e] C. P. Smyth and K. B. McAlpine, *J. Chem. Phys.*, **3**, 347 (1935). [f] J. D. Stranathan, *ibid.*, 6, 395 (1938). [g] H. L. Knowles, THIS JOURNAL, **36**, 2554 (1932). [h] E. M. Moore and M. E. Hobbs, *J. Am. Chem. Soc.*, **71**, 411 (1949). [i] C. P. Smyth, private communication reported in National Bureau of Standards Circular 537, 1953. [j] G. A. Barclay, R. J. W. Le Fevre and B. M. Smythe, *Trans. Faraday Soc.*, **46**, 812 (1950). [k] C. T. Zahn and J. B. Miles, *Phys. Rev.*, **32**, 497 (1928). [l] D. R. Lide, *ibid.*, **87**, 227 (1952). [m] A. A. Maryott, M. E. Hobbs and P. M. Gross, *J. Am. Chem. Soc.*, **63**, 659 (1941). [n] C. P. Smyth and K. B. McAlpine, *J. Chem. Phys.*, **1**, 190 (1933).

than the static value. The difference has been attributed to dispersion associated with molecular inversion and, for symmetric top molecules, it has been found possible to calculate the magnitude of the difference from structural parameters. This paper presents the results of similar measurements on substances of lower molecular symmetry for which exact calculations cannot be made and attempts to give a qualitative interpretation of the results.

Experimental

The apparatus and methods of measurement used were similar to those reported earlier.[2-4] Dielectric constant values were obtained at a series of gas pressures at each of three or more temperatures between 30 and 100°. While the temperature variation of the dielectric constant was not of interest in itself (all gases measured giving the static value for the distortion polarization), it served as a valuable check on the accuracy of the measurements.

All of the materials used were of the purest commercially available grade. Those which are liquid at room temperature were further purified by fractional distillation through an efficient column. Gases were distilled on a vacuum line. In some cases mass spectrometric tests for purity were made.

Results

As in previous measurements, the quantity $(\epsilon - 1)$ was found to vary linearly with pressure and the molar polarization linearly with reciprocal temperature. Table I shows the value of the molar polarization measured or interpolated at 30°, the extrapolated value of the distortion polarization, and the corresponding values for these quantities at low frequency taken from the literature. The last column shows the fractional difference between the orientation polarization at 9400 megacycles and at low frequency.

The average deviation of the measurements on which the results shown in Table I are based ranged between 0.5 and 1%. Additional measurements of considerably lower accuracy were made on six ketones for which low-frequency gas-phase dielectric constant values are not available. Based on the assumptions that the orientation polarization at 9400 Mc. is the same as at low frequency and that the distortion polarization is 5% larger than the molar refraction, the dipole moments of 2-butanone, 3-pentanone, 3-methyl-2-butanone, 4-methyl-2-pentanone, cyclopentanone and cyclohexanone are 2.7, 2.6, 2.7, 2.5, 2.7 and 2.5, respectively.

Discussion

The work of numerous authors[2-9] on both microwave absorption and dielectric dispersion appears to have firmly established the existence of inversion transitions in complex molecules. Using the Van Vleck–Weisskopf equation for pressure-broadening of a spectral line, the dipole moment matrix element for inversion, and assuming the resonant frequency of the inversion to be essentially zero, it has been possible to calculate the observed intensity and frequency variation of microwave absorption in the case of symmetric top molecules where the summation over rotational states can be evaluated.[8] The same model has led to the calculation of the observed difference between the dielectric constant at low frequency and that at microwave frequencies.[4]

There still remain, however, several unresolved problems concerned with such inversion transitions. The transition probability for an inversion occurring at a very low frequency would be ex-

(5) W. D. Hershberger, *J. Appl. Phys.*, **17**, 495 (1946).
(6) J. E. Walter and W. D. Hershberger, *ibid.*, **17**, 814 (1946).
(7) B. Bleaney and J. H. N. Loubser, *Proc. Phys. Soc. (London)*, **A63**, 483 (1950).
(8) G. Birnbaum, *J. Chem. Phys.*, **27**, 360 (1957).
(9) Krishnaji and G. P. Srivastava, *Phys. Rev.*, **109**, 1560 (1958).

pected to be very small, as indeed it must to explain the retention of configuration of optical isomers. Nevertheless, when the spectral line is broadened by pressure into the microwave region, the effect on both microwave absorption and dielectric constant is quite appreciable.

The manner in which the inversion transition occurs is also uncertain. The net effect must be a reversal of the direction of the dipole moment without a rotation of the molecule as a whole. This might be accomplished by a direct inversion, as in ammonia. An alternative and intuitively more reasonable mechanism for a molecule such as methyl chloride involves the internal rotation of one or two of the C–X groups with respect to the remainder, *i.e.*, an extension of a bending or oscillatory mode of vibration.

From the data in Table I it can be seen that many of the substances in the present study show a decreased molar polarization at 9400 Mc. compared with the static value. The last column of Table I shows the fractional difference between the values of the orientation polarization at the two frequencies. For symmetric top molecules, at least, this is a significant quantity since it easily can be shown to be equivalent to $\Sigma f_{JK} \mid \mu_{JK} \mid^2/\mu^2$, the summation over rotational states from which the dielectric constant and absorption can be calculated.

Whether or not the frequency variation in the orientation polarization of the substances shown in Table I is entirely due to inversion is difficult to say. Certainly the asymmetric top molecules will have numerous low-frequency rotational lines which could contribute to the deviation. Such low-frequency lines, however, would be expected to be relatively weak and it is probable that their contribution is negligible. For none of the substances studied was there any indication of a variation of molar polarization with gas pressure. This is an indication that, at the pressures used, the measuring frequency of 9400 Mc. is above the frequency range in which the inversion dispersion takes place.[4] If these presumptions are correct, the last column of Table I gives the fraction of the orientation polarization that is related to inversion transitions, the remainder being associated with rotational transitions.

The values for the inversion contribution given in the last column of Table I are found numerically by taking the difference between two differences (the two orientation polarizations being found by subtracting the distortion polarization from the total polarization). Consequently, they are not highly accurate, having a probable error ranging from 0.01 in the best cases up to perhaps 0.04 for gases where the orientation polarization is small.

It will be noted that the inversion contribution is similar for members of a homologous series. For the first four normal alkyl chlorides the values are 0.09,[2] 0.12, 0.10, 0.11. Methyl and ethyl alcohols give values of 0.06 and 0.08, respectively.

Since the inversion contribution is a measure of the component of the dipole moment parallel to the molecular rotation axis summed over all rotational states it would be expected to be primarily dependent on molecular shape. This is clearly brought out in a qualitative way by the results obtained. For example, the *sec*-propyl bromide and chloride values are similar and considerably larger than those obtained for the normal compounds. In the results previously published,[2,4] the values for CH_3Cl and CH_3Br are 0.09 and 0.06 while those for CHF_3 and $CHCl_3$ are 0.41 and 0.43.

Perhaps the most striking feature in our present results is the absence of any significant difference between the polarizations of CH_2F_2, CH_2Cl_2 and CH_2Br_2 at the two frequencies. CCl_2F_2 also shows no deviation, but for this compound the orientation polarization is so small that a minor difference would not be noted. These four compounds, having C_{2v} molecular symmetry, are non-planar and there is no obvious reason why they should not be able to undergo an inversion transition. Possibly a reason could be understood if the mechanism by which the transition occurs were known. It may also be that a transition does occur, but because of molecular geometry the magnitude of the effect is below our limit of measurement.

Ethyl ether, again, shows only a small difference, well within the limits of experimental error, between its polarization at 9400 Mc. and the static polarization. It may be significant that the polar C–O–C group is planar, with the remainder of the molecule rotating nearly freely. The same sort of situation occurs in the acetone molecule, which has been shown earlier[2] to have the static value of molar polarization at 9400 Mc. If the time required for the inversion process is large compared with the time for internal rotation, the entire molecule would be equivalent to a planar molecule and inversion would be equivalent to rotation.

The trimethylamine molecule, like ammonia, would be expected to undergo inversion easily. Carbon oxysulfide is linear so that no inversion should be possible. For both of these substances, however, the orientation polarization is so small that the differences between the molar polarization observed at 9400 Mc. and the static value are not significant. Dielectric constants have been measured for $CHBrCl_2$ and CH_2BrCl, but low frequency values are not available for comparison. They would both be expected to undergo inversion. The values for the ketones have large enough inaccuracies that the most that can be said is that there is no very large difference between their dielectric constants at 9400 Mc. and at low frequency.

Conclusions

For the asymmetric top molecules studied in this work no calculations of the dielectric dispersion to be expected on the basis of inversion transitions are possible. Nevertheless, many of the substances give the behavior to be expected qualitatively if the same sort of low-frequency inversion occurs that has been suggested for symmetric top molecules. Certain substances, notably those of C_{2v} molecular symmetry, fail to show the observable differences in their dielectric constants that would be expected if they were capable of inversion.

THEORY OF PERMEATION THROUGH METAL COATED POLYMER FILMS[1]

BY W. PRINS AND J. J. HERMANS

Cellulose Research Institute, State University College of Forestry at Syracuse University, Syracuse 10, New York

Received October 25, 1958

It is shown theoretically that if a metal coat on a polymer film contains n circular holes per cm.^{2}, of radius r_0, the permeation flux per cm.^{2} is given approximately by $F = D[(a - b)/s]\theta[1 + 1.18s/r_0)$ when $0 \leqslant \theta \leqslant 1$, where D is the diffusion coefficient, assumed independent of concentration; $(a - b)$ is the concentration drop across the film of thickness s and $\theta = \pi r_0^2 n$ is the fraction of free surface. This theoretical result was confirmed experimentally using an electrical analog, in which the electrical current density in an electrolyte solution between two electrodes was measured, one of the electrodes being coated except for a number of small holes. Calculations and experiments for the inverse case where the coat is applied in the form of a number of impermeable spots of radius r_0, show that the permeability is not affected at all by this kind of coating if $s \gg r_0$ and $(1 - \theta) \ll 1$. Intermediate types of defective coatings are discussed qualitatively.

Introduction

The permeation of gases and vapors through polymer films presents a serious problem in their use as packaging materials. It is well known that the permeation is a diffusion controlled process[2] and extensive determinations of the diffusion flux have been made.[3] In order to reduce the rates of diffusion of gases through membranes, protective metal foils are laminated on to the polymer films or the films may be metalized by vacuum sputtering or other techniques. Although one might expect that the permeability of such coated films would be effectively zero, several experiments have shown[4] that there are sometimes large residual permeabilities, indicating defects in the uniformity of the coating. It is the purpose of this paper to present some calculations and experiments concerning the diffusion of gases through films with incomplete metal coats.

To this end we consider first a film of thickness s, coated with an impermeable metal layer containing a circular hole of radius r_0. We assume that a steady state has been established in which the concentration of the permeating substance in the film at the boundary between the film and the hole is a, while the concentration in the other boundary layer of the film is b. These concentrations will be determined by the pressure of the gas on either side of the film; in a number of cases (N_2, O_2, CO_2), it has been found[3] that the concentrations obey Henry's law, which states that pressure and concentration are proportional to each other. Whether Henry's law is followed or not is immaterial for our calculation. We will assume, however, that the diffusion coefficient of the gas in the film is independent of concentration. This is experimentally found to be true for the gases mentioned, but is not true for water and organic vapors.[3]

We place no restriction on the thickness of the metal layer, although it is conceivable that this will have an influence on the transport through the film in those cases where the holes act essentially as channels. When these channels are comparatively long, the rate of the permeation process may be determined to a certain extent by the diffusion or the flow of the permeating gas or liquid in the channels. This would result in a somewhat lower value of a, but it would not invalidate our treatment of the diffusion through the film.

If the center of the circular hole is taken as origin of a cylindrical coördinate system (x,r) and if x is perpendicular to the film surface, the steady-state equation for the concentration c in the film is

$$\partial^2 c/\partial r + (1/r)\partial c/\partial r + \partial^2 c/\partial x^2 = 0 \qquad (1)$$

with the boundary conditions

$$c(s,r) = b \quad \text{for all } r \qquad (2a)$$

$$c(0,r) = a \quad \text{for } r < r_0 \qquad (2b)$$

$$(\partial c/\partial x)_{0,r} = 0 \quad \text{when } r > r_0 \qquad (2c)$$

An exact solution for the two limiting cases $s \ll r_0$ and $s \gg r_0$ has been found (see Appendix). As an approximation for intermediate cases, the boundary condition (2b) has been replaced by the requirement that the *average* of $c(0,r)$ over the entire hole of radius r_0 is equal to a. If there are n holes per cm.^{2} and if the holes are sufficiently far apart to assume additivity, the flux F per cm.^{2} is obtained by multiplying the result for one hole by n. As shown in the Appendix

$$F = D[(a - b)/s]\theta\lambda/2H(\lambda) \text{ provided } \theta \ll 1 \qquad (3)$$

where $\lambda = s/r_0$ and θ $(= \pi r_0^2 n)$ is the fraction of the surface that is not coated. D is the diffusion coefficient; $H(\lambda)$ is an integral defined by eq. 12 and has been determined by graphical integration. It becomes equal to $\lambda/2 + 0(\lambda^3)$ when λ approaches zero and approaches the value $4/3\pi = 0.425$ when λ becomes infinite. For $\lambda > 0.3$ eq. 3 can be replaced to a good approximation by

$$F = D[(a - b)/s]\theta(1 + 1.18\lambda) \qquad \theta \ll 1 \qquad (4)$$

When the film thickness s is small compared with the radius r_0 of the hole ($\lambda \ll 1$), eq. 3 and 4 give the trivial result

$$F = D\theta(a - b)/s \qquad 0 \leqslant \theta \leqslant 1 \qquad (5)$$

and this is now valid in the entire θ-range. The important feature of the theoretical result (4) is that in the limit of large λ the flux can become many times larger than corresponds with the free surface (eq. 5). Qualitatively this is understandable: the thicker the film compared to the size of the hole, the more the diffusing gas spreads out in the film.

We consider next the inverse case where, instead

(1) Presented at the 134th National Meeting of the American Chemical Society, Division of Polymer Chemistry, September 7–12, 1958, Chicago, Illinois.

(2) R. M. Barrer, "Diffusion in and through Solids," The Macmillan Co., New York, N. Y., 1941.

(3) See *e.g.*, C. Rogers, J. A. Meyer, V. Stannett and M. Szwarc, *Tappi*, **39**, 737 (1956).

(4) V. Stannett, State University College of Forestry, Syracuse, New York, private communication.

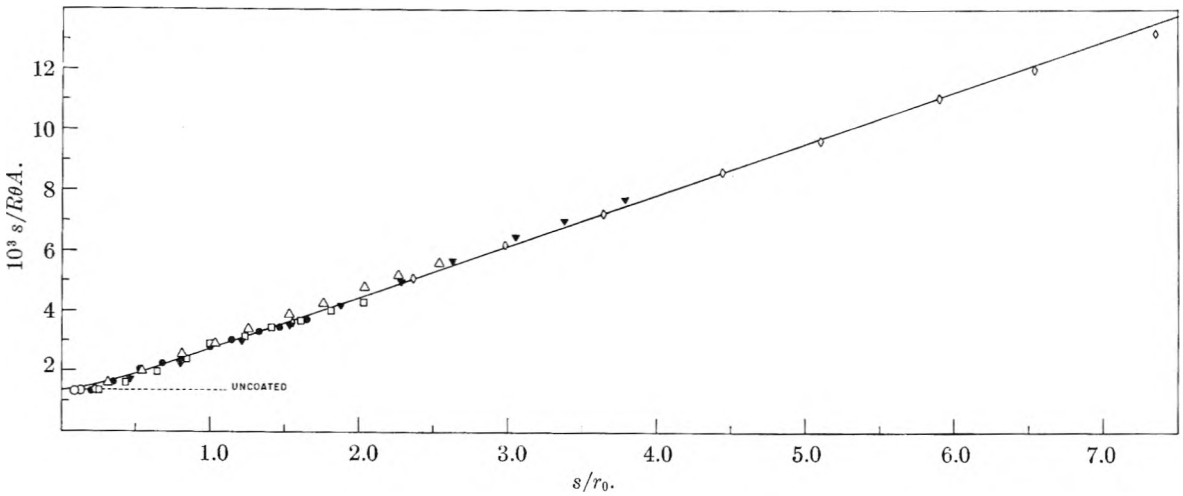

Fig. 1.—Coating containing holes of radius r_0; $s/R\theta A$ as a function of the parameter $\lambda = s/r_0$. The drawn curve is theoretical (eq. 3), the points are experimental. The linear part ($\lambda \geq 0.3$) corresponds to eq. 4 and 4a.

of a hole in an otherwise perfect coating, we have an impermeable island of radius r_0 on an otherwise uncoated polymer film. Now we have to solve eq. 1 with another set of boundary conditions

$$c(s,r) = b \quad \text{for all } r \qquad (6a)$$
$$c(0,r) = a \quad r > r_0 \qquad (6b)$$
$$(\partial c/\partial x)_{0,r} = 0 \quad r < r_0 \qquad (6c)$$

As in the previous case, an exact solution could be found for the two limiting cases $s \gg r_0$ and $s \ll r_0$ (see Appendix). The approximation given for intermediate cases does not obey the condition (6c) but makes the *average* of $\partial c/\partial x$ over the island $r < r_0$ equal to zero. Moreover, the expression obtained for the flux F in this intermediate case is obtained in the form of a double integral which has not been further reduced.

For small λ-values we have, of course, again the trivial answer: $F = D\theta(a - b)/s$ (eq. 5), *i.e.*, the flux is proportional to the free surface θ, which in this case is $(1 - \pi r_0^2 n)$. When $\lambda \gg 1$ we obtain the interesting result

$$F = D(a - b)/s \text{ when } (1 - \theta) \ll 1 \qquad (7)$$

which indicates that small islands of coating on a thick film do not have any influence at all on the permeability of the film. The validity of eq. 7 is restricted to large values of θ (or $1 - \theta \ll 1$) for the same reason as before: the effect of the various islands on the permeability is additive only when they are sufficiently far apart.

The above theoretical results (eq. 4 and 7) were checked by performing simple model experiments. From these experimental results some qualitative predictions can be made for the intermediate cases where θ is neither small nor large.

Model Experiments.—An experimental test of eq. 4 and 7 can be obtained by measuring the current density between two large electrodes of which one is coated completely except for a number of holes of radius r_0. For the inverse case, one electrode is coated with a number of insulating islands of radius r_0. In these model experiments the flux/cm.^{2} is the current density, $F = V/RA$, where V is the potential drop, which replaces $(a - b)$, R is the measured resistance and A the total surface of the blank electrode. The role of the diffusion coefficient is taken over by the specific conductivity K, of the electrolyte solution between the electrodes ($K = s/RA$ for blank electrodes). Equation 4 now reads after rearranging

$$s/R\theta A = K(1 + 1.18\lambda) \text{ when } \theta \ll 1 \qquad (4a)$$

For eq. 7 we get

$$s/RA = K \quad \lambda \gg 1;\ (1 - \theta) \ll 1 \qquad (7a)$$

For the case $\lambda \ll 1$ we have the equivalent of eq. 5

$$s/RA = K\theta \quad 0 \leq \theta \leq 1 \qquad (5a)$$

Two brass discs with a diameter of 11 cm. were gold-plated to suppress polarization potentials, which caused deviations from Ohm's law. At the back, these electrodes were coated with collodion or nail polish. The electrodes were placed in an aqueous 0.01 *N* KCl solution and their spacing varied by means of insulating rings from 1.31 to 10.65 mm. with 1 mm. intervals. The area under the rings was also painted with nail polish leaving an area of 78.5 cm.^{2} for the blank electrodes. Meticulous cleaning of the surfaces with dilute HNO_3, acetone and ether proved necessary in order to obtain linear plots of resistance R *versus* spacing s for the blank electrodes. The resistances, which varied from 1 to 30 ohms, were measured with an accuracy of 0.05 ohms on a Wheatstone bridge operating at 1.5 v. and a frequency of 1000 c./sec.

After measuring the resistance as a function of s for the blank electrodes, one of them was painted with nail polish except for a number of holes of radius r_0, after which the resistance was again measured as a function of s. This was done for holes of various radii, so as to vary the parameter λ from 0 to 7.35 (Fig. 1). In all cases the "holes" were separated by at least one diameter.

For the inverse case small circular pieces of tape of radius 1.65 mm. were punched out by means of a small size cork borer. The resistance was measured at $s = 10.65$ mm., affixing a stepwise increasing number of tapes to the surface of one of the electrodes. In this way θ could be varied from 1 to 0.88, keeping λ constant at the large value 6.5.

Results and Discussion

The curve in Fig. 1 is theoretical (eq. 3), the points are experimental. From the intercept with the $s/R\theta A$ axis we find $K = 0.00137\ \Omega^{-1}$ cm.$^{-1}$, from the slope of the linear part (using eq. 4a): $K = 0.0014\ \Omega^{-1}$ cm.$^{-1}$. The real value for K for the aqueous KCl solution at 23.5° is 0.001385.

A similar plot of $s/R\theta A$ *versus* λ for the inverse case, where we have islands instead of holes, could not be obtained from our experimental results. The error in r_0, as well as in the (small) resistances which we encountered, was too large. Instead, we restricted our measurements to the case where $\lambda \gg 1$ ($\lambda = 6.5$), for which case a theoretical solution is available (eq. 7 and 7a). A plot of s/RA *versus* θ should show a horizontal line, giving the specific conductivity K. As Fig. 2 shows, this is borne out

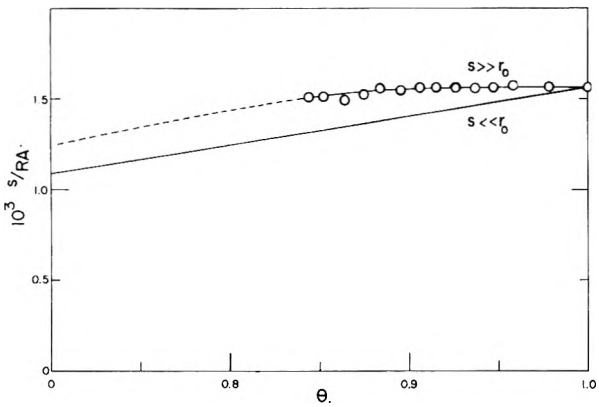

Fig. 2.—Coating consisting of islands of radius r_0; s/RA as a function of θ, the fraction of uncoated surface, at λ = 6.5. Down to θ = 0.86, s/RA equals K, the specific conductivity of the medium, as predicted by eq. 7 and 7a.

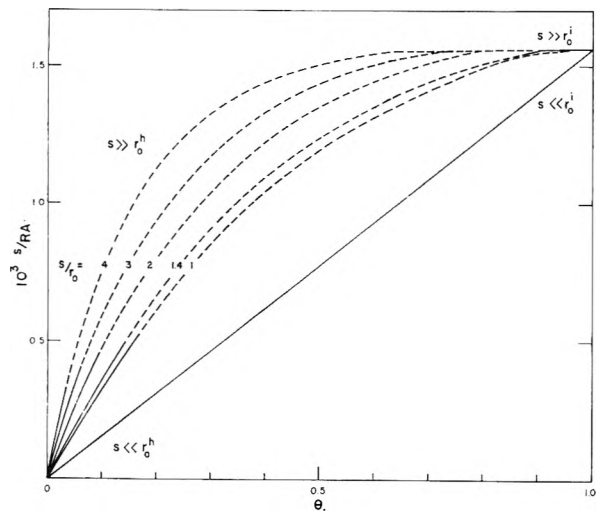

Fig. 3.—Intermediate types of defective coating, the results of Figs. 1 and 2 plotted *versus* θ. The dashed curves represent the probable conductivity at θ values not accessible to theory or experiment.

experimentally: over a range of θ from 1 to 0.86, K equals 0.00156 Ω^{-1} cm.$^{-1}$, whereas the known value at the temperature of the experiment (30°) is 0.001545 Ω^{-1} cm.$^{-1}$.

As pointed out before, both cases treated so far (holes and islands) are restricted to small and large values of free surface, respectively, except when $\lambda \ll 1$. Figure 3 is an attempt to account for the intermediate values of θ from 0.20 to 0.80. The straight line $s/RA = K\theta$ represents the trivial case (eq. 5 and 5a) for $s \ll r_0$, where r_0 can be either the "hole" radius (r_0^h) or the "island" radius (r_0^i). At small θ-values eq. 4 and 4a are valid: plotting s/RA against θ one obtains a number of straight lines, each having its own λ^h value (lines with λ^h = 1, 2, 3 and 4 have been drawn in Fig. 3). At the other extreme, we have only the straight line $s/RA = K$ for λ^i = 6.5, s = 10.65 mm., r_0^i = 1.65 mm. To get an idea of how the straight lines at the bottom left bend over toward the straight line at the upper right, we consider a close packing of "holes" for s = 10.65 mm. and various r_0^h values (thus also various λ^h-values). At close packing we have 91% free surface and 9% coated in the form of "islands" between the close packed holes. We assign an effective radius r_0^i to these islands by the requirement that $\pi(r_0^i)^2$ is equal to the area of one island. When we choose r_0^h = 0.74 (or λ^h = 1.4) we obtain for the "islands" r_0^i = 1.65 mm. We know, therefore, that the straight line at the right should approximately connect with one of the straight lines from the left, to wit the one having λ = 1.4. The slight bending off provides the point where this connection should be made, approximately. It is easy to see that curves with lower λ-values will lie lower than this one and will have a shorter straight stretch at the upper right. For larger λ the opposite will be true.

To interpret the results given in the graphs for the electrical model experiments in terms of permeability, we recall that $s/RA\theta$ has to be replaced by $sF/(a - b)\theta$ and the specific conductivity K by the diffusion coefficient, D.

Although, of course, a variety of defects in metal coated polymer films may exist, the above treatment for holes and islands may serve a useful purpose. Suppose one has a laminated film, which contains holes in the coat. Under the microscope, one can count the number of holes/cm.^{2} and assign an average radius to the holes. These measurements determine θ and r_0. If now the thickness of the film and the permeability of the uncoated film (or its diffusion coefficient for the gas under consideration) are known, eq. 4 and Figs. 1 and 3 will give a fairly precise idea of the permeability of the film with the defective coat. An alternative way of measuring θ would be by means of light transmission.

Another way of obtaining an estimate of the average hole radius can be employed when one can measure the permeability of the metal layer itself, provided that a relation between pore size and permeability is known. For example, if the flow through the holes obeys Poiseuille's law, the flux per cm.^{2} F is $(\Delta p/8\eta l)\Sigma n_i r_i^4$, where Δp is the pressure drop across the metal film of thickness l, and η is the viscosity of the permeating medium. The fraction $\theta = \pi\Sigma n_i r_i^2$ could be estimated from volume and weight measurements. The ratio F/θ then determines a (weighted) average radius.

The consideration of islands of coating may be helpful for coated films that have been obtained by a sputtering technique. Here again a photomicrograph would yield all the necessary information for an estimate of the permeability, using eq. 7 and Figs. 2 and 3.

Appendix

Equation 1 is the well-known equation of Laplace, but the boundary conditions which must be obeyed are of a peculiar type and we have not been able to find a solution in the literature. In the following we will make use of discontinuous integrals involving Bessel functions, most of which can be found in ref. 4. We give no more than an indication of the method and omit the rigorous justification of the various steps made in the calculation.

I. Coat Containing Holes.—We note that $\sinh [t(s - x)]J_0(tr)$ for arbitrary t is a solution of

(4) G. N. Watson, "Theory of Bessel Functions," 2nd Edition, The Macmillan Co., New York, N. Y.

eq. 1 which is zero when $x = s$. Hence

$$c(x,r) = b + \int_0^\infty dt\, f(t)\, J_0(rt) \sinh [t(s - x)] \quad (8)$$

satisfies (1) and (2a) for any function $f(t)$ for which the integral has the necessary properties of convergence. Making use of a discontinuous integral (ref. 4, p. 380), we can satisfy eq. 2c by taking

$$f(t) = BJ_1(r_0t)/t \cosh (st) \quad (9)$$

where B is a constant. The condition (2b) is replaced by the requirement that

$$\int_0^{r_0} 2\pi r\, dr\, c(0,r) = \pi r_0^2 a \quad (10)$$

which determines the value of B. The flux through one hole of radius r_0 is

$$F_1 = -D \int_0^{r_0} 2\pi r\, dr\, (\partial c/\partial x)_{0,r} \quad (11)$$

and the total flux per cm.^{2} is $F = nF_1$. Since $\partial c/\partial x$ is given as an integral over the variable t, eq. 11 for F_1 is a double integral. Changing the order of integration and using the well-known property, $uJ_0(u) = d[uJ_1(u)]/du$ we finally obtain the result given in eq. 3 with

$$H(\lambda) = \int_0^\infty dv\, v^{-2} J_1^2(v) \tanh (\lambda v) \quad (12)$$

This function is, obviously, an odd function of λ. For small values of λ we may replace $\tanh(\lambda v)$ by λv and are thus led to an integral for which the answer is known (ref. 4, p. 403), giving $H(\lambda) = \lambda/2$. At this limit eq. 2b is obeyed exactly. When λ is large, we may replace $\tanh(\lambda v)$ by 1 and obtain (ref. 4, p. 403): $H(\lambda) = 4/3\pi$. It can be easily shown, again using a discontinuous integral (ref. 4, p. 403), that in this limiting case likewise, eq. 2b is satisfied exactly. For finite values of λ, $H(\lambda)$ was obtained by graphical integration, and was found to be represented with fairly good accuracy by

$$H(\lambda) = (\lambda/2)(1 + 1.18\lambda)^{-1}, \text{ provided } \lambda > 0.3$$

II. Coating Consisting of Islands.—To satisfy the boundary conditions (6), we consider the solution

$$c(x,r) = a - (a - b)x/s + \int_0^\infty dt\, g(t)\, J_0(rt) \sinh [(s - x)t] \quad (13)$$

where $g(t)$ is an arbitrary function. This obeys (6a). To satisfy (6b), we make use of the property

$$\int_0^\infty du\, u^{-2}(\sin au - au \cos au) J_0(bu) = \begin{cases} (a^2 - b^2)^{1/2} & \text{when } b < a \\ 0 & \text{when } b > a \end{cases} \quad (14)$$

which can be derived by a process of partial integration from a result given by Whittaker and Watson[5]

(5) E. T. Whittaker and G. N. Watson, "A Course of Modern Analysis," Cambridge University Press, 1927, p. 382.

$$\int_0^\infty du\, u^{-1} \sin (au) J_1(bu) = \begin{cases} ab^{-1} - b^{-1}(a^2 - b^2)^{1/2} & \text{when } b < a \\ ab^{-1} & \text{when } b > a \end{cases} \quad (15)$$

On account of eq. 14 we set

$$g(t) = C(\sin r_0t - r_0t \cos r_0t)[t^2 \sinh (st)]^{-1} \quad (16)$$

and determine the constant C by the condition

$$\int_0^{r_0} 2\pi r\, dr(\partial c/\partial x)_{0,r} = 0 \quad (17)$$

which is an approximation to (6c). The flux is now obtained by integrating $-2\pi Dr(\partial c/\partial x)_{0,r}$ from r_0 to ∞. The term $(a - b)x/s$ in eq. 13 gives the trivial contribution $D(a - b)/s$ to the flux per cm.^{2}. We consider only the remaining part

$$-2\pi D \int_{r_0}^\infty dt\, r\gamma; \quad \gamma = (a - b)/s + (\partial c/\partial x)_{0,r} \quad (18)$$

which is a double integral over r and t. Unfortunately, however, it is not permissible this time to invert the order of integration. This is why we restrict ourselves to the limiting cases $\lambda \ll 1$ and $\lambda \gg 1$, where the integration over the variable t can be carried out explicitly. At the limit of small λ we may replace $\tanh(st)$, which leads to the trivial result eq. 5. At the limit of large λ we replace $\tanh(st)$ by 1 and use two more known discontinuous integrals (ref. 4, p. 405), which lead to the result

$$-(\partial c/\partial x)_{0,r} = \begin{cases} (a - b)/s + C\pi/2 & \text{when } r < r_0 \\ (a - b)/s + C \text{ arc sin } (r_0/r) - Cr_0(r^2 - r_0^2)^{-1/2} & \text{when } r > r_0 \end{cases} \quad (19)$$

Eq. 6c is obeyed when $C = -3(a - b)/2r_0$. It is of some interest to observe that $(\partial c/\partial x)_{0,r}$ for $r > r_0$ has a singularity at $r = r_0$. This is not an artifact caused by the approximation (17); in the limiting case considered ($\lambda \gg 1$), $(\partial c/\partial x)_{0,r}$ is identically equal to zero for all values below r_0, so that we are dealing with the rigorous solution of the problem. Notwithstanding the singularity at $r = r_0$, the integral (18) converges and when worked out leads to the result eq. 7.

NOTE ADDED IN PROOF.—Professor C. J. F. Böttcher (Leiden, Netherlands) kindly drew the author's attention to work on the problem of evaporation from a circular surface which was published more than 40 years ago. Stefan,[6] on the basis of the analogy with electrostatics, predicted theoretically that at the limit of very large values of $\lambda = s/r_0$ (in the notation of the present article), the rate of evaporation is proportional to r_0, in accordance with Eq. 3 or 4 when $\lambda >> 1$.

A review of this work and of some experiments on evaporation was given by Thomas and Ferguson.[7]

Acknowledgment.—The authors are indebted to Dr. V. Stannett (Syracuse, New York) for drawing their attention to this problem and for helpful discussions.

(6) S. Stefan *Wied. Ann.*, **17**, 550 (1882).

(7) N. Thomas and A. Ferguson, *Phil. Mag.* (6) **34**, 308 (1917).

THE KINETICS OF THE POLYMERIZATION OF ETHYLENE WITH TRIETHYLALUMINUM AND TITANIUM TETRACHLORIDE CATALYSTS

BY HANS FEILCHENFELD AND MOSHE JESELSON

Contribution from the Petrochemical Laboratory of the Research Council of Israel and the Physical Chemistry Department, Hebrew University, Jerusalem, Israel

Received October 28, 1958

The polymerization of ethylene was carried out in a heptane solution at 37°. Varying amounts of triethylaluminum and titanium tetrachloride were used as catalysts. The results show that the reaction is of the first order with respect both to ethylene and to titanium tetrachloride as long as an excess of triethylaluminum is present.

Introduction

The publication by Ziegler[1] of his process for the polymerization of ethylene to high molecular polyethylene by the use of mixed catalysts of the type alkyl metal—metal polyhalide has initiated research in different aspects of the reaction. Little of this work has as yet been published; this is particularly true of the system $Al(C_2H_5)_3$–$TiCl_4$ which Ziegler pointed out to be especially efficient. This may be attributed to the extreme reactivity of both components which causes inconvenience in handling. In this paper some results on the kinetics of the reaction will be given. The polymerization of ethylene was carried out in *n*-heptane at partial pressures of ethylene from about 50 to 1000 mm. The catalyst was $Al(C_2H_5)_3$ with small amounts of $TiCl_4$.

Apparatus.—The reaction took place in a flat-bottom flask, the volume of which together with the connecting tubing was 2.2 l. Ethylene obtained from dehydration of ethanol over alumina at 400° was washed in alcohol at −70° and condensed in a trap by liquid air. After enough ethylene was collected the apparatus was evacuated; the liquid air-bath then was removed and the ethylene evaporated until the desired pressure was obtained. The excess ethylene was vented. Three hundred ml. of *n*-heptane (ASTM octane number grade, dried over sodium and freshly distilled before each experiment) was injected into the reaction vessel by means of a syringe, the needle passing through a self-sealing rubber gasket. In the same way the desired amounts of triethylaluminum[2] and titanium tetrachloride[3] were introduced one after the other. The mixture was stirred by a magnetic stirrer at a speed sufficient to make the rate of reaction independent of stirring. Pressure readings were taken. Occasionally gas samples were analyzed by gas chromatography; they showed the presence of small amounts of nitrogen and decomposition products. These were taken into account when calculating the partial pressure of ethylene (p) from the pressure readings. The temperature was kept constant at 37.5 ± 0.5° by means of a water-bath heated with an immersion heater.

Results

Figure 1 shows the rate of change of partial pressure of ethylene with time after the introduction of $TiCl_4$. From the results it appears that there is a very short induction period (more pronounced if, instead of $Al(C_2H_5)_3$ the less reactive $Al(C_2H_5)_2Br$ is used). The rate of reaction then increases rapidly, passes through a maximum and decreases slowly. For the study of the kinetics of the reaction the first period, namely, that of catalyst formation, is not suitable, because it is necessary to work with equal quantities and reactivities of the catalyst; this can only be achieved after the initial period.

To investigate the order of the reaction the experiment was arranged in such a way that from time to time some of the ethylene was suddenly withdrawn by pumping. This procedure allowed the measurement of the rate at different pressures but at the same activity of the catalyst; no further impurities were introduced since no fresh ethylene was fed into the apparatus; in addition, the degree of polymerization before and after withdrawal was virtually the same. The method avoided therefore the comparison of rates at different degrees of polymerization and catalyst activity. The volume of the vapor space was chosen to be rather small in order to reduce shielding effects due to large quantities of polyethylene forming around the active centers.

If a first-order law holds the plot of log p against t should show a straight line the slope of which before withdrawal should be the same as that after withdrawal. Figure 2 shows this plot. Under the given conditions the reaction appears therefore to be of the first order.

To investigate the change of catalyst-activity with time a long run without withdrawals was made. On the assumption that the first-order law holds, as shown in the previous paragraph, the activity on termination of the run after 72 hours had fallen by 50%. By then a little over 100 moles of ethylene had been polymerized per mole of $TiCl_4$. Part or all of the reduction of catalyst activity is no doubt due to poisoning of the catalyst, since in this experiment fresh ethylene was added from time to time.

In another experiment the temperature was changed first to 47 and then to 57°. This had no significant effect on the rate of ethylene uptake. Although no doubt the reaction velocity increased with rise of temperature, this was effectively counterbalanced by the lower ethylene concentrations in the solvent at the higher temperatures.

It was next attempted to investigate the influence of additions of different amounts of $TiCl_4$ while keeping the amount of $Al(C_2H_5)_3$ in excess and constant at 2.5 ml./300 ml. of solvent. This was done by repeating the procedure outlined above, using each time a different amount of $TiCl_4$. An alternative way was to add increasing amounts of $TiCl_4$ while the polymerization was proceeding. The results of both methods agreed among themselves. The constant k', a function of the amount of catalyst, was defined in the usual way by the equation

(1) D. K. Ziegler, E. Holzkamp, H. Breil and H. Martin, *Angew. Chem.*, **67**, 541 (1955).

(2) A. V. Grosse and J. M. Mavity, *J. Org. Chem.*, **5**, 106 (1940).

(3) E. Demarçay, *Compt. rend.*, **104**, 111 (1887).

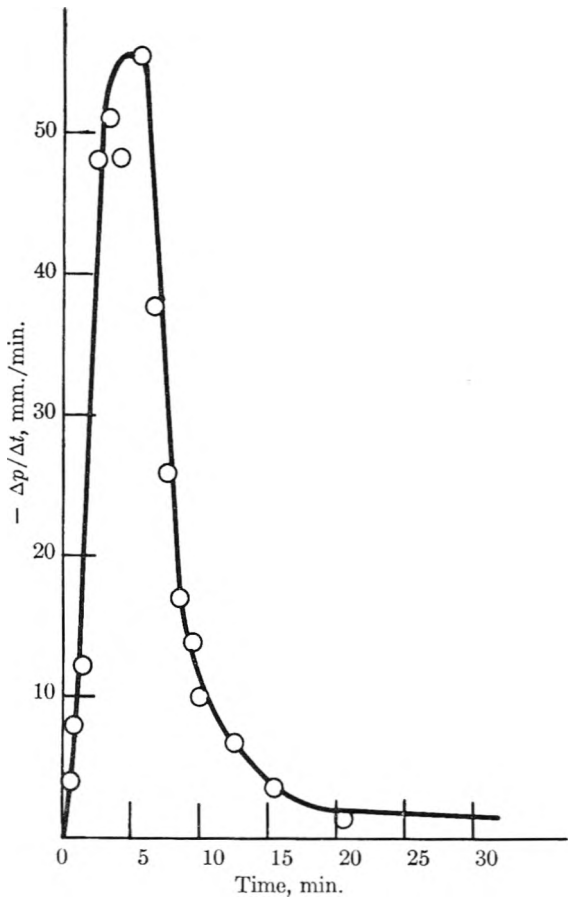

Fig. 1.—Change of rate of polymerization with time.

$$\log p_1/p_2 = k'(t_2 - t_1) \qquad (1)$$

where t is measured in hours. The plot of k' against ml. of $TiCl_4$ added is given in Fig. 3. It can be seen that with an excess of $Al(C_2H_5)_3$ k' increases with increasing amounts of $TiCl_4$. There is a slight tendency toward flattening off at higher concentrations of $TiCl_4$.

On the other hand, working with an excess of $TiCl_4$ over $Al(C_2H_5)_3$ gave a more oily polymer and the reaction did not follow a first-order law.

Discussion

Since the polymerization takes place at the interface between the solid catalyst and the solvent, the first-order kinetic law should have the form

$$r = kAc \qquad (2)$$

where

- r is the rate of polymerization in moles/hr.
- A the active surface area of the catalyst in cm.²
- c the concn. of ethylene in moles/ml. solvent
- k is the rate constant in ml./cm.² hr.

Since stirring was sufficiently rapid the concentration of ethylene was for all practical purposes at its equilibrium value. By Henry's law, therefore

$$c = \alpha p \qquad (3)$$

The rate of polymerization, on the other hand, equals the sum of the rates of disappearance of ethylene from the liquid (u) and the vapor (v) phases

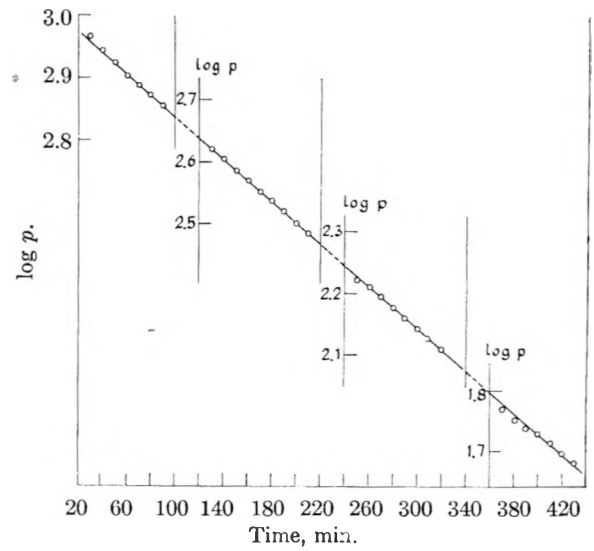

Fig. 2.—Logarithm of partial pressure of ethylene *vs.* time at different ranges of partial pressure; conditions of experiment, solvent, 300 ml. of *n*-heptane; catalyst, 2.5 ml. of $Al(C_2H_5)_3$ + 0.05 ml. of $TiCl_4$; temperature, 37°C.

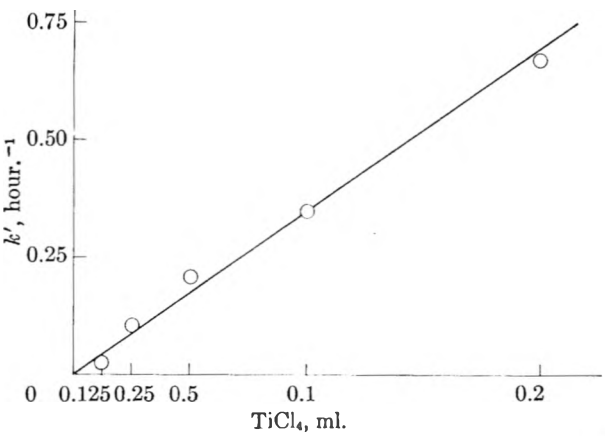

Fig. 3.—Influence of varying amounts of $TiCl_4$ on the rate-constant in the presence of an excess of $Al(C_2H_5)_3$.

$$r = u + v \qquad (4)$$

But

$$u = -V_{\text{liquid}} \frac{dc}{dt} = -\alpha V_{\text{liquid}} \frac{dp}{dt} \qquad (5)$$

$$v = -\frac{dn}{dt} \qquad (6)$$

and n, the number of moles of ethylene in the gas phase

$$n = \frac{V_{\text{gas}}}{RT} p \qquad (7)$$

Since the experiment was run at constant volume and temperature

$$v = -\frac{V_{\text{gas}}}{RT} \frac{dp}{dt} \qquad (8)$$

therefore

$$r = -\left(\alpha V_{\text{liquid}} + \frac{V_{\text{gas}}}{RT}\right) \frac{dp}{dt} \qquad (9)$$

The solubility of ethylene in heptane was determined experimentally and the constant in equation 3 found to be

$$\alpha = 1.2 \times 10^{-4} \text{ moles ml.}^{-1} \text{ atm.}^{-1}$$

If the values for the volume of the gas and liquid phases are inserted in equation 9

$$\alpha V_{\text{liquid}} = 0.036 \text{ and } \frac{V_{\text{gas}}}{RT} = 0.077$$

$$r = -0.113 \frac{dp}{dt} = kAc = kA\alpha p \qquad (10)$$

It follows that the rate of polymerization is about 50% higher than the rate of disappearance of ethylene from the gas phase.

It has been shown in the experimental part that after an initial rise, during which the catalyst surface is formed, the activity of the catalyst remains practically constant for a considerable time. Therefore after the induction period, A remains constant and equation 10 can be integrated to give

$$\log p_1/p_2 = k'(t_2 - t_1) \qquad (11)$$

where

$$k' = \frac{kA\alpha}{2.3 \times 0.113} = 4.6 \times 10^{-4} kA \qquad (12)$$

This is the equation which has been experimentally confirmed (Fig. 2) and which is in accord with the data published by Natta[4] for the system containing $TiCl_3$.

Deviations from the first-order law[5] can be observed in a constant volume system when measurements are made with a freshly precipitated catalyst. The decrease in the rate is then not only due to the decrease in the partial pressure of ethylene but also to a diminution of catalyst surface caused by excessive reduction of the titanium and by the the conglomeration of the particles. If the decrease in catalyst activity is disregarded the order seems higher than it actually is. An alternative explanation for the excessive decrease in the rate before constancy is reached, is the following. In the reaction between $TiCl_4$ and $Al(C_2H_5)_3$ to form the active catalyst, free radicals (or carbanions) are formed. These will react with ethylene, superimposing a transient polymerization reaction over the constant one. The decrease in the rate of disappearance of ethylene will therefore be higher than expected from the first-order law as long as the reaction between $TiCl_4$ and $Al(C_2H_5)_3$ is not complete.

(4) G. Natta, I. Pasquon and E. Giachetti, *Angew. Chem.*, **69**, 213 (1957).

(5) J. C. McGowan and B. M. Ford, *J. Chem. Soc.*, 1149 (1958).

If it is accepted that A, the area of the catalyst surface, is proportional to the volume V of $TiCl_4$ added, $Al(C_2H_5)_3$ being present in excess, equation 11 can be re-written

$$\log p_1/p_2 = k'' V_{TiCl_4}(t_2 - t_1) \qquad (13)$$

Although there is some scatter it can be seen from Fig. 3 that the assumption is not far from the truth. k'' works out to be equal to 3.5 per hour per ml. of $TiCl_4$.

In the constant volume system described, 1 ml. of $TiCl_4$ with an excess of $Al(C_2H_5)_3$ will cause a pressure drop of $^1/_2$ (say from 2 to 1 atm.) to take place in about 5 min. This is the rate of disappearance of ethylene from the gas phase. As has been shown above, the rate of polymerization is about 50% higher. In a constant pressure system where the concentration of ethylene in the liquid phase remains constant both rates are the same. According to equation 10

$$r = -0.113 \frac{dp}{dt} \qquad (14)$$

But from equation 13

$$-\frac{dp}{dt} = 2.3k'' V_{TiCl_4} p \qquad (15)$$

Therefore

$$r = 0.113 \times 2.3 \times 3.5 V_{TiCl_4} p \qquad (16)$$

and the polymerization will proceed at the rate of 0.9 mole/atm./ml. $TiCl_4$/hr. or 26 g./atm./ml. $TiCl_4$/hr.

In the catalyst system consisting of an excess of triethylaluminum over titanium tetrachloride the polymerization of ethylene proceeded at a rate proportional both to the partial pressure of ethylene and to the amount of titanium tetrachloride added. This rate was virtually constant over a long period of time, if the first half hour of catalyst formation is disregarded. The higher rates at the beginning may be due to the transient presence of soluble or colloidal catalyst.

The first-order rate does not prove any definite mechanism. It appears, however, that neither the reducing properties of triethylaluminum nor the partial pressure of ethylene influence the activity of the catalyst once the latter is stabilized.

Acknowledgment.—This work has been carried out with the financial help of the Israel–American Joint Fund for Technical Assistance.

The advice and encouragment of Professor G. Stein are gratefully acknowledged.

HEATS OF FORMATION OF MOLYBDENUM OXYCHLORIDES

BY ROBERT L. GRAHAM AND LOREN G. HEPLER

Contribution from Cobb Chemical Laboratory, University of Virginia, Charlottesville, Va.

Received October 29, 1958

We have prepared $MoO_2Cl_2(c)$ and $MoO(OH)_2Cl_2(c)$ in a very pure state by methods somewhat different from those previously described by others. Heats of reaction of both of these compounds with aqueous sodium hydroxide have been determined and the results of these calorimetric experiments have been used in calculating that the standard heats of formation of $MoO_2Cl_2(c)$ and $MoO(OH)_2Cl_2(c)$ at 298°K. are −169.8 and −245.2 kcal./mole, respectively. We have used these heats of formation as the basis for calculation of equilibrium constants for some interesting reactions of these compounds.

As part of a systematic investigation of the thermochemistry of transition element compounds we have determined heats of formation of $MoO_2Cl_2(c)$ and $MoO(OH)_2Cl_2(c)$. It should be noted that the structure of the second compound is not known and that the formula might well be written $MoO_3 \cdot 2HCl$ or $MoO_2Cl_2 \cdot H_2O$. No values for the heats of formation of these compounds are listed in the National Bureau of Standards Circular 500.[1] We have prepared both compounds in a pure state by methods somewhat different from those previously described by others.

Experimental

The heat of solution calorimeter used in this investigation has been described.[2,3] All of the calorimetric experiments reported in this paper were carried out at 25.0 ± 0.3° with 950 ml. of solution in the calorimeter.

Samples of MoO_2 from two sources were used in the preparation of MoO_2Cl_2. The first sample of MoO_2 was prepared by reducing pure MoO_3 with H_2 in a tube furnace at 490°. This procedure gave us a product that was 88% MoO_2 as determined by reoxidation to MoO_3. Our second sample of MoO_2 was generously given to us by Climax Molybdenum Company and was in the form of pellets 1/4-inch in diameter. No estimate of the MoO_2 content of this sample was made because our work with the first sample showed that a high MoO_2 content was unnecessary for preparation of pure MoO_2Cl_2.

We prepared MoO_2Cl_2 from the first sample of MoO_2 by passing carefully dried Cl_2 over the MoO_2 in a tube furnace maintained at 350°. A round bottom flask, with side arm as exit tube for excess Cl_2, was used as a receiver for the MoO_2Cl_2 that sublimed out of the heated reaction tube. After the reaction was complete the apparatus was cooled and flushed with dry N_2 and then the receiving flask containing MoO_2Cl_2 was connected to another similar flask. The receiver with crude MoO_2Cl_2 was placed in a small furnace that we constructed by winding Nichrome wire on an asbestos-covered can. One end of the furnace can had a small hole for the side arm of the flask containing MoO_2Cl_2 to pass through and the other (removable) end of the furnace can also had a hole in it just large enough to accommodate the tube connecting the two flasks. Dry N_2 was slowly passed through the apparatus as the temperature was raised to 150°, at which temperature the MoO_2Cl_2 slowly sublimed from the hot flask to the cold flask, leaving behind a dark blue residue. After the sample was purified by five sublimations, the Mo content of the product was found to be 47.80 ± 0.05%. We calculated 48.25% Mo for MoO_2Cl_2. Five more sublimations were carried out and the final sublimate, MoO_2Cl_2, was found to contain 48.14 ± 0.02% Mo.

Another sample of MoO_2Cl_2 was prepared from the MoO_2 obtained from Climax Molybdenum Company. Pellets of MoO_2 were placed in the sublimation apparatus and dry Cl_2 was passed up through them. The reaction proceeded fairly rapidly at 150°. The crude MoO_2Cl_2 formed was sublimed ten times and then analyzed and found to contain 48.19 ± 0.02% Mo.

Our observations regarding MoO_2Cl_2 differ considerably from those of Neumann and Cook.[4] Our preparations were carried out at somewhat lower temperatures than were Neumann and Cook's. The crude MoO_2Cl_2 that first collected in the receiver flask was yellow as described by Neumann and Cook but our sublimed and purified MoO_2Cl_2 was a metallic light orange color and was stable for at least 6 months when protected from moisture. Exposure to traces of water vapor caused the pure MoO_2Cl_2 to turn yellow. It may be noted that Neumann and Cook[4] erroneously calculated that MoO_2Cl_2 contains 46.4% Mo (rather than 48.25% Mo) and reported that their MoO_2Cl_2 contained 46.3% Mo.

We prepared $MoO(OH)_2Cl_2$, or $MoO_3 \cdot 2HCl$, in the sublimation apparatus by passing pure dry HCl over pure MoO_3 at 250°. The product of this reaction collected in the cool receiving flask and was then sublimed twice at 150° in a current of dry HCl. This purified $MoO(OH)_2Cl_2$ was found to contain 44.26 ± 0.03% Mo. We calculated that this compound should contain 44.24% Mo. The purified $MoO(OH)_2Cl_2$ was lemon yellow in color and, when stored in a dry atmosphere in a small sealed tube, was sufficiently stable that we were unable to detect any decomposition over a period of 6 weeks. These observations are not in agreement with those of Neumann and Cook.[4]

All of our Mo analyses were carried out by the permanganate method.[5] Rheinhard's solution was used to inhibit oxidation of chloride ion. The analytical method was thoroughly tested on solutions containing known amounts of Mo in the presence of chloride ion. All of our samples of MoO_2Cl_2 and $MoO(OH)_2Cl_2$ were stored in desiccators in a dry box and all manipulations that involved exposing these compounds to the atmosphere were carried out in this same dry box as rapidly as possible.

Results

The heat of reaction of $MoO_2Cl_2(c)$ with 950 ml. of dilute NaOH has been measured. The initial NaOH concentration for each experiment was such that the final NaOH concentration would be 0.011 *M*. The equation for the calorimetric reaction is written as

$$MoO_2Cl_2(c) + 4NaOH(aq) = Na_2MoO_4(aq) + 2NaCl(aq) + 2H_2O(l) \qquad \Delta H_1 \quad (1)$$

Results of our determinations of the heat of reaction 1 are given in Table I. On the basis of these results and estimated heats of dilution, we take $\Delta H_1^0 = -65.3 \pm 0.5$ kcal./mole Mo where ±0.5 indicates our estimate of the total uncertainty due to possible sample impurities, calorimetric errors and heat of dilution uncertainties. We have used this ΔH_1^0 with standard heats of formation from National Bureau of Standards Circular 500[1] and our earlier paper on Na_2MoO_4[3] in calculating that the standard heat of formation of $MoO_2Cl_2(c)$ is −169.8 kcal./mole.

The heat of reaction of $MoO(OH)_2Cl_2(c)$ with 950 ml. of dilute NaOH also has been measured,

(1) "Selected Values of Chemical Thermodynamic Properties," Circular 500, National Bureau of Standards, 1952.

(2) C. N. Muldrow, Jr., and L. G. Hepler, *J. Am. Chem. Soc.*, **79**, 4045 (1957).

(3) R. L. Graham and L. G. Hepler, *ibid.*, **78**, 4846 (1956).

(4) H. M. Neumann and N. C. Cook, *ibid.*, **79**, 3026 (1957).

(5) W. F. Hillebrand, C. E. F. Lundell, H. A. Bright and J. I. Hoffman, "Applied Inorganic Analysis," Second Edition, John Wiley and Sons, Inc., New York, N. Y., 1953, p. 307.

TABLE I

HEAT OF REACTION OF MoO_2Cl_2(c) WITH NaOH(aq)

Sample	Moles MoO_2Cl_2 × 10^3	ΔH_1 (kcal./mole MoO_2Cl_2)
1	1.022	−65.4
1	1.482	−65.0
2	1.883	−65.0
2	2.463	−65.0
2	3.782	−65.1

again with sufficient NaOH present initially to make the final NaOH concentration 0.011 *M*. The equation for the calorimetric reaction is written as

$$MoO(OH)_2Cl_2(c) + 4NaOH(aq) = Na_2MoO_4(aq) + 2NaCl(aq) + 3H_2O(l) \quad \Delta H_2 \quad (2)$$

Results of our determinations of the heat of reaction 2 are given in Table II. On the basis of these results and estimated heats of dilution, we take $\Delta H_2^0 = -58.2 \pm 0.5$ kcal./mole where ±0.5 indicates our estimate of the total uncertainty. We have used this ΔH_2^0 with standard heats of formation from the literature[1,3] in calculating that the standard heat of formation of $MoO(OH)_2Cl_2$(c) is −245.2 kcal./mole.

TABLE II

HEAT OF REACTION OF $MoO(OH)_2Cl_2$(c) WITH NaOH(aq)

Moles $MoO(OH)_2Cl_2$ × 10^3	ΔH_2 (kcal./mole $MoO(OH)_2Cl_2$)
1.231	−57.9
1.687	−57.9
1.818	−58.4
3.197	−58.1
3.767	−57.8

Discussion

In connection with earlier work of Hultgren and Brewer[6] on some gaseous molybdenum oxyhalide systems it would be desirable to calculate ΔH^0 and ΔF^0 for the reaction of H_2O(g) with MoO_2Cl_2(g) to form $MoO(OH)_2Cl_2$(g). Our heats of formation of MoO_2Cl_2(c) and $MoO(OH)_2Cl_2$(c) cannot be used directly for calculation of ΔH^0 of this all-gas reaction but can be used with the heat of formation of H_2O(g)[1] in calculating that $\Delta H_3^0 = -17.6$ kcal./mole at 298°K. for reaction 3 written as

$$MoO_2Cl_2(c) + H_2O(g) = MoO(OH)_2Cl_2(c) \quad \Delta H_3^0 \quad (3)$$

We have, according to Latimer's procedure,[7] estimated that the entropy at 298°K. of $MoO(OH)_2Cl_2$(c) is 9.4 cal./deg. mole greater than the entropy of MoO_2Cl_2(c). This entropy difference estimate and the known entropy of H_2O(g)[1] have been used to calculate $\Delta S_3^0 = -35.7$ cal./deg. mole. We have used ΔH_3^0 and ΔS_3^0 to calculate that $\Delta F_3^0 = -7.0$ kcal./mole, that $K_3 = 1.35 \times 10^5$ and that the H_2O(g) pressure in equilibrium with MoO_2Cl_2(c) and $MoO(OH)_2Cl_2$(c) is 7.4×10^{-6} atm. at 298°K. This is in accord with our observation that MoO_2Cl_2(c) has a great tendency to combine with water. In this connection it should be remembered that $MoO(OH)_2Cl_2$ can be sublimed in a dry atmosphere of HCl without detectable loss of water.

It has been observed several times that $MoO(OH)_2Cl_2$, which might well be written $MoO_3 \cdot 2HCl$, easily loses HCl and that it can be sublimed without decomposition only when excess HCl is present. Our heat of formation of $MoO(OH)_2Cl_2$(c) has been used with data from the literature[1,8,9] and an estimated entropy of $MoO(OH)_2Cl_2$(c) to calculate that the standard free energy change and equilibrium constant for the reaction $MoO(OH)_2Cl_2$(c) = MoO_3(c) + 2HCl(g) are 2 kcal./mole Mo and 3×10^{-2}, respectively. The equilibrium vapor pressure of HCl(g) over MoO_3(c) and $MoO(OH)_2Cl_2$(c) is ~0.17 atm. at 298°K.

Acknowledgment.—We are pleased to express our gratitude to the Alfred P. Sloan Foundation for support of this research.

(6) N. Hultgren and L. Brewer, THIS JOURNAL, **60**, 947 (1956).

(7) W. M. Latimer, *J. Am. Chem. Soc.*, **73**, 1480 (1951).

(8) B. A. Staskiewicz, J. R. Tucker and P. E. Snyder, *ibid.*, **77**, 2987 (1955).

(9) A. D. Mah, THIS JOURNAL, **61**, 1572 (1957).

THE EFFECT OF THE MOLAR Ca/P RATIO UPON THE CRYSTALLIZATION OF BRUSHITE AND APATITE[1]

BY JAMES S. ELLIOT, ROBERT F. SHARP AND LEON LEWIS

From the Poliomyelitis Respiratory and Rehabilitation Center, Fairmont Hospital, San Leandro, California; The Division of Urology, Department of Surgery, University of California School of Medicine, San Francisco, California; The Department of Medicine, Stanford University School of Medicine, San Francisco, California

Received October 30, 1958

Data in the literature indicate that calcium phosphate precipitates from saturated solution as brushite up to *p*H 6.2 and as apatite at higher *p*H levels. In the course of a laboratory investigation concerning the chemical factors responsible for renal calculus growth in paralyzed persons, precipitates in equilibrium with urine saturated with calcium phosphate and having an average molar Ca/P ratio of 3/20 were found to consist of brushite up to *p*H 6.61 and of apatite at higher *p*H levels. In urine specimens with very low Ca/P ratios due to the addition of sodium phosphate the precipitates were composed of brushite up to *p*H 6.93. These observations suggested that the Ca/P ratio in parent solutions and in urine might have considerable effect on the relationship between equilibrium *p*H and the composition of the solid phase. In order to test this hypothesis, solutions of calcium phosphate were prepared having molar Ca/P ratios ranging from 3/1 to 1/100, with the ionic strength maintained at 0.32 by the addition of sodium chloride. Saturation was achieved by adding varying amounts of sodium hydroxide. Solutions were equilibrated with the precipitates for one week at 38°, the solutions filtered, *p*H of the solution determined and the solid phase examined under polarized light and by X-ray diffraction analysis. Results of this study indicate that the maximum *p*H at which brushite is stable is a function of the initial molar Ca/P ratio in solution and the "conversion *p*H" of brushite to apatite increases with a decreasing Ca/P ratio.

Introduction

This paper reports a study of the effect of varying initial Ca/P[2] ratios upon the relationship between equilibrium *p*H and the composition of the solid phase precipitated from solutions saturated with calcium phosphate.

The work was undertaken as part of a comprehensive investigation of the urinary chemistry involved in the formation of renal phosphatic calculi, a common and serious problem in severely paralyzed persons.

Since calcium phosphate is the principal inorganic constituent of human bone, teeth and dental calculus where it occurs as the mineral, apatite, a number of investigators have studied its solubility in aqueous solution and in serum. Although calcium phosphate is the sole or principal constituent of many renal calculi, little attention has been paid to the factors affecting the crystallization of calcium phosphate from urine. In common with other biological phosphatic structures, calcium phosphate occurs usually in renal calculi as the mineral apatite. However, in a small percentage of cases it also occurs as the mineral brushite.

It is well known that the crystalline structure of calcium phosphate is related to *p*H of the solution, and it is generally considered that brushite is unstable above *p*H 6.2, converting to apatite at higher *p*H levels. However, in a previous communication,[3] it was shown that in urine saturated with calcium phosphate by the addition of sodium hydroxide, and in urine specimens which were saturated with calcium phosphate without alteration, the precipitates were composed of pure brushite up to a *p*H of 6.61 and pure apatite above this *p*H level. However, in urine specimens saturated with calcium phosphate by the addition of sodium phosphate, the precipitates consisted of crystalline brushite up to *p*H 6.93. The average Ca/P ratio in urine is 3/20, whereas in the specimens to which sodium phosphate was added, the Ca/P ratios were considerably smaller. The specimen in equilibrium with brushite at *p*H 6.93 had a Ca/P ratio of 3/1000. These observations suggested that the initial Ca/P ratio in the parent solutions might have considerable effect upon the crystalline structure of calcium phosphate precipitated from aqueous solution and urine. Although Neuman and Neuman[4] have stated that the initial Ca/P ratio in solution is a factor which affects the crystalline structure of the precipitate at equilibrium, a review of the literature has indicated that little attention has been paid to this aspect of the chemistry of calcium phosphate.

In a saturated solution of calcium phosphate both the solubility and the crystalline structure of the precipitate are affected by *p*H of the solutions. As shown by Hodge[5] who compared the data from a number of investigators, there is a linear relationship between *p*H of the solution and the molar solubility of calcium. Other observers have shown that *p*H of the solution affects the structure of the crystalline precipitate. In 1925 Holt, La Mer and Chown[6] and later Dallemagne and Melon,[7] and Hodge[8] showed that calcium phosphate crystallizes from a saturated solution as secondary calcium phosphate (brushite) below *p*H 6.2, and as tertiary calcium phosphate (apatite) above *p*H 6.2 when phosphoric acid is titrated with calcium hydroxide. More recently, by means of precipitation and dissolution experiments, Strates, Neuman and Levinskas[9] have shown that brushite is stable at *p*H 6.2

(1) Aided by a grant from the National Foundation for Infantile Paralysis, Inc.

(2) In this paper, the "Ca/P ratio" refers to the initial molar Ca/P ratio in solution.

(3) J. S. Elliot, W. L. Quaide, R. F. Sharp and L. Lewis, *J. Urol.*, **80**, 269 (1958).

(4) W. F. Neuman and M. W. Neuman, *Chem. Revs.*, **53**, 1 (1953).

(5) H. C. Hodge, "Some Considerations of the Solubility of Calcium Phosphate," Conference on Metabolic Interrelations, Transactions of the Third Conference, p. 190, 1951. The Josiah Macy, Jr. Foundation.

(6) L. E. Holt, Jr., V. E. La Mer and H. B. Chown, *J. Biol. Chem.*, **64**, 509 (1925).

(7) M. J. Dallemagne and J. Melon, *Bull. Soc. Chim. Biol.* **28**, 566 (1946).

(8) H. C. Hodge, "Some Observations of the Dynamics of Calcification," Conference on Metabolic Interrelations, Transactions of the Second Conference, p. 73, 1950. The Josiah Macy, Jr., Foundation.

(9) B. W. Strates, W. F. Neuman and G. J. Levinskas, THIS JOURNAL, **61**, 279 (1957).

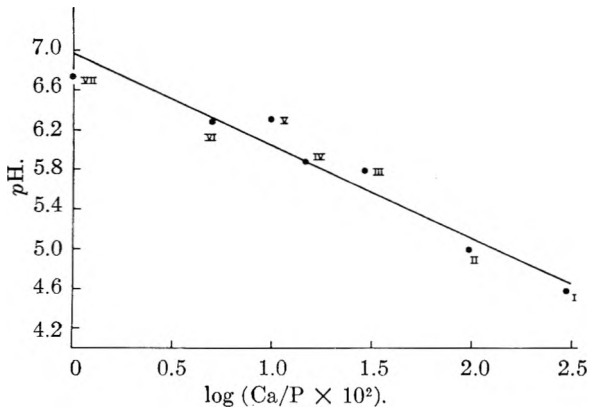

Fig. 1.—Relationship between Ca/P ratio and maximum *p*H at which brushite is found as a single crystalline phase. Roman numerals refer to solution series listed in Table I.

or lower, and at *p*H 6.9 it hydrolyzes rapidly to apatite. In 1947 Melon and Dallemagne[10] studied the solid phase at equilibrium in mixtures of calcium hydroxide and phosphoric acid. In their experiments, brushite did not exist as a stable phase above a *p*H of 6.0. They observed a linear relationship between initial [P] and final *p*H in those samples which contained pure brushite. Brushite was found over a *p*H range from 2.2 to 6.0 with the *p*H increasing as the initial [P] decreased from 0.270 mole/liter to 2.5×10^{-3} mole/liter. The molar Ca/P ratio varied from 0.45 to 0.95 and the ionic strength varied over a wide range. It should be noted that the molar Ca/P ratio in all previously reported investigations did not vary greatly from unity.

Experimental

Seven stock solutions of calcium phosphate were prepared which contained initial molar Ca/P ratios ranging from 3/1 to 1/100. The ionic strength was adjusted to 0.32 (approximating that of normal urine) by added sodium chloride. The initial *p*H of all solutions was 4.3 and no solid phase was present. Varying amounts of carbonate-free sodium hydroxide were added to 100-ml. aliquots of the stock solution in glass stoppered volumetric flasks. The solutions were preserved with toluene. The flasks were incubated at 38° for one week with daily shaking. The contents of the flasks then were filtered at 38° under toluene through Whatman #50 filter paper. The *p*H of each filtrate was determined anaerobically at 38° with the Beckman blood electrode assembly and the Beckman model GS *p*H meter. Beckman buffer standards of *p*H 4.03 and 6.97 at 38° were employed. Precipitates were washed once with 25.0 ml. of distilled water and dried overnight at 38°. Weighing of the dried precipitates indicated that the solid to solution ratios varied from 5.0 to 70.0 mg. with an average of 40.0 mg. per 100 ml. of solution. The composition of the precipitates was determined by examination under polarized light and by X-ray diffraction analysis.[11] Percentage composition of precipitates containing more than one solid phase was estimated by comparison of the X-ray powder patterns with those of known composition. The percentages so determined are considered over all to be accurate to ±10%. In the case of mixtures containing less than 25% brushite, the percentage error is of the order of ±5%.

(10) J. Melon and M. J. Dallemagne, *Bull. soc. chim. Belg.*, **56**, 180 (1947).

(11) Optical and X-ray diffraction analyses were performed by Dr. W. L. Quaide of the Department of Geology, University of California, Berkeley, California.

Observations

Data relating the initial composition of the solutions, the final *p*H and the nature of the solid phase are given in Table I. Examination of this material will show that apatite occurred as a solid phase over a *p*H range of 4.78 to 6.81, and brushite occurred over a *p*H range of 4.31 to 6.74. Further, it is apparent that the maximum *p*H at which brushite is the single crystalline solid increases with a decreasing Ca/P ratio. In Fig. 1 the value, log ([Ca]/[P] × 10²), has been plotted against the maximum *p*H at which pure brushite was found in each of the seven series of solutions. An equation for the regression line was calculated to be: $pH = -0.912 \log ([Ca]/[P] \times 10^2) + 6.95$ with a correlation coefficient of −0.981, indicating essentially a straight line relationship.

TABLE I

RELATIONSHIP BETWEEN COMPOSITION OF THE SOLID PHASE AND THE FINAL *p*H AT VARYING Ca/P RATIOS

Sample no.	(Ca), moles/l. × 10^{-3}	(P), moles/l. × 10^{-3}	Ca/P	*p*H	Compn. of solid phase, % Brushite	Apatite
I-1	60.0	2.00	3/1	4.31	100	
2				4.58	100	
3				4.78	40	60
II-1	20.0	2.00	1/1	4.92	100	
2				5.00	100	
3				5.01	50	50
4				5.08	35	65
5				5.18	40	60
6				5.31		100
III-1	6.00	2.00	3/10	5.72	100	
2				5.79	100	
3				5.83		100
IV-1	6.00	4.00	3/20	5.41	100	
2				5.88	100	
3				5.91	35	65
4				6.03		100
5				6.16		100
V-1	3.00	3.00	1/10	6.22	100	
2				6.30	100	
3				6.50	10	90
4				6.61		100
VI-1	3.00	6.00	1/20	6.21	100	
2				6.28	100	
3				6.41		100
4				6.58		100
VII-1	1.50	15.0	1/100	6.50	100	
2				6.74	100	
3				6.81		100

Summary.—In salt solutions saturated with calcium phosphate having an ionic strength of 0.32, and allowed to equilibrate at 38° for one week, the precipitates were composed of pure brushite over a *p*H range of 4.58 to 6.74. The maximum *p*H at which brushite is stable is a function of the initial molar Ca/P ratio in the solution. The "conversion *p*H" of brushite to apatite increases with a decreasing Ca/P ratio.

SURFACE ACTIVITY OF FLUORINATED ORGANIC COMPOUNDS AT ORGANIC LIQUID–AIR INTERFACES. I. SURFACE TENSION, PARACHOR AND SPREADABILITY[1]

BY N. LYNN JARVIS[2] AND W. A. ZISMAN

U. S. Naval Research Laboratory, Washington 25, D. C.

Received November 1, 1958

A variety of fluorinated compounds, liquids at 20°, were investigated for surface activity at organic liquid–air interfaces. The majority of the compounds had one or more fluorocarbon chains, of varying molecular weights, attached to the hydrocarbon portion of the molecule by an ester, ether or silicate linkage. The surface activity of these fluorinated compounds on a given substrate can be determined to a first approximation by their spreading behavior on that substrate. Their ability to spread upon the following organic liquids was investigated: double end blocked polypropylene oxide, *n*-hexadecane, mineral oil, bis-(2-ethylhexyl)-sebacate, squalene, nitromethane, 1,2-dibromoethylbenzene, 1-methylnaphthalene, tricresyl phosphate, phenoxy bis-(*o*-chlorophenoxy)-phosphate, propylene carbonate and trichlorobiphenyl. Spreadability was thus observed on liquids having a wide range of surface tensions and different surface compositions. Surface tensions and densities were measured for series of fluoroörganosilanes, perfluoroalkanes, fluoroesters and miscellaneous fluorinated compounds. Their molecular parachors and the atomic parachor of fluorine were calculated, the value for fluorine being 22.5. Surface tensions reported for each surface-active agent and substrate liquid were obtained by the pendant drop method. Spreadability of the surface active compounds upon each liquid substrate studied was more pronounced the greater the differences between their surface tensions and that of the substrate. A qualitative discussion is given of the relationship between the molecular structures of the various compounds and their ability to spread on organic liquids. It is shown that for high spreadability at the organic liquid–air interface, the compound must have an amphipathic structure with both organophobic and organophilic groups in the molecule.

Introduction

During recent years increasing interest has been shown in the behavior of surface active agents at organic liquid–air interfaces. Many of the original studies were made of compounds that had proven effective surface active agents in aqueous solutions. McBain and Perry[3] showed that low concentrations of laurylsulfonic acids are able to lower the surface tensions of a group of hydrocarbons. Jones and Saunders[4] measured the surface tensions of a series of *n*-aliphatic acids in nitromethane, and Kaminski[5] observed the adsorption of lauric acid and lauryl alcohol at the mineral oil–air interface using the McBain microtome technique.

Many silicones and fluorochemicals are remarkably surface active in organic liquids. Banks[6,7] reported the formation of stable polydimethylsiloxane films on oleic acid, olive oil, triacetin and ethylene glycol, and Ellison and Zisman[8,9] demonstrated with an all-Teflon film balance the monomolecular nature of films of the linear polymethylsiloxanes and certain perfluorocarbon derivatives adsorbed on mineral oil, *n*-hexadecane and tricresyl phosphate. Other silicones, as well as various polyacrylates, polyalkylene ethers, organosilanes and the protein zein also were shown to be surface active on certain organic substrates. Scholberg, Guenthner and Coon[10] found that certain fluorocarbon derivatives, which were surface active agents in water, also lowered the surface tensions of organic substances more than any other agent ever reported before.

Many classes of compounds are now being specifically synthesized to exhibit surface activity in organic substrates. Blake, Ahlbrecht and Bryce[11] reported a series of polyfluoroquaternary ammonium compounds that in small concentrations reduced the surface tension of selected organic substrates. O'Rear and Zisman[12] and O'Rear, *et al.*,[13] described the synthesis and physical properties of the partially fluorinated esters and ethers, and Ellison and Zisman[14] reported the surface activity of several of these fluoro compounds in *n*-hexadecane and certain chlorinated hydrocarbons. Biswell, *et al.*,[15] investigated a series of polymers containing basic nitrogen substituents which were claimed surface active in hydrocarbon systems.

We report here the surface activity of many new liquid fluorochemicals with respect to a variety of organic substrates, the temperature being held at 20 ± 0.2°. Each compound contains one or more fluorocarbon chains of varying length somewhere in the molecule. The substrate liquids selected have a wide range of surface tensions and surface compositions. Each fluorine-containing compound was examined qualitatively for its ability to spread on a given substrate, as indicated by pushing Teflon indicator powder[8] toward the tray wall. The spreading behavior can be predicted by the well known equation for the initial spreading coefficient.

(1) Presented at "Symposium on Surface Chemical Properties of Fluorochemicals," 134th Meeting of the American Chemical Society, Chicago, Illinois, Sept. 11, 1958.

(2) National Research Council Postdoctoral Fellow.

(3) M. E. L. McBain and L. H. Perry, *J. Am. Chem. Soc.*, **62**, 989 (1940).

(4) D. C. Jones and L. Saunders, *J. Chem. Soc.*, 2944 (1951).

(5) A. Kaminski, "Properties of Surfaces," Nöori-154-T.O. 11, Stanford Research Institute Report, January 12, 1948.

(6) W. H. Banks, *Nature*, **174**, 365 (1954).

(7) W. H. Banks, "Proceedings of the Second International Congress of Surface Activity," Vol. I, Academic Press Inc., New York, N. Y., 1957, p. 16.

(8) A. H. Ellison and W. A. Zisman, THIS JOURNAL, **60**, 416 (1956).

(9) A. H. Ellison and W. A. Zisman, *ibid.*, **59**, 1233 (1955).

(10) H. M. Scholberg, R. A. Guenthner and R. I. Coon, *ibid.*, **57**, 923 (1953).

(11) G. B. Blake, A. H. Ahlbrecht and H. G. Bryce, Am. Chem. Soc., Div. Petrol. Chem., Gen. Papers, No. 32, 131–42 (1954).

(12) J. G. O'Rear and W. A. Zisman, U. S. Patent 2,824,141 (Feb. 18, 1958).

(13) P. D. Faurote, C. M. Murphy, C. M. Henderson, J. G. O'Rear and H. Ravner, *Ind. Eng. Chem.*, **48**, No. 3, 445 (1956).

(14) A. H. Ellison and W. A. Zisman, "Adsorption of Soluble Fluorocarbon Derivatives at the Organic Liquid/Air Interface," Presented at the "Symposium on Surface Chemical Properties of Fluorochemicals," 134th A.C.S. Meeting, Chicago, Ill., Sept. 9, 1958. To be submitted to THIS JOURNAL for publication.

(15) C. B. Biswell, W. E. Catlin, J. F. Fronig and G. B. Robbins, *Ind. Eng. Chem.*, **47**, 1598 (1955).

$$S_{b/a} = \gamma_a - (\gamma_b + \gamma_{ab})$$

where $S_{b/a}$ is the spreading coefficient of liquid "b" upon liquid "a," γ_a is the surface tension of the substrate liquid "a," γ_b is the surface tension of liquid "b" and γ_{ab} is the interfacial tension between "a" and "b." This equation for the initial spreading coefficient may be used in Harkins' well known equivalent form[16]

$$S_{b/a} = W_A - W_C$$

where

$$W_A = \gamma_a + \gamma_b - \gamma_{ab}$$
$$W_C = 2\gamma_b$$

From past studies of surface activity in aqueous solutions, it appears that the ability of a compound to spread on water is a necessary but not sufficient test for surface activity. We can expect the same situation in surveying the surface activity of fluorinated liquids on organic substrates. Further discussion of this point will be deferred to Part II.

Experimental

Materials.—A series of twelve organic liquids covering the ordinary range of surface tensions were selected for use as substrates in this investigation. The mineral oil was U.S.P. grade, light, liquid petrolatum distributed by the Crystal Soap and Chemical Company, Incorporated. *n*-Hexadecane, m.p. 16.2–16.3°, was obtained from the Connecticut Hard Rubber Company; it contained small amounts of *n*-tetradecane. A double end-blocked polypropylene oxide, Ucon Fluid DLB 44 E (free from antioxidant), was procured from Carbide and Carbon Chemical Company. Both tricresyl phosphate (80% para and 20% meta) and nitromethane came from Fisher Scientific Company. Aroclor 1248, trichlorobiphenyl, is a product of Monsanto Chemical Company. Propylene carbonate, 1-methylnaphthalene and squalene, an unsaturated acyclic compound, were Eastman "Practical Grade." Phosphen 4 and Alkazene 42, commercial preparations with average compositions of phenoxy bis-(*o*-chlorophenoxy)-phosphate, and 1,2-dibromoethylbenzene, respectively, are products of Dow Chemical Company. The bis-(2-ethylhexyl)-sebacate used is marketed by Rohm and Haas Company as Plexol 201; it was purified for us by C. M. Murphy of this Laboratory by distillation in a molecular still and was subsequently percolated through an adsorption column containing activated silica and alumina. Squalene, 1-methylnaphthalene, *n*-hexadecane, mineral oil, Ucon DLB 44E, Alkazene 42 and Aroclor 1248 also were freed from polar impurities by slowly passing each through columns of activated silica and alumina. Propylene carbonate and nitromethane were percolated through activated "Florisil" and alumina to remove polar impurities. Tricresyl phosphate and Phosphen 4 were used as received.

Fluorine-containing compounds investigated for surface activity were esters of mono-, di- and tri-carboxylic acids, organosilanes and perfluoroalkanes and their monochloro derivatives. A miscellany of other fluorochemicals investigated included alcohols, phosphates, sulfonates, mercaptans and sulfides. The perfluoroalkanes and their monochloro derivatives were research samples obtained from the Pennsylvania Salt Manufacturing Company and were used as received. Methods of preparing these perfluoroalkanes and many of their physical properties have been reported by Hauptschein, *et al.*[17] They will be designated throughout this paper as follows, in accordance with the nomenclature used by the supplier

$C_3F_7[CF_2CF(CF_3)]_2Cl$	PPCL2
$C_3F_7[CF_2CF(CF_3)]_{3A}Cl$	PPCL3A
$C_3F_7[CF_2CF(CF_3)]_{5A}Cl$	PPCL5A
$C_3F_7[CF_2CF(CF_3)]_{6A}Cl$	PPCL6A
$C_3F_7[CF_2CF(CF_3)]_{3A}F$	PPF3A
$C_3F_7[CF_2CF(CF_3)]_{6A}F$	PPF6A
$\{C_3F_7[CF_2CF(CF_3)]_{2A}\}2$	PPC2A
$\{C_2F_5CF(CF_3)(CH_2CF_2)_{5A}\}2$	BVFC-5

Perfluorokerosene, FCD329, was obtained from du Pont de Nemours & Company. The fluoroörganosilanes and miscellaneous compounds,[18] as well as the remaining fluoroesters and ethers[13,19] were synthesized by J. G. O'Rear and co-workers in this Laboratory. These fluorine-containing surface active compounds were carefully prepared, and nearly all were used as received. Selected physical constants for the fluorochemical surface active agents are given in the 3rd, 4th and 5th columns as well as in the 2nd row of Tables I, II and III.

An abbreviated system of nomenclature adopted by Murphy, *et al.*,[13] will be used here for naming the partially fluorinated compounds. The abbreviations used are

$F(CF_2)_nCOOH$	ϕ-acid
$H(CF_2)_nCOOH$	ψ-acid
$F(CF_2)_nCH_2OH$	ϕ'-alcohol
$H(CF_2)_nCH_2OH$	ψ'-alcohol

This system is extended to the remaining fluorochemicals.

Methods.—Surface tensions of the substrate liquids and surface active agents were measured at 20° using the pendant drop method, following essentially the procedure outlined by Andreas, Hauser and Tucker[20] and using the correction tables compiled by Fordham.[21] Results were reproducible to within approximately ±0.1 dyne/cm. and were shown to be accurate to 2% by calibration measurements on liquids of known surface tensions. Due to their rarity and the small quantities available, most of the fluoro compounds were used as received; hence, several may contain trace impurities. Unless the impurities are fluorinated compounds, it is unlikely they will give rise to significant errors in surface tensions. Density measurements were made at 20° by weighing a known volume of the fluorinated compound as delivered from a calibrated micrometer syringe. With this method a precision of ±0.005 g./cc. was obtained. The resulting surface tensions and densities are recorded in Tables I–III and were used to calculate the parachors listed in the same tables.

To determine the spreadability of each fluorochemical, the substrate liquid was placed in a clean, shallow, glass dish 1.5 inches in diameter. Fine Teflon powder was sprinkled over the surface to serve as an "indicator powder." A small drop of the fluorochemical on the tip of a clean platinum wire was touched to the center of the liquid surface. If the droplet spread over the surface of the substrate moving the Teflon powder to the container wall, the fluorochemical was considered a potential surface-active agent. The relative stability of the spread film could be estimated from the duration of time the Teflon powder indicated a spreading pressure was being exerted upon it. After each spreading test the substrate was discarded and the dish was acid-cleaned before being used again. Results of these experiments are summarized in Tables I–III where an "0" in the table indicates no spreading occurred, "S" denotes spreading was observed and "I" denotes comparative film insolubility because a positive spreading pressure was maintained for several minutes. Compounds observed are listed in the tables in the order of increasing surface tension.

Results

The compounds that exhibited large spreading coefficients on various of the organic liquids and formed stable films, always contained organophilic as well as organophobic groups in the molecule. The effectiveness of any group as an organophilic or organophobic constituent in a compound will obviously vary with the chemical and physical properties of the organic substrate being investigated. The surface activity of a compound in organic liq-

(16) W. D. Harkins, "The Physical Chemistry of Surface Films," Reinhold Publ. Corp., New York, N. Y., 1952, p. 97.

(17) M. Hauptschein, M. Braid and F. E. Lawlor, *J. Am. Chem. Soc.*, **79**, 2549 (1957).

(18) J. G. O'Rear, Naval Research Laboratory, private communication.

(19) P. D. Faurote and J. G. O'Rear, *J. Am. Chem. Soc.*, **78**, 4999 (1956).

(20) J. M. Andreas, E. A. Hauser and W. B. Tucker, THIS JOURNAL, **42**, 1001 (1938).

(21) S. Fordham, *Proc. Roy. Soc. (London)*, **194**, 1 (1948).

TABLE I

PHYSICAL PROPERTIES OF FLUORINATED CARBOXYLIC ESTERS AND THEIR SPREADABILITY ON ORGANIC LIQUIDS[a]

Compound	F/H Ratio	F atomic parachor	Density at 20° (g./ml.)	Surface tension at 20° (dynes/cm.)	Ucon DLB 44 E 23.0	*n*-Hexadecane 27.3	Mineral oil (white) 29.9	Bis-(2-ethylhexyl)-sebacate 30.1	Squalene 31.4	Nitromethane 35.9	Alkazone 42 38.3	1-Methylnaphthalene 38.4	Tricresyl phosphate 40.4	Propylene carbonate 41.0	Phosphen 4 43.5	Aroclor 1248 43.7
Carboxylic esters																
Butyl ϕ-caprylate	1.67	21.7	1.526	18.7	S	S	S I	S	S	S	S I	S	S	S	S	S I
Hexyl ϕ-butyrate[b]	0.54	23.6	1.231	19.2	S	S	S	S	S	S	S	S	S	S	S	S
Bis-(ϕ'-octyl)-3-methylglutarate[b]	2.50	21.5	1.689	19.5	0	S I	S I	S I	S I	S I	S I	S I	S I	S I	S I	S I
Bis-(ϕ'-hexyl)-3-methylglutarate[b]	1.83	23.6	1.539	19.7	S	S	S I	S	S I	S	S I	S	S I	S	S I	S I
Bis-(ϕ'-butyl)-adipate	1.17	21.8	1.504	20.7	0	S	S	S	S	S	S	S	S	S	S I	S I
1,2,3-Trimethylolpropane tris-(ϕ-butyrate)[b]	1.91	22.3	1.614	21.4	0	S	S I	S	S I	S	S I	S	S I	S	S I	S I
1,6-Hexanediol bis-(ϕ-butyrate)	1.17	23.1	1.480	21.5	0	S	S I	S	S I	S	S I	S	S I	S	S I	S I
1,10-Decanediol bis-(ϕ-butyrate)[b]	0.70	23.6	1.359	23.0	0	S	S	S	S	S	S	S	S I	S	S I	S I
ψ'-Nonyl-2-ethylhexanoate	0.89	23.0	1.438	23.1	0	S	S	S	S	S	S	S	S I	S	S I	S I
Bis-(ψ'-nonyl)-3-methyl 2-ethylglutarate	1.78	22.0	1.666	23.2	0	0	S	S	S	S	S I	S	S	S	S I	S I
Tris-(ψ'-amyl)-hemimellitate	2.00	20.6	1.699	24.3	0	0	0	S	S	S	S I	S	S I	S	S I	S I
Bis-(ψ'-nonyl)-3-*t*-butyl adipate	1.45	22.6	1.624	24.9	0	0	0	S	S I	S	S	S	S	S	S I	S I
Bis-(ψ'-heptyl)-phenyl succinate	1.71	21.5	1.652	25.0	0	0	0	S	S	S	S	S	S	S	S	S I
Bis-(ψ'-nonyl)-3-methylglutarate[b]	2.29	23.1	1.714	25.0	0	0	0	S	S	S	S I	S I	S I	S	S I	S I
n-Octadecyl ϕ-butyrate[b]	0.19	23.4	1.056	25.1	0	S	S	S	S	S	S I	S	S I	S	S I	S I
Bis-(ψ'-isohexyl)-adipate	1.43	25.7	1.512	25.6	0	0	0	S	S	S	S	S	S	S	S	S I
Bis-(ψ'-heptyl)-3-methylglutarate[b]	1.71	23.1	1.648	25.6	0	0	0	S	0	S I	S I	S	S	S	S I	S I
Bis-(ψ'-heptyl)-adipate[b]	1.71	23.2	1.652	26.1	0	0	0	S	0	S	S I	S	S I	S	S I	S I
Bis-(ψ'-heptyl)-2-phenylglutarate	1.50	21.2	1.654	26.2	0	0	0	S	S	S	S	S	S	S	S I	S I
ψ'-Heptylhydrogen 3-methylglutarate	1.09	23.3	1.557	26.4	0	0	0	S	S I	S	S	S	S	S	S	S I
Bis-(ψ'-amyl)-3-methylglutarate[b]	1.14	23.3	1.557	26.8	0	0	0	S	0	S	S I	S	S	S	S	S I
Tris-(ψ'-amyl)-benzene 1,2,3-tricarboxylate[b]	5.00	24.6	1.730	26.9	0	0	0	S	0	S	S	S	S	S I	S I	S I
Tris-(ψ'-amyl)-tricarballylate	1.71	22.8	1.680	27.2	0	0	0	S	0	S	S I	S	S	S	S	S I

TABLE I (*Continued*)

Compound	F/H Ratio	F atomic parachor	Density at 20° (g./ml.)	Surface tension at 20° (dynes/cm.)	Ucon DLB 44 E 23.0	*n*-Hexadecane 27.3	Mineral oil (white) 29.9	Bis-(2-ethylhexyl)-sebacate 30.1	Squalene 31.4	Nitromethane 35.9	Alkazene 42 38.3	1-Methylnaphthalene 38.4	Tricresyl phosphate 40.4	Propylene carbonate 41.0	Phosphen 4 43.5	Aroclor 1248 43.7
Bis-(ψ'-amyl)-glutarate[b]	1.33	23.5	1.598	27.5	0	0	0	S	0	S	S	S	S	S	S	S
Bis-(ψ'-amyl)-adipate[b]	1.14	23.6	1.561	27.7	0	0	0	S	0	S	S	S	S I	S	S I	S I
Bis-(ψ'-propyl)-3-methyl-glutarate	0.57	22.0	1.432	29.4	0	0	0	S	0	S	S	S	S	S	S	S
Bis-(ψ'-amyl)-phthalate[b]	1.60	22.5	1.624	28.0	0	0	0	S	0	S	S I	S	S I	S	S I	S I
Bis-(ψ'-amyl)-sebacate[b]	1.71	23.2	1.652	28.2	0	0	0	S	0	S	S	S	S	S	S	S I
Bis-(ψ'-amyl)-diphenate	1.14	21.2	1.555	28.4	0	0	0	S	S	S	S	S	S	S	S	S I
Tris-(ψ'-propyl)-tricarballylate	0.86	21.8	1.560	29.6	0	0	0	0	0	S	S I	S	S	S	S I	S I
Bis-(ψ'-propyl)-diphenate	0.57	19.6	1.431	31.1	0	0	0	0	0	0	S	S	S	S	S	S

[a] "0" indicates no spreading was observed; "S" denotes spreading; "I" denotes formation of insoluble stable film. [b] The surface tensions for the starred compounds were determined by Ellison and Zisman,[13] and their densities by Faurote, *et al.*[18]

TABLE II

PHYSICAL PROPERTIES OF FLUORINATED ORGANOSILANES AND ALKANES AND THEIR SPREADABILITY ON ORGANIC LIQUIDS

Compound	F/H Ratio	F atomic parachor	Density at 20° (g./ml.)	Surface tension at 20° (dynes/cm.)	Ucon DLB 44 E 23.0	*n*-Hexadecane 27.3	Mineral oil (white) 29.9	Bis-(2-ethylhexyl)-sebacate 30.1	Squalene 31.4	Nitromethane 35.9	Alkazene 42 38.3	1-Methylnaphthalene 38.4	Tricresyl phosphate 40.4	Propylene carbonate 41.0	Phosphen 4 43.5	Aroclor 1248 43.7
Organosilanes																
Bis-(*t*-butoxy)-bis-(ϕ'-oxtoxy)-silane	1.36	21.7	1.525	18.4	S	S	S I	S	S I	S I	S I	S I	S I	S I	S I	S I
Bis-(*t*-butoxy)-bis-(ψ'-heptoxy)-silane	1.00	22.5	1.474	20.8	0	S	S	S	S	S	S	S	S I	S	S I	S I
Tetrakis-(1-methyl-ψ'-pentoxy)-silane	1.60	22.3	1.637	22.6	0	0	0	S	S I	S	S	S	S	S	S I	S I
Bis-(1,1-dimethyl-ψ'-propoxy)-bis-(ψ'-heptoxy)-silane	1.45	21.1	1.649	22.7	0	0	0	S	S I	S	S	S	S	S	S I	S I
Tetrakis-(1-trifluoromethyl-heptoxy)-silane	0.20	22.1	1.089	23.0	0	S	S	S	S	S	S	S	S I	S	S I	S I
Tetrakis-(ψ'-pentoxy)-silane	2.67	23.8	1.732	24.6	0	0	0	S	S	S	S	S	S	S	S	S
Perfluoroalkanes																
PPCL2 (volatile)	∞	21.9	1.915	15.1	S	S	S	S	S	S	S	S	S	S	S	S
PPF3A (volatile)	∞	22.0	1.992	16.3	S	S	S	S	S	S	S	S	S	S	S	S
Perfluorokerosene (volatile)	∞	22.5	1.960	16.9	S	S	S	S	S	S	S	S	S	S	S	S
PPCL3A (volatile)	∞	21.7	1.916	17.6	0	S	S	S	S	S	S	S	S	S	S	S
PPF6A	∞	22.3	1.920	17.7	0	0	S	S	S	S	S	S	S	S	S	S
PPCL5A	∞	22.2	1.919	18.4	0	S	S I	S I	S I	S I	S I	S I	S I	S I	S I	S I
PPC2A	∞	21.6	1.996	18.5	0	S	S I	S I	S I	S	S I	S I	S I	S I	S I	S I
BVFC-5	1.90	20.5	1.780	23.6	0	0	0	S	S I	S	S I	S I	S I	S I	S I	S I
PPCL6A (very viscous)	Too viscous				0	0	0	S	S	0	S	S	S	S	S	S

TABLE III

PHYSICAL PROPERTIES OF MISCELLANEOUS FLUORINATED COMPOUNDS AND THEIR SPREADABILITY ON ORGANIC LIQUIDS

Compound	F/H Ratio	F atomic parachor	Density at 20° (g./l.)	Surface tension at 20° (dynes/cm.)	Ucon DLB 44 E 23.0	n-Hexadecane 27.3	Mineral oil (white) 29.9	Bis-(2-ethylhexyl)-sebacate 30.1	Squalene 31.4	Nitromethane 35.9	Alkazene 42 38.3	1-Methylnaphthalene 38.4	Tricresyl phosphate 40.4	Propylene carbonate 41.0	Phosphon 4 43.5	Aroclor 1248 43.7
Miscellaneous																
ϕ'-Octyl chloride	4.67	21.9	1.700	16.9	S	S	S	S	S	S	S	S	S	S	S	S
ϕ'-Octyl alcohol	5.00	22.8	1.734	17.5	S	S	S	S	S	S	S	S	S	S	S	S I
ψ'-Heptyl mercaptan	3.00	23.2	1.663	21.6	0	S	S	S	S	S	S	S	S	S	S	S
Tris-(ω'-amyl)-phosphate	2.67	22.5	1.772	25.0	0	0	0	S	S I	S	S I	S I	S	S	S I	S I
Bis-(ψ'-heptoxyethyl)-sulfide	1.71	23.0	1.653	25.0	0	0	0	S	S	S	S	S	S	S	S	S I
ψ'-Heptyl alcohol	3.00	24.4	1.728	25.2	0	0	0	S	S	S	S	S	S	S	S	S
Bis-(ψ'-heptoxy)-hexane	1.33	23.6	1.578	25.5	0	0	0	S	S	S	S	S	S I	S	S	S I
ψ'-Heptylethane sulfonate	1.50	22.0	1.678	25.9	0	0	0	S	0	S	S	S	S	S	S	S
ψ'-Heptyl mesylate	2.00	22.5	1.741	26.1	0	0	0	S I	0	S	S I	S I	S	S	S I	S I
Bis-(ψ'-heptoxy)-diglycol	2.40	22.3	1.468	26.5	0	0	0	S	S	S	S I	S	S	S	S I	S I

uids is thus dependent upon the nature of the liquid substrate. This is made evident by the data in Tables I–III which give the qualitative spreading behavior of the various compounds observed on a variety of organic substrates. Certain relationships can be identified between the chemical constitutions of the substrates and surface active agents and their spreading behavior; these are discussed below by class of spreading compound.

Fluorinated Carboxylic Esters.—The esters investigated were derived primarily from mono-, di- or tricarboxylic acids treated with one of several fluorinated alcohols. A few are the products of fluorinated acids and non-fluorinated alcohols. Whereas the hydrocarbon portions of the esters are organophilic, the highly fluorinated portions are organophobic. The carboxyl group will be organophobic in hydrocarbons but may be organophilic in polar liquids depending on the presence of active groups with which it may associate. Our data show that surface activity results whenever the fluorine substitution for hydrogen in the esters becomes sufficient to cause the outermost portions of the adsorbed phase of the liquid to be rich in fluorine atoms; in this way the surface tension of the solution becomes less than that of the pure substrate liquid. Table I reveals that spreadability increases with the difference in surface tensions of the surface active agent and substrate. As the fluorine/hydrogen *atomic* ratio of a compound increases, its solubility in the substrate liquid decreases, reducing its spreadability even when there is a large difference between its surface tension and that of the substrate.

As expected, derivatives of ϕ'-alcohols or ϕ-acids were much more effective than the corresponding ψ- and ψ'-compounds in reducing the surface tensions of the esters; hence, they had greater spreadability. For example, the surface tensions of the 3-methylglutarates derived from ψ'-alcohols are about 5 dynes/cm. higher at 20° than those of the corresponding ϕ'-alcohol derivatives. Evidently, this difference results because the terminal hydrogen of the ψ'-derivative increases the surface tension of the ester or ether.

Of the liquid fluoroesters investigated with an F/H ratio between 0.50 and 5.00, only those with surface tensions of 19.7 dynes/cm. or less gave evidence of spreading on the surface of the Ucon fluid. This behavior is similar to the spreading of organic liquids on solids investigated by Fox, Hare and Zisman.[22] By analogy with their work, that surface tension below which the fluoroesters begin to spread on the substrate may be called the critical surface tension, γ_c, of the substrate, with respect to the family of fluoroesters. The critical surface tension of a solid can be determined more precisely because contact angle measurements can be used and the surface tension varied until the angle approaches zero. When the spreading liquid is viscous and the spreading coefficient small, the contact angle is easily measured, whereas spreading may not be observed during a short time of observation, which may lead to low values for γ_c.

(22) H. W. Fox, E. F. Hare and W. A. Zisman, THIS JOURNAL, **59**, 1097 (1955).

Fluoroester liquids on Ucon fluids were observed to have values of γ_c somewhere between 19.7 dyne/cm. where spreading occurred, and 20.7 dynes/cm. where spreading did not. We will estimate γ_c as midway between these two values, *i.e.*, $\gamma_c \cong 20.2$ dynes/cm. Substituting the surface tension of 23.0 dynes/cm. of Ucon fluid for γ_a and γ_c for γ_b in the equation for the initial spreading coefficient and equating $S_{b/a}$ to zero, an approximate value of γ_{ab}, the interfacial tension, can be calculated; this is given in the last row of Table IV. This method of determining the critical surface tension assumes that all spreading compounds having the same general structure will give approximately the same critical surface tension when spread on a given substrate. Because the value of the interfacial tension calculated here is for an interface at which little mixing has taken place, it is really the initial interfacial tension; hence, it would be expected to be higher than that determined under equilibrium conditions. Critical surface tensions and approximate values of the initial interfacial tensions were also estimated from the data of Table I for fluoroesters on mineral oil, *n*-hexadecane, bis-(2-ethylhexyl)-sebacate and squalene. On liquids with surface tensions of 35.9 dynes/cm. or greater, all of the fluorinated compounds investigated spread vigorously; therefore, critical surface tensions could not be calculated for these substrates.

TABLE IV

APPROXIMATE INITIAL INTERFACIAL TENSION OF FLUOROESTER/ORGANIC SUBSTRATE INTERFACE (DATA AT 20°)

	Substrate		
Substrate liquid	Surface tension γ_a (dynes/cm.)	Critical surface tension γ_c (dynes/cm.)	Approximate interfacial tension γ_{ab} (dynes/cm.)
Ucon DLB 44 E	23.0	20.2	2.8
n-Hexadecane	27.3	23.1	4.2
Mineral oil	29.9	23.8	6.1
Bis-(2-ethylhexyl)-sebacate	30.1	29.0	1.1
Squalene	31.4	26.7	4.7

Initial interfacial tensions of the fluoroesters with Ucon DLB 44 E and bis-(2-ethylhexyl)-sebacate were appreciably lower than with the other organic substrates. This is to be expected as these liquids contain ether and ester groups, respectively, which should associate to some extent with the fluoroesters studied. *n*-Hexadecane, white mineral oil and squalene exhibited higher initial interfacial tensions since they do not contain associating or solubilizing groups. As could be expected by extending Pound's rule[23] to non-aqueous systems, the interfacial tensions are in the inverse order of the solubilities of the contacting liquids. The accuracy of these approximate interfacial tension values was verified by measuring several interfacial tensions by the pendant drop method. The initial interfacial tension between bis-(ψ'-heptyl)-3-methylglutarate and hexadecane was determined as 5.4 dynes/cm.; this is to be compared with the estimated value of 4.2 dynes/cm. The measured value of bis-(ϕ'-octyl)-3-methylglutarate against mineral oil of 6.6 dynes/cm. is to be compared with the estimate of 6.1 dynes/cm. These values are in fair agreement, the discrepancies being due to the poor sensitivity of the spreadability method used and to the fact that all compounds in each class in Table I do not have exactly the same orientation and packing in the interfacial phase.

Films resulting from spontaneous spreading have stabilities which are a function of the chemical constitutions of both the surface active agent and the substrate liquid. However, film stability observations on several of the substrates were not reliable due to their high viscosities and the subsequent slow movement of the Teflon powder displaced by the spreading agent. However, several general conclusions can be made regarding the relative stabilities of the films after spreading. A majority of the stable fluoroester films observed were formed on only four of the substrates: Aroclor 1248, Phosphen 4, Alkazene 42 and tricresyl phosphate. These substrate liquids are among those having the highest surface tensions. Propylene carbonate and 1-methylnaphthalene act differently, and it is suggested these substrates do not exhibit such stable films due to their greater ability to dissolve the film.

Solubility plays an important part in these systems. The phosphate substrates apparently have less mutual solubility with the fluoroesters than propylene carbonate, nitromethane or bis-(2-ethylhexyl)-sebacate. 1-Methylnaphthalene exhibited roughly the same solubility properties as mineral oil and squalene. Like Ellison and Zisman,[14] we found that the fluoroesters which were surface active on *n*-hexadecane were also quite soluble in it. Fluoroester derivatives of ϕ'-alcohols and ϕ-acids were less soluble than corresponding ψ- and ψ'-compounds. Any increase in the fluorine content of the molecule decreased the solubility of the surface active agent; however, a decrease in the F/H ratio, additional branching of the organophilic portion of the molecule, or the addition of a phenyl group increased the solubility of the fluoroester in the organic substrate. It also was observed that chlorination in the substrate increased the stability of fluoroester films on most substrates.

Fluoroörganosilanes.—Fluorinated organosilanes spread on the surface of each organic liquid only when their surface tensions were considerably lower than that of the substrate. Critical surface tensions and approximate values of the initial interfacial tensions were estimated from the data of Table II for several of the fluoroörganosilane–organic substrate interfaces, and the results are given in Table V. The initial interfacial tensions between fluoroörganosilanes and the substrate liquids were larger than those with the fluoroesters, indicating greater mutual solubility of these three substrates and the fluoroesters.

Ellison and Zisman[8] obtained the interfacial tensions between mineral oil and two of the organosilanes included in this study, bis-(*t*-butoxy)-bis-(ϕ' octoxy)-silane and bis-(*t*-butoxy)-bis-(ψ'-heptoxy)-silane, by measuring the equilibrium spreading pressure using the method of "piston films."

(23) J. R. Pound, THIS JOURNAL, **30**, 791 (1926).

TABLE V

APPROXIMATE INITIAL INTERFACIAL TENSION OF FLUOROÖRGANOSILANE–ORGANIC SUBSTRATE INTERFACE (DATA AT 20°)

Substrate liquids	Substrate: Surface tension γ_s (dynes/cm.)	Substrate: Critical surface tension γ_c (dynes/cm.)	Approximate interfacial tension γ_{sb} (dynes/cm.)
Ucon DLB 44 E	23.0	20.0	3.0
n-Hexadecane	27.3	21.6	5.7
Mineral oil	29.9	22.3	7.6

They obtained values of 3.9 and 4.4 dynes/cm., respectively, agreeing well with the interfacial tension measurements made by the ring method of 4.0 and 4.5 dynes/cm. These values are much lower than that of 7.6 dynes/cm. calculated here for the typical fluoroörganosilane structure against mineral oil. The higher value for the approximate interfacial tension may again be due to the lack of sensitivity of the spreading tests used in this investigation.

Fluoroörganosilane derivatives of ϕ'-alcohols appear to be more surface active than the ψ'-derivatives, and they generally formed more stable films on the substrates investigated. Compounds containing two long fluorocarbon chains in combination with two hydrocarbon chains were more surface active and insoluble than those with four short fluorocarbon chains, even though they had approximately equal F/H ratios. When the percentage of fluorine in the molecule was small, as in tetrakis-(1-trifluoromethylheptoxy)-silane, the compound showed increased organophilic behavior and the surface tension was higher and nearer that of a non-fluorinated organosilane. When the substrate liquids contained phenyl groups and halogen atoms, and hence had higher surface tensions and viscosities, the films were more stable.

Perfluoroalkanes.—Perfluoroalkanes and their monochloro derivatives exhibited some ability to spread on organic substrates, provided the surface tension of the substrate was sufficiently higher than that of the spreading liquid. Critical surface tensions for Ucon fluid, *n*-hexadecane and mineral oil obtained with respect to the perfluoroalkanes, and the approximate interfacial tensions calculated as in the preceding sections, are listed in Table VI. The interfacial tension of PPCL5A on mineral oil was determined by the pendant drop method to be 7.6 dynes/cm., which is to be compared with the estimated valve of 8.8 dynes/cm.

TABLE VI

APPROXIMATE INITIAL INTERFACIAL TENSION OF PERFLUOROALKANE–ORGANIC SUBSTRATE INTERFACE (DATA AT 20°)

Substrate liquids	Substrate: Surface tension γ_s (dynes/cm.)	Substrate: Critical surface tension γ_c (dynes/cm.)	Approximate interfacial tension γ_{sb} (dynes/cm.)
Ucon DLB 44 E	23.0	17.3	5.7
n-Hexadecane	27.3	19.5	7.8
Mineral oil	29.9	18.5	8.8

Interfacial tensions between these substrates and perfluoroalkanes were higher than those of the fluoroörganosilanes or the fluoroesters, presumably because of the lack of organophilic groups in the molecules. The covalent chlorine atoms present in several of the perfluoroalkanes are somewhat organophilic and increase the stability of the films. Compound BVFC-5 has several methylene groups in each molecule which increases its solubility in these organic substrates and stabilizes the films produced. Compound PPC2A, which is completely fluorinated, exhibited surprising stability. This may arise from its somewhat different structure, or perhaps results from the presence of impurities. Fluoroalkanes of low molecular weight such as PPCL[2], PPF3A, perfluorokerosene and PPCL3A are very volatile; hence, their films evaporated soon after spreading. Compound PPF3A and PPCL6A both spread on many organic substrates, but soon after spreading the Teflon powder slowly moved back to cover completely the surface of the liquid substrate.

Miscellaneous Compounds.—A number of other classes of fluorochemicals, each represented by one or two compounds, were spread on the various organic substrates. Among the various reactive groups to which the fluorocarbon chains were attached, *i.e.*, alcohol, sulfonate, chloride, mercaptan, ether, phosphate and sulfide radicals, some were organophobic, depending upon the substrate with which they were in contact. The greater the number of carbon atoms in the fluorocarbon chain, the more effective it was in increasing spreadability and film insolubility. Again the ϕ'-derivatives were more effective spreading agents than the ψ'-derivatives. Because of the small number of compounds in each class that were available for study, few generalizations can be made about the relation of organic structure to surface activity. These experiments do show, however, that each polar group, when combined with a fluorocarbon chain of appropriate organophobicity, is capable of exhibiting spreadability on the surface of many organic liquids. It is apparent that the greater the degree of internal cohesion or bonding between the active groups in a liquid, the greater its surface tension and the less surface active on organic liquids it will be. In short, as Harkins and Feldman concluded many years ago[24] from their work on spreading upon water, spreadability (and the spreading coefficient) will be decreased by any molecular constitutive change which increases the cohesional energy without increasing the adhesional energy.

Parachors.—Molecular parachors were calculated for the fluorinated liquids whose surface tensions and densities are being reported here for the first time. Molecular parachors for these fluorinated compounds calculated using Quayles'[25] or Vogel's[26] tables of atomic parachors were consistently larger than the observed values. This is caused by the rather large value of 26.1 they reported for the atomic parachor of fluorine. Using Vogel's other atomic parachors, the fluorine parachors were calculated for each compound and are given in Tables I–III. The average value for the atomic parachor

(24) W. D. Harkins and A. Feldman, *J. Am. Chem. Soc.*, **44**, 2665 (1922).

(25) O. R. Quayle, *Chem. Revs.*, **53**, 439 (1953).

(26) A. I. Vogel, *J. Chem. Soc.*, 1833 (1948).

of fluorine calculated from our molecular parachors was 22.5. This agrees well with the value of 22.8 obtained at this Laboratory by Faurote, *et al.*,[13] using some of our surface tensions and Vogel's other atomic parachors. If Sugden's atomic parachors[27] are used, the average calculated atomic parachor of fluorine is 24.9. Values for the atomic parachor of fluorine obtained using Quayles' or Vogel's parachor increments show less variation than those determined using Sugden's values. It is concluded that a value of between 22.5 and 22.8 for the fluorine atomic parachor using Vogel's atomic parachors is more precise and accurate than values previously reported for fluorine covalently bonded to carbon.

General Discussion

A large number of fluorinated organic liquids have been shown to spread spontaneously on the surfaces of a number of organic liquids. In each spreading compound studied, the various fluorocarbon chains were the primary organophobic portions of the molecule, while the hydrocarbon groups were organophilic. Increased substitution of fluorine in the organophobic group in a molecule decreases its surface tension and generally increases its spreading coefficient on a given organic substrate. Provided that structural changes do not make the reversible work of cohesion (W_C) begin to increase with respect to the reversible work of adhesion (W_A), the greater the organophobic/organophilic ratio in such a molecule, the greater the spreading coefficient.

It is concluded that the lower the surface tension of the solute compound and the greater that of the organic solvent or substrate, the greater the spreadability and surface activity of the fluorochemical. Spreadability appears to be a necessary but not a sufficient condition for surface activity. Even when the initial spreading coefficient ($S_{b/a}$) is positive, there is no indication of the extent the surface tension of the substrate will be lowered. Usually, as in this study, the term "surface activity" is reserved for those compounds which in small concentrations effect a large reduction in the surface tension of a given substrate or solvent.

In designing a compound to be surface active on an organic liquid, it is desirable to use those organophilic and organophobic radicals or constituents that contribute least to the surface tension and give a low value of W_C and a high value of W_A. Synthesis of new agents using the ϕ'-alcohols and ϕ-acids results in liquids with much lower surface tensions than the corresponding ψ'-alcohols and ψ-acids. Increased branching of either the organophilic or organophobic part of the molecule, or the addition of an aromatic nucleus, will increase its surface tension and its mutual solubility with many organic substrates, but will also tend to decrease the reversible work of cohesion, W_C. Polar groups will be organophilic or organophobic depending upon the reactive groups present in the substrate. They will generally increase the reversible work of cohesion W_C of the compound, increasing its surface tension. It is a useful guide to realize that the depression of the substrate surface tension by solution of the spreading agent will never be greater than the difference between the surface tensions of the substrate and the surface active agent.

On the basis of these experiments on spreading, many of the new compounds described here are promising as surface active agents for organic liquids. Further work on these compounds is needed, however, to determine their efficiency in lowering the surface tension of the various substrates. In addition, the spontaneous spreading of several of the compounds investigated appears to produce insoluble monolayers on various of the organic substrates which would lend themselves to study by means of the all-Teflon film balance.[8,9]

(27) S. Sugden, "The Parachor and Valency," G. Routledge and Sons, Ltd., London, 1930, p. 38.

THE KINETICS OF THE DECOMPOSITION OF ALKALINE SOLUTIONS OF HYPOBROMITE. SPECIFIC IONIC EFFECTS ON REACTION RATE

BY B. PERLMUTTER-HAYMAN AND GABRIEL STEIN

Contribution from the Department of Physical Chemistry, The Hebrew University, Jerusalem, Israel

Received November 10, 1958

The decomposition of hypobromite in sodium hydroxide solution was reinvestigated. The reaction was confirmed to consist of two consecutive second-order reactions and was found to take place exclusively between the anions. The reactions exhibited a positive salt effect. However, no correlation between the ionic strength and the rate constants was found. At a given cation concentration, the effects of salts containing mono-, di- or trivalent anions were almost identical. Among the 8 anions investigated, only the hydroxyl ion has a specific accelerating effect. The effect of monovalent cations is specific and increases from lithium over sodium and potassium to rubidium and cesium. This specificity is more pronounced at higher hydroxyl ion concentrations.

Introduction

The decomposition of hypobromite solutions into bromate and bromide has been the subject of several investigations,[1] and has been shown to proceed *via* bromite as an intermediate.[1,2] For the reaction in alkaline solutions, Chapin[2] found the reaction rate to be at a minimum at *p*H 13.4, and from there to increase steeply with increasing *p*H (in KOH solution). He found the reaction to be of

(1) P. Engel, A. Oplatka and B. Perlmutter-Hayman, *J. Am. Chem. Soc.*, **76**, 2010 (1954), where previous literature is quoted.

(2) R. M. Chapin, *ibid.*, **56**, 2211 (1934).

second order in normal potassium hydroxide solution.

In the present paper further details on the kinetics of the decomposition in alkaline solution are presented. Furthermore, it has been our object to investigate the influence of added ions on the reaction rate.

Experimental

The chemicals used for the preparation of the reaction mixtures were all analytical grade. In most of the experiments a sample of bromine was used which had been purified locally. Checks were carried out with bromine samples from other sources, and gave identical results. Triply distilled water was used.

The reaction mixtures were prepared by pipetting a suitable amount of bromine into a cooled solution of the required composition. The reaction mixture was then immersed in a thermostat. The "zero" of time was taken as about 15 minutes after immersion. In most cases the reaction was found to be so slow that an uncertainty of several minutes in the zero of time does not influence the results.

The samples used for analysis were first transferred into a test-tube, quickly brought to room temperature, and the time was noted. Measured amounts were then either analyzed directly, or were suitably diluted, and aliquot parts were analyzed. When the time elapsed between the taking of the sample and the titration was more than about 20 minutes, the cooled samples were stored in the refrigerator. At each point 3 analyses usually were carried out: total oxidizing capacity, O, oxidizing capacity with respect to arsenite, P (measuring the normality of hypobromite plus bromite), and the molarity of bromite, B. The analytical methods are those previously described.[1]

The experiments usually were carried out in glass-stoppered erlenmeyer flasks, after a control experiment carried out in a "low Actinic" flask showed that the light to which the solutions are exposed in an ordinary vessel has no measurable influence on the course of the reaction. Direct illumination was avoided. When the reactions took several days, they usually were carried out in sealed ampoules to avoid evaporation. The temperature inside the ampoules was assumed equal to that of the thermostat whereas that in the flasks was found to be constant, but slightly lower.

The initial concentration of hypobromite was usually between 0.030 to 0.055 M. The change of concentration due to expansion was taken into account.

The values of rate constants given below refer to 78.6°, and are given in moles^{-1} l. hr.$^{-1}$.

Results

Reaction Mechanism.—All the experiments followed a course typical for a second-order consecutive reaction, just as in the case of the decomposition at pH $\approx$ 8.[1] We again assume the reaction to be

$$2\mathrm{Br(I)} \xrightarrow{k_1} \mathrm{Br(III)} + \mathrm{Br^-} \qquad (1)$$

$$\mathrm{Br(III)} + \mathrm{Br(I)} \xrightarrow{k_2} \mathrm{Br(V)} + \mathrm{Br^-} \qquad (2)$$

When $k_2 >> k_1$, Br(III) can be considered an unstable intermediate, and a plot of P_0/P against the product of time and initial molarity will yield a straight line whose slope is $3k_1$. Our experimental values did not yield straight lines, but curves which were very flat at the beginning, and approached straight lines as the reaction proceeded. This shows that the steady-state simplification is not applicable. A method of dealing quantitatively with such cases has been developed in our department[3] and the limiting slope has been shown to be smaller than $3k_1$, namely

$$\frac{\mathrm{d}(P_0/P)}{\mathrm{d}(P_0t/2)} = 2k_1\left(\frac{2 + \sqrt{4R^2 - 8R + 1} - 2R}{1 + \sqrt{4R^2 - 8R + 1} + 2R}\right) \qquad (I)$$

where $R \equiv k_1/k_2$.

Furthermore, when suitable correction terms are subtracted from the experimental values of P_0/P, "corrected" values are obtained which, when plotted against the product of time and initial molarity should yield straight lines during the whole course of the reaction, the slope being given by expression I. In order to apply the correction, and in order to calculate k_1 from the slope, one must know R. This quantity was obtained for each experiment by comparing a plot of the experimental values of $4B/P_0$ *vs.* P/P_0 with a family of theoretical standard curves which shows the dependence between these two quantities, for various values of R. The fact that the treatment outlined yielded straight lines proves the applicability of the method, and shows the experimental results to be in quantitative agreement with the proposed mechanism. In particular, a nearly 15-fold variation of the initial concentration did not affect the value obtained for the rate constants (0.4 N NaOH, 1.65 M Na_2SO_4 being added).[4]

Neither the ratio of volume over surface in the vessel used, nor the addition of glass wool had any effect on the reaction rate.

The loss in total oxidizing power was usually zero or very small, in which case the results were corrected accordingly.[5] In some experiments the loss in oxidizing capacity was considerable[6] owing to the presence of traces of an unidentified catalyst. Such experiments were discarded.

Influence of Added Salts.—When at constant hydroxyl ion concentration, sodium sulfate was added to the reaction mixture, a pronounced accelerating effect was noted. The results for $[OH^-] = 0.4$ are shown in Fig. 1 (crosses). Similar results were obtained at $[OH^-] = 0.9$ and 2.7. In another series of experiments, again at $[OH^-] =$

(3) H. J. G. Hayman and B. Perlmutter-Hayman, to be published.

(4) In some cases where the reaction was followed to more than 75% conversion an increase in the slope was observed, which in the range of conversion between 75 and 85% amounted to 10 to 20%. This increase is not in accordance with the above mechanism, and cannot, so far, be explained. The tentative assumption that a concomitant reaction of order one or zero should be responsible for this increase contradicts the independence of the rate constant on the initial concentration; furthermore, even when applied to one particular reaction, the hypothesis did not yield a quantitative fit. Similarly, the suggestion of catalysis by the bromide or bromate formed during the reaction has to be discarded: the rate constants for two experiments carried out in the presence of 0.4 N OH^-, and 2.3 N sodium bromate and perchlorate, respectively, showed an agreement which was well within the limit of experimental error. On the other hand, when perchlorate was replaced by bromide, the rate constant was lowered by about 17%, an effect which can be explained on the assumption that reaction 1 is a reversible one, with a rate constant of the back-reaction equal to about 0.02 that of the forward reaction. (The concentration of bromide usually present in the reaction mixture is so low as to justify our disregarding this reversibility in our kinetic treatment).

(5) The term $P_0\int_{P_0}^{P}\frac{\mathrm{d}O}{P^2}$ was subtracted from the "corrected" values of P_0/P. This correction is exact when the steady-state simplification applies, and is sufficiently accurate in our case since (a) only experiments were considered in which the correction term is small and (b) the value of R is low, *i.e.*, the deviation from the steady state is not very serious. We are indebted to Dr. H. J. G. Hayman for suggesting this correction.

(6) G. Stein and B. Perlmutter-Hayman, *Bull. Res. Counc. Israel*, **4**, 325 (1954).

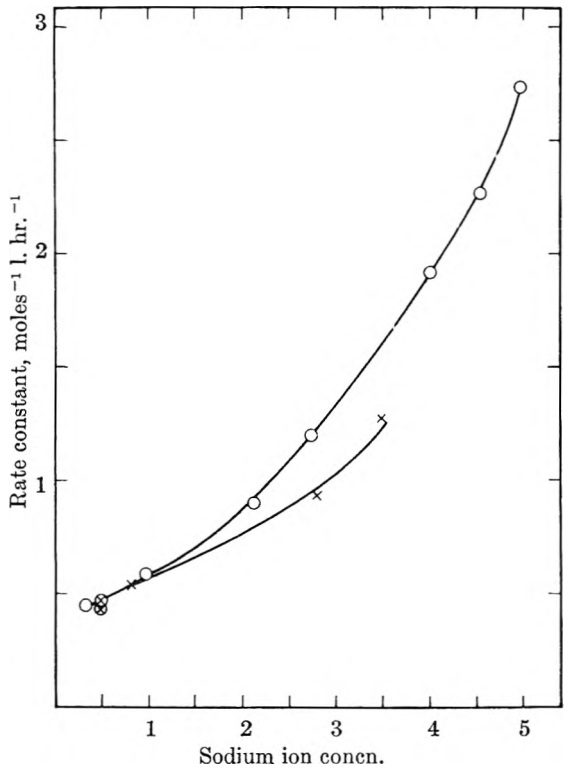

Fig. 1.—The influence of sodium ion concentration on the rate constant: ×, 0.4 N sodium hydroxide plus sodium sulfate; ○, sodium hydroxide. (Approximately 0.1 M of the Na^+ are present in the form of bromide, hypobromite and bromate.)

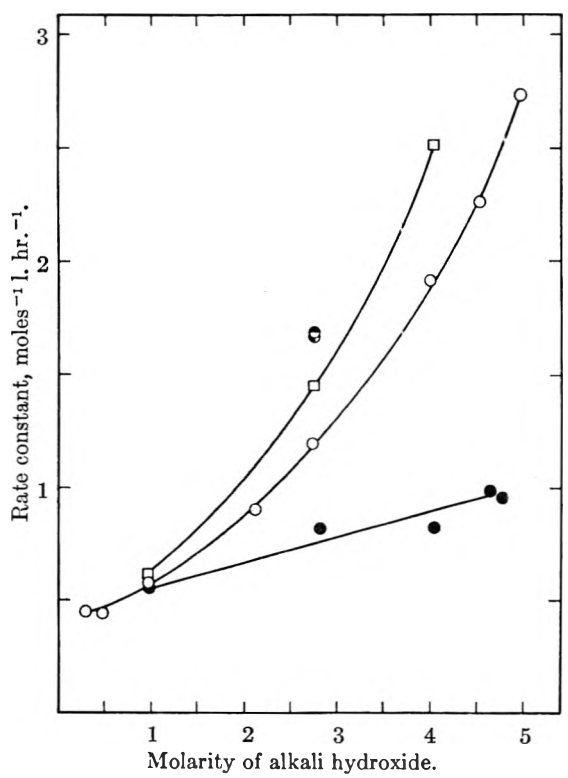

Fig. 2.—Influence of alkali hydroxide concentration on reaction rate: ●, LiOH; ○, NaOH; □, KOH; ◒, RbOH; ◐, CsOH.

0.4, $[Na^+]$ was kept constant at 2.8 M by the addition of various sodium salts. In the presence of 2.3 M sodium bromate, perchlorate, nitrate and chloride (μ = 2.8) the mean value of k_1 was 0.96 ± 0.05 (maximum deviation). When 1.15 M Na_2SO_4 was present (μ = 3.95), k_1 was 0.94, while in the presence of 0.767 M Na_3PO_4 or Na_3AsO_4 (μ = 5.12) it was 1.02 and 1.1, respectively. The univalent anions used have thus no significant specific effect; furthermore, the small differences between uni-, di- and trivalent anions are only slightly more pronounced than those between different anions of the same valency type.

Similarly, when in 0.4 M potassium hydroxide solution the potassium ion concentration was kept in a constant value of 2.8 by the addition of suitable amounts of potassium nitrate and phosphate, the rate constants were 1.14 and 1.24, respectively. It would seem that the influence of anions, though small, is not completely spurious since the ratio of phosphate to nitrate is about 1.1 for both cations.

In a further series of experiments $[OH^-]$ was again kept constant at 0.4 M, and the cation concentration at 2.8 M (usually by the addition of 1.15 M alkali sulfate[7]), while the nature of the cation was varied. The cations were found to have a pronounced specific effect, the values of k_1 being 0.74, 0.94, 1.08 and 1.20 for Li^+, Na^+, K^+ and Rb^+, respectively.

It follows that the accelerating effect of salt concentration on the reaction rate, as exemplified by the results with Na_2SO_4 given above, can be ascribed primarily to a specific effect on the part of the cation, the anion apparently playing only a subsidiary role. In particular it should be noted that the dependence of the rate constant on the salt concentration cannot be expressed in terms of the ionic strength. (The constant varies by ±9% while the ionic strength increases by a factor of 1.7.)

However when instead of other anions OH^- was used to increase the alkali ion concentration, a small but significant accelerating influence over and above that of other alkali compounds was noted; for the case of sodium this is illustrated by Fig. 1, where the influence of sodium sulfate at $[OH^-]$ = 0.4 M (crosses) can be compared with that of sodium hydroxide (circles). Furthermore, this accelerating influence of the hydroxyl ion seems to be enhanced by the presence of the heavier cations. (At an alkali ion concentration of 2.8 M, and $[OH^-]$ = 2.7 M, k_1 = 0.82, 1.20, 1.46, 1.68 and 1.68 for Li^+, Na^+ K^+, Rb^+ and Cs^+, respectively. The ratio of k_1 in experiments were $[OH^-]$ = 2.7 to k_1 in those where $[OH^-]$ = 0.4 thus follows the series 1.11, 1.28, 1.35, 1.40 for the four cations.)

This latter effect becomes especially apparent when the dependence of the rate constant on the alkali hydroxide concentration is investigated. Figure 2 shows the marked specific effect of the various cations.

Bromite Concentration.—The value of k_2 is even more strongly affected by the nature of the cation than is k_1. In the case of lithium, R (the ratio of the rate constants, k_1/k_2) is 0.084 ± 0.003 in 4 experiments where $[Li^+]$ varies between 2.8 and 4.5 M and $[OH^-]$ between 0.4 and 2.7. For so-

(7) In the case of K^+, the value of the rate constant for K_2SO_4 was inferred from the assumption that $k_{K_2SO_4}:k_{KNO_3} = k_{Na_2SO_4}:k_{NaNO_3}$. Potassium sulfate is not sufficiently soluble.

dium, R is 0.058 ± 0.004 as a mean of 25 experiments, at 78.6 and at 59.5°, and at sodium hydroxyl ion concentrations varying between 0.2 to 4.6. There was no perceptible trend with any of these variables although the rate constants k_1 varied up to 3.5 fold at 78.6°, and 2.1 fold at 59.5°. They therefore seem to affect k_2 to the same extent as they affect k_1.

For potassium and rubidium, R = 0.040 ± 0.002 in 4 experiments where the cation concentration was 2.8 and that of OH^- was 0.4. For the heavier cations, however, R is no longer independent of the concentration of alkali hydroxides: for potassium it decreases to 0.02 and 0.01, respectively, in 1.5 and 3.0 N KOH. For rubidium and cesium the effect is still more marked, and in 2.8 N solution of the hydroxides R becomes too small for determination. From the fact that the P_0/P *vs.* t plot no longer shows the form characteristic of a consecutive reaction[3] we conclude $R \leq 0.007$.

The maximum bromide concentration $[BrO_2^-]_{max}$ is connected with R by the expression

$$[BrO_2^-]_{max} = R[BrO^-]_{max}$$

The value of $[BrO^-]_{max}$, the concentration of hypobromite at which the bromite concentration equals $[BrO_2^-]_{max}$ is dependent on R,[3] and decreases from P_0 for negligibly small R to 0.66 P_0 at R = 0.084. From this, we calculate that the percentage of the original hypobromite normality transformed into bromite at its maximum is 11.2 and 8.3 for Li^+ and Na^+, respectively. For K^+ and Rb^+ at 2.8 M and in the presence of 0.4 M OH^- it is 6.2, whereas in 3 M potassium hydroxide solution it is 1.8, and becomes negligible in 2.7 M rubidium and cesium hydroxide.

Energy of Activation in the Presence of Sodium Salts.—Energies of activation were measured by comparing experiments at 59.5 and 78.6°, using the expression

$$E_a = R\left(\mathrm{d}\ln k/\mathrm{d}\frac{1}{T}\right)$$

which gives the apparent energy of activation. The mean value for 8 pairs of experiments is 22.60 ± 0.53 kcal. mole^{-1} in the concentration ranges betweeen 1 to 5 M for sodium ion, and 0.4 to 4.9 for hydroxyl ion. No trend with any of these two variables could be detected.[8] This is somewhat surprising, since in analogy to the effect of ionic strength at lower concentration an increase in the salt concentration might be expected to increase both the frequency factor and the apparent energy of activation.[9] The results are not sufficiently accurate, however, to state conclusively that in this case sodium and/or hydroxyl affect *only* the frequency factor.

Discussion

Influence of Hydroxide Concentration.—Both hypobromous and bromous acids are practically fully dissociated under our conditions.[10] If in this range of pH the change in the dissociative equilibrium between these acids and their respective anions had any influence on the reaction rate, an increase in $[OH^-]$ would cause a sharp decrease in the reaction rate. The opposite has been observed. We may therefore assume the accelerating influence of OH^- to be a *specific* one, and conclude that the reactions in this range take place exclusively between anions, according to

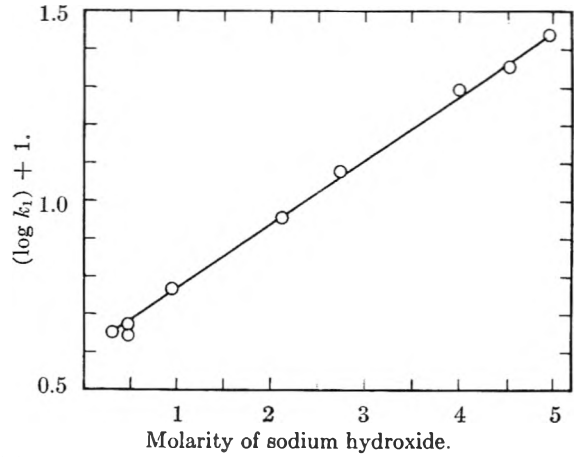

Fig. 3.—The dependence of log k_1 on sodium hydroxide concentration.

$$2BrO^- \longrightarrow BrO_2^- + Br^- \qquad (1a)$$

$$BrO_2^- + BrO^- \longrightarrow Br^- + BrO_3^- \qquad (2a)$$

The Specific Influence of Cations.—The inapplicability of the concept of ionic strength to the kinetics of reactions between ions in solution, and the influence of the valency of the ions of opposite sign on the rate of reaction between ions of like sign have recently been revived by Olson and Simonson.[11] This subsequently was shown[12] to be a natural consequence of Brønsted's original views.[13] The fact that in the presence of polyvalent ions of sign opposite to that of the reacting ions the Debye–Hückel limiting law cannot be applied to evaluate Brønsted's "kinetic factor" is also apparent from the work of La Mer and co-workers.[14,15] The high ability of a polyvalent cation to form an ion-pair with one of the reacting anions has been adduced[16] as an explanation for the fact that in the presence of such cations the experimental results do not agree with the Debye–Hückel–Brønsted theory even at very low ionic strength. More recently[17,18] activated complexes have been formulated in which an ion of opposite sign forms a "bridge" between the two reacting ions of like sign.

(8) Three experiments at 45° were carried out. The average for the activation energies between 59.5 and 45° is 22.61, *i.e.*, identical with the above. The high scatter in the lower range, however, makes this agreement seem fortuitous.

(9) See, *e.g.*, E. A. Moelwyn-Hughes, "The Kinetics of Reactions in Solution," 2nd ed., Oxford Press, New York, N. Y., 1947, p. 103.

(10) The pK of hypobromous acid is 8.7 at room temperature (L. Farkas and M. Levin, *J. Am. Chem. Soc.*, **72**, 5766 (1950)). Even at the lowest value of NaOH used, the undissociated acid constitutes only 2 × 10^{-4} of the hypobromite concentration. Bromic acid may be assumed to be somewhat stronger, and will be still more fully dissociated.

(11) A. R. Olson and T. R. Simonson, *J. Chem. Phys.*, **17**, 1167 (1949).

(12) See, for instance, M. Kilpatrick in "Annual Review of Physical Chemistry," 1951, p. 269.

(13) J. N. Brønsted, *J. Am. Chem. Soc.*, **44**, 877 (1922).

(14) V. K. La Mer and R. W. Fessenden, *ibid.*, **54**, 2351 (1932).

(15) V. K. La Mer, *Chem. Revs.*, **10**, 179 (1932).

(16) V. K. La Mer, *J. Am. Chem. Soc.*, **57**, 2662 (1935).

(17) H. Taube, *et al.*, *ibid.*, **75**, 4119 (1953); **77**, 4481 (1955).

(18) F. M. Beringer and E. M. Gindler, *ibid.*, **77**, 3200 (1955).

The primary factor deciding the influence of the ion of unlike sign usually has been considered to be its valency; special attention to specific effects within a group of ions of equal charge-type has been paid by von Kiss[19] and, more recently—while the present research was in progress—by Sheppard and Wahl.[20] As pointed out by the latter it is not surprising that such specific effects should exist; we might expect them to be particularly pronounced in concentrated solutions. Our results indicate that positive ions are more efficient in promoting the reaction between two hypobromite ions, or a hypobromite and a bromite ion, the smaller their hydration and thus the smaller their radius in solution. This is the expected effect if we assume the role of the ion of unlike sign to lie in helping the two reacting anions to overcome their electrostatic repulsion. In this case it would seem only a matter of definition whether or not the cation is to be considered as a part of the activated complex, forming a bridge between the two anions. Alternatively, the presence of the cation in the activated complex may actually provide a reaction path different from that which is taken in the absence of the cation. (The concentration of such an activated complex would in turn be favored by a high salt concentration.) At present, no decision between the two possibilities can be made.

The accelerating influence of the hydroxyl ion suggests the existence of an alternative reaction path involving transfer of oxygen *via* OH^-. For this reaction between three anions the presence of a cation is certainly even more imperative, and the influence of its radius will be even more pronounced. In this case, it seems natural to look upon the cation as part of the activated complex.

Regarding the relationship between salt concentration and rate constant we found empirical expression (II) to be applicable

$$\mathrm{d} \log k_1/\mathrm{d}c = a \qquad \text{(II)}$$

where c is the salt concentration and a a constant. (See Fig. 3 where log k_1 is plotted *vs.* [NaOH].) Expression II constitutes the rule of Grube and Schmid,[21] proposed by these authors for a reaction of somewhat different type.

(19) A. von Kiss and V. Bruckner, *Z. physik. Chem.*, **128**, 71 (1927).

(20) J. C. Sheppard and A. C. Wahl, *J. Am. Chem. Soc.*, **79**, 1070 (1957).

(21) G. Grube and G. Schmid, *Z. physik. Chem.*, **119**, 19 (1926).

DEUTERIUM EXCHANGE BETWEEN WATER AND BOEHMITE (α-ALUMINA MONOHYDRATE). ACTIVATION ENERGY FOR PROTON DIFFUSION IN BOEHMITE

BY YUNG-KANG WEI AND RICHARD B. BERNSTEIN

Contribution from the Chemistry Department, University of Michigan, Ann Arbor, Michigan

Received November 29, 1958

The kinetics of the exchange of D_2O vapor with crystalline boehmite (particle size *ca.* 1 μ) were studied from 85–151°. The Berthier exchange ratio C (number of exchangeable atoms in the solid relative to vapor phase) ranged from 0.7 to 2.3. The D_2O pressure was varied from 0.41 to 0.95 atm. A rapid initial surface exchange preceded the slower diffusion-controlled exchange with the bulk crystal. After correction for this surface exchange the data followed the appropriate diffusion equation (spherical particle case). Due to the uncertainty in crystallite size absolute values of the diffusion coefficient D are in doubt by a large (but constant) factor. However, the temperature dependence of D furnishes a reliable value for the activation energy: $E_D = 12.9 \pm 0.8$ kcal./mole. Auxiliary exchange experiments carried out with D_2O^{18} showed very slow exchange of O^{18} compared to that of deuterium. This suggests independent migration of protons (deuterons) and oxygen carrier ions through the boehmite lattice.

Introduction

A preliminary study[1] of the exchange of liquid D_2O^{18} with boehmite (α-alumina monohydrate) of sub-micron crystallite size at temperatures above 100° indicated rapid deuterium exchange, with very slow concurrent O^{18} exchange. The results were interpreted on the basis of a slow step involving independent diffusion of protons and oxygen carrier ions. The present investigation was undertaken to obtain more precise data on the kinetics of the deuterium exchange between gaseous water and boehmite of known particle size and specific surface area. From such data the proton diffusion coefficient, the proton mobility and the activation energy for proton diffusion in the boehmite lattice could be evaluated.

(1) R. B. Bernstein, ANL-5889, Argonne National Laboratory, U.S.A.E.C., Aug., 1958.

Experimental

A. Materials.—D_2O (99.8 at. % D) was used in the exchange studies. For the preliminary experiments D_2O^{18} (99.8 at. % D, 1.4 at. % O^{18}) was employed. Boehmite (*Anal.*: Al_2O_3, 84.7; calcd. for AlO_2H, 84.98) was prepared[2] by the reaction of high purity aluminum (>99.99%) with H_2O at 350° for *ca.* 15 hr. X-Ray diffractograms[3] revealed no lines due to crystalline impurities.

For all experiments except the preliminary ones reported in ref. 1, the boehmite was ground in an agate mortar, then fractionated by successive suspensions in water. A "center cut" of particle size was obtained by 3–5 successive sedimentations in water for 30 minute periods. The large agglomerates and the very fine particles were effectively removed by this procedure. The product was dried at 120° for 6 hr., lightly ground and stored in a desiccator. Two

(2) The authors wish to thank J. E. Draley and W. E. Ruther of the Argonne National Laboratory for furnishing the boehmite samples, and R. Banc of the A.N.L. for chemical and spectrographic analyses.

(3) Through the cooperation of S. Siegel and E. Sherry of the A.N.L.

batches were prepared in this way; a third was separated[4] by a more extensive sedimentation procedure. A microphotographic study[4] of these three batches indicated particle size (diameter) distributions with maxima at 1.0, 1.0 and 1.2 μ for batches I, II and III, respectively. However, BET (N_2) surface areas were found[4] to be 7.3, 10.9 and 6.7 m.^{2}/g., corresponding to effective sphere diameters of 0.28, 0.18 and 0.30 μ, respectively. Electron micrographs[4] showed the absence of very fine particles; thus the observed particles probably consisted of agglomerates of smaller crystallites.

B. Analysis.—Water samples (5–10 mg.) were quantitatively converted to H_2–HD–D_2 by reaction with hot zinc, then analyzed (±1 at. % D) mass spectrometrically using a calibration curve. Deuterated boehmite samples were analyzed by dehydration at 450° *in vacuo* after an initial evacuation at room temperature. Preliminary experiments showed that 96–98% of the stoichiometric amount of water was liberated. X-Ray diffraction[3] showed the residual crystalline solid to be γ-Al_2O_3.

In a number of cases[1] the total oxygen was removed from the boehmite by treatment with $KBrF_4$ at 500°.[5] Oxygen yields of 97–99% were obtained. For the O^{18} experiments the oxygen was assayed mass spectrometrically[6] and compared with oxygen evolved from the stock D_2O^{18} by treatment with BrF_3.[7]

C. Procedures.—The conditions for the preliminary exchanges of boehmite with liquid D_2O^{18} have been described.[1] For the experiments with gaseous D_2O, the procedure was as follows. A weighed amount (4–12 g.) of boehmite was placed in a 2-liter flask and evacuated at 120–150° for several hours. A known weight of D_2O was introduced as a vapor into the flask, which was then sealed and rotated on a glycerol-bath. The whole system was enclosed in a constant temperature oven (±1°). During the reaction period small amounts (*ca.* 5 cc. atm.) of vapor were withdrawn from the flask (by gas pipetting) at definite times and assayed for deuterium. A number of the deuterated solid samples were also analyzed at the end of the exchange experiments; the assay agreed within experimental error with that calculated from the analysis of the corresponding vapor sample.

The pressure in the reaction flask was calculated from the quantity of water introduced; it ranged from 0.41 to 0.95 atm. Temperatures studied were from 85–151°. The Berthier exchange ratio C (number of exchangeable atoms in the solid relative to vapor phase) was adjusted from 0.7 to 2.3; most experiments were carried out at a value of $C = 1$.

Results

In all cases it was found that a rapid initial exchange (presumably with the first few surface layers) preceded the slow, diffusion-controlled exchange with the bulk crystal. The magnitude of this surface exchange (determined from the intercepts of plots of the fraction exchanged *vs.* the square root of the time) was somewhat variable; the average value was *ca.* 10%.

The data may be treated using a 3-phase model based on an intact solid particle surrounded by a film which is in labile isotopic equilibrium with the gas phase. The symbols n_s, n_f and n_g represent the number of gram atoms of hydrogen plus deuterium in the solid, the film and the gas phase, respectively. The fraction of total solid phase which is labile is thus $\lambda = n_f/(n_s + n_f)$ and the Berthier ratio is $C = (n_s + n_f)/n_g$. The symbols x_s, x_f and x_g denote the (average) atom fraction deuterium in each phase. The true fraction exchange in the bulk solid is $f^* = x_s/x_\infty$ and the apparent fraction exchange based on assay of the gas phase is $f_a = (x_0 - x_g)/(x_0 - x_\infty)$. Here x_0, x_g and x_∞ represent values of the atom fraction deuterium in the gas phase originally, after time t and at equilibrium. It is noted that $x_0/x_\infty = 1 + C$. From material balance at any time, $x_s n_s + x_f n_f + x_g n_g = x_0 n_g$. Assuming $x_f = x_g$, one obtains the relation: $f^* = 1 - (1 - f_a)(1 + c\lambda)/(1 - \lambda)$. Letting f_a^0 denote the apparent "zero-time" fraction exchange (the initial exchange with the film; *i.e.*, the intercept on a plot of f_a *vs.* $t^{1/2}$) and x_g^0 be the atom fraction deuterium in the gas phase directly after the initial exchange, $f_a^0 = (x_0 - x_g^0)/(x_0 - x_\infty)$ and $\lambda = f_a^0/[1 + C(1 - f_a^0)]$. This leads to the result

$$f^* = (f_a - f_a^0)/(1 - f_a^0) \qquad (1)$$

An estimate of the equivalent thickness of the labile film obtained from the magnitude of λ (*ca.* 0.05) and the average value of the effective sphere diameter (*ca.* 0.25 μ) is approximately 20 Å. The presence of a surface layer of $Al(OH)_3$ would account in part for this (apparent) high value. All data were corrected for the observed initial exchange using eq. 1 before attempting to evaluate the diffusion coefficient.

The kinetics of isotope exchange between a well-stirred fluid phase and a bed of uniform spherical particles were treated by Berthier,[8] following upon the earlier work of Wagner[9] and Zimens.[10] Crank[11] portrays Berthier's results in graphical form.

The procedure used to treat the present data is described. Curves of f^* *vs.* $t^{1/2}$ (initially linear) were compared to the theoretical curve (from Berthier's table) of fraction exchange *vs.* $\tau^{1/2}$ at a given value of the Berthier ratio C. Here $\tau = D^*t$, $D^* = D/a^2$, D is the diffusion coefficient and a is the sphere radius. Values of D^* (the "relative" diffusion coefficient) thus obtained were compared with similar values deduced from an alternate procedure. This involved comparison of plots of log $(1 - f^*)$ *vs.* t with theoretical plots of log $(1 - f^*)$ *vs.* τ (linear for $\tau >> 1$). The agreement was within the experimental uncertainty of 5–10% in D^*. There was an indication of a slight decrease in D^* as the average atom fraction deuterium in the solid phase built up beyond about 35%. The concentration dependence of the diffusion coefficient was small, however. Experiments to investigate this using low initial deuterium concentrations (*ca.* 20 at. % D) were less precise and somewhat inconclusive; the over-all magnitude of the effect is estimated to be less than 10% in the diffusion coefficient over the whole concentration range available.

Experiments showed that D^* was indeed independent of the Berthier ratio C. In addition, it was found that there was no significant dependence of D^* upon the D_2O pressure over the range studied.

Table I summarizes the results for one particular batch (II) of boehmite.

(4) By the Fine Particles Group of the Armour Research Foundation, Chicago, Ill., under the supervision of S. Katz.

(5) I. Sheft, A. Martin and J. Katz, *J. Am. Chem. Soc.*, **78**, 1557 (1956). Thanks are due to I. Sheft and M. Roemer of the A.N.L. for their cooperation in this connection.

(6) O^{18} assays through the cooperation of D. Hutchison and H. Rest of the A.N.L.

(7) H. Hoekstra and J. Katz, *Anal. Chem.*, **25**, 1608 (1953).

(8) G. Berthier, *J. chim. phys.*, **49**, 527 (1952).

(9) H. Dünwald and C. Wagner, *Z. physik. Chem.*, **B24**, 53 (1934).

(10) K. Zimens, *Arkiv. Kemi. Mineralogi Geologi*, **20A**, No. 18, 1 (1945).

(11) J. Crank, "Mathematics of Diffusion," Oxford Press, New York, N. Y., 1956.

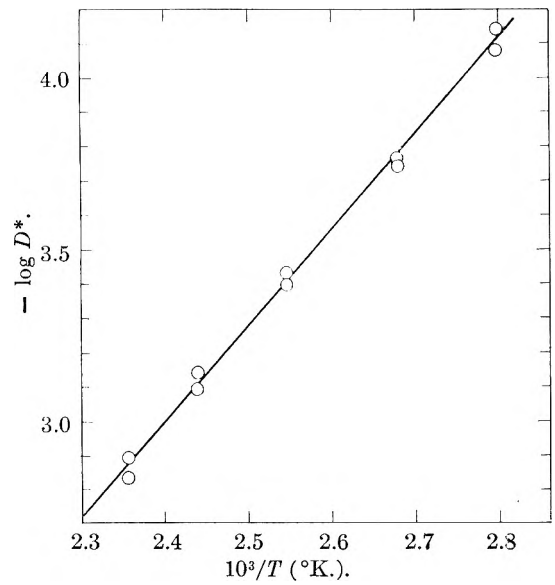

Fig. 1.—Temperature dependence of the relative diffusion constant; activation energy 12.9 kcal./mole.

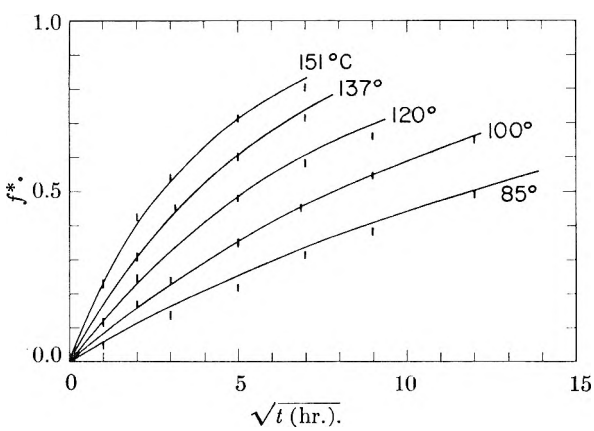

Fig. 2.—Exchange of D_2O(g) and α-AlOOH; 1:1 g. atom ratio H:D. Solid lines are calculated (see text).

TABLE I

TEMPERATURE DEPENDENCE OF THE RELATIVE DIFFUSION COEFFICIENT D^*

T (°C.)	P (atm.)	Berthier C	$10^4 \times D^*$ (hr.$^{-1}$)
85	0.46	0.86	0.81
85	.41	0.90	0.72
100	.73	1.00	1.72
100	.70	1.09	1.78
120	.75	0.83	4.00
120	.70	1.06	3.71
137	.77	1.02	7.70
137	.56	1.44	8.20
151	.64	1.01	14.6
151	.86	0.84	12.8

Figure 1 shows the temperature dependence of the relative diffusion coefficient D^*(hr.$^{-1}$). A least-square line through the data yields an equation

$$D^* = 1.7 \exp(-12{,}900/RT) \qquad (2)$$

with D^* now expressed in sec.$^{-1}$. The activation energy for the diffusion coefficient is 12.9 ± 0.8 kcal./mole. Less extensive results with other batches of boehmite served to confirm this value.

Using eq. 2, values of D^* were calculated at temperatures from 85–151° and theoretical graphs of f^* *vs.* $t^{1/2}$ at $C = 1$ were plotted. Figure 2 shows the fit of the experimental data (for those experiments in which C was close to 1) to the calculated curves based on diffusion in uniform spherical particles. It is to be noted that the data could not be fitted to the theoretical curves for diffusion through infinite plane sheets.

It was of interest to make an estimate of the absolute value of the diffusion coefficient from the D^* measurements for the different batches of boehmite. Equivalent sphere radii based on the BET surface areas were used. For a series of comparison experiments at 137° the results were: $10^{17} \times D$ (cm.^{2} sec.$^{-1}$) = 1.2, 1.8 and 3.0 for batches I, II and III, respectively. The large range is due in part to the unsolved problem of inhomogeneity of crystallite size and agglomeration of crystallites to form the large (1 μ) particles.

Using these values in conjunction with the usual equation $D = D_0 \exp(-E_D/RT)$, one estimates a value of D_0 of the order of 2×10^{-10} cm.^{2} sec.$^{-1}$. An estimated upper limit for D_0 (obtained by assuming the equivalent sphere diameter equal to the particle diameter) is about 5×10^{-9} cm.^{2} sec.$^{-1}$.

Experiments[1] with D_2O^{18} were of a preliminary nature and are not exactly comparable with those described above. They were carried out in sealed tubes using liquid water under its saturated vapor pressure at temperatures up to 230°. The boehmite powder had not been fractionated and therefore contained an appreciable (but unknown) percentage of fine particles (the BET area was 12.2 m.^{2}/g.). In typical experiments,[1] the total deuterium exchange (surface plus bulk exchange) was 49% after 24 hr. at 100°; at 230° in 39 hr. there was 84% exchange.

In computing the per cent. exchange of O^{18} it was assumed that only one-half of the O atoms in the AlOOH are ultimately exchangeable. The data on the O^{18} content of the separate phases after exchange could not be reconciled without this assumption.[12] Using this basis of calculation, typical results were as follows: at 100° in 22 hr., 12% O^{18} exchange; at 230° in 39 hr., 10% exchange. Even after 27 days at 230° only 28% of the exchangeable O atoms had undergone exchange (corresponding to 14% of the total O atoms in the boehmite). It is to be noted that surface exchange probably accounts for a considerable fraction of the observed total exchange.

A number of miscellaneous deuterium exchange experiments were carried out using boehmite samples which contained as impurities varying amounts of iron and silicon (up to an estimated 1% of each). The usual rapid surface exchange occurred, but the rate of the subsequent bulk exchange was very much lower than in the case of pure boehmite. No quantitative data on the influence of impurities on the diffusion coefficient were obtained in the present study, however.

(12) Due to the slowness of the O^{18} exchange (low bulk diffusion coefficient) it was not possible to achieve equilibrium and obtain conclusive evidence on this point.

Discussion

The very slow exchange of O^{18} relative to that of deuterium suggests independent migration of protons (deuterons) and oxygen-bearing carriers (such as OH^-, $O^=$ or H_2O) through the boehmite crystal lattice. As might be expected, the diffusion coefficient of the proton is appreciably greater than that of any oxygen carrier.

The crystal structure of boehmite was studied first by Reichertz and Yost[13] and subsequently by Milligan and McAtee.[14] One-half of the oxygen atoms (type I) can be assigned to Al–O–Al links while the other half (type II) are associated with hydrogen bonds (Al–O–H–O–Al). It has been suggested[13] that cleavage of boehmite crystals occurs along the sheets of hydrogen atoms in the H-bonds to give the orthorhombic crystals. Recent work by Holm, *et al.*,[15] has indicated that the O–H–O bond is asymmetric.

It is postulated here that (1) hydrogen diffusion occurs along the sheets of bonded hydrogens, and (2) the observed oxygen exchange is limited to the type II oxygen atoms, accessible through the sheets of hydrogen bonds.

It is of interest to compare the boehmite case with that of ice. The conductivity and proton mobility in polycrystalline ice has been measured by Spernol.[16] Below $-15°$ an activation energy of 3.9 ± 0.2 kcal./mole was obtained for the mobility. Using the Einstein relation between the diffusion coefficient and the mobility (v): $D = (kT/e)v$, (where k is the Boltzmann constant and e is the proton charge), the activation energy for the proton diffusion coefficient is $E_D = E_v + RT$, which gives a value of 4.5 kcal./mole for the case of ice. It is not surprising that the value for E_D in boehmite is significantly greater than this result.

Recently Kuhn and Thuerkauf[17] reported measurements on the O^{18} and D diffusion coefficients in polycrystalline ice at $-2°$. They found these to be the same (with a value of 1.0×10^{-10} cm.^{2} sec.$^{-1}$), from which they deduced that the diffusing species in ice is the water molecule. This value for the diffusion coefficient of water in ice is, of course, considerably larger than that of the proton in boehmite.

The low value of D_0 for proton diffusion in boehmite implies an unusually large negative entropy of activation. It would be of interest to extend this work to the study of proton diffusion in other crystalline hydrous oxides.[18]

Acknowledgments.—The authors appreciate the partial support of this research by the U. S. Atomic Energy Commission, Division of Research (Contract No. AT(11-1)-321) and the Argonne National Laboratory (Chemistry and Metallurgy Divisions). Special thanks are due to J. E. Draley and H. H. Hyman of the A. N. L. for a number of valuable discussions.

(13) P. Reichertz and W. Yost, *J. Chem. Phys.*, **14**, 495 (1946).
(14) W. Milligan and J. McAtee, THIS JOURNAL, **60**, 273 (1956).
(15) C. H. Holm, C. R. Adams and J. A. Ibers, *ibid.*, **62**, 992 (1958).
(16) A. Spernol, *Z. Elektrochem.*, **59**, 31 (1955).
(17) W. Kuhn and M. Thuerkauf, *Helv. Chim. Acta*, **41**, 938 (1958).
(18) In this connection it should be noted[1] that the proton mobility in bayerite (β-$Al(OH)_3$) was found to be at least an order of magnitude greater than that in boehmite.

NOTES

ELECTRODE POTENTIALS IN FUSED SYSTEM. V. CELLS WITH TRANSFERENCE

BY KURT H. STERN

Chemistry Department, University of Arkansas, Fayetteville, Arkansas

Received March 14, 1958

Laity[1] recently has discussed fused salt concentration cells with transference. In particular he studied the cell

$$Ag|AgNO_3(X_1),\ NaNO_3;\ NaNO_3,\ AgNO_3(X_2)|Ag$$

Mobilities of silver and sodium ions are the same in $AgNO_3$–$NaNO_3$ solutions over the entire composition range. It follows that the measured potential of the cell arises only from the difference in the activity of the $AgNO_3$ in the two electrode compartments.

In the present work we treat a still simpler case: that in which the concentrations of the ions to which the electrodes are reversible are the same. Any measured potential $\neq 0$ can then be expressed in terms of events occurring in the liquid junction alone, *e.g.*, in terms of the difference in the mobilities of the ions to which the electrodes are *not* reversible.

The cells studied are: (1) Cl_2 | AgCl; NaCl | Cl_2, (2) Cl_2 | NaCl; KCl | Cl_2 and (3) Cl_2 AgCl; KCl | Cl_2.

Experimental

Materials.—All salts were of C.P. grade. Matheson tank Cl_2 was bubbled through concentrated H_2SO_4 and over anhydrous $CaSO_4$ before passing into the cells.

Apparatus.—The cell consisted of a 15 mm. i.d. Vycor U-tube having a graphite membrane (spectrographic carbon) sealed into the bottom and separating the cell compartments. The permeability of this membrane could be varied by changing its thickness; 2–3 mm. were sufficient to prevent diffusion for an hour or so. Separate tanks of Cl_2 were used for each compartment and the Cl_2 was passed over the carbon electrodes. Other details of measurement were as described previously.[2] Cells recovered quickly after having current passed through them, indicating that reversible potentials were measured. All measurements were made isothermally at several temperatures between 800 and 900°.

(1) R. W. Laity, *J. Am. Chem. Soc.*, **79**, 1849 (1957).
(2) K. H. Stern, THIS JOURNAL, **60**, 679 (1956).

Results

All the above cells showed zero potential, within experimental error (±0.5 mv.). In some runs AgCl was added to one side or the other of cells containing NaCl and KCl in the two compartments. In no case did the potential vary from zero.

Discussion

The measured potentials of the above cells can be attributed to events at the liquid junction. If we write the cell $A_2 \mid M'A;\ M''A \mid A_2$ it is clear that composition in the "junction" must change continuously from M'A to M"A. The analysis which follows[3] applies to this region.

Consider a system containing at any point x_1 moles of M'A and x_2 moles of M"A, with transference numbers t_1 for M', t_2 for M", and t_A for A, and corresponding mobilities u_1, u_2 and u_A. At any point the conductance is proportional to $u_1x_1 + u_2x_2 + u_A$. Then

$$t_1 = u_1x_1/(u_1x_1 + u_2x_2 + u_A)$$

and

$$t_1 + t_2 + t_A = 1$$

The material flux per faraday at any point is

$$t_1M' + t_2M'' - t_AM_A = t_1M'A + t_2M''A - A$$

The last term is independent of the position in the cell and may be combined with the electrode process. In these cells they cancel exactly, so

$$-(\mathfrak{F}/RT)dE = t_1 \text{ d ln } a_1 + t_2 \text{ d ln } a_2 \qquad (1)$$

where $a_1 = a_{M'}a_A$ and $a_2 = a_{M''}a_A$. Hence, using the Gibbs-Duhem equation[1]

$$-(\mathfrak{F}/RT)dE = \frac{u_1x_1 \text{ d ln } a_1 + u_2x_2 \text{ d ln } a_2}{u_1x_1 + u_2x_2 + u_A} = \frac{(u_1 - u_2)x_1 \text{ d ln } a_1}{u_1x_1 + u_2x_2 + u_A} \qquad (2)$$

$dE = 0$ if $u_1 - u_2 = 0$, as Laity[1] has found for the nitrates. The liquid junction potential, *i.e.*, the potential of our cells, is also zero if

$$\int_A^B \frac{(u_1 - u_2)x_1 \text{ d ln } a_1}{u_1x_1 + u_2x_2 + u_A} = 0 \qquad (3)$$

where the integration is carried out over the whole range of composition. It might be assumed that $(u_1 - u_2)$ is positive for some ranges of composition and negative for others, the whole integral being zero, but this possibility appears very unlikely in view of some recent measurements by Murgulesco and Marchidan[4] on the concentration cell with liquid junction in which the mole fraction of AgCl in

Ag | AgCl ‖ AgCl, KCl | Ag

the right-hand compartment was varied from 0.1 to 0.8. They report that the diffusion potential is zero within experimental error (~1 mv.) in the system over this concentration range, as Laity had found for the nitrates. On the basis of this evidence it is reasonable to conclude that the integral (3) is zero because $u_1 - u_2 = 0$. It seems likely that this explanation is valid for the AgCl–NaCl and KCl–NaCl systems also.

Acknowledgment.—I wish to thank Dr. G. Scatchard for his derivation of equation 2 and Drs. F. R. Duke and R. W. Laity for some stimulating discussions.

(3) G. Scatchard, personal communication.

(4) I. G. Margulesco and D. I. Marchidar, *Rev. Chim., Acad. de la Repub. Populaire Roumaine*, III, No. 1 (1958).

VISCOSITY OF AQUEOUS SODIUM PERCHLORATE SOLUTIONS

BY E. R. NIGHTINGALE, JR.

Department of Chemistry, University of Nebraska, Lincoln 8, Nebraska

Received July 17, 1958

Accurate viscosity data for dilute aqueous sodium perchlorate solutions are not available in the literature.[1] In conjunction with diffusion studies being conducted in these laboratories, the viscosities of sodium perchlorate solutions at 25° have been measured in the concentration range 0.001 to 2 *M*. These results are reported here.

Experimental

To purify reagent grade sodium perchlorate sufficient sodium hydroxide was added to a 6 *M* sodium perchlorate solution to give *p*H 10. After standing 24 hours, the solution was filtered through a fine porous glass funnel to remove the insoluble heavy metal hydroxides. The solution was acidified to *p*H 6 with perchloric acid and then boiled to concentrate the solution. Upon incipient precipitation of the anhydrous sodium perchlorate, the solution was cooled to 55° and filtered rapidly through a heated porous glass funnel. Care must be exercised not to cool the solution below about 55° and thus permit the crystallization of the monohydrate. The anhydrous sodium perchlorate was removed from the funnel and dried at 110° for 4 hours.

The sodium perchlorate solutions were prepared by diluting weighed quantities of the purified salt to volume. The densities of the solutions were measured at 25.0 ± 0.1° using 25-ml. specific gravity bottles, and the densities are precise to 0.0001 g./ml.

The viscosities of the solutions were measured at 25.00 ± 0.01° using an Ostwald viscometer with a flow time of 170 seconds for water. Flow times were measured to 0.02 sec. with a stopwatch. The average deviation for five to eight measurements of a single sample did not exceed ±0.05 sec. The average flow times for replicate samples of a single solution agreed within ±0.04 sec. The viscometer was calibrated with water, benzene and 20% and 30% sucrose solutions by means of equation 1

$$\eta/\rho = Kt - L/t \qquad (1)$$

where η is the absolute viscosity, ρ is the density, and t is the flow time of the calibrating solution. The characteristic viscometer constants K and L were 0.00005291 and 0.0011, respectively. The absolute viscosities of water, benzene and the sucrose solutions were taken as 0.008903,[2] 0.006010,[3] and 0.01701 and 0.02741[4] poise, respectively; the densities of the solutions were taken as 0.99707,[5] 0.87370,[3] and 1.07940 and 1.12517[4] g./ml., respectively.

Results and Discussion

The viscosities of the sodium perchlorate solutions were computed by means of equation 1. The relative and absolute viscosities for ten solutions in the concentration range 0.001 to 2 *M* are presented in Table I. The values for the 1 and 2 *M* solutions compare well with those reported for concentrated solutions by Miller and Doran.[6] The data have

(1) R. Reyner, *Z. physik. Chem.*, **2**, 744 (1888).

(2) J. R. Coe and T. B. Godfrey, *J. Applied Phys.*, **15**, 625 (1944).

(3) American Petroleum Institute Research Project 44, "Selected Values of Physical and Thermodynamic Properties of Hydrocarbons and Related Compounds," Carnegie Press, Pittsburgh, 1957, tables 21a, 21c.

(4) E. C. Bingham and R. F. Jackson, *Nat. Bur. Standards (U.S.), Tech. News Bull.*, **14**, 59 (1918).

(5) N. E. Dorsey, "Properties of Ordinary Water-Substance," Reinhold Publ. Corp., New York, N. Y., 1940, p. 201.

(6) M. L. Miller and M. Doran, THIS JOURNAL, **60**, 186 (1956).

TABLE I

RELATIVE AND ABSOLUTE VISCOSITIES OF AQUEOUS SODIUM PERCHLORATE SOLUTIONS AT 25°

C, moles/l.	η/η_0	η, poise
0.0008987	1.0002	0.008905
.004499	1.0005	.008907
.01000	1.0009	.008911
.01600	1.0012	.008914
.03600	1.0021	.008922
.06054	1.0029	.008929
.1000	1.0038	.008937
.3948	1.0101	.009003
1.0008	1.049	.009339
1.9975	1.150	.01024

been analyzed using the Jones–Dole[7] equation

$$\eta/\eta_0 = 1 + A\sqrt{C} + BC \qquad (2)$$

where η/η_0 is the viscosity of the salt solution relative to that of the solvent, water, C is the molar concentration, and A and B are constants characteristic of the electrolyte. The A-coefficient represents the contribution from interionic electrostatic forces and was first derived by Falkenhagen and Vernon.[8] The B-coefficient appears to represent the contribution of the co-spheres of the ions,[9,10] although no satisfactory theoretical treatment has yet been given. This constant is a specific and approximately additive property of the ions of a strong electrolyte at a given temperature.[11] Rearranging equation 2 and plotting $(\eta/\eta_0 - 1)/\sqrt{C}$ *vs.* $\sqrt{C}$, the A-coefficient is the ordinate intercept, and the B-coefficient is given by the slope of the resulting straight line. The experimental value for the A-coefficient of 6.8×10^{-3} compares well with the theoretical value of 6.4×10^{-3}. The experimental value for the B-coefficient is observed to be $+0.03$ for sodium perchlorate at 25°. Taking the value for the B-coefficient for the sodium ion to be $+0.086$,[9,10] we calculate -0.056 as the magnitude of the B-coefficient for the perchlorate ion at this temperature.

Recently, Gurney (ref. 9) has discussed the relation between the viscosity B-coefficient for individual ions and the partial molar ionic entropy. This relation has been the basis for his selection of -5.5 e.u. as the absolute partial molar entropy of the hydrogen ion at 25°.[12] In a separate study to be described in another paper,[13] it will be demonstrated that a self-consistent set of radii for hydrated ions can correlate all the features of the viscosity B-coefficient/ionic entropy relations. In addition, if allowance is made for the configurational contributions to the ionic entropy (*e.g.*, rotational entropy), the absolute partial molar ionic entropy can be shown to be a single linear function of the viscosity ionic B-coefficient. Using these relations, the B-coefficient for the perchlorate ion has been estimated to be -0.05, and this compares favorably with the value of -0.056 reported in this study. By virtue of its minimum solvation, the hydrated perchlorate ion is sufficiently small to loosen or disrupt locally the pseudo-tetrahedral structure of the water in the co-sphere about the ion and hence decrease the viscosity of the solvent about this ion. Such behavior is commonly observed only in water, and only for the few ionic species whose effective hydrated radii are minimal.

Acknowledgment.—The assistance of Mr. H. D. Russell in measuring some of the densities of the sodium perchlorate solutions is acknowledged.

(7) G. Jones and M. Dole, *J. Am. Chem. Soc.*, **51**, 2950 (1929).

(8) H. Falkenhagen and E. L. Vernon, *Physik. Z.*, **33**, 140 (1932).

(9) R. W. Gurney, "Ionic Process in Solution," McGraw-Hill Book Co., Inc., New York, N. Y., 1953, p. 160 ff.

(10) M. Kaminsky, *Z. Naturforsch.*, **12a**, 424 (1957).

(11) W. M. Cox and J. H. Wolfenden, *Proc. Roy. Soc. (London)*, **A145**, 475 (1934).

(12) K. H. Laidler, *Can. J. Chem.*, **34**, 1107 (1956).

(13) E. R. Nightingale, Jr., to be published.

THE VIRIAL TREATMENT OF THE INTERACTION OF GAS MOLECULES WITH SOLID SURFACES[1]

BY ROBERT S. HANSEN

Institute for Atomic Research and Department of Chemistry, Iowa State College, Ames, Iowa

Received July 31, 1958

The virial treatment of gas–solid interactions developed by Halsey and co-workers[2–5] was extended to interaction potentials based on the Lennard-Jones 6–12 potential for intermolecular attraction, which is known to give a better representation of gas second virial coefficients than does the rigid sphere model used by Halsey and co-workers.[6,7] Independently, this problem also has been attacked by DeMarcus, Hopper and Allen[8] and by Freeman.[9] This paper will therefore be limited to conclusions other than those reached by these workers.

The second virial coefficient for gas–solid interaction, including correction for quantum effect[7,8] is given by

$$\lim_{P\to 0}\left(\frac{NkT}{P} - V\right) = A\left\{\int_0^\infty (e^{-\epsilon(x)/kT} - 1)\,dx - \frac{\hbar^2}{24mk^2T^2}\int_0^\infty \frac{\partial^2\epsilon}{\partial x^2} e^{-\epsilon(x)/kT}\,dx\right\} \qquad (1)$$

where $\epsilon(x)$ is the potential energy of a gas molecule at a distance x from the solid, taken as a semi-infinite slab. The molecular 6–12 potential has been taken in the form suggested by Hirschfelder, Curtiss and Bird[7] to facilitate use of their tabular parameter data

$$\varphi(r) = 4\epsilon^0\left[\left(\frac{\sigma}{r}\right)^{12} - \left(\frac{\sigma}{r}\right)^{6}\right] \qquad (2)$$

where $\varphi(r)$ is the interaction potential energy of two

(1) Work was performed in the Ames Laboratory of the Atomic Energy Commission.

(2) W. A. Steele and G. D. Halsey, Jr., *J. Chem. Phys.*, **22**, 979 (1954).

(3) W. A. Steele and G. D. Halsey, Jr., THIS JOURNAL, **59**, 57 (1955).

(4) M. P. Freeman and G. D. Halsey, Jr., *ibid.*, **59**, 181 (1955).

(5) G. Constabaris and G. D. Halsey, Jr., *J. Chem. Phys.*, **27**, 1433 (1957).

(6) R. H. Fowler and E. A. Guggenheim, "Statistical Thermodynamics," The University Press, Cambridge, 1949.

(7) J. O. Hirschfelder, C. F. Curtiss and R. B. Bird, "Molecular Theory of Gases and Liquids," John Wiley and Sons, Inc., New York, N. Y., 1954.

(8) W. C. DeMarcus, E. H. Hopper and A. M. Allen, A.E.C. Bulletin K1222 (1955).

(9) M. P. Freeman, THIS JOURNAL **62**, 723 (1958).

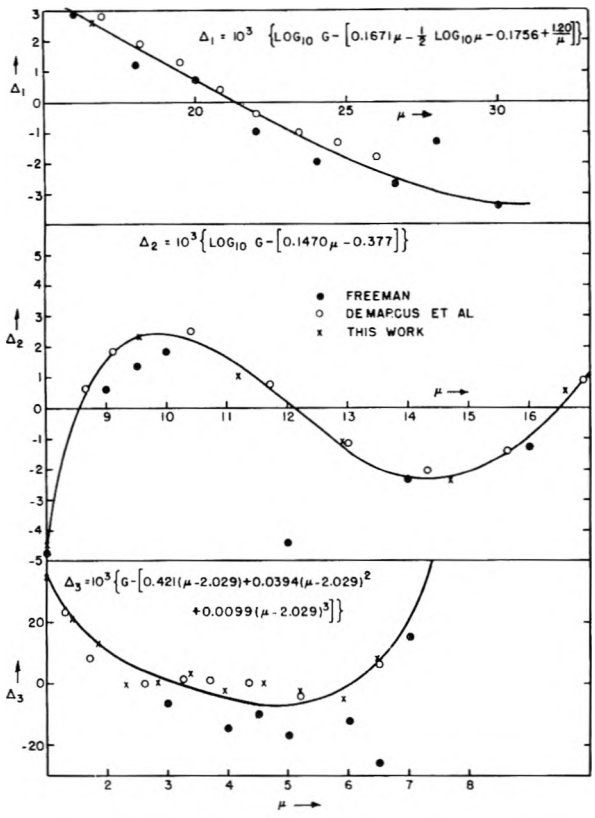

Fig. 1.

molecules (in this case, one in the gas, one a molecule of the solid). By integrating this expression over all molecules in the semi-infinite solid, we obtain, where ρ is the number of molecules per unit volume in the solid

$$\epsilon(x) = -\frac{2\pi\epsilon^0\rho\sigma^3}{3}\left[\left(\frac{\sigma}{x}\right)^3 - \frac{2}{15}\left(\frac{\sigma}{x}\right)^9\right] \quad (3)$$

If this potential is substituted in eq. 1, it is possible to perform the indicated integrations to obtain convergent power series expressions for the second virial coefficient. These are

$$\lim_{P\to 0}\left(\frac{NkT}{P} - V\right) = \sigma A\left\{G(\mu) - \frac{A}{T}R(\mu)\right\} \quad (4)$$

where

$$G(\mu) = \frac{1}{9}\left(\frac{2}{15}\right)^{1/6}\mu^{1/3}\sum_{n=0}^{\infty}\frac{\mu^{2n/3}}{n!}\Gamma\left(\frac{3n-1}{9}\right) \quad (4a)$$

$$R(\mu) = \mu^{-1/3}\sum_{n=0}^{\infty}\frac{\mu^{2n/3}}{n!}\left(\frac{n}{5}+\frac{1}{9}\right)\Gamma\left(\frac{3n+1}{9}\right) \quad (4b)$$

with

$$\mu = \frac{T_0}{T} = \frac{\pi\epsilon^0\rho\sigma^3}{kT}\left(\frac{10}{3}\right)^{1/2}, \quad A = \left(\frac{15}{2}\right)^{1/6}\frac{5\hbar^2}{12m\sigma^2 k} = \frac{28.1}{M\sigma_A^2}$$

$M = N_0 m$ = molecular weight of the gas, $\sigma_A = 10^8\sigma = \sigma$ in ångström units.

Results of DeMarcus, *et al.*,[8] and Freeman[9] are in a somewhat different form because different forms of the 3–9 potential eq. 3 were used; their parameters and quantities compare with those in the present work as

$$\frac{\epsilon}{kT}\text{ (DeMarcus, } et\ al.\text{)} = \frac{\epsilon^*}{kT}\text{ (Freeman)} = \frac{2\sqrt{3}}{9}\mu = 0.3849\,\mu$$

$$z_0\text{ (DeMarcus, } et\ al.\text{)} = S_0\text{ (Freeman)} = \left(\frac{2}{15}\right)^{1/6}\sigma$$

$$-I_1\text{ (DeMarcus, } et\ al.\text{)} = \frac{B_{AS}}{AS_0}\text{ (Freeman)} = \left(\frac{15}{2}\right)^{1/2}G(\mu)$$

$$I_2\text{ (DeMarcus, } et\ al.\text{)} = \frac{15\sqrt{3}}{\mu}R(\mu)$$

Asymptotic equations for $G(\mu)$ and $R(\mu)$ can be based on the fact that, if $f(x)$ has a strong maximum at x_0

$$\int_0^\infty g(x)\exp\{f(x)\}\,dx \sim g(x_0)\exp\{f(x_0)\}\int_{-\infty}^{\infty}\exp\left\{\left(\frac{d^2f}{dx^2}\right)_{x_0}\frac{u^2}{2}\right\}d\mu \quad (5)$$

which leads to

$$G(\mu) \sim \left\{\frac{\pi}{3}\left(\frac{2}{15}\right)^{1/2}\left(\frac{5}{2}\right)^{1/6}\right\}^{1/2}\mu^{-1/2}\exp\left\{\frac{2\mu}{3\sqrt{3}}\right\} \quad (6a)$$

$$R(\mu) \sim \left\{3^{1/6}\frac{3\pi}{25}\right\}^{1/2}\mu^{1/2}\exp\left\{\frac{2\mu}{3\sqrt{3}}\right\} \quad (6b)$$

valid for large μ.

The series 4a and 4b are slowly convergent; the following empirical analytical forms were therefore developed for convenient representation

$$\log G(\mu) = 0.1671\mu - \frac{1}{2}\log\mu - 0.1756 + \frac{1.20}{\mu} \pm 0.003 \text{ for } 16 < \mu < 30 \quad (7a)$$

$$\log G(\mu) = 0.1470\mu - 0.377 \pm 0.002 \text{ for } 8.2 < \mu < 17.4 \quad (7b)$$

$$G = 0.421(\mu - 2.029) + 3.94\times 10^{-2}(\mu - 2.029)^2 + 9.9\times 10^{-3}(\mu - 2.029)^3 \pm 0.01,\ 2 < \mu < 6.5 \quad (7c)$$

$$\log R(\mu) = 0.1671\mu + \frac{1}{2}\log\mu - 0.1721 + \frac{0.420}{\mu} \pm 0.001,\ 12 < \mu < 26 \quad (8a)$$

$$\log R(\mu) = 0.1294 + 0.1981\mu - 6.76\times 10^{-4}\mu^2 \pm 0.001,\ 1 < \mu < 14 \quad (8b)$$

The first three terms on the right in equations 7a and 8a derive in each case from the asymptotic expressions (6a) and (6b); the terms in $1/\mu$ are empirical corrections. Equations 7a and 8a have been tested to the upper limits indicated, but may be expected to apply reasonably well above these limits. Figure 1 compares calculations of the present work, those of DeMarcus, *et al.*, and those of Freeman in difference plots against eq. 7a, 7b, 7c, permitting accurate corrections to these empirical equations if desired.

Equation 6b is particularly useful in the evaluation of parameters; many of the data of Halsey and co-workers is in the range covered by this formula, so that the slope of the linear portion of a plot of $\log \lim_{P\to 0}(NkT/P - V)$ against $1/T$ divided by 0.1470 gives the ratio of μ to T, *i.e.*, $T_0 = (10/3)^{1/2}\times\pi\epsilon^0\rho\sigma^3/k$.

Omission of the quantum correction (term in $R(\mu)$) causes little error in the surface area calculated by this treatment; the correction in $\lim_{P\to 0}(NkT/P - V)$ amounts to 7% for the system He–

carbon black[2] at 78°K. and 3% for the same system at 194°K. The deviations due to quantum effects should, however, be observable.

Data represented by equation 4, omitting the term in $R(\mu)$, in the range $8 < \mu < 17$ will be almost equally well represented by the treatment of Steele and Halsey based on a rigid sphere – inverse r^3 potential model, relevant parameters corresponding as follows: ϵ^*/k (Steele and Halsey) $= 0.422T_0$; (AD_0) (Steele and Halsey) $= 1.695\ (A\sigma)$. The range of agreement can be extended toward lower values of μ by choosing different geometric volumes in the two treatments. Accurate high temperature data will resolve between the two models since the model based on the 6–12 potential leads to zeros in $\lim_{P\to 0}(NkT/P - V)$ at $\mu = 2.029$ and at $\mu = 0$ with an intervening minimum at $\mu = 0.166$ ($G(0.166) = -0.545$), while the model of Steele and Halsey leads to a single zero at $\mu = 3.4$ and a monotone decrease to $-AD_0$ at $\mu = 0$.

Treatments of gas imperfections due to gas–solid interactions based on eq. 4 or on the model of Steele and Halsey determine the products $A\sigma$ or AD, and evaluation of the surface area A requires the independent evaluation of the parameters σ or D. Previous workers[2–5,9] have estimated these parameters from the Kirkwood–Mueller formula for intermolecular forces; Steele and Halsey[2] comment on the low values thus obtained. It is also reasonable to calculate the parameters σ and ϵ^0 from the "combining laws" cited by Hirschfelder, Curtiss and Bird (ref. 7, pp. 168–9), *i.e.*, $\sigma_{12} = 1/2(\sigma_{11} + \sigma_{22})$, $\epsilon^0_{12} = (\epsilon^0_{11}\epsilon^0_{22})^{1/2}$. The values of σ_{12} thus calculated are higher than those obtained by the Kirkwood–Mueller formula, and the surface areas computed by their use are lower. For the carbon black "Black Pearls 71" studied by Steele and Halsey, surface areas obtained by them using Ne and A were 367 and 262 m.²/g. compared to a B.E.T. nitrogen surface area of 337 m.²/g. Results obtained using eq. 4 and the "combining law" evaluation of σ were 151 and 160 m.²/g. for Ne and A, respectively. Freeman[9] reports an argon area of 162 m.²/g. for this adsorbent using the Kirkwood–Mueller formula and a treatment with the same basis as eq. 4 but using different data. Surface areas computed from gas imperfection data appear to be generally less than those evaluated by the B.E.T. method for the same adsorbent.

A film on the surface of the adsorbent whose thickness is of the order σ (*i.e.*, molecular dimensions) should have an important effect on gas imperfections due to gas–solid interaction. Suppose there is a film of thickness Δ on the surface of the semi-infinite slab which serves as a model for the solid adsorbent. Let ϵ^0_f and σ_f be the parameters of eq. 2 corresponding to the film material, and let ρ_f be the number of molecules per unit volume in the film. Then the analog of eq. 3 becomes

$$\epsilon(x) = -\frac{2\pi\epsilon^0_f\rho_f\sigma_f^3}{3}\left\{\left(\frac{\sigma_f}{x}\right)^3 - \frac{2}{15}\left(\frac{\sigma_f}{x}\right)^9 - \left(\frac{\sigma_f}{x+\Delta}\right)^3\left[1 - \frac{\epsilon^0\rho}{\epsilon^0_f\rho_f}\left(\frac{\sigma}{\sigma_f}\right)^6 + \frac{2}{15}\left(\frac{\sigma_f}{x+\Delta}\right)^9\left[1 - \frac{\epsilon^0\rho}{\epsilon^0_f\rho_f}\left(\frac{\sigma}{\sigma_f}\right)^{12}\right]\right\} \quad (9)$$

Now at least at sufficiently low temperature the asymptotic evaluation of first integral in eq. 1 indicates that $\ln \lim_{P\to 0}(NkT/P) - V$ must vary linearly with $1/T$, and the slope must be $-(\epsilon(x_0)/k)$, where x_0 is the value of x at which $\epsilon(x)$ has a minimum. Evidently if $\Delta \sim \sigma_f$ or $\Delta > \sigma_f$ $\epsilon(x_0)$ will depend importantly on Δ, ρ_f, ϵ^0_f, and σ_f, *i.e.*, on parameters of the film. The presence of such a film on carbon surfaces is to be strongly suspected from the work of Anderson and Emmett[10] unless rigorous outgassing procedures have been followed.

Acknowledgment.—I am indebted to Dr. Mark P. Freeman for calling my attention to the work of DeMarcus, Hopper and Allen, for furnishing me a copy of his own paper on this subject in advance of publication, and for stimulating oral and written discussion.

(10) R. B. Anderson and P. H. Emmett, THIS JOURNAL, **51**, 1308 (1947).

A METHOD FOR THE CALCULATION OF BOND MOMENTS FROM ELECTRONEGATIVITY DATA[1]

BY RICARDO DE CARVALHO FERREIRA

Escola Superior de Química, University of Recife, Brazil

Received November 10, 1958

The purpose of this note is to describe a method for the calculation of the polarity of simple bonds based on the principle of electronegativity equalization of Sanderson.[2] We will show that this principle is completely general and may be applied for the determination of the charge distribution in simple molecules.

Sanderson's principle may be derived as follows: let us suppose that the electronegativity of a certain atom A is greater than the electronegativity of another atom B, $X_A(0) > X_B(0)$. If these atoms combine to form a molecule AB, then after the sharing of one electron-pair, A will acquire a partial negative charge and B will acquire a partial positive one. The electronegativity of A will thus decrease and that of B will increase until the charge distribution in the molecule AB is such that $A^{-\delta}$ and $B^{+\delta}$ have the same electronegativity.

At this point it will be interesting to examine the meaning of the concept of electronegativity in the light of Sanderson's principle. Electronegativity as defined by Pauling,[3] Mulliken,[4] Gordy[5] and others,[6,7] has the dimensions of *energy*. However, chemists have always used the concept of electronegativity as a characteristic atomic *potential:* the power of an atom in a molecule to attract electrons to itself.[8] Now, this is precisely what is borne out by the principle of electronegativity

(1) This work has been supported by the Conselho Nacional de Pesquisas, Rio de Janeiro.

(2) R. T. Sanderson, *Science*, **114**, 670 (1951).

(3) L. Pauling, *J. Am. Chem. Soc.*, **54**, 3570 (1932).

(4) R. S. Mulliken, *J. Chem. Phys.*, **2** 782 (1934).

(5) W. Gordy, *Phys. Rev.*, **69**, 604 (1946).

(6) T. L. Cottrell and L. E. Sutton, *Proc. Roy. Soc.* (*London*), **A207**, 49 (1951).

(7) H. O. Pritchard and H. A. Skinner, *Chem. Revs.*, **55**, 745 (1955).

(8) L. Pauling, "The Nature of the Chemical Bond," Cornell University Press, Ithaca, N. Y., 1939, p. 58.

equalization: the electronegativities (potentials) of two atoms are equalized during the formation of a chemical bond.

The electronegativity X of an atom is a function of the net atomic charge q. Developing $X(q)$ in powers of q and disregarding higher terms

$$X(q) = X(0) + q(dX/dq)(0) \qquad (1)$$

Thus, as a first approximation we may suppose that there is a linear relationship between electronegativity and charge. Pauling,[3] Haissinsky,[9] and Daudel and Daudel[10] have shown how to calculate (dX/dq) from the electronegativity scale. These authors admitted that the screening constant of one valence electron for another is independent of their electronic wave functions. A more accurate treatment is as follows:

When one goes from an element of atomic number Z to the next one, $(Z + 1)$, the effective nuclear charge increases by $1 - s_k$, where s_k is the screening constant of the differentiating electron of the element $(Z + 1)$. When the element Z loses one valence electron the effective nuclear charge increases by s_i, the screening constant of the lost electron. Hence the increase in the electronegativity of an atom B caused by a positive unitary charge resulting from the complete removal of the i electron of atom B is

$$\Delta X_i^+ = \frac{s_i}{1 - s_k}(X_{Z+1} - X_Z) \qquad (2)$$

Similarly the decrease in the electronegativity of an atom A caused by a unitary negative charge resulting from the complete acceptance of the j electron by atom A is given by

$$\Delta X_j^+ = \frac{s_j}{1 - s_h}(X_Z - X_{Z-1}) \qquad (3)$$

where s_j and s_h are, respectively, the screening constants of the differentiating electrons of elements $(Z + 1)$ and Z. From equation 1

$$X_A(-nq) = X_A(0) - q\sum_{j=1}^{n} \Delta X_j^- \qquad (4)$$

and

$$X_B(+mq) = X_B(0) + q\sum_{i=1}^{m} \Delta X_i^+ \qquad (5)$$

In these equations n and m are the oxidation numbers of atoms A and B, and q is the fractional charge (in electronic units) the atoms will acquire when their oxidation numbers are, respectively, -1 and $+1$. From the principle of electronegativity equalization it follows that

$$q = \frac{X_A(0) - X_B(0)}{\sum_{j=1}^{n} \Delta X_j^- + \sum_{i=1}^{n} \Delta X_i^+} \qquad (6)$$

It is seen that in principle it is possible to calculate the charge distribution of simple molecules from electronegativity data. However, a difficulty arises in the choice of suitable screening constants. The screening constant of one valence electron for another varies with the electronic wave function and with the atomic number. Besides, it is well known that different screening constants must be used for different properties (ionic size, ionization potential, electron-affinity, etc.).[11] In fact, Hartree[12] recently proposed the use of the term *screening parameter* instead of *screening constant* because the quantity s is not constant for variations of any of the variables of which it might be considered a function.

Screening constants for electronegativities are not known. However, if we use Mulliken's definition, $X = I + E$, and since the ionization potential (I) is generally much greater than the electron-affinity (E), we may use the ionization potential screening constants calculated by Kohlrausch[13] without introducing very serious errors.

We have followed this procedure for the calculation of the charge distribution of the hydrogen halides, using the corrected electronegativity values of Mulliken's scale as given by Pritchard and Skinner.[7] Applying equations 2 and 3 we obtained the values: $\Delta X_H^+ = 2.62$; $\Delta X_F^- = 2.40$; $\Delta X_{Cl}^- = 1.92$; $\Delta X_{Br}^- = 2.39$; $\Delta X_I^- = 2.42$.

Table I shows the values of q obtained from equation 6 and the values of the dipole moments (μ_{calcd}) obtained by multiplying the charge q by the experimental interatomic distances H–X. This is strictly correct only if the pure covalent function Ψ_{H-X} describes a state of zero dipole moment.[14] For the molecules HX the theoretical calculations are contradictory,[15,16] and our values are in good agreement with the experimental values of the dipole moments[17-19] shown in the second column of Table I.

TABLE I

Compound	q (electronic) units	$\mu_{expt.}$ D	$\mu_{calcd.}$ D
HF	0.32	1.91	1.39
HCl	.16	1.03	1.01
HBr	.10	0.78	0.68
HI	.05	0.38	0.38

Acknowledgments.—We wish to thank Professor G. Beck and Dr. J. Danon for valuable discussions.

(9) M. Haissinsky, *J. Phys.*, **7**, 7 (1946).
(10) P. Daudel and R. Daudel, *ibid.*, **7**, 12 (1946).
(11) L. Pauling and J. Sherman, *Z. Krist.*, **81**, 1 (1932).
(12) D. R. Hartree, *Rev. Mod. Phys.*, **30**, 63 (1958).
(13) K. W. F. Kohlrausch, *Acta Phys. Austr.*, **3**, 452 (1949).
(14) C. A. Coulson, *Proc. Roy. Soc. (London)*, **A207**, 63 (1951).
(15) D. Z. Robinson, *J. Chem. Phys.*, **17**, 1022 (1949).
(16) P. N. Schatz, *ibid.*, **22**, 695 (1954).
(17) C. T. Zahn, *Phys. Rev.*, **27**, 455 (1926).
(18) R. P. Bell and I. E. Coop, *Trans. Faraday Soc.*, **34**, 1209 (1938).
(19) N. B. Hannay and C. P. Smyth, *J. Am. Chem. Soc.*, **68**, 171 (1946).

BOILING POINTS OF NORMAL PERFLUOROALKANES

BY WILLIAM POSTELNEK

Materials Laboratory, Wright Air Development Center, United States Air Force, Wright-Patterson Air Force Base, Ohio

Received August 28, 1958

Previously, no simple equations have been proposed which relate the number of carbon atoms of fluorocarbons to their boiling points. However, many empirical relationships have been proposed for calculation of boiling points of normal hydro-

TABLE I

BOILING POINTS OF NORMAL PERFLUOROALKANES (T = °K.)

No. of carbon atoms (n)	Formula	T(obsd.)	T(calcd.)	No. of carbon atoms (n)	Formula	T(obsd.)	T(calcd.)
1	CF_4	145[2]	142	8	C_8F_{18}	377[13]	
2	C_2F_6	194[3]	194.2			380[11]	379.6
3	C_3F_8	234[1]		9	C_9F_{20}	395.5–6.5[13]	
		237[5]	237.2			398.3[15]	
4	C_4F_{10}	271.3[6]				400[11]	400
		274[4]	273.4	10	$C_{10}F_{22}$	417.2[15]	418.8
		277[7]				423[11]	
5	C_5F_{12}	303.1[8]	304.8	11	$C_{11}F_{24}$	433.8[15]	436.2
6	C_6F_{14}	329[9]		12	$C_{12}F_{26}$		452.4
		330[10]		13	$C_{13}F_{28}$	466–9[11]	467.6
		331[11]		14	$C_{14}F_{30}$		481.8
		333[12]	333.2	15	$C_{15}F_{32}$		495.3
7	C_7F_{16}	355[13]		16	$C_{16}F_{34}$	511–13[16]	508
		355.5[14]	357.2				

carbons. Notable among these is that of Egloff, Sherman and Dull,[1] who observed this relationship to exist (equation 1)

$$T = a \log (n - b) + k \qquad (1)$$

where T is the boiling point in degrees Kelvin, n is the number of carbon atoms in a hydrocarbon molecule and a, b and k are empirical constants. Equation 2 was derived from evaluation of the observed boiling points of normal alkanes and subsequent curve-fitting.[1]

$$T = 745.42 \log (n + 4.4) - 416.31 \qquad (2)$$

By application of equation 1 to the observed boiling points of normal perfluoroalkanes, and by curve-fitting according to the method of least squares, the constants a, b and k were evaluated to give the proposed equation 3

$$T = 540.87 \log (n + 3) - 183.67 \qquad (3)$$

Boiling points were calculated for normal perfluorocarbons from CF_4 to $C_{16}F_{34}$ using equation 3.

Calculated boiling points are compared with observed boiling points in Table I. Since an appreciable variation exists in boiling points reported for the same compound by different investigators, it is not possible to effectively assess the accuracy of equation 3 at this time, and the accuracy of this equation can be said to be in the order of ±3.5°. However, good agreement is noted to exist between the calculated boiling point and at least one of the observed boiling points in most of the cases studied. The chief reason for the variation in the observed boiling points as reported for a given fluorocarbon probably can be attributed to isomerization which might have occurred during the fluorination process to give branched compounds which were not detectable by analytical means available during the early periods of fluorocarbon research. The 3 degree anomaly for the first member of the series was not unexpected, since Egloff observed an 18 degree difference between the observed and calculated boiling point of methane.

The boiling points for n-$C_{12}F_{26}$, n-$C_{14}F_{30}$, and n-$C_{15}F_{32}$ which have not been reported at this time are predicted to be 452.4, 481.8 and 495.3°K., respectively.

(1) G. Egloff, J. Sherman and R. B. Dull, THIS JOURNAL, **44**, 730 (1940).

(2) J. D. Calfee and L. A. Bigelow, *J. Am. Chem. Soc.*, **59**, 2072 (1937).

(3) O. Ruff and O. Bretschneider, *Z. anorg. allgem. Chem.*, **210**, 173 (1933).

(4) R. N. Haszeldine, *J. Chem. Soc.* 3559 (1953).

(5) P. Lebeau and A. Damiens, *Compt. rend.*, **191**, 939 (1930).

(6) R. D. Fowler, J. M. Hamilton, *et al.*, *Ind. Eng. Chem.*, **39**, 375 (1947).

(7) J. H. Simons and L. P. Block, *J. Am. Chem. Soc.*, **59**, 1407 (1937).

(8) L. L. Burger and G. H. Cady, *ibid.*, **73**, 4243 (1951).

(9) M. Hauptschein and A. V. Grosse, *ibid.*, **74**, 4454 (1952).

(10) R. N. Haszeldine and E. G. Walaschewski, *J. Chem. Soc.*, 3607 (1953).

(11) A. F. Benning and J. D. Park, U. S. Patent 2,490,764 (1949).

(12) J. H. Simons and L. P. Block *J. Am. Chem. Soc.*, **61**, 2962 (1939).

(13) M. Stacey, *Roy. Inst. Chem. G. Brit. and Ireland*, 1 (1948).

(14) G. D. Oliver, S. Plumkin and C. W. Cunningham, *J. Am. Chem. Soc.*, **73**, 5722 (1951).

(15) R. N. Haszeldine, *J. Chem. Soc.*, 3617 (1950).

(16) W. B. Burford, R. D. Fowler, *et al.*, *Ind. Eng. Chem.*, **39**, 319 (1947).

DIPOLE MOMENTS OF SOME AMINE EXTRACTANTS IN BENZENE

BY W. J. MCDOWELL AND KENNETH A. ALLEN

Oak Ridge National Laboratory, Oak Ridge, Tennessee[1]

Received August 29, 1958

Previous studies of the long chain amines in liquid–liquid extraction systems have shown that the sulfate and bisulfate salts of these extractants do not behave as would be expected for monomeric solutes.[2] Recent light scattering measurements[3] have shown, indeed, that the sulfates of most of the amines investigated are aggregated, but to widely varying degrees, depending on chain branching and class. In the present investigation, the dielectric behavior of these solutes was examined as a further means of elucidating their structures.

Experimental

Capacitance measurements were made in the range 15 Kc.

(1) Operated for the U. S. Atomic Energy Commission by Union Carbide Nuclear Company.

(2) K. A. Allen, THIS JOURNAL, **60**, 239, 943 (1956); W. J. McDowell and C. F. Baes, Jr., *ibid.*, **62**, 777 (1958); K. A. Allen, *J. Am. Chem. Soc.*, **80**, 4133 (1958).

(3) K. A. Allen, THIS JOURNAL, **62**, 1119 (1958).

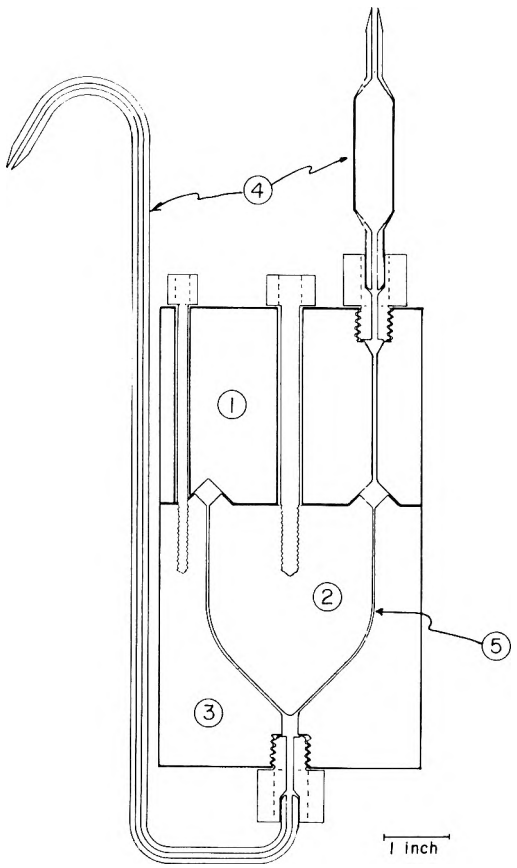

Fig. 1.—Dielectric constant cell: the Teflon block (1) supports the gold-plated brass electrodes (2,3) by means of the central bolt and six peripheral bolts of stainless steel. The glass fittings (4) were press-fitted into Teflon plugs. The annular space (5) between the electrodes was 0.020".

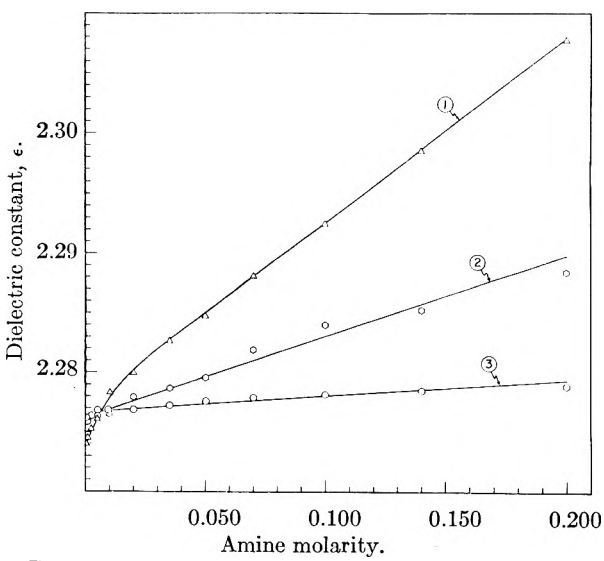

Fig. 2.—Dielectric constants of benzene solutions of amines: (1) 1-(3-ethylpentyl)-4-ethyloctylamine; (2) di-*n*-decylamine; (3) tri-*n*-octylamine.

to 5 Mc. using a General Radio capacitance bridge (Type 716-CS1) and signal generator (Type 1330A). Sensitive radio receivers of the appropriate frequency coverage were employed as null detectors. The cell for the solution samples is shown in Fig. 1. This cell allowed the use of small volumes (*ca.* 30 ml.) and provided for easy and thorough cleaning while in a fixed position in the constant temperature bath. Its capacitance with air was *ca.* 300 $\mu\mu$f.; the measurements were made to within 0.05 $\mu\mu$f. The capacitance of the cell was temperature dependent; however, thermostatting at 25.00 ± 0.01° proved to be sufficiently close temperature control to make thermal fluctuations in the capacitance immeasurably small. The dielectric constant ϵ was computed from the relation

$$\epsilon_x - \epsilon_a = (C_x - C_a)\frac{\epsilon_s - \epsilon_a}{C_s - C_a}$$

where the subscripts refer to the ϵ and C (capacitance) values with dry air, a, cyclohexane, s, and solution, x, in the cell.[4]

For the measurements at frequencies higher than 5 Mc. a Boonton Type 170-A "Q" meter having a frequency range of from 30 to 200 Mc. was used. A small sample cell containing two parallel plates was attached directly to the binding posts used for measuring small (*ca.* 1.5 to 2.5 $\mu\mu$f.) unknown capacitances. The differences in the capacities of the cell with air, standard and solution were obtained on maximizing the LC current in the meter circuit by appropriate adjustments of the built-in precision condenser. These measurements were, of course, much less accurate than those obtained at lower frequencies; however, they were reproducible to within 1%, and the conclusions drawn below with respect to anomalous frequency dispersion are considered quite reasonable.

The amines are characterized in Table I. The dry amine solutions were dehydrated over metallic sodium. Sulfate salts of the amines were prepared by contacting benzene solutions of the amines with aqueous sulfuric acid solutions. As a consequence, the amine sulfate solutions prepared in this way contained equilibrium concentrations of water: that soluble in the benzene at 25° (*ca.* 0.5 mg./ml.)[5] plus that associated with the extractant species, presumably as water of hydration. While the presence of such water lessens the validity of comparing the present results with those of others who used anhydrous materials (*e.g.*, C. A. Kraus[9]), it was of importance to observe the dielectric behavior of the actual extractant systems, such as those for which the aggregation behavior had already been obtained from light scattering measurements.[3] For comparison, measurements also were made on a nearly anhydrous preparation of di-*n*-decylamine sulfate, one of the solutes of greatest previous theoretical interest.[2,3] The dry di-*n*-decylamine sulfate was prepared by evaporating the solvent benzene and removing water from the salt by evacuation. The dry salt then was dissolved in dried benzene (the dried benzene averaged *ca.* 0.06 mg. H_2O/ml.). The analytical methods for the organic amine, sulfate and water determinations have been described elsewhere.[2]

TABLE I

AMINE COMPOSITION AND PURITY

Amine	Neutr. equil. Found	Neutr. equil. Theor.	Composition, % Primary	Composition, % Secondary	Composition, % Tertiary
1-(3-Ethylpentyl)-4-ethyloctyl	255	255	>99	<0.5	<0.5
Di-*n*-decyl	300	298	<0.5	98	2
Tri-*n*-octyl	354	354	<0.5	<0.5	>99

Results and Discussion

Dielectric constant measurements as a function of frequency on 0.05 to 0.10 *M* benzene solutions of di-*n*-decylamine sulfate over the range 15 Kc. to 195 Mc. did not show a dielectric dispersion in this region which was detectable with the available

(4) The use of the equation above with a standard liquid dielectric and a permanently-fixed arrangement of electrical components eliminates the effects of lead capacitances. Cyclohexane was chosen as a standard dielectric rather than the commonly used benzene principally because it is much more easily dried and maintained free of water than benzene. The value ϵ_s = 2.0173 for cyclohexane at 25° was taken from the work of L. Hartshaw, J. V. L. Parry and L. Essen, *Proc. Phys. Soc.* (*London*), **68B**, 422 (1955). The value ϵ_a = 1.006 was taken from R. J. W. LeFevre "Dipole Moments," Methuen and Co., London, 1948.

(5) G. G. Joris and H. S. Taylor, *J. Chem. Phys.*, **16**, 45 (1948).

equipment. According to calculations by the Debye equation, from the molecular weight found by light scattering measurements (*ca.* 30,000) for di-*n*-decylamine sulfate in benzene,[3] a dispersion should occur at around 40 Mc. if this entire particle is acting as a single dipole.[6] The fact that no such dispersion is observed suggests that the bonding in the aggregate is not of such a nature as to prevent the orientation of the monomers in the electric field. Thus, it is probable that the bonds holding the aggregate together are quite weak, possibly not more than a few kcal./mole. Since di-*n*-decylamine sulfate exhibits the largest particle size of any of the amine sulfates examined by light scattering methods, the absence of a dispersion for this solute made it unlikely that such dispersions would be observed for the other amine sulfates. Consequently, further study was restricted to measurements of the dielectric constants of the solutions as functions of concentration, at a fixed frequency of 1 Mc., for which optimum accuracy was obtainable from the electronic equipment.

The dielectric constants of benzene solutions of the various amines and their sulfate salts as functions of concentration are shown in Figs. 2, 3 and 4. Apparent dipole moments calculated by the method of Guggenheim[7] may be seen in Table II. In the two cases where two values of the moment are shown, the first was computed from a high slope of the ϵ *vs.* M line observed at low concentrations (<0.010 M for 1-(3-ethylpentyl)-4-ethyloctylamine and <0.0015 M for dry di-*n*-decylamine sulfate). The second value of μ resulted from the slopes above the fairly abrupt transition between the two dependences (see Fig. 5; the "limiting" slopes for these second values were obtained from the points above the transition, ignoring the points used for the first values), and is representative of a much wider concentration range, as is apparent from the figures.

In addition to the changes of slope at low concentrations, it will be noticed that several of the ϵ *vs.* M plots show a pronounced curvature at higher concentrations. Hooper and Kraus[8] found such

(6) The validity of the Debye–Stokes equation $\tau_d = 4\pi a^3\eta/kT$, for the relaxation time τ_d in terms of a, the molecular diameter and η, the viscosity of the medium (P. Debye, "Polar Molecules," Reinhold Publ. Corp., New York, N. Y., 1929), and particularly its application to molecular weight determinations, has been questioned by some authors (see *e.g.*, R. E. Powell and H. Eyring in "Advances in Colloid Science," E. O. Kraemer, editor, Interscience Publishers Inc., New York, N. Y., 1942, Vol. I, pp. 213–223). However, it is probably good to within a factor of two, and since the measurements extended to *ca.* 200 Mc., and since in addition the dielectric constants appeared to increase slightly at the higher frequencies rather than decrease, it was considered reasonable to assume the absence of a detectable dispersion in the predicted frequency range.

(7) In the Guggenheim method of calculating dipole moments (E. A. Guggenheim, *Trans. Faraday Soc.*, **45**, 714 (1949)), the quantity $\Delta = (\epsilon - n^2) - (\epsilon_1 - n_1^2)$, where ϵ = dielectric constant of solution, n = refractive index of solution, ϵ_1 = dielectric constant of solvent and n_1 = refractive index of solvent, is plotted against c, the concentration of polar solute in moles per cc. The limiting slope of the line $(\Delta/c)_0$, is then used to calculate the moment by means of the equation

$$\mu^2 = \frac{9kT}{4\pi N_0} \frac{3}{(\epsilon_1 + 2)(n_1^2 + 2)} (\Delta/c)_0$$

where N_0 is Avogadro's number. As a matter of convenience, for the present data Δ was plotted against the concentration in moles per liter, M, and the resulting slope was multiplied by 1000.

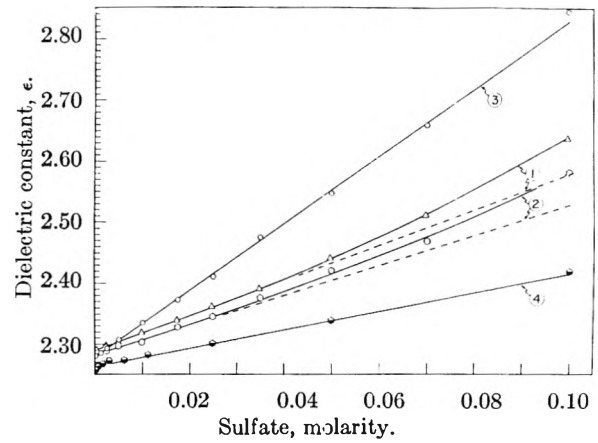

Fig. 3.—Dielectric constants of benzene solutions of amine sulfates: (1) 1-(3-ethylpentyl)-4-ethyloctylamine sulfate; (2) di-*n*-decylamine sulfate (the broken line is an extension of the straight portion at low concentrations to illustrate the deviations from linearity); (3) tri-*n*-octylamine sulfate; (4) di-*n*-decylamine sulfate, dry.

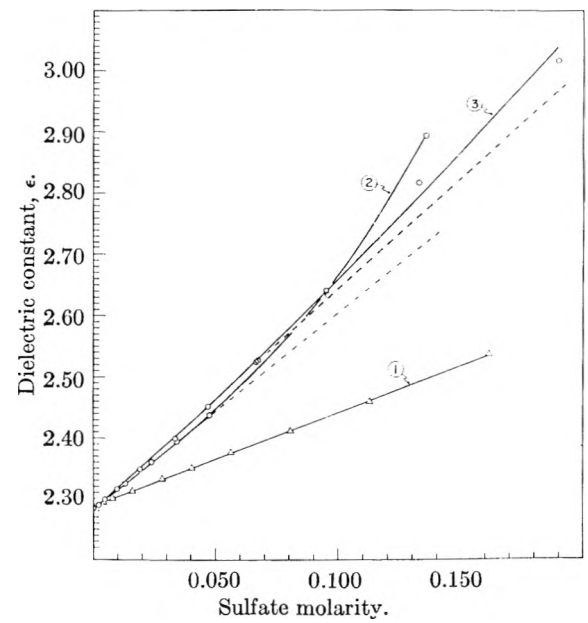

Fig. 4. —Dielectric constants of benzene solutions of amine bisulfates: (1) 1-(3-ethylpentyl)-4-ethyloctylamine bisulfate; (2) di-*n*-decylamine bisulfate; (3) tri-*n*-octylamine bisulfate.

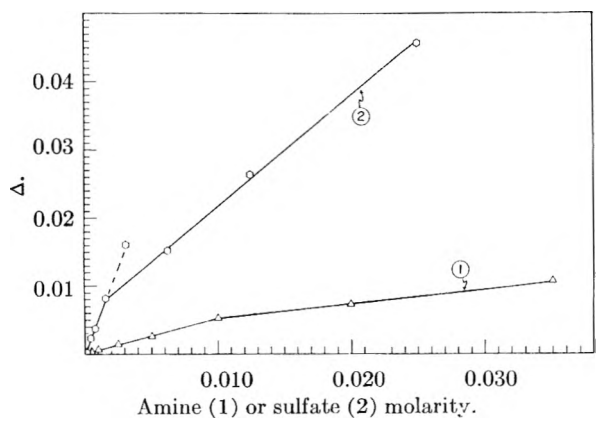

Fig. 5.—Guggenheim slope of lower concentration range of: (1) 1-(3-ethylpentyl-ethyloctylamine and (2) di-*n*-decylamine sulfate, dry.

TABLE II

DIPOLE MOMENTS AT 1 MC.

Form	Condition of prep.	$[H_2SO_4]/[\Sigma R]$	$[H_2O]/[\Sigma R]$	$\mu \times 10^{18}$
A. 1-(3-ethylpentyl)-4-ethyloctylamine				
Amine	dry	(No H_2SO_4)	0.1 to >1	5.07, 4.08
Sulfate	wet	0.500	4	4.95
Bisulfate	wet	.808	3	3.59
B. Di-*n*-decylamine				
Amine	dry	(No H_2SO_4)	<1	2.05
Sulfate	dry	0.515	0.05 to >1	4.4, 3.67
Sulfate	wet	.500	1.5	4.67
Bisulfate	wet	.674	no analysis	5.13
C. Tri-*n*-octylamine				
Amine	dry	(No H_2SO_4)	<1	0.277
Sulfate	wet	0.494	2.5	6.77
Bisulfate	wet	.943	0.94	5.40

deviations from linearity in the measurement of dielectric constants of various tri- and tetraalkylammonium picrates and bromides in benzene. They attributed this effect to an increase in aggregation with concentration, and noted that very symmetrical molecules showed little deviation from linearity, while very unsymmetrical ones showed large deviations. For the present solutes, the light scattering measurements indicated monodisperse aggregates; in addition, there is apparently little or no correlation between the non-linearity observed here and molecular symmetry. It seems likely that some other effect is responsible for the deviations observed.

It is to be noted that the magnitude of the dipole moments in Table II are in a reasonable range for such compounds, although all are somewhat lower than the picrate, acetate and halide salts of some tertiary amines recorded by Geddes and Kraus.[9]

Compound	$\mu \times 10^{18}$
Tri-*n*-butylammonium picrate	13.1
Tri-isoamylammonium picrate	13.3
Tri-*n*-butylammonium iodide	8.09
Tri-*n*-butylammonium bromide	7.61
Tri-*n*-butylammonium chloride	7.17

These differences are to be expected from the more symmetrical arrangement of two alkyl ammonium groups associated with the sulfate radical. Of the compounds investigated here the dipole moments of the free amines show the expected trend, *i.e.*, primary > secondary > tertiary. In the case of the amine sulfates, however, the tertiary amine shows a higher dipole moment than either the primary or secondary amine. Since the latter amine sulfates are known to be aggregated,[3] while tri-*n*-octylamine sulfate is monomeric, this suggests that the moments due to the primary and secondary amine sulfate monomers in the aggregates are partially cancelled by their spatial arrangement. The bisulfates of these amines are likewise out of the expected order. Tri-*n*-octylamine bisulfate, which is known to be dimeric, shows a sharp decrease in polarity from the sulfate, again in qualitative accord with masking due to the molecular grouping.

Understanding of the dielectric behavior of these solutes is, of course, far from complete. Among the questions remaining to be answered is the role of water in the apparent dipole moment and in the degree of aggregation of the amine salts in organic diluents. In this connection the behavior shown by a relatively dry sample of di-*n*-decylamine sulfate is interesting (see Fig. 5). The solution contained a small amount of water (*ca.* 0.06 mg./ml.), and a change in slope of the dielectric constant curve for this solute occurs in the region of two waters per mole of amine sulfate.[10] This suggests the possibility of a stoichiometric hydrate, which may be of importance in controlling the extent and/or the stability of the aggregation.

(8) G. S. Hooper and C. A. Kraus, *J. Am. Chem. Soc.*, **56**, 2265 (1934).

(9) J. A. Geddes and C. A. Kraus, *Trans. Faraday Soc.*, **32**, 585 (1936); C. A. Kraus, THIS JOURNAL, **60**, 129 (1956).

(10) Since the initially dry amine sulfate was dissolved in and successively diluted with benzene containing *ca.* 0.06 mg./ml., as the concentration of amine sulfate was reduced the ratio $[H_2O]/[\text{Amine sulfate}]$ increased.

ELECTROLYTIC JUNCTIONS WITH RECTIFYING PROPERTIES

BY B. LOVREČEK,[1] A. DESPIĆ[2] AND J. O'M. BOCKRIS

John Harrison Laboratory of Chemistry, University of Pennsylvania, Philadelphia, Pa.

Received September 2, 1958

Reiss[3] and Fuller[4] have pointed out that the excess and decess of electrons in, *e.g.*, Si and Ge, containing impurities, corresponding to n- and p-type semiconductors, respectively, have a strong analogy to the excess and deficiency of protons in water, corresponding to acid and alkaline solutions. It follows that there should be a possibility of achieving, utilizing only aqueous electrolytes, the well known rectification of alternating electric current which occurs at a junction of n- and p-type semiconductors. The purpose of this communication is to report that this has been achieved.

The idealized electrolytic analogy to the p-n junction would consist of an electrolytic solution (A) containing an excess of highly mobile protons, together with corresponding anions so large as to be entirely immobile; and in contact with this a second solution (B), containing an excess of highly mobile hydroxyl groups, together with corresponding cations so large as to be entirely immobile. Suppose that inert electrodes are introduced into A and B and an alternating current applied across them. During the phase in which A is positive and B negative, the current carrying H^+ and OH^- ions will be impelled toward each other, meet at the interface, and, in principle, form water. For this phase, therefore, current flow will be easy. In the reverse phase, the mobile current carriers cannot flow freely in the opposite direction to that considered in the first case, because they would have to be supplied by the dissociation of water at the interface between the two liquids, and this is slow (rate constant $K_d = 2.6 \times 10^{-5}$).[5] Consequently, rectification should occur.

(1) University of Zagreb, Zagreb, Yugoslavia.

(2) University of Belgrade, Belgrade, Yugoslavia.

(3) H. Reiss, *J. Chem. Phys.*, **21**, 1209 (1953).

(4) C. S. Fuller, *Rec. Chem. Progr.*, **17**, 75 (1956).

In practice, rectification of alternating currents has been observed with the following practical approximations to the above idealized system.

(1) One electrolyte is an aqueous solution of a strong polyacid; the other is an aqueous solution of a strong polybase. The polyacid and polybase should both be of the highest practical molecular weight. The two electrolytes are separated by a thin dialyzing membrane and one electrode is immersed in each.

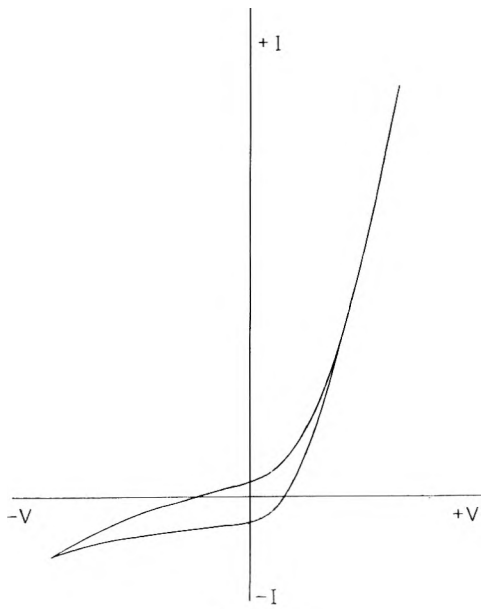

Fig. 1.

(2) The electrolytes are a cation-exchange membrane in H^+ form and an anion exchange membrane in OH^- form. The membranes are pressed against each other. To make the electrical contacts, each membrane has an adjacent electrode compartment filled with a suitable electrolyte in which an inert electrolyte is immersed.

Both types (1) and (2) were constructed and the rectification effects detected. For type (1), solutions of polyvinyltoluenesulfonic acid and polyvinyltrimethylbenzylammonium hydroxide (kindly supplied by the Dow Chemical Co.) were used. Dialyzing parchment was used as a membrane. A rectifying element of type (2) was constructed of Nepton-CR-61AD and Nepton AR-111AD membranes in H^+ and OH^- form, respectively. A thin perforated Teflon sheet (0.02 mm. thick) was placed between the membranes to reduce the active surface of the rectifier in respect to outer surfaces in contact with electrolytes. In most experiments the electrolytes were pure water. Platinum gauze electrodes were used.

A.c. voltage (60 c.p.s.) was applied across the electrodes and the resulting current–voltage relation was observed directly on a CRO screen. A typical rectification curve obtained is shown in Fig. 1.

A multi-element device was also composed by connecting a number of single elements of type (2) in series. Each "sandwich" was separated from the next by a thicker Teflon spacer, the free space being filled with water. Electrode compartments were added to the end elements on both sides. Rectification efficiencies up to 85% were observed.

It is known that certain biological systems also exhibit rectification properties.[6] The above described model of a rectifying electrolytic junction may possibly be applicable also to these systems.

(5) M. Eigen and L. De Maeyer, *Z. Elektrochem.*, **59**, 986 (1955).
(6) T. Teorell, *Z. physik. Chem. Neue Folge*, **15**, 385 (1958).

PORE STRUCTURE OF SINTERED GLASS FROM DIFFUSION AND RESISTANCE MEASUREMENTS

By I. Fatt

Division of Mineral Technology, University of California, Berkeley 4, California

Received September 2, 1958

Barrer[1] recently has proposed the use of transient diffusion measurements in porous media to determine the tortuosity factor of these media. He also called attention to the suggestion of Wyllie and Rose[2] that tortuosity can be derived from the ratio of the specific electrical resistance of a porous medium saturated with a conducting fluid to the specific resistance of the fluid itself. The purpose of this note is to show that for a given sintered glass body the tortuosity calculated from precise transient diffusion measurements is exactly equal to the tortuosity calculated from the specific resistance. Furthermore, this equality of the tortuosities indicates that the sintered glass has no "dead end" pore space or at least none which can influence the transient diffusion. (Dead end pore space is considered to be pore space which is connected to the main pore space but through which there is no diffusion or electrical flux when a diffusion or electrical potential is applied across the porous body.)

Dr. K. J. Mysels has very kindly made available to the author, for the purpose of making resistivity measurements, the sintered Pyrex discs used by Mysels and Stigter[3] in their development of a transient diffusion method for measuring the self-diffusion coefficient of micelles. Mysels and Stigter had previously measured the transport of sodium chloride in these discs. The tortuosity factor was calculated from the pore volume and length of the discs, and the slope of the transport ratio *versus* square root of time curves published by Mysels and Stigter.[4]

The transport equation for transient diffusion across an interface between two solutions was given by Mysels and Stigter as

$$\frac{dR_t}{d\sqrt{t}} = \frac{q(V_L + V_u)}{V_L V_u}\sqrt{\frac{D}{\pi}} \qquad (1)$$

for their experimental arrangement and in the range $0 < R_t < 0.6$. R_t is the transport ratio, t is time, q is the cross-sectional area open for diffusion, V_L and V_u are the pore volume of the lower and upper chambers, respectively, and D is the diffusion coefficient. When the chambers are replaced by porous discs the open area, q, of the upper disc, into which diffusion is taking place, can be obtained from $q = V_u/L_u$ where L_u is the bulk length of the upper disc. Equation 1 then becomes

$$\frac{dR_t}{d\sqrt{t}} = \frac{(V_L + V_u)}{L_u V_L}\sqrt{\frac{D}{\pi}} \qquad (2)$$

Mysels and Stigter used sodium chloride solution in the range 0.2 to 0.7 N as the diffusing material.

(1) R. M. Barrer, THIS JOURNAL, **57**, 35 (1953).
(2) M. R. J. Wyllie and W. Rose, *Nature*, **165** 972 (1950).
(3) K. J. Mysels and D. Stigter, THIS JOURNAL, **57**, 104 (1953).
(4) K. J. Mysels and D. Stigter, 1st Technical Report, ONR Project No. NR 054-254, Library of the University of Southern California or Library of Congress.

D varies only slightly with concentration in this range and can be taken as 1.474×10^{-5} cm.^{2}/sec.

Measured pore volumes, bulk lengths and D, when substituted into equation 2 gives $(dR_t/d\sqrt{t})_{calcd}$ for a system of open area q and length L_u. The observed values of $dR_t/d\sqrt{t}$ taken from Mysels and Stigter are for a system of open area q and length l_u where l_u is the actual fluid path length through the porous medium. The ratio $(dR_t/d\sqrt{t})_{calcd}/(dR_t/d\sqrt{t})_{obsd}$ is then a tortuosity, k_1, where $k_1 = l_u/L_u$.[5] The tortuosity so obtained should be characteristic of the pore geometry only. It gives the ratio of the length of fluid path through the porous disc to the bulk length of the disc.

The Mysels and Stigter solution of the transient diffusion equation is based on the assumption that the porous material is equivalent to a bundle or network of capillary tubes and that there are no dead end pores which can act as sources or sinks of diffusing material.

Columns 2 and 3 in Table I give the calculated and observed values of $dR_t/d\sqrt{t}$. Column 4 gives the tortuosity, k_1, calculated from these transient diffusion measurements.

TABLE I

COMPARISON OF TORTUOSITES FROM DIFFUSION AND CONDUCTANCE

1	2	3	4	5
Disc	$\left(\frac{dR_t}{d\sqrt{t}}\right)_{calcd}$	$\left(\frac{dR_t}{d\sqrt{t}}\right)_{obsd}$	k_1 (from diffusion)	k_1' (from conductance)
2 U	0.01765	0.01331	1.325	1.315
4 U	.02713	.02000	1.365	1.375
5 U	.02620	.01875	1.396	1.395
6 U	.02610	.01874	1.391	1.385

Many authors[6-8] have shown that the pore geometry characteristic called the tortuosity above can also be calculated from electrical resistance measurements on a porous material saturated with a conducting fluid. The relation is

$$k_1' = \sqrt{\frac{rV}{\rho L^2}} \qquad (3)$$

where r is the measured resistance of a porous body of pore volume V, length L, and saturated with a fluid of specific resistance ρ. Equation 3 is also based on a model of a porous medium that does not include dead end pore space.

If the tortuosities calculated from transient diffusion and electrical resistance measurements on a given porous material are the same then there is no dead end pore volume or not enough to influence transient diffusion. This must be true because dead end pore volume will not have the same effect on tortuosities calculated from transient diffusion and electrical resistance.

The porous discs listed in Table I were saturated with sodium chloride solution for which $\rho = 257$ ohm cm. at 23°. For this solution, about 0.05 M, in porous glass the surface conductance has been shown to be less than one per cent. of the total conductance.[8] The resistance of the saturated discs was measured between gold-plated brass electrodes by use of a conductance bridge operating at 1000 c.p.s. An electrolyte-saturated piece of blotting paper was placed between the discs and the electrodes to ensure contact. The resistance of the two saturated pieces of blotting paper alone was also measured. This resistance was subtracted from the total to give the resistance of the porous disc. The resistance of the paper was 5% of the total and could be reproduced to ±5%. The uncertainty in the resistance of the porous disc introduced by use of the blotting paper as contact material was no greater than 0.25%. The total uncertainty in the resistance is probably 0.5%.

Column 5 of Table I gives k_1' calculated from resistance measurements by use of equation 3.

The tortuosities given in columns 4 and 5 are identical within the precision of the measurements. This can be taken to mean that the tortuosity of sintered porous glass is the same in transient diffusion as in electrical conductance.

Schofield and Dakshinamurti[6] already have shown that the tortuosity of a given porous material is the same in steady state diffusion and electrical conductance. Their conclusion means simply that Fick's first law of diffusion and Ohm's law for a porous body are analogous. The conclusion drawn here, that for sintered porous glass the tortuosity is the same in transient diffusion and electrical conductance, is more significant. It indicates that Fick's second law of diffusion, when applied to sintered porous glass, has no source function and can be integrated directly to give Fick's first law which is in turn analogous to Ohm's law. That is, $G(x,t) = 0$ in

$$\frac{\partial C}{\partial t} = D\frac{\partial^2 C}{\partial x^2} + G(x,t) \qquad (4)$$

where $G(x,t)$ is the strength of the source or sink in unidimensional diffusion. A dead end pore can act as a source or sink because it can add or subtract from the transient diffusion flux. If $G(x,t) = 0$ for sintered glass then there are no dead end pores in this material or at least none which can influence transient diffusion of the kind carried out by Mysels and Stigter.[3,4]

Studies are now under way in this Laboratory to evaluate the effect of dead end pores on transient diffusion.

The author wishes to thank the American Petroleum Institute and the Institute of Engineering Research of the University of California, Berkeley, for the financial support of pore structure studies in this Laboratory.

(5) This is not the same tortuosity used by Barrer[1] and Wyllie and Rose.[2] Their tortuosity is equal to k_1^2. The difference lies in the use here of an open cross-sectional area equal to V_u/L_u whereas Barrer, Wyllie and Rose, and others have used V_u/l_u.

(6) P. C. Carman, "Flow of Gases Through Porous Media," Academic Press, New York, N. Y., 1956, p. 46.

(7) R. K. Schofield and C. Dakshinamurti, *Disc. Faraday Soc.*, **3**, 56 (1948).

(8) L. J. Klinkenberg, *Bull. Geol. Soc. Amer.*, **62**, 559 (1951).

(8) H. L. White, F. Urban and B. Monagham, THIS JOURNAL, **45**, 560 (1941).

γ-RADIOLYSIS OF ETHYLENE

BY KANG YANG AND PETER J. MANNO

Radiation Laboratory, Continental Oil Company, Ponca City, Oklahoma

Received October 10, 1958

It appears that the gaseous products formation in γ-radiolysis of ethylene has not been investigated.[1]

We have studied the problem and summarize our results in this note.

Experimental

Matheson C. P. grade ethylene and Matheson nitric oxide (min. 99%) were degassed by freeze-pump technique and subjected to bulb-to-bulb distillation on a vacuum line. The only detectable impurities in the purified gases were 0.007% ethane in ethylene and 0.3% nitrous oxide in nitric oxide. The irradiation vessel was made of Pyrex glass and equipped with break-off seal and capillary constriction at opposite ends. Four fuel elements from a Materials Testing Reactor, shielded by 5.5 meters of water, were used as an irradiation source. All experimental data were obtained at 22.5 ± 1° (the temperature of pool water). Gamma field intensity was obtained by ionization-chamber technique, calibrated with a cerious–ceric chemical dosimeter.[2] Ionization chamber readings before and after each run were averaged. In a week of irradiation the γ-field intensity decreased 14%. After irradiations, gaseous products were analyzed by gas–liquid partition chromatography.

Results and Discussion

Gamma irradiation of ethylene yielded H_2, CH_4, C_2H_2, C_2H_6 and n-C_4H_{10} as gaseous products,[3] with G-values independent of energy input rate. G-values were also independent of initial ethylene pressure (Table I) and surface-to-volume ratio of the glass reactors (Table II). In order to identify the presence of free radicals, nitric oxide was added to a standard run. The results summarized in Table III show that the formation of ethane was completely inhibited by the presence of 5% nitric oxide. In electron bombardment of ethylene,[4] hydrogen atoms and methyl radicals are formed by direct detachment and by ion–molecule reactions. Similar reactions could occur in γ-radiolysis. Hence, ethane probably is formed by free radical reactions, such as

$$H + C_2H_4 \longrightarrow C_2H_5$$
$$C_2H_5 + H \longrightarrow C_2H_6$$

and

$$CH_3 + CH_3 \longrightarrow C_2H_6$$

The G-values for hydrogen, acetylene and n-butane were not affected by nitric oxide. This suggests that the reactions resulting in these products do not involve free radicals.

TABLE I

G-VALUES OF GASEOUS PRODUCTS IN γ-IRRADIATION OF ETHYLENE AT DIFFERENT ETHYLENE PRESSURES

Energy input rate: 2×10^{19} e.v./g. hr.

Ethylene pressure (cm.)	G (molecules per 100 e.v.)				
	C_2H_2	H_2	CH_4	C_2H_6	n-C_4H_{10}
120.0	3.2	1.9	0.05	0.56	0.48
99.8	3.0	1.8	[a]	.48	.45
80.0	3.7	2.0	.04	.59	[a]
60.0	3.7	2.0	.06	.67	.89
40.0	3.9	2.0	.10	.85	.89

[a] G-value not measured.

(1) E. Collinson and A. J. Swallow, *Chem. Revs.*, **56**, 482 (1956).

(2) J. Weiss, *Nucleonics*, **10**, No. 6, 28 (1952).

(3) Negative results of Hayward and Bretton to identify these gaseous products may be due to the ineffectiveness of their analytical technique, *viz.*, copper oxide reduction method. (See J. C. Hayward, Jr., and R. H. Bretton, *Chem. Eng. Progr. Symposium Series*, **50**, 78 (1954)).

(4) F. H. Field, J. L. Franklin and F. W. Lampe, *J. Am. Chem. Soc.*, **79**, 2419 (1957).

TABLE II

EFFECT OF GLASS SURFACE UPON THE GASEOUS PRODUCTS FORMATION IN THE γ-RADIOLYSIS OF ETHYLENE

Ethylene pressure, 120 cm.; energy input rate, 2×10^{19} e.v./g. hr.

Surface area, vol. $cm.^{-1}$	G (molecules per 100 e.v.)				
	C_2H_2	H_2	CH_4	C_2H_6	n-C_4H_{10}
0.8	3.6	2.2	0.06	0.36	0.30
5.7[a]	3.2	1.9	.05	.56	.48

[a] Packed with glass beads (4 mm. in diameter).

TABLE III

EFFECT OF NITRIC OXIDE ON THE GASEOUS PRODUCTS IN THE γ-IRRADIATION OF ETHYLENE[a]

Ethylene pressure, 100 cm.; energy input rate, 2×10^{19} e.v./g. hr.

Nitric oxide pressure (cm.)	G (molecules per 100 e.v.)			
	C_2H_2	H_2	C_2H_6	n-C_4H_8
0.0	3.0	1.8	0.48	0.45
5.0	3.6	1.8	.00	[b]
10.0	3.9	1.7	.00	.40
20.0	4.1	1.9	.00	.37
30.0	4.1	1.7	.00	.41

[a] Due to the overlap of methane and nitric oxide peaks in chromatographs using silica gel columns, the effect of nitric oxide on the G-value for methane was not obtained. [b] G-value not measured.

MISCIBILITY RELATIONS OF LIQUID HYDROGEN CYANIDE

BY ALFRED W. FRANCIS

Socony Mobil Oil Company, Inc.
Research and Development Laboratory, Paulsboro, N. J.

Received September 19, 1958

Published miscibility relations of hydrogen cyanide are meager, perhaps because of its toxicity. Several handbooks indicate complete miscibility with water or alcohol; and distribution at low concentrations is reported[1–6] between benzene and water or aqueous solutions. Freezing curves of four binary systems of hydrogen cyanide have been observed.[6–8] Its unique structure suggested studies of binary and ternary solubilities.

Hydrogen cyanide was distilled from a cylinder and condensed in a large tube in an ice-bath. It was kept at 0° (its b.p. is 26°) in a glass stoppered vessel. All operations were conducted in a hood, and no odor of cyanide was noted during the investigation.

Samples of hydrogen cyanide were taken by a 1-ml. graduated pipet connected to a "propipette,"[9] and mixed with other liquids in a small graduated glass stoppered tube which could be shaken for equilibrium studies. In view of the small samples,

(1) A. Hantzsch and F. Sebaldt, *Z. physik. Chem.*, **30**, 258 (1899).

(2) A. Hantzsch and A. Vagt, *ibid.*, **38**, 705 (1901).

(3) P. Gross and K. Schwarz, *Monatsh. Chem.*, **55**, 287 (1930).

(4) P. Gross and M. Iser, *ibid.*, **55**, 329 (1930).

(5) M. Randall and J. O. Halford, *J. Am. Chem. Soc.*, **52**, 192 (1930).

(6) "Solubilities of Inorganic and Metal-Organic Compounds," A. Seidell, Ed., D. Van Nostrand Co., New York, N. Y., 1940, pp. 569–70.

(7) J. E. Coates and N. H. Hartshorne, *J. Chem. Soc.*, 657 (1931).

(8) A. L. Peiker and C. C. Coffin, *Can. J. Research*, **8**, 114 (1933).

(9) Instrumentation Associates, New York 23, N. Y.

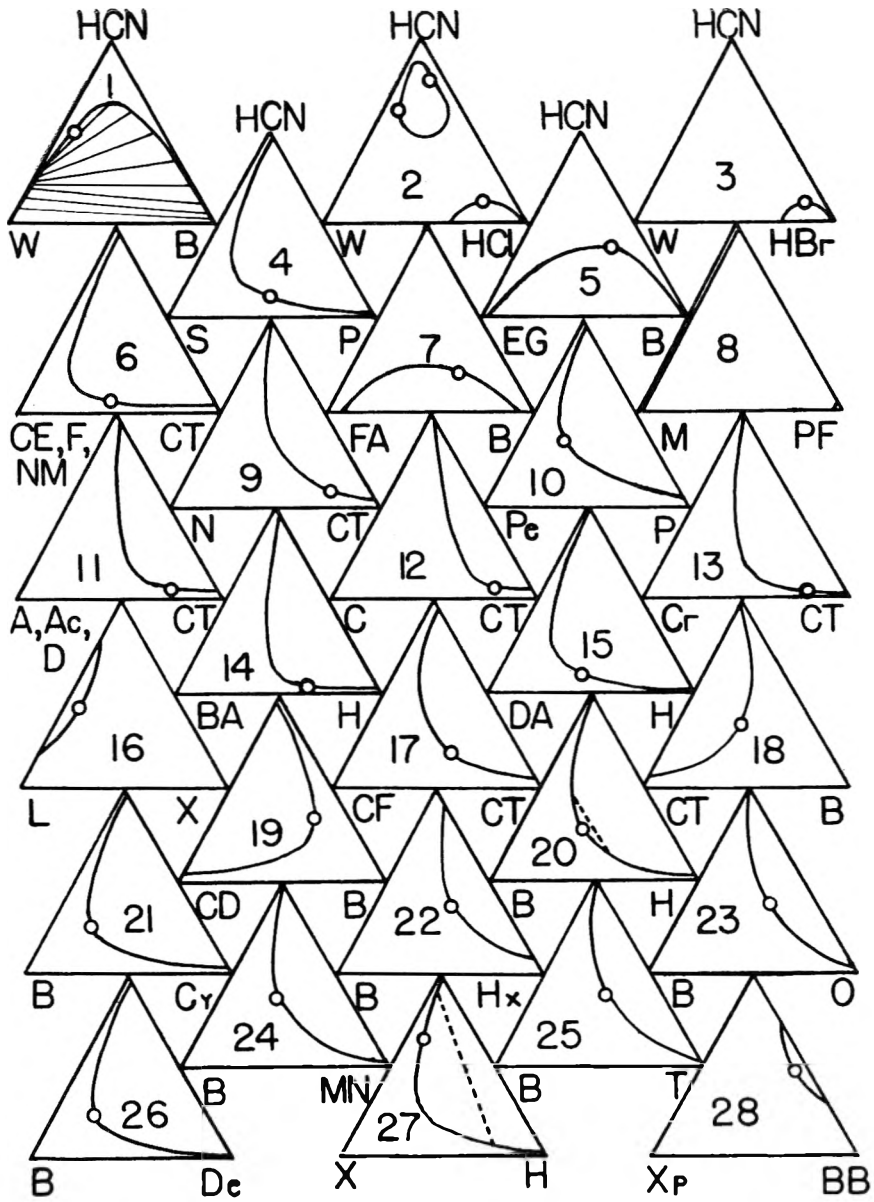

Fig. 1.—Ternary systems of hydrogen cyanide.

solubilities are only approximate. Liquids (including condensed gases) found miscible with hydrogen cyanide were matched for ternary systems with other liquids known to be immiscible with HCN, and *vice versa*. This gives a better idea of miscibility relations than do binary solubilities alone. A gaseous reagent was condensed into a cooled thick-walled glass tube containing the other components. The tube was sealed, weighed, shaken, then cooled, reopened, more reagent added and resealed, etc.

Table I lists 23 liquids found completely miscible with hydrogen cyanide at room temperature. The "codes" are letters suggestive of the names, referring to graphs in Fig. 1. Table II lists 13 liquids not miscible with hydrogen cyanide, with estimates of the two solubilities. From their structures many more substances could be added to each of these groups with reasonable certainty. Thus, most liquid organic oxygen compounds up to C_{10} and aromatic hydrocarbons up to C_9 are completely miscible with hydrogen cyanide and would be included in Table I. Olefins above C_5 and all paraffins and naphthenes are probably only par-

TABLE I

LIQUIDS COMPLETELY MISCIBLE WITH HYDROGEN CYANIDE (AT 25°)

Code	Solvent	Code	Solvent
Ac	Acetonitrile	F	Furfural
A	Aniline	HBr	Hydrogen bromide
B	Benzene	HCl	Hydrogen chloride
BA	*n*-Butyl alcohol	M	Methanol
C	Chlorex	N	Nitrobenzene
CE	β-Chloroethanol	NM	Nitromethane
CF	Chloroform	Pe	Propylene
Cr	*m*-Cresol	S	Sulfur dioxide
DA	Decyl alcohol	W	Water
D	Dioxane	X	*m*- and *p*-Xylenes
EG	Ethylene glycol	Xp	*p*-Xylene
FA	Formic Acid		

tially miscible with hydrogen cyanide and would be included in Table II.

TABLE II

MUTUAL SOLUBILITIES OF HYDROGEN CYANIDE. (AT 25°)

Code	Solvent	Solubility, wt. % Of HCN	In HCN
BB	*sec*-Butylbenzene	30	30
CD	Carbon disulfide	5	2
CT	Carbon tetrachloride	5	2.5
Cy	Cyclohexane	5	3
De	Decalin	3	2
H	*n*-Hexane	2	2
Hx	1-Hexene	10	10
L	Lauryl alcohol	20	20
MN	α-Methylnaphthalene	5	5
O	1-Octene	5	5
PF	Perfluorodimethylcyclohexane	2	2
P	Propane	5	2
T	Tetralin	5	5

Figure 1 presents 32 ternary systems on 28 graphs arranged concisely as in systems of liquid carbon dioxide.[10] In each graph the top corner represents hydrogen cyanide. The other components are indicated by letters referring to the codes in the tables. The left hand component is the non-hydrocarbon, when present, or the more polar component. However, the usual measures of polarity are distorted since benzene and xylenes are miscible with hydrogen cyanide while carbon disulfide and carbon tetrachloride are not.

The majority of the graphs have simple binodal curves on the right side, though the depths of the curves and the positions of the plait points vary. Five of the systems have binodal curves on the bottom and three on the left sides. Graphs 20 and 27 have isopycnics[10,11] as represented by dashed tie lines indicating equal densities for the two layers. Other tie lines are shown only on Graph 1, based partly on references 1, 2, 6. These tie lines are solutropic (reversing in slope). This system also contains isoöptics[11,12] (not shown) for some tie lines, indicating equal refractive indices for the two layers. Tie lines in the other systems can be approximated from the positions of the plait points.

Graph 2 is unusual in showing a binodal curve and a separate island curve, and so has three plait points. The island may be related to the complex noted by Peiker and Coffin.[8] This island is larger than in the other published graph of this type, namely, the aqueous system of dioxane with hydrogen chloride.[13] The system water–hydrogen bromide–dioxane is certainly of the same type. However, there is no island in the HBr–HCN system, Graph 3. Two graphs, 6 and 11, represent three systems each because those of each graph are identical within the accuracy of the observations.

An actual extraction in the benzene–hexane system, graph 20, indicated a fair selectivity of hydrogen cyanide for benzene. However, other less toxic substances show higher selectivities.

Acknowledgment.—The author is indebted to his colleague, Dr. R. D. Offenhauer, who suggested the investigation, and prepared the sample of hydrogen cyanide.

(10) A. W. Francis, THIS JOURNAL, **58**, 1099 (1954).
(11) A. W. Francis, *Ind. Eng. Chem.*, **45**, 2789 (1953).
(12) A. W. Francis, THIS JOURNAL, **56**, 510 (1952).
(13) A. W. Francis, *ibid.*, **62**, 579 (1958), Fig. 2.

A SPECTROPHOTOMETRIC INVESTIGATION OF OUTER-SPHERE ASSOCIATION OF HEXAMMINECOBALT(III) ION AND HALIDE ION[1]

BY EDWARD L. KING, JAMES H. ESPENSON AND ROBERT E. VISCO

Department of Chemistry, University of Wisconsin, Madison 6, Wisconsin

Received September 27, 1958

This paper presents the results of experiments which indicate that the values of Q_1, the equilibrium quotients for the reactions

$$Co(NH_3)_6^{+3} + X^- \rightleftharpoons Co(NH_3)_6^{+3}\cdot X^-$$

with $X^- = Cl^-$ and Br^- are much lower than the values reported by Evans and Nancollas.[2] Very small values of the absorbancy enhancement have been relied upon in this earlier work to obtain values of Q_1.[3] The present study was made with the concentration of hexamminecobalt(III) ion held at a low and constant value and the concentration of halide ion varied up to 0.9 *M*. The results obtained in the present study at λ 250 mμ for $X^- = Cl^-$ and λ 260 mμ for $X^- = Br^-$ are presented in Fig. 1. It is seen that the absorbancy enhancement in each series of measurements is, within the experimental uncertainty, proportional to the concentration of halide ion over the entire range of concentration.

Curvature in a plot of the apparent molar absorbancy index of hexamminecobalt(III) ion ($\bar{a} = (\log I_0/I)/[Co^{III}]b$, where b is the cell length and $[Co^{III}]$ is the stoichiometric molar concentration of hexamminecobalt(III) ion) *versus* $[X^-]$ sets in with increasing $[X^-]$ when $Q_1[X^-]$ becomes appreciable compared to unity, as shown by the equation

$$\bar{a} = \frac{a_0 + a_1Q_1[X^-]}{1 + Q_1[X^-]} \qquad (1)$$

where a_0 and a_1 are the molar absorbancy indices of $Co(NH_3)_6^{+3}$ and $Co(NH_3)_6^{+3}\cdot X^-$, respectively. If $Q_1[X^-] << 1$, equation 1 reduces to

$$\bar{a} = a_0 + a_1Q_1[X^-] \qquad (2)$$

It is clear that only values of the product of a_1 and Q_1 are obtained from the experiments such as those reported in Fig. 1. The values of this product for each system at several wave lengths are given in Table I. In Fig. 1 are also shown the lines which correspond to $Q_1 = 0.2$ associated with the Q_1a_1 product which gives the best fit to all of the

(1) This work was supported in part by a grant from the United States Atomic Energy Commission (Contract AT(11-1)-64, Project No. 3).

(2) M. G. Evans and G. H. Nancollas, *Trans. Faraday Soc.*, **49**, 363 (1953).

(3) The enhancement of log I_0/I at one of the highest concentrations of chloride ion and hexamminecobalt(III) ion studied at 35° at 248 mμ was only 0.026 (if δ of the paper[2] refers to one cm. of light path).

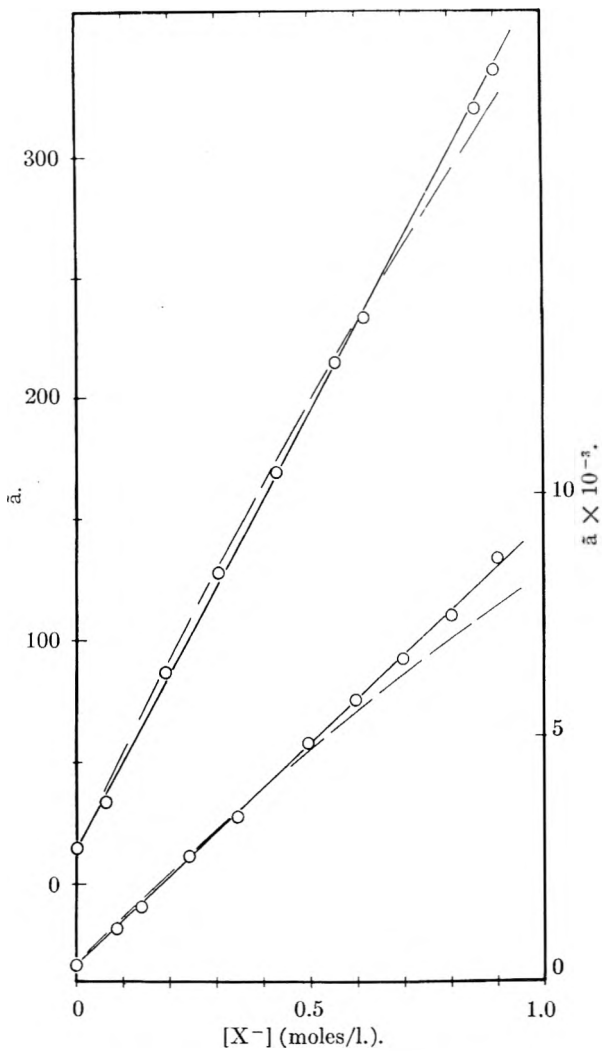

Fig. 1.—The apparent molar absorbancy index of hexamminecobalt(III) ion as a function of the concentration of chloride ion and bromide ion. $T = 35.1°$; I (ionic strength) = 0.9, maintained with sodium perchlorate; $[Co(NH_3)_6^{+3}] = 3\text{–}5 \times 10^{-4}$ molar; upper curve, X = chloride, λ 250 mμ left hand ordinate; lower curve, X = bromide, λ 260 mμ, right hand ordinate.

points. The enhancement of absorbancy in these systems, if interpreted in terms of the formation of an outer-sphere complex, suggests, therefore, the value of the association equilibrium quotient at 35° and an ionic strength of 0.9 for each of these reactions to be definitely less than 0.2.[4] Evans and Nancollas[2] interpret their absorbancy data obtained at $I = 0.054$ and 35° to give Q_1 values of 91 ± 4 and 51 ± 2 for $X^- = Cl^-$ and Br^-, respectively. Is the factor of ≥250 between the Q_1 values reported by Evans and Nancollas[2] and the upper limit suggested by the present work possibly to be attributed to the ionic strength dependence of the value of Q_1? A rough approach to this problem is the use of the relative change of the sixth power of $\gamma_\pm$ for a strong 1-1 electrolyte with ionic strength as an estimate of the relative change with ionic strength of Q_1 for these reactions with $\Delta Z^2 = -6$. The value of $(\gamma_\pm)^6_{RbI}$ (for 25°) changes by a factor of ~7 over this range of I. (Of those 1-1 electrolytes which are certainly strong, rubidium iodide shows about as dramatic a change in $\gamma_\pm$ over this range of ionic strength as do any.) There is, therefore, an apparently irreconcilable discrepancy between the Q_1 values reported here and those reported by Evans and Nancollas.[2] In view of the larger absorbancy enhancement upon which the conclusions of the present paper are based, the upper limit of Q_1 reported here is considered the more reliable.

Table I

The Values of the Quantity Q_1a_1 at 35.1° in Aqueous Solution with $I = 0.9$ for $Co(NH_3)_6^{+3}X^-$

λ (mμ)	Q_1a_1 $X^- = Cl^-$	Q_1a_1 $X^- = Br^-$
245	680	
250	360[a]	
255	180	1150
260	97	900[a]
265		680
270		520

[a] This is the slope of the straight line in Fig. 1.

It would appear that the data of Evans and Nancollas[2] are not, however, in drastic disagreement with the data presented here. From the plots in their Fig. 3, it is to be concluded that the values of a_1Q_1 for the chloride and bromide systems at ionic strength 0.054 are ~10 ± 3 times the values of this quantity obtained in the present work. This factor is not very different than the factor ~7 already suggested as a reasonable ionic strength dependence of Q_1 over the range $I = 0.9$ to $I = 0.054$. (This suggests only minor variations in the values of a_1 with changing ionic strength.)

On the basis of conductance measurements upon solutions of hexamminecobalt(III) chloride, Jenkins and Monk[5] assign a value of ~30 for $K_1^0 = [Co(NH_3)_6^{+3}\cdot Cl^-]/[Co(NH_3)_6^{+3}]\cdot[Cl^-]$ at 25°. A reasonable extrapolation of this admittedly very uncertain value to $I = 0.05$ gives $Q_1 \cong 10$.

It is of interest to note that the upper limit placed upon the value of K_1^0 by the present work corresponds in the Bjerrum treatment of ion association[6] to a rather large distance of closest approach. If one uses the activity coefficient curve for rubidium iodide as a model for the ionic strength dependence of $(Q_1)^{-1/6}$, one concludes that K_1^0 is less than ~5, which corresponds to a distance of closest approach of greater than ~10 Å.; the value of q, the distance of separation in the Bjerrum theory, within which a pair of ions of charge +3 and −1 are considered to be associated in water at 35° is 10.8 Å. It appears that the association of hexamminecobalt(III) ion and univalent anions is less extensive than that

(4) It has been asserted by S. R. Cohen (This Journal, **61**, 1670 (1957)) that the spectrophotometric study of ion-pair association reactions yields a low value of the equilibrium quotient if distant ion-pairs do not manifest their presence by a change in absorbancy compared to the unassociated ions. This assertion is not correct; the value of Q_1 obtained by the correlation of absorbancy data with equation 1 is the sum of the Q_1 values for the reactions forming all 1-1 species, and the a_1 value obtained is the weighted average of the absorbancy indices of all such species. (This has been pointed out by E. Grunwald and J. E. Leffler (see S. D. Ross, M. M. Labes and M. Schwarz, *J. Am. Chem. Soc.*, **78**, 343 (1956)); see also L. E. Orgel and R. S. Mulliken, *ibid.*, **79**, 4839 (1957).) Thus the value 0.2 is the upper limit for the sum of the Q_1 values for all "isomeric" 1-1 species which form rapidly from $Co(NH_3)_6^{+3}$ and X^-.

(5) I. L. Jenkins and C. B. Monk, *J. Chem. Soc.*, 68 (1951).

(6) N. Bjerrum, *Kgl. Danske Vidensk. Selskab.*, **7**, No. 9 (1926).

predicted on the basis of the Bjerrum theory using a value of the distance of closest approach which corresponds to the dimensions of the unhydrated ions (*i.e.*, 4–5 Å.). The logical conclusion to be drawn is that hexamminecobalt(III) ion and the univalent anions chloride and bromide do not succeed in mutually desolvating one another of water molecules.

Experimental

Hexamminecobalt(III) chloride was prepared using the method of Bjerrum and McReynolds.[7] Hexamminecobalt(III) perchlorate was prepared by addition of perchloric acid to a solution of the chloride salt in water. Each compound was recrystallized from water two or more times. It was demonstrated that further recrystallization of the hexamminecobalt(III) perchlorate used in the measurements reported here does not alter the absorbancy of the solutions containing hexamminecobalt(III) ion and halide ion. (Some early measurements using a less pure cobalt(III) salt gave appreciably higher absorbancy enhancement than reported here.)

Reagent grade sodium chloride and sodium bromide were used without further purification.

Sodium perchlorate was prepared by reaction of a slight excess of perchloric acid with reagent grade sodium carbonate. The solid obtained by the evaporation of water from the filtered solution was twice recrystallized from water.

Absorbancy measurements were made using a Beckman model DU spectrophotometer. Cells of 2 and 10 cm. length were used with a thermostated cell holder.

Acknowledgment.—One of us (E. L. K.) wishes to acknowledge that Professor H. Taube called his attention to the fact that the Q_1 values reported by Evans and Nancollas[2] were probably too high, thus suggesting the present study.

(7) J. Bjerrum and J. P. McReynolds, "Inorganic Syntheses," Vol. II, McGraw-Hill Book Co. Inc., New York, N. Y., 1946, pp. 217–218.

FREEZING POINTS OF MIXTURES OF WATER WITH HEPTAFLUOROBUTYRIC ACID

By John R. Hollahan and George H. Cady

Contribution from the Department of Chemistry, University of Washington, Seattle, Washington

Received October 4, 1958

Heptafluorobutyric acid is miscible in all proportions with water. Like its homologs this acid is highly ionized in dilute solutions. Its freezing point is given in the literature as −17.5°.[1] This datum is used in Fig. 1.

The acid for this study was obtained from the Minnesota Mining and Manufacturing Co. It was distilled, the middle portion being used. A mixture of the acid with its anhydride was obtained by adding some of the acid to phosphorus pentoxide and then distilling away the liquid.

Two methods were used for determining freezing points and compositions: (1) a mixture of the acid with water was partially frozen in a Dewar vessel and the mixture was stirred until equilibrium was established between solid and liquid. The temperature then was observed with a thermocouple, and a sample of the liquid was removed using a hypodermic needle covered at the tip with a filter of glass-wool. The sample was analyzed to determine the acid by titration with sodium hydroxide or to determine the water, in mixtures containing over 45 mole % acid, by titration with Karl Fischer reagent. (2) In the second method, a sample of a mixture of the acid with its anhydride was placed in a flask which could be weighed. To this weighed portions of water were added as needed using a vacuum line to make the transfers. After each addition of water, the freezing point of the solution was determined by finding the temperature (using a thermocouple in a tube with a closed end dipping into the liquid) at which a very small part of the sample would continue to exist as solid while shaken with the liquid for at least a few minutes. By making a graph of freezing point *vs.* weight of water added, two maxima in the temperature were found. One maximum corresponded to the pure acid and the other to the compound $C_3F_7COOH \cdot H_2O$. From these the compositions of all other solutions in the run were calculated. The second method gave more precise compositions than the first.

(1) Page 1 of Heptafluorobutyric Acid, Minnesota and Mining and Mfg. Co., St. Paul, Minnesota (about 1950).

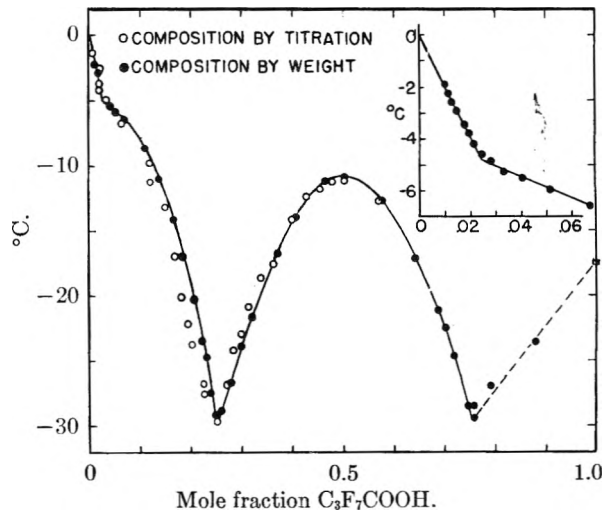

Fig. 1.

Results are represented in Fig. 1, the line being based upon the second experimental method. Two features of the graph are of interest: (1) the acid forms a monohydrate as does trifluoroacetic acid[2] but it does not form a tetrahydrate (trifluoroacetic acid does). (2) There is a break in the curve at a mole fraction of 0.026 and −4.9°. This probably indicates the existence of micelles in solutions above this concentration. At this point one mole of acid in 1000 g. of water lowers the freezing point about 3.3°. Upon shaking a solution of composition within the micelle region a foam, like soap suds, is obtained for concentrations of acid less than mole fraction 0.14.

The inset in Fig. 1 represents in detail the part of the system involving solutions of mole fraction below 0.065. All of the points shown in the inset were obtained by the second experimental method.

The monohydrate melts at −11.0°. There is an eutectic point at −29.9° and a mole fraction of acid of 0.750 and a second eutectic point at −29.7° and a mole fraction of 0.255.

Acknowledgment.—This work was supported in part by the Office of Naval Research.

(2) H. H. Cady and G. H. Cady, *J. Am. Chem. Soc.*, **76**, 915 (1954).

ANION TRANSPORT NUMBER IN PURE MOLTEN SILVER NITRATE

By H. Bloom and D. W. James

University of Auckland, Auckland, N. Z.

Received October 16, 1958

A method to determine transport number in molten salts was described recently by Bloom and

Doull[1] who measured (*e.g.*, for $PbCl_2$) volume increase of anolyte, when a known quantity of electricity was passed through the melt which was divided into two compartments by a sintered disc. These compartments terminated in capillaries in which were situated molten lead electrodes which were open to the atmosphere. The apparatus was made horizontal to prevent gravitational flow. Lorenz and Janz[2] have shown that liquids which do not wet glass (*e.g.*, molten lead), required considerable pressure to cause their displacement in a glass capillary. To eliminate the possible sticking at the interfaces between molten metal and air, the present authors have modified the apparatus so that only the molten salt in the capillaries is in contact with air. In the present method, there are advantages in using solid metal electrodes, *e.g.*, silver. It was decided, therefore, to investigate molten silver nitrate, this being one of the few suitable silver salts which wets glass.

Experimental

The vitreous silica apparatus consisted of a short tube (bore 0.6 cm.) divided into two compartments by an ultrafine (porosity 4) disc and terminating at each end in a uniform capillary tube (bore 0.1 cm.). Current from an electronically stabilized power supply was introduced by platinum wires sealed through a small hole in the side of each compartment into large beads of pure silver which form the electrodes. The cell was heated in a furnace capable of rotation. It was filled with melted analytical grade $AgNO_3$ in the vertical position and then rotated into the horizontal position, where the boundaries of molten $AgNO_3$ in the capillaries were observed using a cathetometer. After levelling the apparatus to prevent gravitational movement of the melt, current was passed for measured time intervals and the resulting movement of the boundaries measured. A range of current from 26 ma. (for 15 min.) to 100 ma. (for 3 min.) was used. Silver "trees" were formed at the cathode, *cf.* Aziz and Wetmore,[3] but electrolysis was interrupted before they extended to the disc. Reversal of polarity caused the trees to break. Temperature was kept constant to $\pm 0.1°$ during each run.

Results and Discussion

The transport number of the anion is given by

$$t_- = \frac{96{,}500 V \rho}{qE}$$

where V in cc. is the volume increase of the anolyte (*i.e.*, the volume increase due to movement of electrolyte boundary plus the volume of silver anodically dissolved); ρ in g. cc.$^{-1}$, the density of the molten salt; q in coulomb, the quantity of electricity passed; and E, the equivalent weight of the electrolyte. For 25 runs using different cells and currents from 26 to 100 ma., $t = 0.251 \pm 0.014$ (95.5% confidence limits) at $232 \pm 4°$. In contrast with Bloom and Doull's method, ultrafine discs must be used as the prevention of gravitational mass transfer through the disc is difficult with coarser discs even with careful levelling of the furnace. Lorenz and Janz[2] likewise found that melts such as $AgNO_3$, which wet glass, can be displaced in glass capillaries by very small pressure. The present value of t is in good agreement with the approximate value predicted by Aziz and Wetmore[3] for the same salt and, within experimental error, is identical with the value of 0.25 which Laity and Duke[4] obtained by a bubble cell method. In each case the only moving interface is between air and molten $AgNO_3$.

Assistance from the University of New Zealand Research Fund for the purchase of apparatus is gratefully acknowledged.

(1) H. Bloom and N. J. Doull, THIS JOURNAL, **60**, 620 (1956).

(2) M. R. Lorenz and G. J. Janz, *ibid.*, **61**, 1683 (1957).

(3) P. M. Aziz and F. E. W. Wetmore, *Canadian J. Chem.*, **30**, 779 (1952).

(4) R. E. Laity and F. R. Duke, *J. Amer. Electrochem. Soc.*, **105**, 97 (1958).

THE INFRARED SPECTRA OF GASEOUS MAGNESIUM CHLORIDE, MAGNESIUM BROMIDE AND NICKEL CHLORIDE AT ELEVATED TEMPERATURES[1]

BY STERLING P. RANDALL, FRANK T. GREENE AND JOHN L. MARGRAVE

Department of Chemistry, University of Wisconsin, Madison 6, Wisconsin

Received October 11, 1958

The infrared absorption spectra of gaseous $MgCl_2$, $MgBr_2$ and $NiCl_2$ have been observed by means of a Beckman IR 2 infrared spectrophotometer, using a Vycor tube (2.5 cm. diameter, 70 cm. long) fitted with potassium bromide windows as the gas cell. A nichrome wound resistance furnace was used for heating this cell. The temperature was measured and controlled by means of a chromel P–alumel thermocouple in conjunction with an Amplitrol and potentiometer. The temperatures at which absorption was observed were: $MgCl_2$, 1000°; $MgBr_2$, 1000°; $NiCl_2$, 850°.

Electron diffraction measurements of the vaporized group II halides[2] indicate that these molecules are linear. $MgCl_2$ and $MgBr_2$ should therefore exhibit two infrared active fundamental frequency absorptions[3] at frequencies ν_3 for the antisymmetric stretching vibration and ν_2 for the bending vibration. The one absorption maximum observed for each salt undoubtedly is due to the antisymmetric stretching vibration. Since the Beckman IR 2, with potassium bromide optics, has a long wave length limit of about 400 cm.$^{-1}$, one does not expect to observe the bending absorption which occurs at still longer wave lengths.

The structure of $NiCl_2$ in the gas state has not been determined, but one may tentatively assign a linear structure to this molecule. If $NiCl_2$ possessed a bent symmetrical structure, it would have three infrared active fundamental frequencies. The symmetric and antisymmetric stretching vibrations should have fairly similar magnitudes, while the bending vibration would absorb at longer wave lengths. Only one absorption maximum for $NiCl_2$ was observed, and this is ascribed to the antisymmetric stretching vibration of a linear molecule. This assumption of linearity is tentative since there is a possibility that a bent $NiCl_2$ molecule might have symmetric and antisymmetric stretching frequencies differing considerably in magnitude so that one absorption might fall outside the

(1) Paper presented at the fall meeting of the American Chemical Society at Chicago, Illinois, September 11, 1958.

(2) P. A. Akishin and V. P. Spiridonov, *Kristallografiya*, **2**, 475 (1957).

(3) G. Herzberg, "Infrared and Raman Spectra," D. Van Nostrand Co., Inc., New York, N. Y., 1945.

wave length region studied, or the bent molecule might possess frequencies so similar that, especially at high temperatures, the absorptions might superimpose to give one resulting maximum.

The three absorption maxima observed were: $MgCl_2$, 588 cm.$^{-1}$; $MgBr_2$, 490 cm.$^{-1}$; $NiCl_2$, 505 cm.$^{-1}$. Buchler and Klemperer have recently published work on the infrared spectrum of vaporized $MgCl_2$,[4] and report a value of 597 cm.$^{-1}$ for the antisymmetric stretching frequency.

The frequency of the symmetric bond stretching vibration for these molecules is not found in the literature. This precludes the calculation of the interaction force constant. In the few examples for inorganic molecules of this type where the bond–bond interaction force constant is known[3,5] the value is quite small. If one assumes a value of zero for this interaction constant, the stretching force constant, k_1, may be obtained from valence force field equations.[3] Also, the infrared inactive frequency due to the symmetric stretching vibration may be calculated.

The calculated force constants for the XY_2 molecules are shown in Table I. The force constants for the diatomic XY molecules as obtained from known ν_1 values[6] are included for comparison. The calculation of the force constant, k, for the diatomic species is based on the 0–1 transition, *i.e.*, the effect of anharmonicity is included in the calculation. The observed frequency for the antisymmetric stretching vibration and the calculated frequency for the symmetric stretching frequency for the three compounds also are shown.

TABLE I

VIBRATIONAL FREQUENCIES IN CM.$^{-1}$ AND FORCE CONSTANTS IN 10^5 DYNES/CM. FOR TRIATOMIC AND DIATOMIC HALIDES

	ν_3 (obsd.)	ν_1 (calcd.)	k_1 XY_2	k XY
$MgCl_2$	588	297	1.83	1.77
$MgBr_2$	490	178	1.48	1.48
$NiCl_2$	505	341	2.41	2.26

It is interesting to note, especially for the magnesium compounds, that the force constants for the triatomic and diatomic species are of nearly equal magnitude, on the assumption that the interaction constant in the XY_2 molecule is zero. Additional work is in progress in an effort to determine the exact value of this constant.

(4) A. Buchler and W. Klemperer, *J. Chem. Phys.*, **29**, 121 (1958).
(5) W. Klemperer and L. Lindeman, *ibid.*, **25**, 397 (1956).
(6) G. Herzberg, "Spectra of Diatomic Molecules," D. Van Nostrand Co., Inc., New York, N. Y., 1950, Second Edition.

RADIATION INDUCED RACEMIZATION OF *l*-MANDELIC ACID IN AQUEOUS SOLUTION[1]

BY PAUL Y. FENG AND STEPHEN W. TOBEY

Physics Research Department, Armour Research Foundation, Chicago, Illinois

Received October 17, 1958

Wright[2] has found that the optical activity of solid mandelic acid is reduced by pile irradiation, and that benzaldehyde is a reaction product. The reaction mechanism was however not understood. It was not clear whether the reduction of optical activity was due to racemization, or simple destruction of the mandelic acid.

This paper reports on the γ-radiolysis of aqueous solutions of mandelic acid. Both racemization and destruction were found to occur. These phenomena may be explained by conventional radical mechanisms.

Experimental

Irradiation Samples.—The samples were prepared by introducing aqueous solutions of optically active mandelic acid[3] into Pyrex sample tubes, which were subsequently frozen, evacuated and sealed. These samples were irradiated at the Gamma Irradiation Facility of the Argonne National Laboratory.[4]

Measurements.—Optical activity measurements were made with the sodium-D line using a Fric polarimeter. The irradiated mandelic acid was isolated by first treating a portion of the irradiated sample with dilute sodium hydroxide solution and extracting some of the decomposition products four times with diethyl ether. The aqueous phase then was acidified with dilute hydrochloric acid and the acidic ingredients were extracted four times with ether. This latter ethereal phase was evaporated to dryness and the mandelic acid so recovered was recrystallized twice from benzene. Finally, the acid was dissolved in water, and the optical activity was measured.

Results

The mandelic acid solutions became turbid upon irradiation and water-insoluble products were observed at higher irradiation dosages. Invariably, the specific rotations of the solutions were lowered. Benzaldehyde was produced (identified by the mixed melting point method as the 2,4-dinitrophenylhydrazine derivative). Phenylacetic acid, though a possible product, was not positively identified by either infrared spectrometry or wet analysis.

Within the range of the irradiation dosages used, the optical activity decreased steadily with dose (Table I). In addition, measurements of the

TABLE I

RADIATION INDUCED RACEMIZATION OF *l*-MANDELIC ACID IN AQUEOUS SOLUTION

Sample concn. (g./100 ml.)	Irradiation dosage (10^{20} e.v./g.)	Initial optical rotation (degrees)	Final optical rotation (degrees)	Indirect action G-values for the disappearance of optically active mandelic acid
1.662	5.53	−4.73	−2.77	4.9 ± 0.2
1.662	4.95	−4.73	−3.00	4.7 ± .2
1.662	4.08	−4.73	−3.20	5.2 ± .2
1.662	3.96	−4.73	−3.21	5.3 ± .2
9.85	5.8	−28.0	−25.6	6 ± 1
9.85	4.8	−28.0	−26.5	5 ± 1
9.85	3.4	−28.0	−27.3	3 ± 2
9.85	3.2	−28.0	−27.4	3 ± 2

mandelic acid recovered from the irradiated samples showed that both destruction and racemization of the mandelic acid molecules occurred. In a sample where the total reduction of optical activity amounted to 30%, the fraction of optical activity lost by destruction of the mandelic acid molecules was twice as large as the fraction of optical activity lost by racemization.

(1) This work was supported by the ARF reactor research program.
(2) J. Wright, *Disc. Faraday Soc.*, **12**, 64 (1952).
(3) Prepared according to the procedure of R. H. Manske and T. B. Johnson, *J. Am. Chem. Soc.*, **51**, 1909 (1929).
(4) The cooperation of Miss Gladys Swope is gratefully acknowledged.

Discussion of Results

Primary Mode of Interaction.—Examination of the experimental data suggests that the reactions induced in an irradiated mandelic acid solution proceed *via* a free radical indirect mechanism involving both the H· and OH· radicals as well as H_2O_2 molecules. The primary attack is believed to be

$$H_2O \rightsquigarrow a\text{H}\cdot + b\text{OH}\cdot + c\text{H}_2 + d\text{H}_2\text{O}_2 \quad (1)$$

$$C_6H_5CHOHCOOH + \text{H}\cdot\ (\text{or OH}\cdot) \longrightarrow C_6H_5\dot{C}OHCOOH + \text{H}_2\ (\text{or } H_2O) \quad (2)$$

These hydrogen abstraction reactions are suggested by analogy to the results of the irradiation of aqueous solutions of acetic acid,[5] hydroxy acids[6] and toluene,[7] with the formation of, respectively, succinic acid, keto-acids and side chain hydroxylated derivatives of toluene. Furthermore, the fact that benzaldehyde but no appreciable amount of phenylacetic acid was detected in the irradiation products also indicated the hydrogen abstraction reaction.

The radical species $C_6H_5\dot{C}OHCOOH$ so produced probably reacts with other H· or OH· radicals, H_2O_2, or another $C_6H_5\dot{C}OHCOOH$ radical.

$$C_6H_5\dot{C}OHCOOH + \text{H}\cdot \longrightarrow C_6H_5CHOHCOOH\ (\text{racemic}) \quad (3)$$

$$C_6H_5\dot{C}OHCOOH + \text{OH}\cdot \longrightarrow [C_6H_5C(OH)_2COOH] \xrightarrow{-H_2O} C_6H_5COCOOH \xrightarrow{-CO_2} C_6H_5CHO \quad (4)$$

Both the reaction between a $C_6H_5\dot{C}OHCOOH$ radical with H_2O_2

$$C_6H_5\dot{C}OHCOOH + H_2O_2 \longrightarrow [C_6H_5C(OH)_2COOH] + \text{OH} \quad (5)$$

and the reaction between two $C_6H_5\dot{C}OHCOOH$ radicals

$$2C_6H_5\dot{C}OHCOOH \longrightarrow C_6H_5COCOOH + C_6H_5CHOHCOOH\ (\text{racemic}) \quad (5)$$

are energetically permissible. Reaction 6 was advanced to explain the observed extent of radiation induced reaction in optical activity. Reactions with other degradation products are not important in the initial period.

The G-Values of the Radiation Induced Reactions.—It is possible to make the following simplified observations.

One pair of $C_6H_5\dot{C}OHCOOH$ radicals disappearing by reaction 6 would result in racemization or destruction of two original mandelic acid molecules with the expenditure of two radicals, whereas a single $C_6H_5\dot{C}OHCOOH$ radical disappearing by some other mechanism would result in the destruction or racemization of one original mandelic acid molecule also with the expenditure of two radicals. (For the purpose of this consideration, the H_2O_2 produced can be considered as being equivalent to two radicals.) Designating by X the fraction of $C_6H_5\dot{C}OHCOOH$ radicals which disappear according to reaction 6, we have, at the beginning of irradiation

$$-G(\text{op. activity}) = \frac{1-X}{2}[g(\text{H}) + g(\text{OH}) + 2g(H_2O_2)] + X[g(\text{H}) + g(\text{OH}) + g(H_2O_2)]$$

where $-G$ (optical activity is the reduction of optically active mandelic acid molecules (due to either racemization or destruction) per 100 e.v., and the g-values are the 100 e.v. primary radical and molecular yields in irradiated water. Although the various g-values for mandelic acid solutions (pH ~ 2) are not determined, they should lie somewhere between the g-values in 0.8 N H_2SO_4 and those in neutral water. As a first approximation, the g-values[8] for 0.8 N solutions of H_2SO_4 probably can be used, and we have

$$g(\text{H}) = 3.70,\ g(\text{OH}) = 2.92 \text{ and } g(H_2O_2) = 0.78$$

If the initial G-value for reduction of optical activity is taken, by extrapolation of the experimental data, to be 5.5, the value of X becomes 0.42, which compares with the experimental value of 0.33.

Acknowledgment.—The authors thank Dr. L. Reiffel for suggesting this work.

(5) H. Fricke, E. Hart and H. Smith, *J. Chem. Phys.*, **8**, 229 (1938).
(6) A. Pratt and F. Putney, *Rad. Res.*, **1**, 234 (1954).
(7) A. Kailan, *Sitzber. Akad. Wiss Wien, Math. Naturw. Klasse, Abt. IIa*, **128**, 831 (1919).
(8) Calculated from the G_F, G_R, G_E values of A. O. Allen, *Proc. Int. Conf. Peaceful Uses Atomic Energy*, **7**, 513 (1956).

THE SOLUBILITY OF SILVER CHLORIDE IN NITRATE MELTS

By Ralph P. Seward

College of Chemistry and Physics, The Pennsylvania State University, University Park, Pennsylvania

Received October 25, 1958

In many instances it has been shown that fused salt mixtures are close to ideal solutions. For example, at 300° solid silver chloride is at equilibrium with a liquid which is 0.55 mole fraction silver chloride and 0.45 mole fraction silver nitrate.[1] This within the uncertainty of the solubility measurement, agrees with the value calculated from the melting point of pure silver chloride, 455°, and the calorimetrically determined heat of fusion, 3080 cal. mole^{-1}.[2]

In contrast, the solubility of silver chloride in sodium and potassium nitrate is very small and, at sufficiently high temperatures, two liquid phases are formed. By means of potentiometric titrations Flengas and Rideal[3] found the product of silver and chloride ion molalities in the presence of solid silver chloride in an equimolar sodium–potassium nitrate solvent to be 4.8×10^{-6} at 248°. In the absence of excess of either silver or chloride this is a solubility of 2.2×10^{-3} molal or 2.05×10^{-4} mole fraction silver chloride. From the variation of the solubility product with temperature, these authors calculated the heat of solution of silver chloride into the melt to be 18.3 kcal. mole^{-1}. These solutions appeared to be ideal in that the silver chloride activity was proportional to the product of the silver ion and chloride ion concentrations, although far from ideal in terms of departure from Raoult's law.

(1) "International Critical Tables," Vol. IV, McGraw-Hill Book Co., Inc., New York, N. Y., 1928, p. 58.
(2) K. K. Kelley, U. S. Bureau of Mines, Bulletin 476, 1949.
(3) S. N. Flengas and E. Rideal, *Proc. Roy. Soc.* (*London*), **233**, 443 (1955).

The large differences in the solubility and heat of solution of silver chloride in silver nitrate and in the alkali metal nitrate solvent suggested the solubility measurements reported here. The solubility of silver chloride in sodium nitrate, in potassium nitrate, in various mixtures of potassium nitrate with silver nitrate, lead nitrate, thallous nitrate and barium nitrate has been measured, in each case over a temperature range of 60° or more.

Experimental

The various salts were reagent quality used without further purification, except silver chloride which was made from silver nitrate and hydrochloric acid.

Sufficient solvent salt or mixture to yield a liquid volume of about 60 ml. was fused in a glass tube which rested in a small furnace, the temperature being controlled manually by means of a variable voltage transformer to ±1°. Solid silver chloride was then added and the mixture stirred mechanically for about one hour. The consistency of the results indicated that equilibrium was reached in this time. Stirring was stopped and, after a few minutes, samples of 2–20 g. were removed with a preheated glass pipet. As undissolved silver chloride settled on the bottom or collected on the stirrer or side walls of the tube, filtration was not needed. After cooling, the samples were weighed, soluble salt extracted with water, and silver chloride weighed as such in a sintered glass disc crucible. Temperatures, which varied from 180 to 400°, were measured with a calibrated chromel–alumel thermocouple. The hot junction, protected with a thin glass tube, was under the liquid surface of the fused salt. It is thought that uncertainty in solubility measurements is of the order of ±2%.

Results and Discussion

If it is assumed that both silver chloride and the solvent are completely dissociated to simple ions, the product of the silver and chloride ion mole fractions, calculated on this assumption, would be constant at a fixed temperature, providing that the ion activity coefficients were constant. The symbol K is used below to designate the ion mole fraction product, where the ion mole fraction is the ratio of the number of moles of the ion to the sum of the number of moles of all ions. Furthermore, the heat of solution of silver chloride might be calculated from the slope of a plot of log K *versus* reciprocal absolute temperature. This was done for each solvent and in all cases plots which were linear within experimental error were obtained. The results are shown in condensed form in Table I which shows the solvent composition, $-\log K$ at 300°, the molality of silver chloride at 300°, and ΔH, the apparent heat of solution, calculated as $-2.3R\ \mathrm{d}(\log K)/\mathrm{d}(1/T)$.

TABLE I

THE SOLUBILITY OF SILVER CHLORIDE IN VARIOUS NITRATE MELTS

Solvent composition, mole %	$-\log K$ (300°)	Moles AgCl/kg. solvent (300°)	ΔH, kcal. mole^{-1}
$NaNO_3$ 100	7.17	0.00625	22.0
KNO_3 100	6.93	.00679	24.0
KNO_3 95, $AgNO_3$ 5	4.86	.0105	9.9
KNO_3 90, $AgNO_3$ 10	4.16	.0254	8.9
KNO_3 75, $AgNO_3$ 25	2.97	.137	7.3
KNO_3 50, $AgNO_3$ 50	1.83	.885	5.8
KNO_3 25, $AgNO_3$ 75	1.25	2.44	3.8
$AgNO_3$ 100[a]	0.83	7.35	3.4
KNO_3 90, $TlNO_3$ 10	6.39	0.0106	22.0
KNO_3 86, $Pb(NO_3)_2$ 14	5.69	.0229	16.5
KNO_3 87.5, $Ba(NO_3)_2$ 12.5	6.89	.0063	

[a] Reference 1.

Inspection of Table I shows that the product of silver and chloride ion mole fractions at a given temperature is a function of the other cations which are present. There is a small (8% in molality at 300°) but significant (compared to estimated 2% precision) difference between sodium and potassium, a very strong dependence on excess silver ion, and somewhat lesser dependence on lead and thallous ions. Addition of barium nitrate did not cause a significant change in K, although there was a decrease in silver chloride molality. While these effects suggest complexes of the form $Ag_nCl^{(n-1)+}$ or Ag_n^{n+}, no quantitative agreement with such assumptions could be found and the observed behavior may arise from quite different causes.

Although the slopes of the log K *versus* $1/T$ lines for silver chloride in sodium nitrate and potassium nitrate are greater than those corresponding to the value of 18.3 kcal. found by Flengas and Rideal,[3] extrapolation to 248° gives 0.0023 ± 0.0001 molal for the solubility of silver chloride in both sodium nitrate and potassium nitrate in agreement with Flengas and Rideal at this temperature. Since the heats of solution designated as ΔH in Table I are based on an assumption as to the nature of the solution, they should not be considered reliable until confirmed by calorimetric measurements.

The solubility of silver chloride is also increased greatly by the addition of chloride ion. In a 90 mole % potassium nitrate, 10 mole % potassium chloride solvent, the silver chloride solubility at 300° was found to be 0.16 molal. As the eutectic temperature in this system is above 300°, this value was obtained by extrapolation of measurements made at higher temperatures. These solubility measurements show that a silver chloride–silver indicator electrode can have but limited application in fused nitrate melts.

The freezing point of the silver chloride used in the solubility measurements was found to be 454 ± 1°. On the addition of sufficient potassium nitrate to form a two phase liquid system, the freezing point of the silver chloride layer was found to be lower by 4.6°. Assuming both potassium nitrate and silver chloride in the silver chloride phase to be completely dissociated and taking the heat of fusion of silver chloride as 3080 cal. mole^{-1}, the mole fraction of dissolved potassium nitrate was calculated to be 0.0067. As extrapolation of the solubility of silver chloride in potassium nitrate to 450° gives a silver chloride mole fraction of 0.0065, the mutual solubilities appear to be substantially equal.

FLUORINE N.S.R. SPECTROSCOPY. I. RELIABLE SHIELDING VALUES, ϕ, BY USE OF CCl_3F AS SOLVENT AND INTERNAL REFERENCE

BY GEORGE FILIPOVICH AND GEORGE V. D. TIERS

Contribution No. 152, Central Research Dept., Minnesota Mining and Manufacturing Co., St. Paul 6, Minnesota

Received October 27, 1958

At present, there is no accurate method by which fluorine nuclear spin resonance (n.s.r.) spectra can

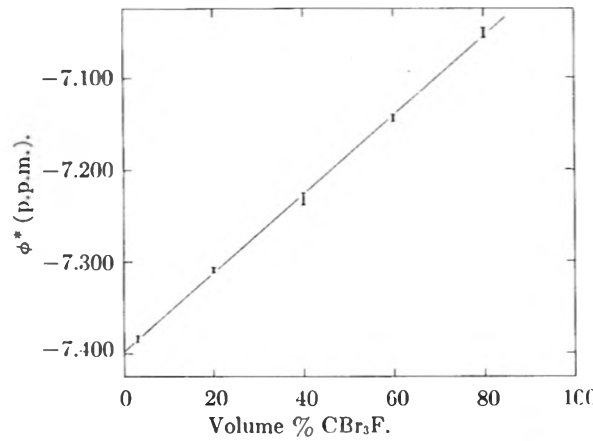

Fig. 1.—Plot of the apparent shielding value, ϕ^*, *vs.* concentration of CBr_3F in CCl_3F.

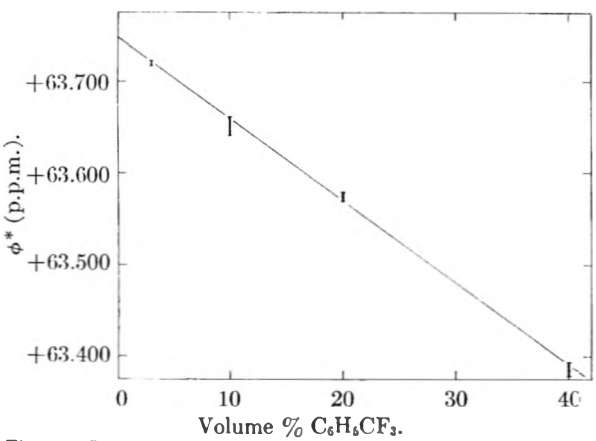

Fig. 2.—Plot of the apparent shielding value, ϕ^*, *vs.* concentration of $C_6H_5CF_3$ in CCl_3F.

be compared, since no reliable means of recording spectral position has been reported. There is obviously a need for a practical means of making such measurements, but recent papers have cast doubt on the possibility of doing so; a marked effect of solvent upon spectral position has been reported.[1,2] It has been suggested that intermolecular effects may be evaluated exactly by extrapolation to zero polarization (*i.e.*, gas phase at low pressures).[2] Such procedures are at best rather troublesome, particularly in view of the relatively low solubility of fluorocarbon materials in non-fluorinated solvents; furthermore, the long extrapolation to zero polarization is difficult to perform with precision. For these and other reasons[3] we have developed a simplified, internally referenced,[3] alternative procedure for determining and tabulating reliable fluorine n.s.r. shielding values. Shielding values may be referred to any physically-defined state (*e.g.*, vacuum), but it is desirable to choose an experimentally appropriate state; we have found CCl_3F to be an excellent solvent for fluorinated materials[4] and have accordingly chosen infinite dilution in CCl_3F as the standard state for measurement of fluorine shielding values. The strong, sharp, readily-identified peak of CCl_3F is used as the internal reference, and is assigned the value $\phi = \pm 0.000$ by definition of the ϕ-scale. For other peaks ϕ^* (in p.p.m.) $= 10^6(H_{obs} - H_{CCl_3F})/H_{CCl_3F}$, and $\phi = \phi^*$ at infinite dilution. Increasing values of ϕ signify increasing shielding of the fluorine nucleus.

The n.s.r. equipment and measurement techniques were as previously described,[3] except that sweep rates were such that 1.0 p.p.m. occupied about 50 mm. of chart (25 mm. for n-$C_6H_{13}F$ and for Et_2SiF). The very inexpensive pure solvent, CCl_3F, obtained commercially in cylinders,[5] was transferred to bottles for convenience; refrigerator storage is desirable in view of its low b.p., 24°. Pipetting and handling were most easily done in slightly-cooled equipment; for this purpose it was convenient to use a chip of Dry Ice held in a towel. The fluorine compounds studied were available in these laboratories and had in most cases been obtained from suppliers of laboratory chemicals.[6]

In Table I are presented the observed ϕ^*-values for a wide variety of compounds having highly dissimilar types of fluorine atoms. The variations in

TABLE I

APPARENT FLUORINE N.S.R. SHIELDING VALUES, ϕ^*

Compound	Vol., % concn. in CCl_3F	ϕ^* (p.p.m.)	Std. dev.
$C_6H_5SO_2F$	5	−65.509	±0.005
	20	−65.547	± .006
$CFBr_3$	3	−7.384	± .004
	20	−7.309	± .002
	40	−7.231	± .007
	60	−7.143	± .003
	80	−7.052	± .003
CF_2Br_2	2	−6.768	± .002
	10	−6.763	± .004
	80	−6.768	± .005
$BrCF_2CF_2Br$	10	+63.394	± .005
	40	+63.373	± .009
	80	+63.332	± .007
$C_6H_5CF_3$	3	+63.719	± .003
	10	+63.651	± .010
	20	+63.574	± .005
	40	+63.385	± .009
$CFCl_2CFCl_2$	5	+67.753	± .006
	20	+67.762	± .006
CF_3CO_2H	5	+76.542	± .005
	20	+76.552	± .006
CF_3CCl_3	3	+82.209	± .002
	10	+82.220	± .008
	40	+82.230	± .009
C_6H_5F	10	+113.150	± .002
	40	+113.231	± .003
$(CF_2CCl_2)_2$	2	+114.086	± .009
	15	+114.086	± .003
$(C_2H_5)_3SiF$	10	+176.24	± .02
	40	+176.240	± .006
n-$C_6H_{13}F$	10	+219.017	± .006
	40	+219.002	± .013

(1) D. F. Evans, *Proc. Chem. Soc.*, 115 (1958).

(2) R. E. Glick and S. J. Ehrenson, THIS JOURNAL, **62**, 1599 (1958).

(3) G. V. D. Tiers, *ibid.*, **62**, 1151 (1958).

(4) Miscible at −20° with n-C_8F_{18}, $(n$-$C_6F_{13})_2O$, $(n$-$C_4F_9)_3N$, cyclo-C_4F_8, $C_6H_5CF_3$, α-$C_{10}H_7I$, CS_2, CH_3NO_2, CH_3CN. Solubility parameter, δ (J. H. Hildebrand and R. L. Scott, "The Solubility of Non-Electrolytes," 3rd Ed., Reinhold Publ. Corp., New York, N. Y., 1950, p. 253 *et seq.*) estimated as 7.4 by means of the empirical relation $\delta = 32.0(n^2 - 1)/(n^2 + 2)$ for liquids of low polarity.

(5) Trade names: "Freon-11" (duPont Co.) or "Genetron-11" (General Chem. Co.).

(6) Matheson, Coleman and Bell Co.; Eastman Kodak Co.; Peninsular Chemical Co. (Gainesville, Fla.); Columbia Organic Chemical Co. (1012 Drake St., Columbia, S. C.).

ϕ^* with concentration may seem negligible in view of the great breadth of the fluorine spectrum (300 p.p.m. or more); however, overlapping ϕ^*-values are shown by two compounds in Table I. It is noteworthy that the error in measurement of ϕ^* is less than 1% as large as the maximal solvent dependence of ϕ^* exhibited by one compound, $C_6H_5CF_3$. For analytical purposes, at least, crude ϕ^*-values cannot be relied upon directly, but must be converted into ϕ-values by extrapolation to infinite dilution.

Our procedure for extrapolation is illustrated by Figs. 1 and 2, in which (within our limits of error) the plot of ϕ^* *vs.* volume percentage of solute appears completely linear. The cases chosen, $CFBr_3$ and $C_6H_5CF_3$, respectively, are the only ones from the present data which permit a serious test of linearity. Table II contains a selection of ϕ-values thus obtained.

TABLE II

FLUORINE N.S.R. SHIELDING VALUES, ϕ, OBTAINED BY THE EXTRAPOLATION OF ϕ^*-VALUES TO INFINITE DILUTION IN CCl_3F

Compound	ϕ, p.p.m.	Std. dev.
$C_6H_5SO_2F$	−65.497	±0.007
$CFBr_3$	−7.397	± .004
CF_2Br_2	−6.768	± .002
$BrCF_2CF_2Br$	+63.403	± .006
$C_6H_5CF_3$	+63.747	± .003
$CFCl_2CFCl_2$	+67.750	± .008
CF_3CO_2H	+76.539	± .007
CF_3CCl_3	+82.204	± .002
C_6H_5F	+113.123	± .002
$(CF_2CCl_2)_2$	+114.086	± .010
$(C_2H_5)_3SiF$	+176.24	± .03
n-$C_6H_{13}F$	+219.022	± .009

There are several points of practical significance to be drawn from Tables I and II. (1) For dilute solutions (2 to 10%) the difference between ϕ^* and ϕ is hardly greater than experimental error, and extrapolation may safely be omitted unless the highest degree of discrimination is required. In cases of limited solubility, or when weak, broad multiplets are observed, extrapolation may prove very difficult (*e.g.*, Et_3SiF). (2) Rather good ϕ-values are obtained by extrapolation of ϕ^* even when *only* highly concentrated solutions are used. This is particularly significant for the identification of minor impurities in a sample. (3) The presence of 1% or less of impurity in the CCl_3F produces negligible error in the ϕ-values; accordingly it would be permissible to add 1% of the excellent reference compound, tetramethylsilane,[3] if proton τ-values were also to be measured.

Externally-referenced measurements made on pure liquids[7-10] cannot accurately be converted to ϕ-values. Substantial errors would be incurred in substituting such measurements for ϕ-values, as illustrated in Table III. In many cases errors even of this magnitude cannot alter the interpretation of the spectrum; the data of Table III (not elsewhere available) are therefore of some utility for the intercomparison of measurements listed in references 7–10.

TABLE III

APPARENT SHIELDING VALUES OBTAINED BY EXTERNAL REFERENCING WITH CCl_3F

Pure compound	Apparent shielding value	Std. dev.	Error,[a] $\Delta\phi$
$C_6H_5SO_2F$	−65.38	±0.02	+0.12
$CFBr_3$[b]	−8.85	± .005	−1.45
$BrCF_2CF_2Br$	+63.32	± .01	+0.08
$C_6H_5CF_3$[b]	+63.95	± .01	+ .20
$CFCl_2CFCl_2$	+67.27	± .02	− .48
CF_3CO_2H	+78.45	± .02	+1.91
C_6H_5F[b]	+113.68	± .01	+0.56
$(CF_2)_4$[b]	+138.03	± .01	—
$(C_2H_5)_3SiF$	+176.78	± .02	+ .54
n-$C_6H_{13}F$	+219.42	± .01	+ .40

[a] Error incurred in substituting these apparent shielding values for the ϕ-values listed in Table II. [b] First measured by Dr. J. R. Zimmerman at the suggestion of one of the authors (G.V.D.T.). Our measurements agree with his within ±0.02 p.p.m.

It is concluded that subsequently reported fluorine n.s.r. data should and can be presented easily in a truly interconvertible system of units; we prefer ϕ-values, but would welcome any equivalent system.

We thank Dr. John R. Zimmerman of the Magnolia Petroleum Co., not only for communicating to us the results of several precise measurements comparable to those of Table III, but also for making valuable suggestions concerning n.s.r. techniques. The assistance of Mr. Donald Hotchkiss in obtaining and measuring many of the spectra is gratefully acknowledged.

(7) L. H. Meyer and H. S. Gutowsky, THIS JOURNAL, **57**, 481 (1953); H. S. Gutowsky, D. W. McCall, B. R. McGarvey and L. H. Meyer, *J. Am. Chem. Soc.*, **74**, 4809 (1952).

(8) N. Muller, P. C. Lauterbur and G. F. Svatos, *ibid.*, **79**, 1043, 1807 (1957).

(9) J. J. Drysdale and W. D. Phillips, *ibid.*, **79**, 319 (1957); W. D. Phillips, *J. Chem. Phys.*, **25**, 949 (1956).

(10) G. V. D. Tiers, *J. Am. Chem. Soc.*, **78**, 2914 (1956); **79**, 5585 (1957).

THE CRYSTALLIZATION RATE OF LOW PRESSURE POLYETHYLENE[1]

BY S. BUCKSER AND L. H. TUNG

Polychemicals Research Department, High Pressure Laboratory, The Dow Chemical Company, Midland, Michigan

Received October 28, 1958

The crystallization rate of the more branched, high pressure polyethylene has been studied dilatometrically by Kovacs.[2] He observed a rapid crystallization followed by a slow volume contraction which varied linearly with the logarithm of time. The slow volume contraction was attributed to the rearrangement of amorphous material by the author. Similar processes in the crystallization of polyhexamethylene adipamide and polyethylene terephthalate have been observed by Morgan, *et al.*,[3] who called the respective processes primary and secondary crystallization. No work on the

(1) Preliminary results of this note were presented in a paper entitled "Effect of Molecular Weight on the Crystallinity and the Rate of Crystallization of Polyethylene" at the 133rd ACS meeting in San Francisco, April, 1958.

(2) A. J. Kovacs, *Ricerce Sci.*, **25A**, 668 (1955).

(3) F. D. Hartley, F. W. Lord and L. B. Morgan, *ibid.*, **25A**, 577 (1955).

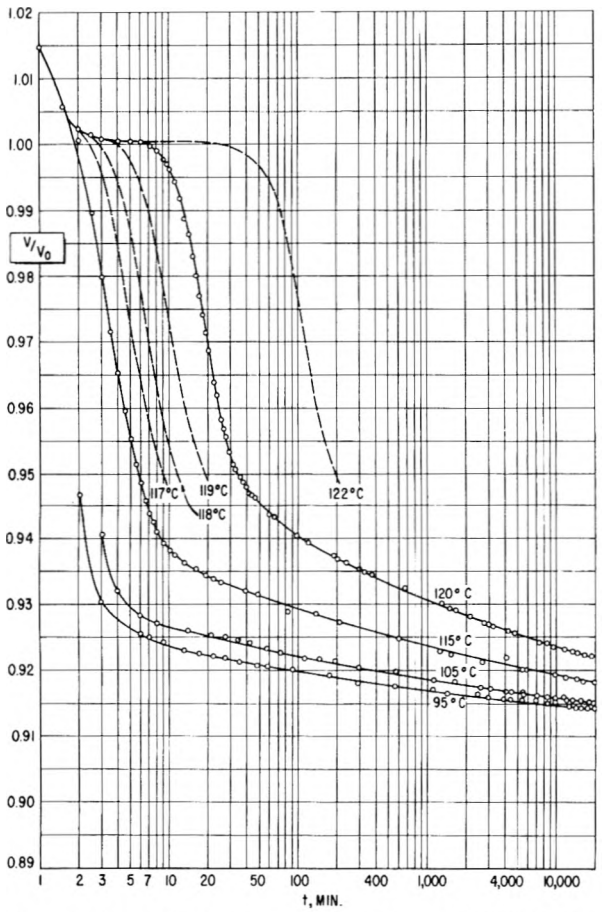

Fig. 1.—Crystallization curves of mol. wt. 110,000 polyethylene fraction.

simpler less branched polyethylenes has been reported except the rapid primary crystallization of polymethylene observed by Mandelkern.[4] In the present work the crystallization rates of several Ziegler-type low pressure polyethylene samples were measured dilatometrically. Some experiments were carried on for as long as two weeks to examine the long-term, slow volume contraction reported by Kovacs.

Experimental

The technique of dilatometry has been described in an earlier article.[5] An auxiliary temperature bath was used to hold the samples at 165° for at least 30 minutes. The dilatometer was then transferred rapidly to the other temperature bath controlled at the temperature of crystallization and the volume contraction was observed through a precision cathetometer.

Results and Discussion

The samples used for the experiments were an unfractionated Ziegler-type polyethylene of viscosity average molecular weight 98,000, and three fractionated samples of molecular weights 110,000, 53,000 and 2,100. The melting points and method of fractionation of these samples have been reported before.[5] A set of crystallization curves of the 110,000 molecular weight fractionated samples at four different temperatures is represented by the solid lines in Fig. 1. In the figure, v is the specific volume of the polymer and v_0 is the specific volume of the amorphous phase extrapolated to the crystallization temperature from the specific volume of the same sample above its melting point. The crystallization curves of the other three samples are similar to the ones shown in Fig. 1. At high crystallization temperatures an apparent induction period was observed. Following the apparent induction period was the rapid primary crystallization. At lower temperatures of crystallization the induction period disappeared and the crystallization started before the sample reached thermal equilibrium, but the slow, long contraction curves remained about the same.

In order to obtain more information for the rapid primary crystallization, a few short runs were made at temperatures from 6 to 16 degrees below the melting points of the respective samples. The results on the 110,000 molecular weight sample are shown by the dotted lines in Fig. 1. The actual experimental points of these runs have been omitted from the plot as they were very close together and fell right on the curves. The early portions of these curves are superimposable, and the rate increased with the lowering of the crystallization temperature as in the case of polymethylene observed by Mandelkern.

The primary crystallization of polymers can usually be described by Avrami's equation[6]

$$a = e^{-Kt^n} \qquad (1)$$

where a is the fractional amount of the original crystallizable amorphous phase remaining at time t, K is a rate constant and the index n is equal to 2, 3 or 4 depending on the nature of the nucleation and growth processes of the spherulites. The analysis of the present data was, however, complicated by the fact that the primary crystallization was not readily separable from the secondary volume contraction. In order to compare the crystallization rates we used the early portion of the crystallization curves and assumed that n was equal to 4 to calculate the constant K. This assumption implied that the nucleation of spherulite centers was homogeneous and the growth of spherulites was spherical with a linear radial growth rate. The fit between the calculated and the experimental curves consequently was confined only to the early stage of crystallization. The experimental points became higher than the $n = 4$ curves at the later stage of crystallization. The rate constants K so calculated are listed in Table I.

In Table I, ΔT is defined as the temperature difference between the melting point and the temperature of crystallization. The rate constants K are shown to decrease with the increase of molecular weights. The unfractionated sample, based on its viscosity-average molecular weight, seems to have exceptionally large rate constants. Owing to the broadness of molecular weight distribution the number average molecular weight of the unfractionated sample was estimated to be between those of samples 3 and 4. Thus the present data indicate that the crystallization rate depends on the number average molecular weight.

According to the treatment of Mandelkern,

(4) L. Mandelkern, *Chem. Revs.*, **56**, 903 (1956).

(5) L. H. Tung and S. Buckser, THIS JOURNAL, **62**, 1530 (1958).

(6) M. Avrami, *J. Chem. Phys.*, **8**, 212 (1940).

TABLE I

CRYSTALLIZATION RATE CONSTANT K OF THE RAPID PRIMARY CRYSTALLIZATION PERIOD

Sample 1, M_v 98,000 (unfractionated)			Sample 2, M_v 110,000 (fraction)		
T, °C.	ΔT	K (1/min)[4]	T	ΔT	K
119	10	9.11×10^{-5}	117	13	4.39×10^{-4}
120	9	1.82×10^{-5}	118	12	1.68×10^{-4}
112	7	5.71×10^{-8}	119	11	3.03×10^{-5}
123	6	7.71×10^{-10}	120	10	2.80×10^{-6}
			122	8	2.42×10^{-9}
Sample 3, M_v 53,000 (fraction)			Sample 4, M_v 2,100 (fraction)		
T	ΔT	K	T	ΔT	K
113	16	2.48×10^{-3}	111	12	2.80×10^{-3}
115	14	9.16×10^{-4}	113	10	3.76×10^{-4}
117	12	2.44×10^{-4}	114	9	1.59×10^{-4}
119	10	1.76×10^{-5}	115	8	3.67×10^{-4}
121	8	1.77×10^{-7}			

Quinn and Flory,[7] log K should vary linearly with the term $(T_m/\Delta T)^2 1/T$, where T_m is the melting temperature of the polymer. From the slope of such a plot shown in Fig. 2, the interfacial surface energy can be calculated. With the exception of the data for the highest molecular weight sample, the slopes of all curves seem to be independent of molecular weight. It is not obvious that the data of the highest molecular weight sample should have a different slope in Fig. 2, but the uncertainties involved in calculating the constant K and the fact that a small error in the melting point determination would cause a radical change in the slopes and the positions of the lines in Fig. 2, could easily have caused such an anomaly. The interfacial surface energy calculated from the three parallel lines in Fig. 2 is in the order of 4 ergs per cm.^{2}. This value, though not too far from what Mandelkern, Quinn and Flory have found for other polymers, is small in comparison to the value found by Burnett and McDevit[8] from the direct microscopic observation of Nylon spherulite growth.

The slow secondary volume contraction of the present low pressure polyethylene samples is slightly different from that of high pressure polyethylene observed by Kovacs. Kovacs found that the volume change varied linearly with the logarithm of time whereas the slopes of the curves in Fig. 1 change continuously with the logarithm of time. The tail portions of the present curves actually can be fitted by a simple relaxation equation of the type

$$v/v_0 - v_\infty/v_0 = Ce^{-K't} \qquad (2)$$

where v_∞ is the equilibrium specific volume, K' is the rate constant and C is another constant. The data of the high temperature runs followed equation 2 at about 5,000 minutes (3.5 days) after the start of crystallization. For lower temperature runs equation 2 begins to fit the data as early as 2,000 minutes after the start of crystallization. The calculated values of the constant K' listed in Table II are relatively insensitive to the variation of molecular weight and temperature indicating that a diffusion controlled process which has a relatively

(7) L. Mandelkern, F. A. Quinn, Jr., and P. J. Flory, *J. Appl. Phys.*, **25**, 830 (1954).

(8) B. B. Burnett and W. F. McDevit, *ibid.*, **28**, 1101 (1957).

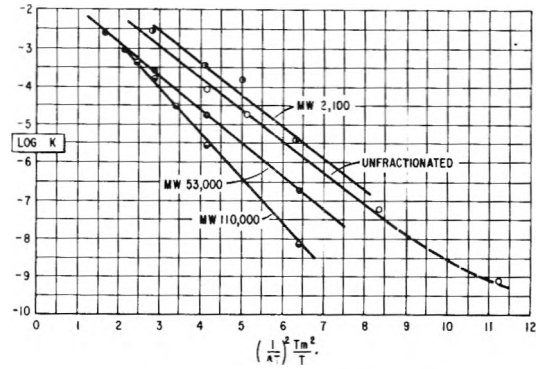

Fig. 2.—Log K *vs.* $(1/\Delta T)^2(T_m^2/T)$.

large temperature coefficient is not likely to be alone responsible for the slow volume contraction. It is interesting to note that the long term crystallization behavior observed by Russell and discussed by Dunning[9] on vulcanized rubber also fitted an equation similar to equation 2.

TABLE II

THE RATE CONSTANT K' (IN 1/MIN.) FOR THE TAIL PORTIONS OF THE SLOW SECONDARY VOLUME CONTRACTION

Temp., °C.	Sample 1 M_v 98,000 (unfractionated)	Sample 2 M_v 110,000 (fraction)
120	1.35×10^{-4}	1.02×10^{-4}
115	1.06×10^{-4}	1.15×10^{-4}
105	1.34×10^{-4}	1.24×10^{-4}
95	1.39×10^{-4}	0.64×10^{-4}
Temp., °C.	Sample 3 M_v 53,000 (fraction)	Sample 4 M_v 2,100 (fraction)
120	1.30×10^{-4}	...
115	1.27×10^{-4}	0.70×10^{-4}
105	1.55×10^{-4}	1.52×10^{-4}
95	1.36×10^{-4}	0.99×10^{-4}

Although the tail portions of the present crystallization curves can be fitted by equation 2, the entire crystallization process shown in Fig. 1 is obviously not a simple composite of the processes described by equations 1 and 2. It is conceivable that the secondary nucleation and the subsequent growth of crystallites during the development of spherulites set up stresses in the polymer. The slow volume contraction, resulting from the decay of such stresses is likely to be more complicated than can be described by a single, simple relaxation equation.

(9) W. J. Dunning, *Trans. Faraday Soc.*, **50**, 1115 (1954).

RADIATION-INDUCED CATIONIC POLYMERIZATION OF BUTADIENE[1]

BY W. S. ANDERSON

Shell Development Company, Emeryville, California

Received November 3, 1958

Chapiro[2] has reported that butadiene is slowly polymerized when exposed to ionizing radiation. Although most radiation-induced vinyl polymerizations are known to proceed *via* free radical inter-

(1) Presented at the San Francisco Meeting of the American Chemical Society, April 14, 1958.

(2) A. Chapiro, *J. chim. phys.*, **47**, 764 (1950).

mediates, there is evidence[3] that irradiation of well-chosen hydrocarbon monomers leads to polymerization by an ion–molecule mechanism. We have found that irradiation of butadiene leads to polymerization by the ionic route.

The infrared spectrum of polymer prepared by electron-irradiation of butadiene at 0 to −180° is similar to that of polymer obtained by Ferington and Tobolsky and Lewis acid catalysis.[4] With the absorptivities of Hampton[5] it can be calculated that 72% of the double bonds lie in *trans*-1,4 monomer units and 28% in vinyl groups. The *cis*-1,4 units in polybutadienes prepared by free radical initiation absorb at 13–14 μ; this absorption is absent from the polymer made by irradiation. If, however, an emulsion of butadiene in 5% aqueous soap solution is irradiated at 40°, that is, irradiated under conditions suitable for emulsion polymerization of butadiene, then the resulting polymer displays the absorption at 13–14 μ normally expected for radical-propagated polybutadiene.

Polymers prepared at 0, −40, −78 and −180° have identical infrared spectra and therefore the same distribution of double bond types. This effect is explained as follows: lifetimes of ions in the liquid phase are of the order of 10^{-12} to 10^{-14} second,[6] or about the interval required for a molecular vibration. Within this time an ion must undergo reaction or else suffer neutralization by a thermal electron. In such a short lifetime, a growing ion cannot attain thermal equilibrium before neutralization or the addition of a monomer unit. It would be expected, therefore, that the polymer double bond distribution be kinetically, not thermodynamically determined. In radical-propagated polybutadiene the *cis/trans* ratio is a function of polymerization temperature[7] and probably lies at the thermodynamic equilibrium value.[8]

TABLE I

POLYMERIZATION OF BUTADIENE WITH IONIZING RADIATION[a]

Temp., °C.	Conversion, %	Intrinsic viscosity,[b] dl./g.
20	6.1, 6.1	1.1, 1.1
0	6.7, 6.2	1.4, 1.3
−78	7.4, 7.3	2.1, 2.1

[a] The entire sample was exposed to 3-mev. electrons for 20 minutes; dose, 10^7 rads. [b] In toluene, 25°.

Rate of radiation-induced polymerization increases with decreasing polymerization temperature as shown in Table I. A negative temperature coefficient is common among cationic polymerizations; for example, the aluminum chloride catalyzed butadiene polymerization[9] is twice as fast at −110° as at −75°. Radical propagation of butadiene requires a large positive activation energy,[10] and in this respect differs from an ion–molecule reaction.[11] It seems likely that radical propagation in radiation-induced polymerization is defeated by the fast coupling of butadiene radicals.[12]

In order to obtain high molecular weights at high rates in the homogeneous radical polymerization of butadiene, very high temperature must be used.[13] However, in the radiation-induced polymerizations of Table I, the highest molecular weights are attained at −78°. This is further evidence that a non-radical mechanism is operating.

Intrinsic viscosities in the range of 1–2 dl./g. imply degrees of polymerization of at least 10^2–10^3. The growing ion therefore undergoes at least 10^2–10^3 collisions before its neutralization. If the estimated ion lifetime of 10^{-12} to 10^{-14} second is correct, then the ion–molecule collision frequency in the liquid state is, as in the dilute gas, greater than the intermolecular collision frequency. Owing to possible chain transfer by the charge transfer[14] type of ion–molecule reaction, the frequency of ion–molecule collisions may be even higher than that indicated by polymer molecular weight.

Acknowledgment.—The author wishes to acknowledge the valuable help and advice of D. P. Stevenson, E. R. Bell, C. R. Wagner and V. A. Campanile of the Shell Development Company.

Experimental

On a manifold equipped with a mercury diffusion pump, degassed Phillips Pure Grade butadiene in a bulb at −78° was distilled into ten-ml. ampoules. The monomer was then degassed again and the ampoules, containing about a five-gram charge, were sealed and irradiated with 3-mev. electrons from a van de Graaff generator. To determine yields of polymer, the ampoules were chilled to −78°, opened, and the contents were transferred to an aluminum dish where monomer was allowed to evaporate and polymer was weighed. Infrared spectra were obtained by dissolving the polymer residue in benzene, casting a film on a sodium chloride plate and recording the spectrum on a Beckman IR-4 instrument.

(3) W. N. T. Davison, S. H. Pinner and R. Worrall, *Chemistry and Industry*, 1274 (1957); W. J. Burlant and D. H. Green, *J. Polym. Sci.*, **31**, 227 (1958).

(4) T. E. Ferington and A. V. Tobolsky, *ibid.*, **31**, 25 (1958).

(5) R. Hampton, *Anal. Chem.*, **21**, 923 (1949).

(6) J. L. Magee, *Ann. Rev. Nuclear Sci.*, **3**, 171 (1953); A. H. Samuel and J. L. Magee, *J. Chem. Phys.*, **12**, 1080 (1953); M. Burton, J. L. Magee and A. H. Samuel, *ibid.*, **26**, 760 (1952).

(7) F. E. Condon, *J. Polymer Sci.*, **11**, 139 (1953).

(8) M. A. Golub, *ibid.*, **25**, 373 (1957).

(9) C. S. Marvel, *et al.*, *ibid.*, **6**, 483 (1958).

(10) M. Morton, P. P. Salticllo and H. Landfield, *ibid.*, **8**, 279 (1952).

(11) D. P. Stevenson, THIS JOURNAL, **61**, 1453 (1957).

(12) C. Walling, "Free Radicals in Solution," John Wiley and Sons, Inc., New York, N. Y., 1957, p. 208.

(13) C. E. Schildknecht, "Vinyl and Related Polymers," John Wiley and Sons, Inc., New York, N. Y., 1952, pp. 85, 119.

(14) E. F. Gurnee and J. L. Magee, *J. Chem. Phys.*, **26**, 1237 (1957); G. G. Meisels, W. H. Hamill and R. R. Williams, *ibid.*, **25**, 790 (1956); S. O. Thompson and O. A. Schaeffer, *J. Am. Chem. Soc.*, **80**, 556 (1958).

THE SORPTION EFFECT OF CELLULOSE TRINITRATE IN CAPILLARY VISCOMETRY

BY M. M. HUQUE,[1] M. FISHMAN AND D. A. I. GORING

The Pulp and Paper Research Institute of Canada, and McGill University, Montreal, Canada

Received December 1, 1958

In a recent study on the solution properties of cellulose trinitrate[2] it was found that an anomalous increase of η_{sp}/c occurred at low concentrations. This now familiar phenomenon has been reported by several workers for various polymer solvent sys-

(1) Colombo Plan Scholar from Dacca, Pakistan.

(2) M. M. Huque, D. A. I. Goring and S. G. Mason, *Can. J. Chem.*, **36**, 952 (1958).

tems.[3-9] Whether it is caused by an adsorbed layer on the wall of the capillary[4] or by molecular expansion at low concentration[3,7] is still uncertain. The present note summarizes results for a sample of high molecular weight cellulose trinitrate obtained with two multishear viscometers of different radii. Solvents were acetone and ethyl acetate.

A sample of raw ramie nitrate was purified by solution in acetone, centrifugation at 24,000 *g*, precipitation by addition of water and drying *in vacuo*. Solutions were made up by weight in redistilled acetone or ethyl acetate by shaking mechanically for 64 hours. Solutions and solvent were clarified by centrifugation and filtration, respectively.

Viscosity was measured at 25°. Viscometers were of the Schurz and Immergut[10] type having four bulbs and permitting dilution *in situ*. Capillary radii were 0.13 and 0.28 mm. Volumes and heights of bulbs were such that solvent flow times of 85 to 233 sec. were obtained. Kinetic energy corrections were made. The Kroeplin shear rate G for solvent ranged from 400 to 4000 sec.$^{-1}$ in the narrow capillary and from 400 to 3000 sec.$^{-1}$ in the wide capillary. From graphs of η_{sp}/c *vs.* log G or log η_{sp}/c *vs.* log G values of η_{sp}/c at constant G were obtained.

In 11 experiments a definite upward curvature of the η_{sp}/c *vs.* c plot was detected 10 times. However the regularity and quantitative reproducibility of the data were not good. The irreproducibility observed was not caused only by limitations in precision of the viscometers but indicated differences in behavior from one solution to the next.

A set of results for solutions in acetone is shown in Fig. 1. Data obtained with ethyl acetate as solvent were very similar. The following general trends were noted in all the results. (1) The increase in η_{sp}/c was more marked in the small capillary. (2) There was no gross effect of shear rate on the phenomenon in the range 500 to 2000 sec.$^{-1}$. (3) The minimum value of η_{sp}/c appeared at a slightly higher concentration in the large capillary.

The irregularity of the results did not allow calculation of the layer thickness by the extrapolation method of Öhrn.[4] However, for acetone and ethyl acetate solutions in both capillaries the points obtained lay approximately on theoretical curves derived by assuming an adsorbed layer of 500–1000 Å. on the walls of the capillary.

No consistent evidence was found of a decrease in η_{sp}/c at very low concentrations. This indicated that the layer, once adsorbed, did not desorb when more dilute solutions were run through the capillary. This point was tested further by rinsing out the viscometer with solvent after the run and taking an efflux time for solvent. This efflux time was higher than the efflux time taken before the run. In one case the difference persisted after rinsing the viscometer three times with solvent. The efflux time returned to its usual value when the viscometer was cleaned with chromic acid. The equivalent thickness a of the adsorbed layer was computed from

$$a = \frac{r\Delta t}{4t} \qquad (1)$$

where r is the radius of the capillary and Δt is the difference in the efflux time t before and after the run. Values of a are shown in Table I. With the exception of one experiment, they lie between 500 and 1000 Å.

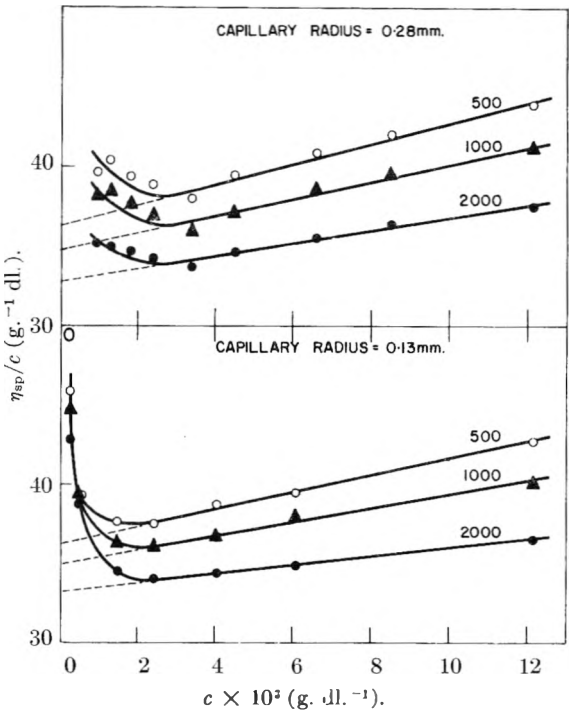

Fig. 1.—Anomalous increase of η_{sp}/c at low values of c for cellulose trinitrate in acetone. The $[\eta]$ values obtained by extrapolation of the linear portion show some shear dependence in contrast to previously published data.[2] The present range of shear is about 4 times that used previously. From the above data, the shear dependence can be computed over the range 300 to 700 sec.$^{-1}$ as previously studied. The resulting spread in $[\eta]$ corresponds to the small error of ±1.5%.

TABLE I

THICKNESS OF ADSORBED LAYER CALCULATED FROM INCREASE ON SOLVENT EFFLUX TIME AFTER RUN

Solvent	Capillary radius (mm.)	a (Å.)
Acetone	0.28	700
Acetone	.13	900
Ethyl acetate	.28	300
Ethyl acetate	.13	600

From relationships obtained in a previous study,[2] the weight average molecular weight and Z-average root mean square radius of gyration were 2.2×10^6 and 1600 Å., respectively. Thus the adsorbed layer was probably no thicker than one molecule unless it was formed by the preferential adsorption of smaller molecules. If one molecule was assumed to occupy 10^6 Å.^{2} of surface, the maximum weight in a monolayer over the complete inner surface of the viscometer would be approximately 10^{-5} g., *i.e.*, 0.5% of the cellulose trinitrate in the volume of solution added. Therefore effects due to concentration changes probably are small. For a given value of a in eq. 1, Δt increases as r decreases. With fine capillaries this effect could be used to study the

(3) D. J. Streeter and R. F. Boyer, *J. Polymer Sci.*, **14**, 5 (1954).
(4) O. E. Öhrn, *ibid.*, **17**, 137 (1955).
(5) M. Takeda and R. Endo, THIS JOURNAL, **60**, 1202 (1956).
(6) C. A. F. Tuijnman and J. J. Hermans, *J. Polymer Sci.*, **25**, 385 (1957).
(7) T. Kawai, K. Saito and W. Krigbaum, *ibid.*, **26**, 213 (1957).
(8) O. E. Öhrn, *Arkiv Kemi*, **12**, 397 (1958).
(9) S. Gundiah and S. L. Kapur, *J. Polymer Sci.*, **31**, 202 (1958).
(10) J. Schurz and E. H. Immergut, *ibid.*, **9**, 279 (1952).

dimensions of adsorbed polymer layers in systems where such small changes in concentration are difficult to measure.

Finally it should be pointed out that the irreproducibility from solution to solution supports Öhrn's adsorption theory. If the effect were due to some fundamental hydrodynamic change in the solution there should be no difficulty in reproducing it. On the other hand, an adsorption process would probably be sensitive to variable traces of water or dissolved gases in the solvent as well as to the condition of the glass surface of the capillary.

COMMUNICATION TO THE EDITOR

THE PREPARATION OF MONODISPERSED EMULSIONS

Sir:

A method has been devised for preparing oil in water emulsions of narrow size distribution, as indicated by the presence of the colors of the higher order Tyndall spectrum.[1] Basically, the method consists of generating a monodispersed aerosol in either the Sinclair–La Mer,[2] or the Rapaport–Weinstock generator,[3] charging the particles by passing them through a corona discharge,[4] and bubbling them into a vessel containing an electrically grounded bulk phase. The dispersed phases have been paraffin oil, Nujol, mercury, and dioctyl phthalate. The choice is limited to compounds insoluble in water which have vapor pressures low enough at room temperature for a stable aerosol to be prepared. The average particle radii cover the range 0.05 to 0.9 micron; extension to larger and smaller sizes can be accomplished easily.

The bulk phase can be pure water or contain an emulsifier, except in the case of an oil which spreads on the surface of pure water. In this case enough emulsifier must be added to lower the surface tension of the bulk phase sufficiently to prevent the oil from spreading. Two emulsifiers have been used, Triton X-100 (Rohm and Haas) and Myrj-52 (Atlas Powder Company).

The rate of emulsification depends on the concentration of the original aerosol, the magnitude of the charge on the particles, the surface tension of the bulk liquid, and the geometry of the bubbling device used to introduce the aerosol into the liquid.

(1) I. Johnson and V. K. La Mer, *J. Am. Chem. Soc.*, **69**, 1184 (1947).

(2) D. Sinclair and V. K. La Mer, *Chem. Revs.*, **44**, 245 (1949).

(3) E. Rapaport and S. Weinstock, *Experientia*, **11**, 363 (1955).

(4) G. Goyer, R. Gruen and V. K. La Mer, THIS JOURNAL, **58**, 137 (1954); A.E.C. Handbook on Aerosols, Washington, D.C., 1950.

The number concentration of the aerosol is important since it limits the ultimate concentration which can be attained in reasonable time. The Rapaport–Weinstock generator is to be preferred in this respect because the aerosol number concentration is generally higher. However, it needs modification to permit the dispersion of solids, whereas many solids may be dispersed with the Sinclair–La Mer generator.

The rate of emulsification is low if the aerosol particles are uncharged, but rises rapidly when a few charges are placed on each particle. Further increase in the magnitude of the charge may increase the rate slightly, but the effect is too small to be observed in the experiments performed to to date. Decreasing the surface tension increases the rate of emulsification.

The geometry of the bubbling device determines the efficiency of the emulsification. The number of particles entering the interface depends on the size of the bubbles and the time the bubbles remain in the liquid. The emulsion cell consists of four capillary tubes evenly spaced around the bottom of a 250-ml. beaker, fitted with a magnetic stirrer which reduces the size of the bubbles appreciably due to the shearing effect of the moving liquid. A flat disc, placed directly over the stirring magnet, increases the time required for the bubbles to rise. A single capillary tube with the gas bubbles directed toward the stirring magnet also is satisfactory.

At present we are preparing emulsions using as disperse phases sulfur and stearic acid, studying the quantitative relationships of the variables involved, and increasing the efficiency of the emulsification method. A study of the effect of emulsifiers, size and charge distributions upon the properties of emulsions is contemplated.

COLUMBIA UNIVERSITY
NEW YORK 27, N. Y.
RONALD E. WACHTEL
VICTOR K. LA MER

RECEIVED APRIL 1, 1959